A STUDY OF FATIGUE LOADING ON AUTOMOTIVE AND TRANSPORT STRUCTURES

by

Johann Wannenburg

A thesis submitted for the degree of
PhD (MECHANICAL ENGINEERING)
in the Faculty of Engineering, the Built Environment
and Information Technology
of the
University of Pretoria

August 2007

Dedicated to my late father,
Jan Wannenburg,
who introduced me to thesis writing
(Wannenburg (1966))
at an early age and with who's help
this thesis may have been completed years earlier.

ABSTRACT

It is accepted that defective structural designs are mostly caused by insufficient knowledge of input data, such as material properties or loading, rather than inadequate analysis or testing methods. In particular, loads associated with automotive and transport (trucks, trailers, containers, trains) structures are nontrivial to quantify. Such loads arise from stochastic and ill-defined processes such as driver/operator actions and structure-terrain interaction. The fundamental processes involved with the determination of input loading are measurements, surveys, simulation, estimation and calculation from field failures. These processes result in design criteria, code requirements and/or testing requirements. The present study deals with methods for the establishment of input loading for automotive and transport structures. It is attempted to generalise and unify new and existing techniques into a cohesive methodology. This is achieved by combining researched current theory and best practices, with lessons learned during application on, as well as new techniques developed for, a number of complex case studies, involving road tanker vehicles, light commercial vehicles, industrial vehicles, as well as tank containers. Apart from the above, the present study offers four individual, unique contributions. Firstly, two methods, widely applied by industry, namely the Remote Parameter Analysis (RPA) method, which entails deriving time domain dynamic loads by multiplying measured signals from remotely placed transducers with a unit-load static finite element based transfer matrix, as well as the Modal Superposition method, are combined to establish a methodology which accounts for modal response without the need for expensive dynamic response analysis. Secondly, a concept named *Fatigue Equivalent Static Load (FESL)* is developed, where fatigue load requirements are derived from measurements as quasi-static g-loads, the responses to which are considered as stress ranges applied a said number of times during the lifetime of the structure. In particular, it is demonstrated that the method may be employed for multi-axial g-loading, as well as for cases where constraint conditions change during the mission of the vehicle. The method provides some benefits compared to similar methods employed in the industry. Thirdly, a complex analytical model named *Two Parameter Approach (TPA*) is developed, defining the usage profile of a vehicle in terms of a bivariate probability density distribution of two parameters (distance/day, fatigue damage/distance), derived from measurements and surveys. Based on an inversion of the TPA model, a robust technique is developed for the derivation of such statistical usage profiles from only field failure data. Lastly, the applicability of the methods is demonstrated on a wide range of comprehensive case studies. Importantly, in most cases, substantiation of the methods is achieved by comparison of predicted failures with 'real-world' failures, in some cases made possible by the unusually long duration of the study.

OPSOMMING

Dit is bekend dat defektiewe struktuurontwerpe meestal veroorsaak word deur onvoldoende kennis van insette, soos materiaaleienskappe of belastings, in stede van ontoereikende analise- of toetstegnieke. In besonder is belastings geassosieer met voertuig- of vervoertoerustingstrukture, nie triviaal om te bepaal nie. Sulke belastings word veroorsaak deur stogastiese en ongedefinieerde prossesse soos drywer/operateur aksies en struktuur-terrein interaksie. Die fundamentele prosesse betrokke by die bepaling van insetbelastings is metings, vraelyste, simulasie, estimasie en berekening uit falingsdata. Hierdie prosesse het dan as uitsette, ontwerpkriteria, kodevereistes, en/of toetsvereistes. Die huidige studie handel oor metodes vir die bepaling van insetbelastings vir voertuig- en vervoerstrukture. Daar word gepoog om bestaande en nuwe tegnieke in 'n omvattende en generiese metodologie saam te vat. Dit word bereik deur 'n kombinasie van bestaande teorieë en beste praktyke soos gevind in die literatuur, lesse geleer uit die toepassing daarvan op, asook nuwe tegnieke ontwikkel vir 'n aantal komplekse gevallestudies, wat tenktrokke, ligte kommersiële voertuie, industriële voertuie en tenkhouers insluit. Bykomend tot bogenoemde doelwit, maak die studie ook vier unieke, individuele bydraes. Eerstens is twee tegnieke, wyd toegepas deur die industrie, naamlik die Indirekte Parameter Analise tegniek, wat behels om belastings in die tyd-domein te bereken deur vermenigvuldiging van indirek geplaasde meetkanaal resultate met 'n oordragfunksie, verkry uit die resultate van 'n statiese eenheidlas eindige element analise, sowel as die Modale Superposisie tegniek, saamgevoeg om 'n tegniek te vestig waar modale responsie in ag geneem kan word sonder die nodigheid van duur dinamiese responsie analises. Tweedens is 'n konsep, genoem *Vermoeidheids-Ekwivalente Statiese Belasting,* ontwikkel, waar vermoeidheidsbelastingvereistes gedefinieer word as kwasi-statiese inersiële belastings, die responsies waarvan beskou word as spanningsbereike wat 'n spesifieke aantal kere toegepas word gedurende die leeftyd van die komponent. In besonder is daar gedemonstreer dat die tegniek toepaslik is in gevalle van multi-assige inersiële belasting, asook wanneer randvoorwaardes verander gedurende die missie van die voertuig. Die metode bied 'n paar voordele bo soortgelyke tegnieke wat deur die industrie gebruik word. Derdens is 'n komplekse analitiese model, genoem die *Twee Parameter Metode,* ontwikkel, waar die gebruikersprofiel van 'n voertuig gedefinieer word in terme van 'n bivariate waarskynlikheidsdigtheidsfunksie van twee parameters (afstand/dag, vermoeidheidskade/afstand), bepaal uit rekstrokiemetings en vraelyste. Gebaseer op 'n inverse van die model, is 'n robuuste tegniek ontwikkel wat die bepaling van so 'n statistiese gebruikersprofiel, slegs uit veldfalingsdata, moontlik maak. Laastens is die toepaslikheid van die tegnieke gedemonstreer op 'n wye verskeidendheid van omvattende gevallestudies. Van spesifieke belang is die feit dat in meeste gevalle, die geldigheid van die tegnieke bewys kon word deur vergelyking tussen voorspelde falings en praktyk falings, waarvan sommige slegs moontlik was as gevolg van die ongewone lang tydsduur van die studie.

ACKNOWLEDGEMENTS

I want to express my sincere gratitude to the following persons for their involvement in, and contribution to this study:

- Anton Raath, Waldo von Fintel, Herman Booysen, Jurie Niemand, Theunis Blom and the other personnel at the University of Pretoria laboratories, who performed measurements and testing and provided insight,
- Rudy du Preez, Ettienne Prinsloo, Kenneth Mayhew-Ridgers, Lajos Vari and the other personnel at BKS Advantech who performed finite element analyses and data processing,
- De Wet Strydom and Sarel Beytell at Anglo Technical Division who performed measurements and finite element analyses,
- Stephan Heyns for his mentorship and encouragement,
- the personnel at the various vehicle manufacturing companies, for their support during the different case study projects,
- my children, Jamie, Willem and Stefanie, for their many years of sacrifices,
- and finally, my wife Letitia for her constant and unselfish love and support.

The Author
August 2007

TABLE OF CONTENTS

LIST OF SYMBOLS

ρ	Correlation coefficient
γ	Irregularity factor
σ	Stress
ε	Total local true strain
$\Delta\varepsilon$	Local strain range
$\Delta\sigma$	Nominal stress range
$\Delta\sigma_e$	Equivalent nominal stress range
$\Delta\sigma_l$	Local stress range
$\sigma(t)$	Stress as a function of time
σ_{1g}	Stress due to 1 g inertial loading
σ_a	Stress amplitude
σ_c	Stress at critical position
Δe	Engineering strain range
γ_f	Load factor
ε_f	True fracture ductility
Δg	Range of applied inertial loading
Δg_e	Range of equivalent applied inertial loading
ΔK	Stress intensity range
γ_m	Material factor
ϕ_r	Mode shape
ω_r	Natural frequency
η_r	Principal coordinate
μ_y	Mean of random variable y
σ_y	Variance of random variable y
[B]	Stress-load matrix
[c]	Damping matrix
[C]	Damping matrix in principal coordinates
[D]	Rigid body transformation matrix
[k]	Stiffness matrix
[K]	Transfer matrix, stiffness matrix in principal coordinates
[m]	Mass matrix
[M]	Mass matrix in principal coordinates
$[P_y]$	Load covariance matrix
A	Area
a	Crack length, acceleration
a(t)	Acceleration as a function of time
b	Fatigue strength exponent
C	Fatigue crack growth (Paris) equation coefficient
c	Fatigue ductility exponent
D	Fatigue damage
D_f	Damage to failure
D_{tt}	Damage induced by test track
e	Engineering strain
E	Young's modulus
F	Force
FF	Fatigue factor
f	Frequency
f(x)	Probability density function of variable x
g	Gravitational acceleration
G	Power Spectral Density
I	Second moment of area

IRI	International roughness index
k	Stiffness
K	Stress intensity factor
K'	Cyclic strength coefficient
K_t	Theoretical stress concentration factor
L	Length, load
m	Mass, fatigue crack growth (Paris) equation exponent, gradient of curve, spectral moment
n	Number of applied cycles
N	Number of cycles to failure
n'	Cyclic strain hardening exponent
n_e	Number of equivalent applied cycles
N_e	Number of equivalent cycles to failure
n_i	Number of applied cycles for i^{th} stress range
N_o	Number of positive sloped zero crossings per second
N_p	Peaks per second
p	Forces
P	Forces
P_f	Probability of failure
P_{RR}	PDF of rainflow ranges
P_s	Survival probability
S_f	Fatigue coefficient
t	Time
TD	Total fatigue damage
u	Displacement
v	Velocity
V	Volts
x_1	Damage per kilometre
x_2	Kilometre per day

LIST OF ABBREVIATIONS

A/D	Analogue to digital
APD	Amplitude probability density
ASME	American Society of Material Engineers
BS	British standard
ECCS	European Commission for the Construction of Steel
FDRS	Fatigue damage response spectrum
FEA	Finite element analysis
FESL	Fatigue equivalent static load
FF	Fatigue factor
FFT	Fast Fourier transform
HAZ	Heat affected zone
IFFT	Inverse fast Fourier transform
IRI	International roughness index
ISO	International Standards Organisation
LHD	Load haul dumper
LTV	Ladle transport vehicle
MAM	Mode acceleration method
MDM	Mode displacement method
PC	Personal computer
PDF	Probability density function
PSD	Power spectral density
RAM	Random access memory
RPA	Remote parameter analysis
RPC	Remote parameter control
SN	Stress – life
SRS	Shock response spectrum
TPA	Two parameter approach
US	United States

1. INTRODUCTION

The engineering discipline of structural mechanics comprises specialist fields such as structural dynamics, strength of materials, finite element methods, fatigue, durability testing and fracture mechanics. In basic terms, each of these subjects is based on mathematical models used to simulate the behaviour of structures in terms of outputs such as deflections, stresses, vibration and various failure mechanisms. All structural mechanics models may be written in the following form:

$$[\text{Deflection, stress, strain, stress intensity, etc.}] = f(\text{Geometry, material properties, loading})$$

The sophistication of these mathematical models range from being based on fundamental principles such as equilibrium and compatibility, to power law curve fitting on regions of empirical data. Sufficiently accurate models are however available for most practical cases.

In a study into the sources of inaccuracies in fracture mechanics calculations, Broek (1985) shows that inherent mathematical modelling inexactness is mostly orders of magnitude less contributing than erroneous input data. Svensson (1997), states that variations caused by, for instance, different wind loads, roads or drivers, can be of considerable importance for the prediction uncertainty of fatigue calculations. Dressler and Kottgen (1999) state that in industries that cannot closely control the usage of their products by their customers, such as the ground vehicle industries, loading and its variation due to different customer usage profiles is the most important variable in fatigue – more important than the usual scatter of material properties. Socie and Pompetzki (2004) state that it is much more difficult to assess the variability in service loading than in the material properties. Similar comments are made by Rhaman (1997), concerning finite element calculations. It may therefore be argued that defective structural designs, excluding failures caused by manufacturing defects, are mostly caused by insufficient knowledge of input data.

Of the input data required, geometry is usually well-defined. In some cases, notably with fatigue crack initiation and propagation analysis, the accuracy of material properties presents difficulties. In the vast majority of practical applications, however, the major concern involves the determination of input loading. Quantification of the structural loading associated with earthquakes and wind forces for buildings, wave forces for offshore platforms and ships, aerodynamic forces during aircraft manoeuvres and digging forces for earthmoving equipment, could be cited as examples.

Similarly, loads associated with automotive and transport (trucks, trailers, containers, trains) structures are nontrivial to quantify. Such loads arise from stochastic and ill-defined processes such as driver/operator actions and structure-terrain interaction.

The present study deals with practical methods for the establishment of input loading for automotive and transport structures through measurements and other methods and its application to structural design, finite element analysis and testing, with the purpose of assessing fatigue durability. It is attempted to also formulate a generalised unified methodology, generalising and unifying the new techniques and existing methods into a cohesive methodology.

The fundamental processes involved with the determination of input loading are measurements, surveys, simulation, estimation and calculation from field failures. These processes result in design criteria, code requirements and/or testing requirements. A number of complex case studies are presented to develop and illustrate the concepts. These case studies involve light commercial vehicles, road tankers, industrial vehicles, as well as ISO tank containers.

The structure of the thesis is based on the above logic. In Chapter 2, the case studies are defined. Chapter 3 deals with the current theory and practice of structural analysis and testing, as well as input loading determination. In Chapter 4, measurement, surveying and simulation methods, developed by the author and applied to the case studies, are presented. In Chapter 5 these results are processed to establish design and testing requirements. Chapter 6 serves the dual purpose of presenting a method for derivation of a usage profile based field failure data, as well as substantiation and correlation of the previous results, using field failure data. In Chapter 7, the processes and techniques presented in the study are formalised and final conclusions are drawn in Chapter 8.

The principal objectives and hypotheses of the study may be summarised as follows:

- It is argued that the formalised determination of input loading is not given its deserved prominence in the research of design and testing technology of automotive and transport structures.
- It is assumed that the fatigue failure mechanism is the major cause of failures of automotive and transport structures.
- It is suggested that accurate prediction of field failures is possible, using well established analysis and testing methods, if input loading is scientifically determined.
- It is proposed that the usefulness of input loading determination methods would be greatly enhanced in industry if it results in quasi-static, inertial loading, since thereby it would be design independent and would avoid the need for expensive dynamic analyses.
- While it is supposed that in most cases, uni-axial, road induced, vertical loading, dealt with in a quasi-static, deterministic manner, would be the predominant load case causing fatigue in automotive and transport structures, it is endeavoured to also address multi-axial loads, modal responses, as well as the stochastic nature of input loading.

2. DEFINITION OF CASE STUDIES

2.1 SCOPE

In this chapter the various case studies dealt with during this study, are defined in terms of problem definitions and basic methodologies.

2.2 LIGHT COMMERCIAL VEHICLES

2.2.1 Minibus

The case study is also described by Wannenburg (1993).

2.2.1.1 Problem definition

Durability qualification testing of new motor vehicle models involves the (usually accelerated) simulation of normal operational conditions on test routes, test tracks, or in the structural testing laboratory. In most cases however, the definition of normal operational conditions presents a major challenge. Often this definition is achieved rather unscientifically, based on decades of experience with similar models. Ideally, an optimal durability test requirement should be set such that an optimum balance is achieved between the costs of testing and development, and the cost of having failures occur in service (due to warranty claims, loss of market confidence, etc.). For safety critical components, the cost of testing and development is not a driver, but the imperative of defining operational conditions accurately is as apparent.

For this case study, a scientific methodology is presented, based on a probabilistic approach, which aims to define operational conditions in a statistical manner in terms of fatigue damage. The results thus obtained empower manufacturers to scientifically establish optimal durability requirements.

The development of the methodology that will be presented has been based on a rather unique problematic situation facing manufacturers of 12 - 16 seat minibus vehicles for the Southern African market. In this region, where third-world rural areas and first-world cities are situated close together, minibus vehicles are largely employed as taxis in an extensive transportation industry to transport commuters of the rural areas to and from the cities. This industry is very competitive and speed and number of passengers carried on each trip are survival issues. This often leads to serious overloading of the vehicles, which are then driven at high speeds on overworked secondary tar and dirt roads.

Since these extreme conditions have not been included in the original usage profiles by the developers of the vehicles, it is often necessary to adapt the vehicle designs for this market. Adapted designs require qualification through testing and there was therefore a need to establish optimal durability requirements for these vehicles.

2.2.1.2 Methodology

The process comprised five phases:

- Measurements were performed on typical routes across the country used by taxis. A typical minibus vehicle was instrumented with strain gauges for this purpose. A durability test track was also measured.

- Fatigue calculations were performed on the measured signals to obtain relative damage caused by each category of road.
- The data obtained from a questionnaire survey filled in by taxi operators was used to determine relative damage per kilometre induced on the vehicles by each participant by multiplying the percentages driven on each category road with the damage/km for each category road obtained from the fatigue calculations. Probability density functions were fitted to this data as well as to the data concerning the distance travelled per day by each participant, which could then be used to derive durability requirements in terms of years without failure or distance without failure. Verification of these results was achieved by using the results to obtain a theoretical prediction of the failures that had occurred in practice on a specific chassis crossmember and comparing this to the actual failure data.
- The first step of the verification was to perform laboratory tests on the component, by simulating an appropriate sequence of the durability track in a test rig until failure occurred to determine the relative damage to failure.
- Based on the test results as well as data of sales of vehicle type in question, the theoretical distributions obtained from the measurements, fatigue calculations and questionnaires, were used to predict the failures of the component in practice. These predicted results were then compared to actual failure results. Based on this comparison the theoretical distributions were adjusted to achieve close correspondence between theory and practice.

2.2.2 Pick-up Truck

The pick-up truck case study is also described by Van Rensburg and Wannenburg (1996).

2.2.3 Problem definition

The need was identified to qualify a 1 tonne pick-up truck for South African conditions. It was proposed to perform a road simulator durability test and in parallel perform an exercise to establish the usage profile with respect to structural fatigue inputs for South African road conditions. The purpose of the latter was to be able to establish the severity of testing in terms of customer road usage unique to South African conditions.

It was agreed that the road simulator test would be continued until the equivalent of a set target distance of road usage for a set percentile customer, had been simulated. Failures experienced during this test were then to be evaluated in terms of failure rate predictions that may be experienced by the customer fleet, based on the established statistical usage profile.

This case study report deals with the details and results of the testing and the usage profile establishment, as well as the failure rate prediction.

2.2.3.1 Methodology

The project comprised seven phases:

- Measurements were performed on typical roads across the country used by these vehicles. A vehicle was instrumented with accelerometers and strain gauges for this purpose.
- Measurements were also performed on a vehicle test track with a fully laden and unladen vehicle.

- Fatigue calculations were performed on the measured strain data as well as the test rig response strain data to obtain a relative damage per km per channel for all types of road and test sections.
- The data obtained from a questionnaire completed by pick-up truck owners was used to determine relative damage per kilometre induced on the vehicles by each participant by multiplying the percentages driven on each category road with the damage/km for each category road obtained from the fatigue calculations.
- An accelerated laboratory durability fatigue test was conducted on the vehicle.
- The data contained in the questionnaires was used to determine the usage profile of the vehicles.
- The usage profile distributions were then used to quantify failures experienced on the test rig in terms of usage profile distances.
- Using the established usage profiles, as well as other input data such as sales history, failure rate predictions for critical components that had failed during the test, were performed, using a statistical simulation model. The results of this simulation essentially are to be used for decision making with respect to the structural integrity of the vehicle.

2.3 FUEL TANKER

2.3.1 Problem definition

A new dual purpose, aluminium road tanker was developed (See Figure 2-1). The trailers are designed with flat decks to facilitate the transport of dry load cargo. This enables the operator to transport liquid loads in one direction (e.g. in South Africa from the coastal oil refineries to Gauteng) and general freight on the decks during the return trip. The profitability of the vehicle is greatly improved.

The design presented challenges in terms of the box shaped design of the tanks, requiring significant internal reinforcing, the use of aluminium in combination with the drive towards a lightweight design, implying concerns in terms of fatigue durability, as well as the uniqueness of the application, presenting the problem of determining the loading conditions.

2.3.2 Methodology

The durability assessment comprised the following steps:

- Finite element assisted design according to available design code prescribed loads.
- Building of prototype vehicle.
- Strain gauge measurements on prototype vehicle for typical operational cycles.
- Establishment of design criteria for fatigue loading.
- Redesign and extensive fatigue assessment using finite element and measurement results.

Figure 2-1 Fuel tanker

2.4 ISO TANK CONTAINER

2.4.1 Problem Definition

Tank containers transport bulk products (mostly liquid and often dangerous) by ship, rail and truck. The container structures are subjected to exceptionally harsh dynamical loading conditions such as impact loading in train shunting yards, abusive handling by cranes and forklifts in depot yards, dynamic loading in storms when stacked 8 high in ship holds and fatigue loads induced by rough roads.

Figure 2-2 ISO tank container

Design loads for ISO tank containers are prescribed by codes such as ISO 1496-3:1991(E). Such loads are static and attempt to account for dynamic and fatigue effects through safety factors. Field failures, often resulting from abusive loading events, but sometimes resulting from normal fatigue loading, have been experienced by all manufacturers on designs that have passed the ISO static loading and impact tests. This prompted detailed finite element analyses to solve such problems, which showed up structural weaknesses, mostly in terms of fatigue, which did not show during ISO testing.

The knowledge gained through such exercises was used by manufacturers to design new models. Detailed finite element analysis methods were used during these design efforts, using ISO loads as inputs, as well as measured impact loading, but still without quantitive knowledge of normal fatigue loading.

In order to further reduce possible risks associated with the new designs, consideration was given to perform structural dynamic testing, especially to determine the fatigue durability of the designs. It was however argued that to be able to perform fatigue life estimates through finite element analysis, or through testing, both require prescribed loading magnitudes and number of cycles (performing tests with guessed loads would not be sensible). This argument prompted the project. The purpose of the project was thus to determine from extensive measurements, the characteristics of normal, abnormal and abusive loads on tank containers.

2.4.2 Methodology

- A specialised instrument (datalogger) was developed, which was fitted to a number of tanks that were sent into operation.
- A number of tank containers was instrumented with strain gauges and accelerometers and continuous measurements over long periods of time were accumulated and sent via the internet to a data collection facility.
- Special algorithms were developed and implemented to derive from the data new design and testing criteria for tank containers.
- The results thus obtained were unique in the industry (from the point of view of comprehensiveness) and would facilitate both safer, as well as more optimised (lower tare) designs.

2.5 INDUSTRIAL VEHICLES

2.5.1 Load Haul Dumper

2.5.1.1 Problem definition

Load Haul Dumpers (LHD) (refer to Figure 2-3), are employed in underground mines to load blasted rock at the stope face and transport it to tipping stations, from where the product is transported via conveyors. Such vehicles operate in the harshest of road conditions and this, coupled to high dynamic loads induced during loading and dumping, imply fatigue problems. The need for structural design criteria for such vehicles arises from the production requirement for reliable vehicles with predictable lives.

2.5.1.2 Methodology

- Finite element models of two different LHDs, operating in different mines, were generated, and used to determine suitable positions where strain gauges could be located to measure the input load responses.
- The vehicles were instrumented with strain gauges, and the strains during the typical operational cycles of the vehicles were recorded.
- The results of these measurements were used to calculate static equivalent fatigue loads, which in turn could be introduced into the finite element model to perform fatigue life predictions on the total vehicle structure.
- Due to the fact that significant fatigue failures have been experienced on one of the vehicle types, it was also possible to verify the methodology, by comparing the predicted failures with actual failures.

Figure 2-3 Load Haul Dumper (LHD)

2.5.2 Ladle Transport Vehicle

2.5.2.1 Problem definition

A newly designed Ladle Transport Vehicle (LTV) is to be put into operation in an Aluminium Smelter plant. The vehicle has an articulated arrangement, with the trailer having a U-shaped chassis and lifting bed, which allows the vehicle to reverse into a ladle mounted on a pallet. The filled ladle may then be lifted and locked for transport. In the tilting version of the design, the ladle can be tilted at the off-loading station. The lifting bed is lifted vertically, guided by vertical pillars and when reaching the top, commences tilting (refer to Figure 2-4). The case study presented here deals with the non-tilting version of the design.

The objective of the project was to determine input loads during typical operation, to allow a fatigue durability assessment of the vehicle structures to be performed.

2.5.2.2 Methodology

A finite element model of the LTV structure was generated and used to determine suitable positions where strain gauges could be located to measure the input load responses.

- A vehicle was instrumented with strain gauges and the strains during the typical operational cycles of the vehicles were recorded.
- The results of these measurements were used to calculate static equivalent fatigue loads, which in turn could be introduced into the finite element model to perform fatigue life predictions on the total vehicle structure.
- From the results of the measurements, it was realised that account would also have to be taken of higher order mode shapes.

Figure 2-4 Ladle Transport Vehicle (LTV)

2.6 CLOSURE

The case studies defined in this chapter are each dealt with in detail in the following chapters. The presentation logic emphasises a structured treatment of the techniques developed and employed for the establishment of input loading for vehicular structures, which implies the fragmentation of the case study arrangement in the different chapters. The processes followed for each case study are shown as part of the generalised methodology in diagrams presented in Chapter 7.

3. FUNDAMENTAL THEORY AND METHODOLOGIES

3.1 SCOPE

In this chapter, the fundamental theory underpinning the techniques covered in the present study, as well as methodologies with regard to the determination of input loading, structural fatigue design and testing of vehicular structures, are presented. The chapter firstly deals with the various analysis and testing methods, involved in vehicle structural design and assessment and then discusses the techniques used to determine inputs for these methods.

The various methods and techniques described in this chapter are summarised at the end of the chapter. In particular, the fatigue design methods, as opposed to the testing methods, are contextualised using a diagram. The framework for this diagram is depicted in Figure 3-1. Load inputs are obtained from either measurements, or simulation. These loads are used as inputs for stress analyses, which may be either quasi-static, or dynamic, as well as either in the time domain, or in the frequency domain. The outputs of these analyses are then used in fatigue analyses.

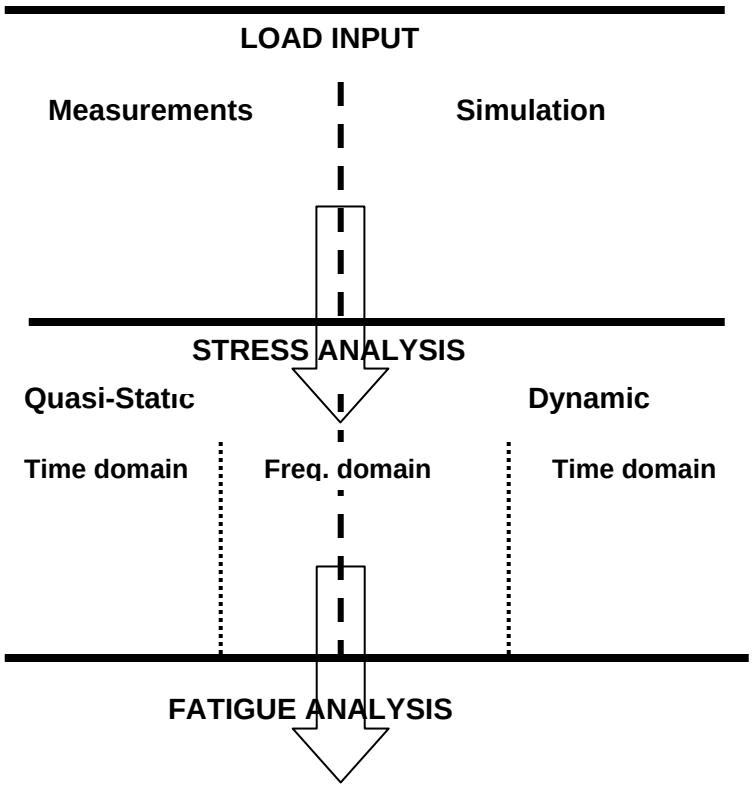

Figure 3-1 Framework for Summary of Fatigue Design Methods

3.2 FINITE ELEMENT ANALYSIS

3.2.1 General

The finite element method has become an indispensable tool for the design of vehicle and transport structures. Computing power and software sophistication have increased dramatically over the past decades, bringing the technology into the economic grasp of most of the transport industry. It is the present author's experience that there are some transport equipment manufacturers, even in Europe and the USA, which still regard the finite element method as 'high-tech' and therefore still rely on hand-calculations. A possible reason for this is that the method is considered to be inaccurate and therefore not worth the additional effort. One of the principal causes of these inaccuracies, albeit not commonly thus understood, may be the undefined input loading.

It would be defendable to state that using the finite element method instead of hand-calculation methods, or sticking to existing designs, is indeed not worth the additional effort unless input loading is well defined. In cases where high volumes imply high risks, and/or the market is very competitive, demanding lighter and more durable structures, such as in the automotive industry, finite element methods and testing have been extensively used and comprehensive efforts are expended in defining input loading.

In the following sub-sections, some aspects of the Finite Element Method are discussed, with specific reference to its capability of calculating variable stresses/strains, resulting from variable input loads, which then may be used to perform fatigue calculations.

3.2.2 Static Load Analysis

3.2.2.1 General

The use of static load finite element analyses in the design process of vehicular structures are commonplace and well documented. In many instances design codes would prescribe static design loads, where fatigue and dynamic considerations are catered for by prescribing large safety factors.

More sophisticated methods are also employed, staying within the economic domain of static analyses, where dynamic stress responses, used for detailed fatigue analysis, are calculated. These methods are called 'quasi-static' and are described in the following subsections.

3.2.2.2 Quasi-static finite element analysis

The basic quasi-static finite element analysis method, described by Bishop and Sherratt (2000) and in the MSC.Fatigue 2003 User's Manual (2002), involves calculating the stress response (σ_{ij}) for all elements (i), or of critical elements (i), caused by applying static unit loads ($L_{j\text{-}unit}$), one at a time, for all loads acting on the structure.

These results are used to establish a quasi-static transfer matrix [K] between element stresses and loads. Known time histories of each load ($L_j(t)$) are then multiplied with the inverse of the transfer matrix, achieving, by the principle of superposition, stress time histories ($\sigma_i(t)$) at each element (i):

$$[K]=[\sigma_{ij}]$$
$$\{\sigma_i(t)\}=[K]^{-1}\{L_j(t)\}$$

Eq. 3-1

The method is depicted on the summary framework in Figure 3-2.

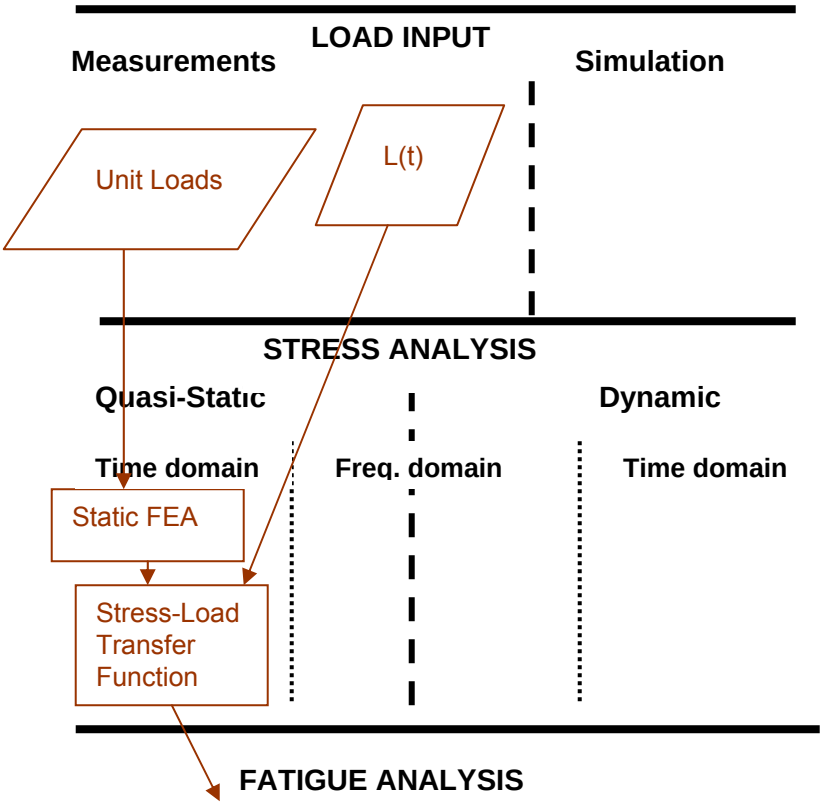

Figure 3-2 Quasi-Static Method

A derivative of this method, employed by Ford Motor Company to perform a durability analysis on a vehicle body-structure in the concept design phase, using the finite element method, is described in Kuo and Kelkar (1995). They state that the absence of detailed design and correct loads at the concept design stage makes upfront fatigue life predictions difficult. A process was developed to overcome these difficulties. The process involves the following:

- Identify relative stress sensitivities by applying unit loads to each body/chassis attachment location, one at a time, using the inertial relief method (the applied load is balanced by an inertial load). A small number of elements are identified which are sensitive to each load (normally in the vicinity of the applied load).

- Identify critical load paths by calculating the fatigue damage at the most critical element for each load, by using the linear relationship between the unit load and the stress at that element to provide a stress history when multiplied with a measured load history. High fatigue damages imply critical load paths. Softening (to reduce loads) or strengthening (to reduce stresses) of the critical load paths can then be applied.
- Identify critical road events by comparing fatigue damages calculated as above for different road events.
- Compute fatigue lives at critical areas by superposition of synchronised time histories for critical load paths and critical road events.

In many instances, inputs for concept design work would however be derived from multi-body simulation (refer to paragraph 3.3), or from measurements performed on previous models.

3.2.3 Dynamic Analysis

3.2.3.1 General

The most direct way of theoretically assessing the integrity of structures for dynamic and fatigue loading, is by dynamic finite element analysis. The objective would be to solve for the stresses as time functions, when the model is subjected to time series of loads. Additional to the difficulty in defining such loads, there are several restrictions with regard to the use of dynamic finite element analyses, especially for fatigue assessment. These are dealt with in this subsection. It is due to these restrictions that quasi-static methods, some dealt with in this chapter and others presented as part of the present study, are required to be able to perform finite element based fatigue analyses in practice.

3.2.3.2 Explicit and implicit codes

There are several finite element techniques employed for dynamic analysis of vehicle structures. Explicit codes assume small displacements, which makes it impossible to include the relatively soft suspension in the same model as the relatively stiff structure. The input forces of the suspension onto the structure therefore need to be defined. Implicit codes are able to circumvent this restriction, as the solution is achieved by iteration, but demands on computing power are extreme for large models. Such codes are therefore normally only used for analysis of dynamic events of short duration, such as crash worthiness analyses.

3.2.3.3 Direct integration method

A further differentiation may be made for explicit codes in terms of the solving method, according to Bathe (1996) and Bishop and Sherratt (2000). One group of methods uses the direct integration method (called ‘dynamic transient analysis’ by Bishop), solving for the displacements after each small time increment by direct integration. A complete analysis is therefore performed at each time step, except for the compilation of the mass, damping and stiffness matrices, which need only be computed once. Again, the computing power demands are high, normally restricting such analyses to simulation durations of minutes, if not seconds.

The usefulness of such short duration analyses for fatigue assessment purposes is then questionable. Only if the short duration input loading is representative of operational

loading, such as may be the case if the loading is stationary random, could such analysis results be useful. The direct integration method is depicted on the summary framework in Figure 3-3. Load inputs to this method may be obtained through measurements or simulation.

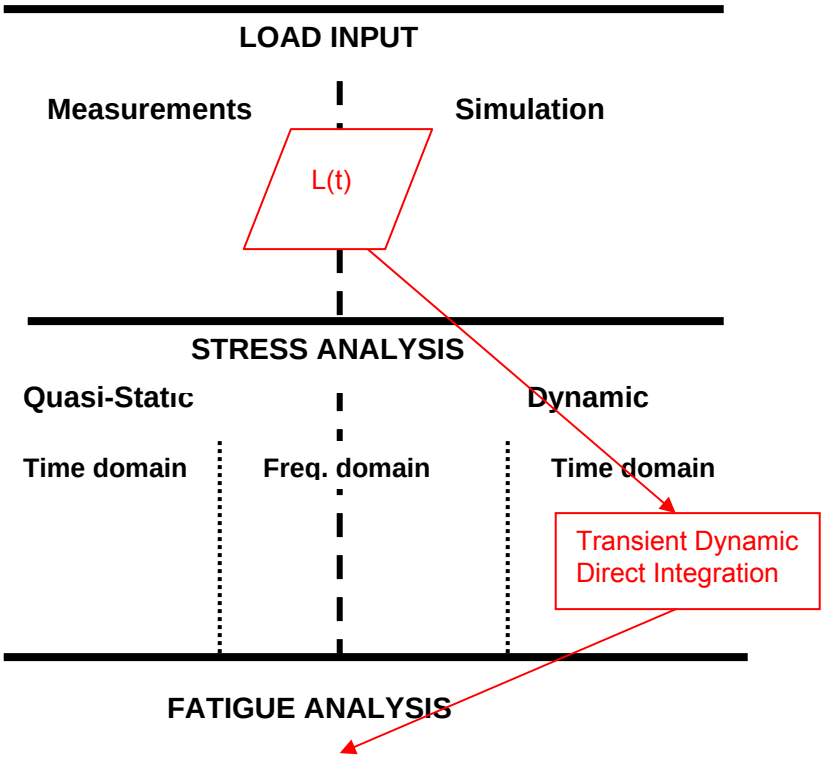

Figure 3-3 Direct Integration Method

3.2.3.4 Modal superposition

A further solving method involves the superposition of forced response mode shapes (the deformed shapes of the structure when vibrating at its natural frequencies), calculated in either the time domain, or the frequency domain, for each eigenvalue solution partially excited by the input loading spectra. The basis of the method is described in various text books, e.g. by Bathe and Wilson (1976). A dynamic system may be described by the following equilibrium equation:

$$[m]\{\ddot{u}\} + [c]\{\dot{u}\} + [k]\{u\} = \{p\}$$

with u = displacement

m = mass

c = damping

k = stiffness

p = excitation loading

Eq. 3-2

In general, the m, c and k matrices would have non-zero coupling terms so that solving the equation in the above form would require simultaneous solution of N equations in N unknowns (N being the number of degrees of freedom of the system).

The first step of the modal superposition method is to obtain the natural frequencies (ω_r) and modes (ϕ_r) of the system, by solving the following equation:

$$([k] - \omega_r^2[m])\{\phi\}_r = \{0\}$$

Eq. 3-3

The modes are then collected to form the modal matrix, $[\Phi] = [\phi_1\ \phi_2\ \phi_3\ \ldots\ldots]$.

The key step is to introduce the coordinate transformation:

$$\{u\} = [\Phi]\{\eta\} = \sum_r \phi_r \eta_r$$

$$\eta_r = \text{principal coordinates}$$

Eq. 3-4

Substituting Eq. 3-4 into Eq. 3-1 and premultiplying with $[\Phi]^T$ gives the equation of motion in principal coordinates, namely:

$$[M]\{\ddot{\eta}\} + [C]\{\dot{\eta}\} + [K]\{\eta\} = \{P\}$$

with $\eta = \text{principal coordinates}$

$$[M] = [\Phi]^T[m][\Phi]$$

$$[C] = [\Phi]^T[c][\Phi]$$

$$[K] = [\Phi]^T[k][\Phi]$$

$$\{P\} = [\Phi]^T\{p\}$$

Due to the orthogonality of the principal coordinate system, the mass and stiffness matrices are diagonal. Therefore, in the case of zero damping, or in the special case where the modal damping matrix is also diagonal, the equations of motion are uncoupled. The total response (η) can then be obtained as a superposition of the response due to initial conditions alone and the response due to the excitation alone.

The economy of the modal superposition method in comparison with the direct integration method is realised if the system response involves only a relatively small subset of the modes of the system.

Two solution methods are discussed, both using mode truncation.

3.2.3.4.1 Mode-Displacement Solution

In this case, the displacement (u) is approximated by:

$$\{u\} = [\Phi]\{\hat{\eta}\} = \sum_{r=1}^{\hat{N}} \phi_r \eta_r$$

$$\eta_r = \text{principal coordinates}$$

$$\hat{N} = \text{number of truncated modes} < N$$

Eq. 3-5

The principal coordinates are then solved from the following uncoupled equations:

$$[M_r]\{\ddot{\eta}_r\} + [K_r]\{\eta_r\} = \{P_r\}$$
$$\text{with } r = 1,2,3,.....\hat{N}$$
$$[M_r] = [\phi_r]^T [m][\phi_r]$$
$$[K_r] = [\omega_r^2][M_r]$$
$$\{P_r\} = [\phi_r]^T \{p\}$$

Eq. 3-6

It is often found that the mode-displacement solution fails to give accurate results. Convergence may be slow and many modes may be required to give accurate results, thereby negating the economy advantage over the direct integration method. Modes of the elements through which the loads are transferred into the structure also need to be included, otherwise the structure is mathematically 'cushioned' from the loads.

3.2.3.4.2 Mode-Acceleration Solution

A method with superior convergence properties is the mode-acceleration method (MAM), described by Rixen (2001). Eq. 3-1 (without damping) is rearranged as follows:

$$[m]\{\ddot{u}\} + [k]\{u\} = \{p\}$$
$$\therefore \{u\} = [k]^{-1}(\{p\} - [m]\{\ddot{u}\})$$

Eq. 3-7

Differentiating Eq. 3-5 twice and substituting into Eq. 3-7:

$$\{u\} = [k]^{-1}\{p\} - [k]^{-1}\sum_{r=1}^{\hat{N}} [m]\phi_r \ddot{\eta}_r$$

but,

$$[k]^{-1}[m] = \left[\frac{1}{\omega_r^2}\right]$$

$$\therefore \{u\} = [k]^{-1}\{p\} - \sum_{r=1}^{\hat{N}} \frac{1}{\omega_r^2}\phi_r \ddot{\eta}_r$$

Eq. 3-8

The first term in the above equation is the pseudo-static response, while the second term superimposes the effects of the truncated number of modes. The superior accuracy of this method compared to the mode-displacement method (MDM), can be attributed to the fact that modes disregarded (normally the higher frequency modes, which are required to construct the rigid body displacements), leading to the inaccuracies of the MDM, are implicitly accounted for by the first term of Eq. 3-8, that represents such rigid body displacements.

Ryu et al. (1997) describe the application of the MAM to compute dynamic stresses on a vehicle structure for fatigue life prediction. Input loads are obtained from Multi Body Dynamic Simulation of the vehicle traversing a ground profile. Input loading may also be obtained through measurements. The modal superposition method may be employed in either the time domain, or the frequency domain.

The modal superposition method is depicted on the summary framework in Figure 3-4.

This method was employed in one of the case studies, when it was found that complex modes were excited.

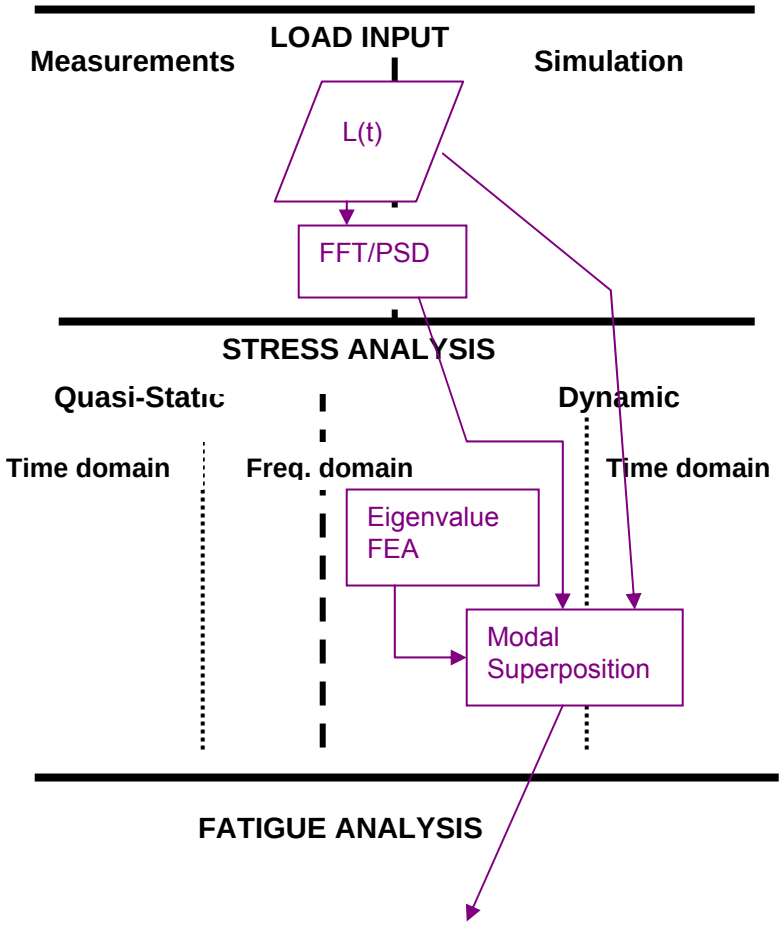

Figure 3-4 Modal Superposition Method

3.2.3.5 Frequency domain analysis

A third method, called 'vibration (fatigue) analysis' by Bishop, involves calculating power spectrum densities of the stresses using input power spectrum densities and cross power spectrum densities, as well as transfer functions computed from the finite element model. This method requires that the input data is stationary random and complicates the fatigue analysis (as described in paragraph 3.4.5), but allows for economic analysis, even for a large number of load sequences. The vibration fatigue method is depicted on the summary framework in Figure 3-5.

3.2.3.6 Static condensation

To reduce the calculation effort required, a smaller model can be obtained via static condensation (Aja (2000)) to include only the carefully chosen degrees of freedom required to fully describe the important mode shapes. Back-substitution is then performed after modal superposition to obtain stress and deformation results as functions of time or frequency.

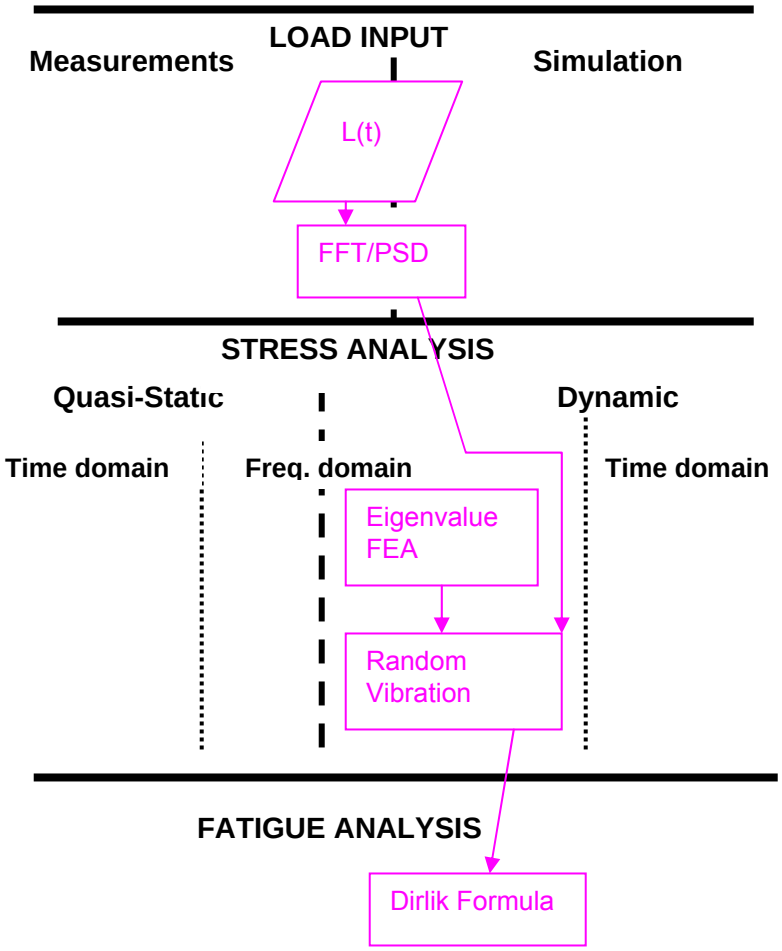

Figure 3-5 Random Vibration Method

3.2.3.7 Inputs to dynamic analysis

In most cases, inputs for dynamic analyses will be obtained from measurements. On vehicles, the quantities that are typically measured, are accelerations, displacements and/or forces.

3.2.3.7.1 Force inputs

Should forces have been measured, direct solving of the equilibrium equation (Eq. 3-2) can be performed, since the unknown displacements are on one side of the equation. The measured forces, represented by the L(t) block in the diagrams in Figure 3-2 to Figure 3-5 before, are used as inputs to the various methods.

3.2.3.7.2 Acceleration inputs

It is normally difficult to directly measure forces introduced through the suspension of a vehicle to the vehicle structure. Accelerations are often measured. Direct solving of Eq. 3-2 is then not possible, since prescribed motion terms are part of the {ü} vector on the left-hand side of the equation. Three methods may be used to circumvent these problems, according to the MSC/NASTRAN User's Guide.

- Large mass-spring method: This method entails adding an element with a large mass or stiffness at the point of known acceleration. Large forces, calculated as the large mass multiplied by the desired accelerations (or stiffness multiplied by known displacements) are applied to obtain the required motion. The method is not exact and may produce various errors if used with inputs required at more than one point.
- Relative displacement method: This method entails input accelerations defined as the inertial motion of a rigid base to which the structure is connected. The structural displacements are then calculated relative to the base motion. The displacement vector {u}, can be defined as the sum of the base motion $\{u_o\}$ and the relative displacement $\{\delta u\}$:

$$\{u\} = \{\delta u\} + [D]\{u_o\}$$

Eq. 3-9

where [D] is the rigid body transformation matrix that includes the effects of coordinate systems, offsets and multiple directions. If the structure is a free body, the base motions should only cause inertial forces:

$$[k][D] = [0]$$
$$[c][D] = [0]$$

Eq. 3-10

Substituting Eq. 3-9 and Eq. 3-10 into Eq. 3-2 yields:

$$[m]\{\delta\ddot{u}\} + [c]\{\delta\dot{u}\} + [k]\{\delta u\} = \{P\} - [m][D]\{\ddot{u}_0\}$$

Eq. 3-11

For a vehicle structure, six accelerations may be measured to define the base motion. These may typically be three vertical accelerations (measured on the structures at the two front and one rear suspension mounting points), one longitudinal (it is normally assumed that any rigid position on the vehicle structure would be sufficient to establish the braking and pulling away accelerations), as well as two lateral accelerations, measured on one front and one rear suspension mounting positions.

The vehicle structure would then be fixed to the base at the positions and in the directions of the measured accelerations. The one missing vertical input must then be measured as a force and introduced as a force on one free suspension mounting point. Lateral forces only occur during cornering and it may be assumed that the largest component of such forces would be carried on the inside wheel. Otherwise, two lateral force inputs need to be measured. It is mostly assumed that left and right longitudinal inputs are equal and for pulling away, only the driven wheels are attached to the base, whereas for braking, all four wheel positions may be attached, or only two, with an assumption as to the percentage braking force between front and rear, corrected for by introducing forces at the unattached wheel positions, calculated as the percentage multiplied by the measured longitudinal acceleration, multiplied by the suspended mass of the vehicle. The benefits of this seemingly cumbersome method is a significant saving with regard to the measurement exercise, as well as the avoidance of rigid body modes, which may occur with the other methods due to slight measurement errors.

- Lagrange multiplier technique: This technique requires adding additional degrees of freedom to the matrix solution that are used as force variables for the constraint functions. Coefficients are added to the matrices for the equations that couple the constrained displacement variables to the points at which enforced

motion is applied. The technique produces indefinite system matrices (zero, or relatively small diagonal values) that require special resequencing of variables for numerical stability.

These methods are depicted in Figure 3-6.

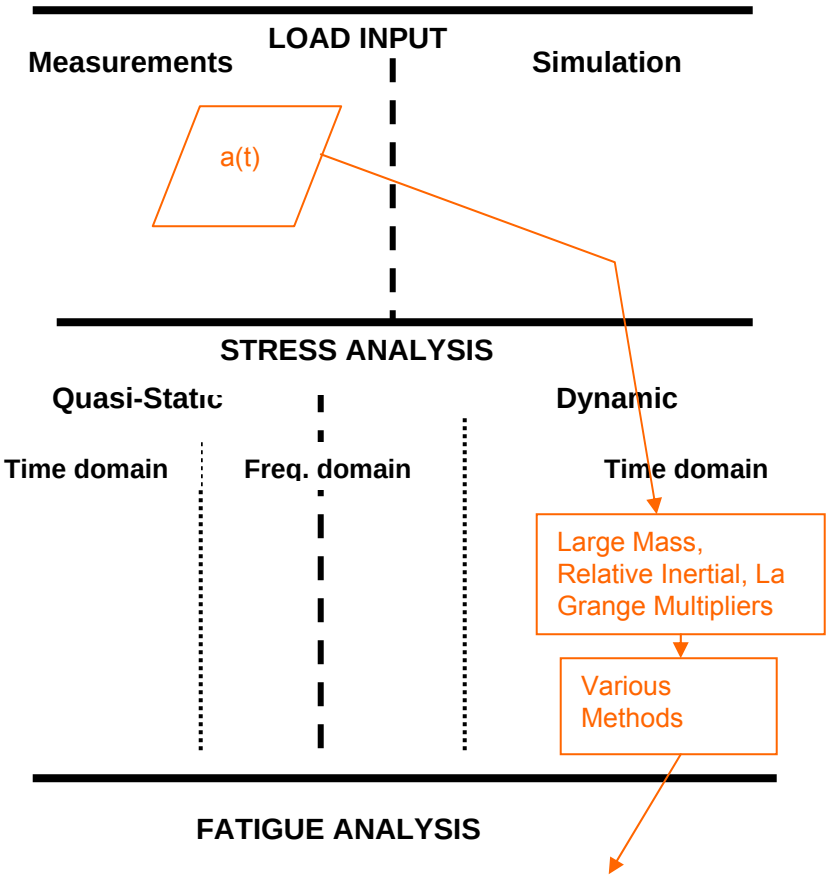

Figure 3-6 Large Mass, Relative Inertial, La Grange Multipliers Methods

3.2.3.8 Covariance method

A method is described by Dietz et al. (1998), making use of a dynamic simulation model of a train to establish the dynamic loads onto a bogey, after which quasi-static, as well as condensed dynamic finite element analyses, are performed to obtain stress histories for subsequent fatigue analysis.

The distinction is made between linear operational conditions and non-linear events. Linear conditions are assumed when driving straight over a track, where the inputs are small and caused by track irregularities (input into the simulation as spectral densities and output into the dynamic finite element process as a load covariance matrix, [P(y)], i.e. in the statistical/frequency domain).

Non-linear events, such as driving through a ramp or over a crossing, are dealt with in the simulation by direct integration in the time domain, producing time histories of input forces to the finite element process.

Due to the large finite element model, it is said to be impracticable to perform dynamic finite element analyses, using the force histories for the non-linear events as inputs. Maximum load time steps are rather identified and quasi-static analyses are performed to calculate the resulting stresses.

For the linear conditions, the covariance matrices of the input forces are used in a condensed dynamic finite element analysis process in the statistical/frequency domain.

A stress load matrix [B] is calculated for only the critical areas of concern, with,

$$[\sigma_c(t)] = [B]\,[L(t)] \qquad \textbf{Eq. 3-12}$$

where $[\sigma_c(t)]$ are the stress tensors at the critical locations, [L(t)] are the various input loads (forces and accelerations as a function of time) and [B] contains the stress tensor results from static unit load analyses for each input load, as well as the eigenmode stresses obtained from dynamic finite element analysis. Eq. 3-12 is equivalent to Eq. 3-1 with $[B] = [K]^{-1}$.

The time independent stress load matrix allows transformation of the load covariance matrix into a stress covariance matrix:

$$[P(\sigma)] = [B]\,[P(y)]\,[B]^T \qquad \textbf{Eq. 3-13}$$

Although the resulting stress covariance matrix only contains information about the amplitude distribution of stresses, the number of cycles can be derived by assuming a probability density function for a stationary random process, thereby allowing fatigue analyses to be performed at the critical positions.

This method is therefore a quasi-static method in the frequency domain.

This method is depicted in Figure 3-7.

3.2.4 Sources of inaccuracies

Bathe (1996) and Rhaman (1997) discuss sources of inaccuracies when performing finite element analyses. Appart from inaccuracies occurring due to inaccurate input loads, the following are important:

- Discrepancies between model and real structure
- Boundary conditions
- Simplifying assumptions
- Element type
- Mesh refinement
- Material properties

Any of these, or a combination, could render finite element analysis results unusable.

3.2.5 Summary

As is clear from the above discussion, dynamic finite element analysis of vehicle structures, is a non-trivial problem. Several choices exist as to which method to apply,

mostly dependent on the type of input data available. Generally, it is not practical to perform dynamic analyses to obtain fatigue stresses, unless stationary random data is assumed, and/or the model is condensed. Measurements performed to obtain input data for these analyses, require careful planning. Due to economy considerations, as well as the fact that dynamic analysis requirements would mostly be too complex for inclusion in design codes and standards, quasi-static methods are mostly employed, therefore the emphasis of the present study.

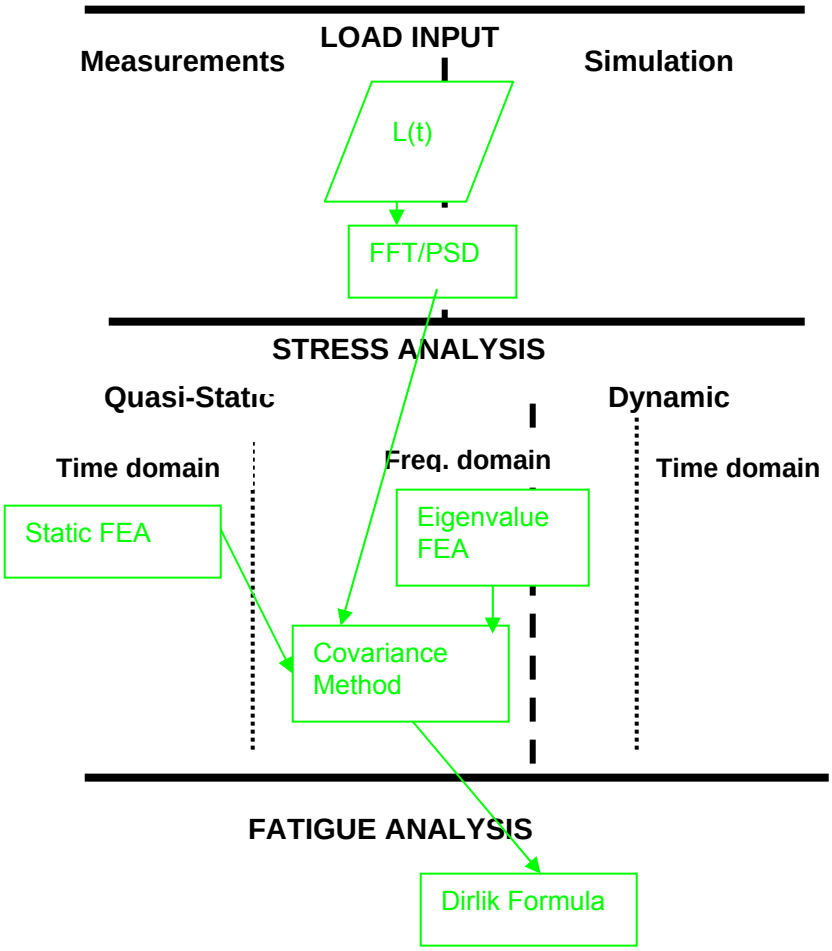

Figure 3-7 Covariance Method

3.3 MULTI-BODY DYNAMIC SIMULATION

An important technique to establish dynamic input loading for vehicle structures when measurements are not possible, is multi-body dynamic simulation. A dynamic (mass-spring-damper) model of the vehicle system is constructed. The traversing of the vehicle over terrain with known statistical or geometric profiles (such as digitised proving ground section profiles) is then simulated to solve for the dynamic input loading. These loads may then be applied to finite element models.

Examples of this process are reported on by Dietz et al. (1998) (dealt with in the previous subsection) and by Oyan (1998), where the fatigue life prediction for a railway bogie and a passenger train structure is performed using dynamic simulation.

For trackless vehicles, one of the fundamental difficulties for accurate dynamic simulation of input loads, is related to the complexity of modelling of the tyres. Analytical tyre models are described by Captain et al (1979) and tyre modelling by finite element methods is discussed by Faria et al. (1992). Mousseau states in SAE Fatigue Design Handbook (1997), that simplified tyre models may lead to significant errors in terms of simulating durability loading.

For the durability assessment of a complete body structure of a vehicle using finite element methods, dynamic simulation is often employed to solve for the high number of loads acting on body attachment locations, due to the practical difficulties in measuring these loads, as discussed by Gopalakrishnan and Agrawal (1993). Measured wheel loads, using a specialized loadcell, are introduced to a dynamic model, which then solves for the attachment point loads.

The same process may be followed, using measured wheel accelerations, as described by Conle and Chu (1991). Difficulties are however usually encountered with the double integration of the acceleration signals to obtain displacements. Table 3-1 summarises the different types of dynamic simulation applications.

Table 3-1 Types of Dynamic Simulation Applications

	MULTI-BODY DYNAMIC SIMULATION		
	Type 1	**Type 2**	**Type 3**
Purpose	To obtain FEA load inputs without the availability of measurements	To obtain FEA load inputs on suspension hard points	To obtain FEA load inputs on suspension hard points
Input	Digitised road profiles	Measured spindle loads	Measured wheel accelerations
Difficulty	Require complex tire model	Require specialised loadcell	Double integration of measured accelerations present problems

The multi-body dynamic simulation process is depicted in Figure 3-8.

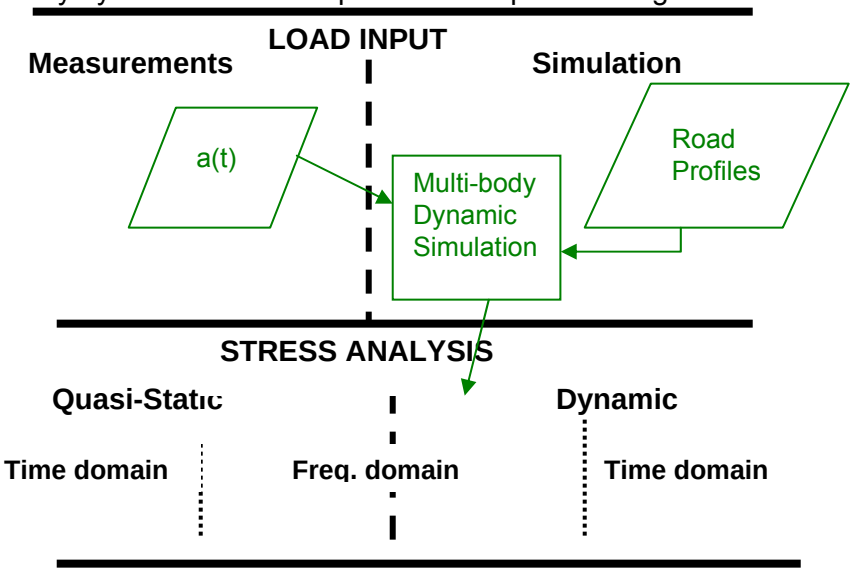

Figure 3-8 Multi-body Dynamic Simulation Method

3.4 DURABILITY ASSESSMENT

3.4.1 General

According to Dressler and Kottgen (1999), six different fatigue durability assessment methods, adapted to different development stages, are currently used in the vehicle industry:

- Test drives on public roads.
- Drives on test tracks.
- Laboratory testing with edited time histories.
- Laboratory testing with synthetic service loading.
- Numerical analysis based on the nominal stress approach (stress-life).
- Numerical analysis based on the strain-life approach.

3.4.2 Fatigue Analysis

3.4.2.1 Stress-life approach

The stress-life approach is described by Bannantine et al. (1990). The approach is based on the experimentally established material fatigue response curve (the SN curve, or Wöhler curve – see Figure 3-9), which plots number of cycles (N) or reversals (2N) to failure (mostly defined as the initiation of an observable crack) vs nominal stress range ($\Delta\sigma$) or amplitude (σ_a).

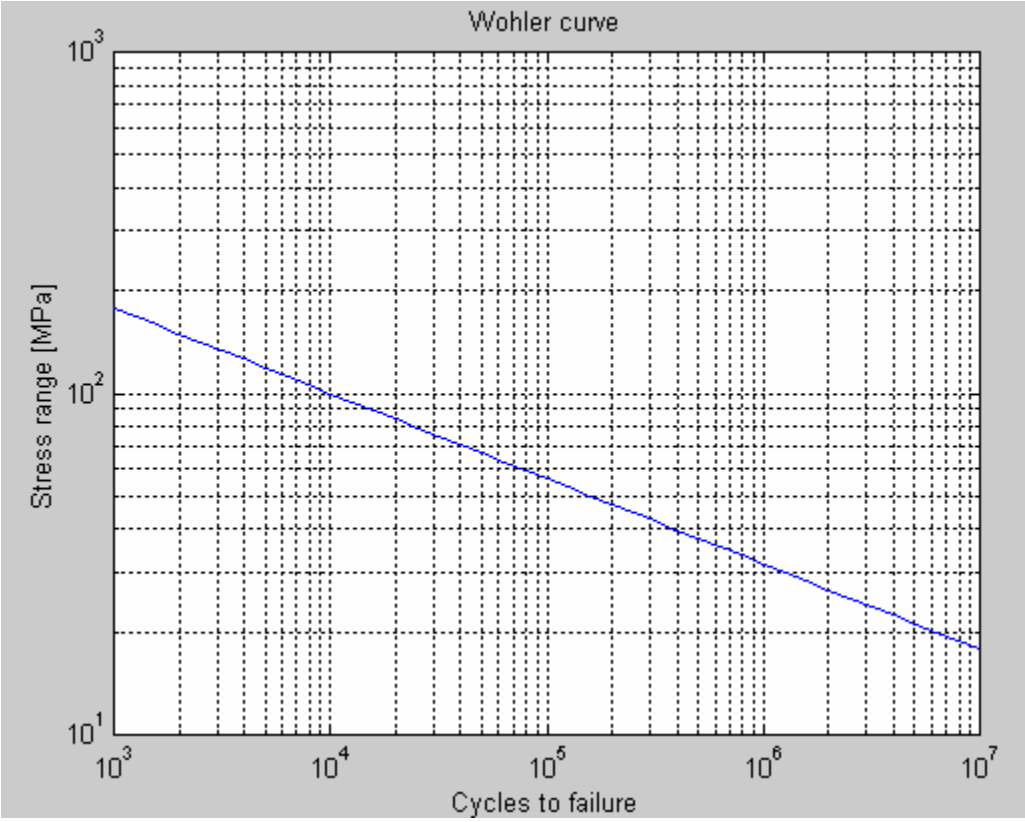

Figure 3-9 Typical SN (or Wöhler) curve

On a log-log plot, an approximate straight line is observed, resulting in a power-law relationship:

$$\Delta\sigma = S_f N^b$$
$$S_f = \text{fatigue coefficient}$$
$$b = \text{fatigue exponent}$$

Eq. 3-14

3.4.2.2 Strain-life approach

The strain-life or local strain approach is essentially an extension of the stress-life approach into the elastic-plastic regime. The theory is described by Bannantine et al. (1990). The strain life equation describes the local strain range ($\Delta\varepsilon$) as a function of four material parameters, as well as the number of cycles to failure (N):

$$\frac{\Delta\varepsilon}{2} = \frac{S_f}{E}(2N)^b + \varepsilon_f(2N)^c$$
$$\text{with}: S_f = \text{Fatigue strength coefficient}$$
$$\varepsilon_f = \text{Fatigue ductility coefficient}$$
$$b = \text{Fatigue strength exponent}$$
$$c = \text{Fatigue ductility exponent}$$

Eq. 3-15

The local strain range is expressed as a function of the local stress range ($\Delta\sigma_l$) using the cyclic stress-strain relationship:

$$\frac{\Delta\varepsilon}{2} = \frac{\Delta\sigma_l}{2E} + \left(\frac{\Delta\sigma_l}{2K'}\right)^{1/n'}$$
$$\text{with}: n' = \text{Cyclic strain hardening exponent}$$
$$K' = \text{Cyclic strength coefficient}$$
$$E = \text{Elasticity modulus}$$

Eq. 3-16

The stress and strain ranges at a local stress concentration are related to nominal stress range ($\Delta\sigma$) and strain range (Δe) through the Neuber equation (see Neuber (1969)):

$$\sqrt{\Delta\sigma_l \Delta\varepsilon} = K_t\sqrt{\Delta\sigma \Delta e E}$$

Eq. 3-17

with the stress concentration factor = K_t.

The process to calculate fatigue damage is a more complex one, with the point by point calculation of the local stress-strain history by simultaneous numerical solution of the above equations, as described in the SAE Fatigue Design Handbook (1997).

The strain-life approach is considered to be a better model of the fundamental mechanism of fatigue initiation compared to the stress-life approach, since it takes

account of the notch root plasticity, with the cyclic plastic strain being the driving force behind the fatigue mechanism.

For high-cycle fatigue applications, the stress-life and strain-life techniques converge, since the effects of plasticity would be small (i.e. the first term of Equation 3-15 would be dominant and the second negligible). The transition between high-cycle fatigue and low-cycle fatigue is defined by the intersection point of the curves representing these two components, named the transition life. This transition life is found to be material dependent, increasing with decreasing hardness. According to Bannantine et al. (1990), a medium carbon steel in a normalized condition would have a transition life of 90 000 cycles (implying that the plastic term would still significantly contribute for a number of cycles of more than 10^5), whereas the same steel in a quenched condition would have a transition life of 15 cycles (implying that the plastic term would not be significant).

It may be argued that, in the case of vehicle structures, where the number of cycles to failure would typically be millions (for example, the rigid body natural frequency of the body on its suspension may be typically 2 Hz, implying that a million cycles would occur in 140 hours), stress life methods should often suffice. The loading are however of a stochastic nature and therefore, the number of cycles are not so simply defined. The major contributors to damage accumulated on a specific component, may be large, impact driven stress response, induced during events that occur infrequently.

3.4.2.3 Fracture mechanics approach

The fatigue mechanism is normally described as consisting of two phases, namely the crack initiation phase, as well as the crack propagation phase. This is however an engineering distinction, rather than a physical distinction, due to the difficulty of measuring very small cracks. The stress- and strain-life approaches dealt with above, are usually employed to predict the number of cycles to either separation failure (initiation plus propagation), or initiation of a visible (measurable) crack, depending on the definition of the life to failure.

The propagation of a crack is governed by the Paris equation (Broek (1985)):

$$\frac{da}{dN} = C\Delta K^m$$
$$\text{with : } C, m = \text{material properties}$$
$$\frac{da}{dN} = \text{crack growth per cycle}$$
$$\Delta K = \text{stress intensity range}$$

Eq. 3-18

The fracture mechanics approach finds very few applications in vehicle structural analysis, even though for welded components the life to failure is dominated by the propagation phase, due to pre-existing defects. The fatigue analysis of welded components, however is performed using an approach similar to the stress-life approach, as explained in the next section.

3.4.2.4 Fatigue of welded components

The fatigue analysis of welded components, very important in vehicular structures, is based on original work done by Gurney (1976). SN-curves, equivalent to the material

properties used in the stress-life method, are derived from extensive tests performed on different weld joint specimens.

3.4.2.4.1 Reference stress

For most joint classifications, the reference stress used in the SN-curve is the nominal principal stress in the direction indicated by the joint classification detail, at the weld toe and uninfluenced by the weld geometry itself. It is therefore a stress that does not exist in reality. The weld geometry formed part of the component test and its effect is therefore accounted for in the SN-curve. Stress concentrations other than due to the weld geometry need to be additionally accounted for. The proper use of strain gauge measured stresses or finite element results require careful consideration. A strain gauge placed at the weld toe would include weld geometry effects and would therefore yield conservative results. Stresses measured too remotely may exclude bending stress or stress concentration gradients and therefore need to be extrapolated to the weld toe. The same principle applies to stresses calculated with finite element methods. Shell element models do not include the geometry of the weld itself, but for T-joints, will exhibit high stress concentration at the perfectly square and sharp joint, also depending heavily on how fine the mesh is.

Niemi and Marquis (2003) recommend a pragmatic rule, ensuring elements the size of the weld throat next to the joint, where the nominal stress can be taken as the stress in the second element away from the joint.

3.4.2.4.2 Conservativeness

The Gurney paper provides the mean, first standard deviation, as well as second standard deviation curves (the latter curves are mostly used in design codes and implies a probability of failure of 2.3 %). When performing failure predictions to be compared to actual failures, it would be more accurate to use the average curves. The stress range values for a class F2 weld (fillet weld of T-joint across stressed member) at 2 million cycles are as follows:

- Mean = 85 MPa
- First standard deviation = 71 MPa
- Second std = 60 MPa

There is therefore typically a two classifications jump from the 2.3% curve to the average curve.

3.4.2.4.3 SN-curve gradient (fatigue exponent)

In most fatigue design codes (e.g. ECCS (1985), BS 8118 (1991)), the fatigue exponent for all welded joints is generalised to be b = –0.333. It is argued that this generalisation is possible due to the fact that b = –1/m, with m being the exponent of the Paris equation (approximately 3 for many metals), because the fatigue life of a welded joint is governed by propagation of a pre-existing defect.

Integration of Eq. 3-18 yields:

$$N = C\Delta\sigma^{-m}\int_{ai}^{af}\left(\sqrt{\pi a}\right)^{-m}da$$

Eq. 3-19

$$\Delta\sigma \propto N^{-\frac{1}{m}}$$

A value of b = –0.333 is therefore often used when performing relative damage calculations for vehicle structures when weld failures are expected.

3.4.2.4.4 Mean stress

No mean stress effects need to be taken into account, since it is argued that the as-welded specimens would have had residual welding stresses close to yield stress already.

3.4.2.4.5 Design standards

Numerous fatigue design standards or codes are based on the above method. For steel, the European code, ECCS (1985) and for aluminium the British code BS 8118 (1991), are employed in the present study.

3.4.2.4.6 Equivalent constant range stress

The steel code uses the concept of an equivalent constant range stress at an arbitrary number of applied cycles to replace random stress signals after rainflow counting, before estimating fatigue life. This is done on the basis that the equivalent stress range and number of cycles combination should induce the same damage as the random signal. The formula is derived in Section 5.4.2 in a slightly different format and forms the basis of the Fatigue Equivalent Static Load method developed during the present study.

In both codes, the classification of welds are denoted according to their stress range strengths in MPa at 2 million cycles, instead of the symbols A,B,C,.. employed by Gurney. This is the main reason for calculating equivalent constant range values at 2 million cycles.

3.4.2.4.7 Hot-spot stress

Leever (1983) and Stephens et al. (1987) describe methods using the ‘hot-spot’ stress for fatigue calculations. This is of importance when a complex joint which cannot be classified according to the design codes, requires analysis. The hot-spot stress is the maximum principal stress at the weld toe, which may be calculated by finite element analysis with solid elements, which include the weld geometry.

3.4.2.5 Fatigue of spot welds

The fatigue prediction of spot-welds is of importance for vehicle design. Again the essential fatigue mechanism is a crack propagation mechanism, where the initial crack front is in fact the sharp edge formed by the joined plates at the weld boundary. A method similar to the SN approach has been empirically developed (Rupp (1989), Rui et al. (1993)), which makes it possible to use the calculation techniques developed during the present study also for spot-welded structures.

3.4.2.6 Multi-axial fatigue

Chu (1998) states that the need to use multi-axial fatigue methods for non-proportional loading has been recognised by the significant improvement in fatigue life prediction accuracy these analyses yield over the traditional uni-axial method. A methodology is presented, based on the strain-life approach, which includes a three-dimensional cyclic stress-strain model, the critical plane approach, which requires the fatigue analysis to be performed on various potential failure planes before determining the lowest fatigue life, a bi-axial (normal and shear stress) damage criterion, as well as a multi-axial Neuber

equivalencing technique, used to estimate from elastic finite element stress results, the multi-axial stress and strain history of plastically deformed notch areas.

The present study is limited to the use of uni-axial fatigue methods. More accurate determination of input loading (the aim of the present study), may, in many instances, outweigh the inaccuracies caused by neglecting multi-axial effects.

3.4.2.7 Summary of fatigue analysis methods

The various Fatigue Analysis methods described in Paragraph 3.4.2 are depicted on the summary diagram in Figure 3-10. All these methods require an intermediate step, collectively named Cycle Counting, to convert frequency domain, or time domain stress histories to stress ranges and numbers of cycles. Methods of Cycle Counting are discussed in the next paragraph. All the Fatigue Analysis methods also require material property inputs, as depicted in the diagram.

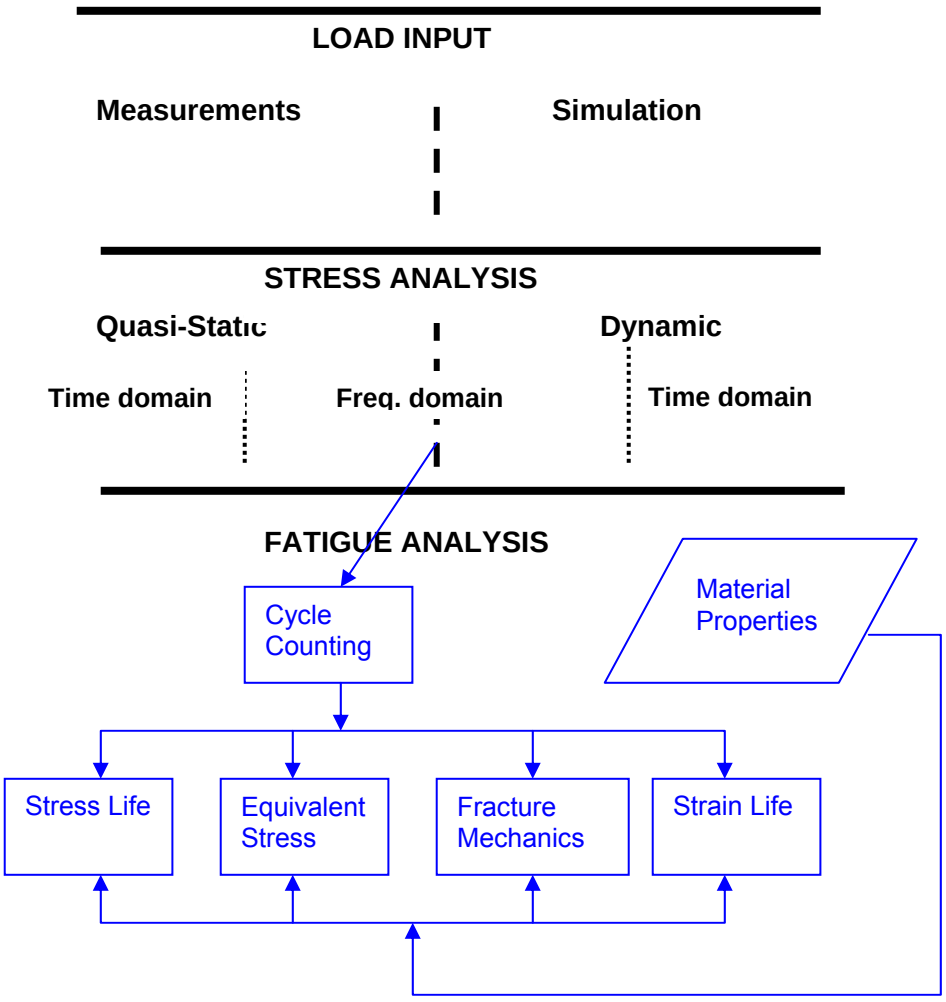

Figure 3-10 Fatigue Analysis Methods

3.4.3 Cycle Counting

3.4.3.1 Rainflow counting

3.4.3.1.1 Hand counting method

The rainflow counting method is described in SAE Fatigue Design Handbook (1997). The original logic of the method was based on the extraction of closed hysteresis loops from the elastic-plastic stress-strain history. The method however logically counts half cycles with different ranges from random stress histories, making it possible to use the stress-life approach and Miner's damage accumulation rule for fatigue life estimation (Miner (1945)).

3.4.3.1.2 Computerised counting method

An algorithm which is more easily computerized, also called the range-pair-range method is described in SAE Fatigue Design Handbook (1997).

In principle, the algorithm searches for a sequential four point pattern shown below, commencing at the first 4 points of the reduced signal (where only peaks and valleys are kept):

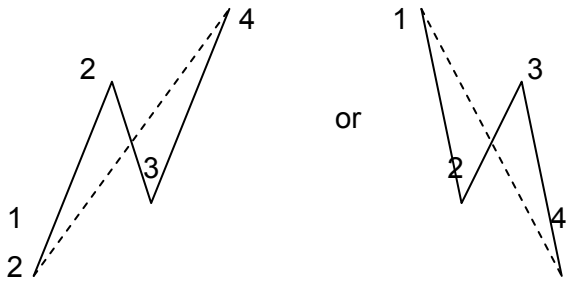

Point 1 must be lower or equal to point 3 and point 4 must be higher or equal to point 2 (and the opposite for the mirror pattern).

When a pattern is found, a half cycle is recorded with a range between the values of points 2 and 3. Points 2 and 3 are then deleted and points 1 and 4 connected, as shown by the dashed lines. The algorithm then steps back by 2 points and continues the search. This process continues until the end of the signal is reached. A list of counted cycle ranges ($\Delta\sigma_i$) results, with i from 1 to the number of half cycles counted.

3.4.3.1.3 Standard counting method

A standardized counting method is prescribed in ASTM E 1049-85 (1989). The method is based on the range-pair-range method, but yields the same results as the rainflow counting method and is usually referred to also as rainflow counting.

3.4.3.1.4 Statistical properties of rainflow counts

The computation of statistical properties of rainflow counts is described by Olagnon (1994).

3.4.3.2 Rainflow reconstruction

Measured data is often only available in the compressed fatigue domain (Rainflow matrix) format. For laboratory testing to be performed it is necessary to reconstruct time domain data from the rainflow data, according to Lund and Donaldson (1992). Specialised techniques are required.

3.4.3.3 Multi-axial, non-proportional loading

Cycle counting methods for multi-axial, non-proportional loading, are summarized by Dressler and Kottgen (1999). The intention is to count cycles such that a multi-axial fatigue calculation (e.g. according to the critical plane approach) may be performed from reconstructed data. A notch simulation approach is used where a pseudo stress time history is used to compute the full elastic-plastic stress and strain tensor histories required to calculate the fatigue damage in different directions. This pseudo stress ($^{e}\sigma$) at a location (s) and time (t) is a superposition of the response from (n) different load components (L_m) acting at time (t) on the structure:

$$^{e}\sigma_{ij}(t,s) = \sum_{m=1}^{n} c_{ij,m}(s).L_m(t) \qquad \textbf{Eq. 3-20}$$

where $c_{ij,m}(s)$ are dimensional proportionality constants similar to stress concentration factors. A number of discrete combinations of these constants are chosen to cover the total range of possible contributions of the different loads to a stress state at any position, which then results in a finite number of rainflow matrices being counted. The stress state at any specific position will then correspond to one of these matrices. Load reconstruction may then be performed, where-after the damage in the most critical direction may be computed using the strain-life approach.

This method also makes it possible to filter non-proportional loading, where only time intervals producing loops smaller than the filter value for all the load projections, are filtered.

3.4.4 Damage Accumulation

The process to calculate fatigue damage caused by random loading is based on the linear damage accumulation approach, proposed by Miner (1945). The total damage (D) caused by a combination of cycles of different ranges is calculated as the linear sum of the fraction of the applied number of cycles at that range (n_i) divided by the number of cycles to failure at that range (N_i). Failure is expected if the total damage reaches unity.

$$D = \sum \frac{n_i}{N_i} \qquad \textbf{Eq. 3-21}$$

The process to calculate fatigue damage from random stress histories, is depicted in Figure 3-11 (shown here for the stress-life approach).

3.4.5 Frequency Domain Fatigue Life

Methods for estimating fatigue life from frequency domain data are described by Sherratt (1996). Although the fatigue failure mechanism is essentially dependent on amplitudes and number of occurrences (parameters determined through cycle counting from time domain data), data storage space and communication restrictions often imply the need to find more compact data formats, such as the direct storage of real time cycle counted

results, or the statistical information represented by the frequency domain. In the present study, a case study is presented where both these domains were employed.

Data stored in a Power Spectral Density (PSD) format, represents averaged statistical information concerning the energy contained in the original time domain signal at each frequency. Since the energy will be related to amplitudes and the frequencies to number of cycles, intuitively it should be possible to calculate fatigue damage.

A key step is to predict the distribution of peaks and valleys in the time history. For a time history x, a peak and valley will occur when dx/dt = 0. A peak will occur when d^2x/dt^2 is negative and a valley if it is positive. There are links between x, dx/dt, d^2x/dt^2 and various moments of the PSD around the frequency axis. The n^{th} spectral moment is defined as:

$$m_n = \int_0^\infty f^n G(f) df$$

Eq. 3-22

where G(f) is the value of the PSD as a function of frequency (f).

According to statistical theory, the variance of x = m_0 (the area of the PSD, or energy), the variance of dx/dt = m_1 and the variance of d^2x/dt^2 = m_2 . It is normally assumed that x follows a Gaussian distribution.

It is then possible to derive values for number of cycles vs range as follows:

- Estimate the number of times a given boundary at a value α will be crossed in one second with x increasing.
- Apply this at α = 0 to estimate the number of positive-going zero crossings in one second.
- Estimate the number of positive-going zero crossings of dx/dt in one second. This will be the number of valleys per second and be equal to the number of peaks.
- Use the level-crossing information from the first step to estimate the number of peaks at each level.

The ratio of positive–going zero crossings per second N_0 (step 2 above), to the number of peaks per second N_p (irregularity factor γ = N_0/N_p), is a measure of how irregular the time history is. If it is near unity, the record passes through zero after almost every peak and cycles may be formed by pairing every peak with every valley at the same level below (the peak values are therefore an indication of amplitude). This will be the case if the PSD is narrow-band.

In the wide-band case, the assumption which links peaks and valleys at similar levels above and below zero, gives a conservative estimate of damage. This may be understood if it is compared with the rainflow algorithm, which links peaks with valleys closer to it's own level.

An alternative way to calculate damage from PSD data would be to produce time data from it which can be cycle counted directly, using the inverse FFT method (IFFT). For this, phase information needs to be created (not kept by the PSD calculation), by creating a random phase record. The effect of this method is to reduce the conservative damage result for wide-band data by some 20%.

Sherratt (1996) describes the Dirlik formula (refer to Eq. 3-24) which estimates the probability density function (PDF) of rainflow ranges as a function of moments of the PSD. This formula is empirically derived from the results of IFFTs of a number of PSDs with random phases. This formula allows closed form estimation of fatigue damage from PSD data.

It is lastly important to note that a fundamental assumption made when using frequency domain data is that the time data is stationary, meaning that PSDs taken on any partial duration of the data would be similar. This would be true for data obtained from a vehicle travelling on a road of constant roughness, but will certainly exclude transient events, such as hitting a curb.

$$P_{RR}(S) = \frac{(D_1 e^{-Z/Q})/Q + (D_2 Z e^{-(Z/R)^2/2})R^2 + D_3 Z e^{-Z^2/2}}{2(m_0)^{1/2}}$$

with :

$P_{RR}(S) =$ PDF of rainflow ranges of S

$$\gamma = \frac{m_2}{(m_0 m_4)^{1/2}}$$

$$x_m = \frac{m_1 m_2^{1/2}}{m_0 m_4^{1/2}}$$

$$D_1 = \frac{2(x_m - \gamma^2)}{x_m + \gamma^2}$$

$$D_2 = \frac{1 - \gamma - D + D_1^2}{1 - R}$$

$$D_3 = 1 - D_1 - D_2$$

$$Q = 1.25\frac{\gamma - D_3 - D_2 R}{D_1}$$

$$R = \frac{\gamma - x_m - D_1^2}{1 - \gamma - D_1 - D_1^2}$$

$$S = 2m_0^{1/2} Z$$

Eq. 3-23

3.4.5.1 Errors induced by signal processing and cycle counting

Errors induced by signal processing and cycle counting are discussed in the SAE Fatigue Design Handbook (1997) and by Broek (1985). The planning the measurement configuration requires carefull consideration of the following aspects:

- Transducer sensitivity, accuracy and range
  It is good practice to perform trial measurements to confirm that, e.g. no overloading would occur, before commencing with actual measurements.
- Sample frequency, aliasing and filtering
  From a frequency domain point of view, the sample frequency should be at least twice the highest frequency of concern contained in the signal. From a time domain point of view, peak definition would be inadequate should the sample

rate be chosen on this basis and sample rates at 5 – 10 times the relevant input frequencies are required. Small errors in defining peak values are amplified when performing fatigue life prediction, due to the fatigue exponent effect.

- Noise protection
- Capacity, resolution and gains
- Strain gauge temperature compensation

Load sequencing is known to have a significant effect on fatigue crack propagation, due to an effect known as crack retardation. Fracture mechanics models exist to take account of this effect, but it is mostly ignored when performing stress-life or strain-life predictions.

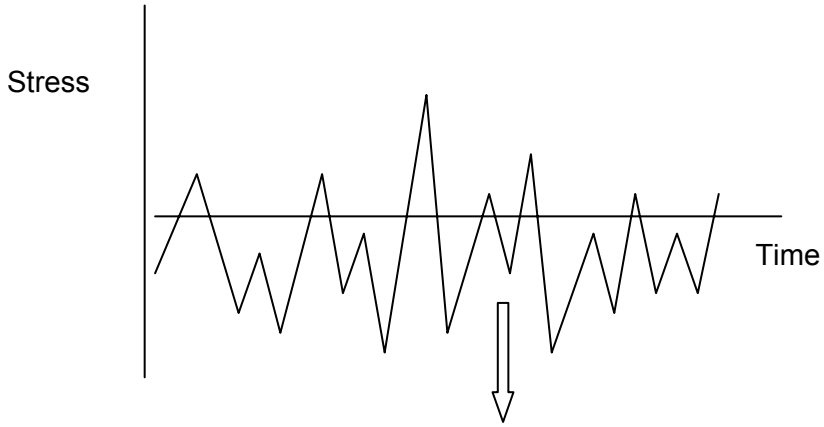

Rainflow cycle counting

$\Delta\sigma_i$	Cycles (n_i)
200	5
180	24
--	--

$$N_i = \left(\frac{\Delta \sigma_i}{S_f} \right)^{1/b}$$

$$Damage = \sum \frac{n_i}{N_i}$$

Figure 3-11 Fatigue damage calculation process

3.4.5.2 Summary of cycle counting methods

The two Cycle Counting methods are depicted on the summary diagram in Figure 3-12. Rainflow counting is performed using time domain data and the Dirlik method is used with frequency domain data.

3.4.6 Durability Testing

3.4.6.1 Test development and correlation

3.4.6.1.1 General

Generally, durability qualification testing of engineering systems should conform to two basic requirements for validity, namely, the accurate simulation of possible service failures and failure modes, as well as a known relation between test duration and actual service life. Testing with the purpose to infer reliability data has the additional requirement of having to be able to relate the test results to expected service lifetimes within statistical confidence intervals.

The first requirement implies that simulation of the mission profile in terms of loading conditions, environmental conditions etc. should be sufficiently comprehensive so as to include all possible causes of failure. It also implies that, should the test be accelerated, the failure modes that may occur in service would still be induced during the test.

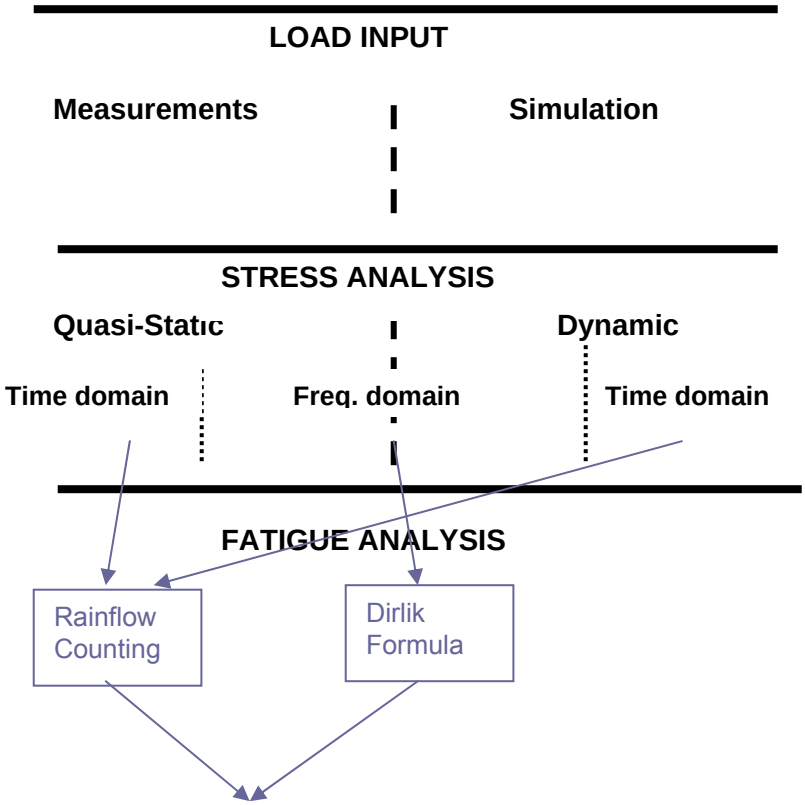

Figure 3-12 Cycle Counting Methods

The second requirement implies the obvious condition in that it is imperative to know the factor by which a test is accelerated, should accelerated testing be performed. The added complication is that the acceleration factor must be known for all possible modes of failure (an accelerated test in terms of vibration loads would for example achieve different acceleration factors for mechanical components than for electronic components).

The third requirement implies that it is necessary to employ a statistical approach to be able to take account of statistical variables which could influence the performance of the system. This becomes necessary since it is obviously only possible to perform durability tests on a sample population.

The development of a testing methodology that would conform to the above validity requirements is logically set out in Table 3-2. Different levels of testing are logically developed. The lowest level test involves the idealized case where the total population of fully assembled systems are tested for the total lifetime, being subjected to all loading conditions experienced during service.

In order to develop a practical test (on a higher level of sophistication), certain technical aspects need to be addressed, as listed in the last row of the table. The optimal level of testing may be derived by balancing the cost of testing (a low level test implies a high cost due to large samples, long durations and comprehensive simulation of loading conditions) and the cost of developing a higher level of testing (the expertise required to address the technical aspects is costly).

For each higher level of testing all technical considerations listed at the lower levels need to be addressed.

Table 3-2 Levels of durability testing

Level	**0**	**1**	**2**	**3**	**4**
Assembly level	Complete system	Complete system	Complete system	Complete system	Component level
Acceleration	None	None	None	Accelerate	Accelerate
Sampling	Total population	Large sample	Limited sample	Limited sample	Limited sample
Comprehensiveness of loading	Comprehensive	Comprehensive	Reduced Inputs	Reduced inputs	Reduced inputs
Application method	Actual service	Simulate	Simulate	Simulate	Simulate/ single amplitude
Technical considerations	None	What to simulate? How to simulate? Statistics	Insignificant inputs? Statistics of limited samples	Acceleration factors?	Interaction effects?

The technical considerations listed in the above table are individually dealt with in the following paragraphs:

- Mission profile
  In order to design a lifetime test it is imperative to detail the mission profile of the system in terms of all loading conditions. These include consideration of operational modes, operational life, external inputs, environmental conditions, operator influence and others. No valid test method could be developed without establishing the mission profile.

- Simulation methods
  Methods to simulate all loading conditions must be designed. Lower level testing involves true laboratory simulation of actual loading conditions. Simulation of vibration inputs typically requires that acceleration measurements be performed on an actual system in service, which could then be reconstructed in the laboratory.

  For higher level testing, simulation of actual (random) loading conditions may be replaced with idealized simulation such as block loading or single amplitude loading. In this case it is necessary to determine the damage content of the idealized loading in terms of the actual loading conditions. It is therefore required to develop failure models for all possible failure modes.

- Insignificant inputs
  Simulation of all loading conditions could be severely restrictive in terms of economic viability. It is therefore necessary to identify insignificant loading conditions. This will require that all possible failure modes be identified and that failure models of all modes should be established. These failure models would involve mathematical expressions of life to failure in terms of loading parameters.

- Acceleration
  Required operational life would typically imply impractical testing durations. It is therefore necessary to accelerate the test. Acceleration is achieved by testing under more severe conditions to what would be expected in service, i.e. test with higher loads. In order for the test to be valid, it is necessary to establish the factor with which the test is accelerated. Typically, a power law (for fatigue failure) or inverse power law (for bearing failure) failure model is assumed. With knowledge of the failure model constants, it is then possible to relate the expected service life under normal loading to the test life under increased loading.

  It is therefore imperative to derive failure models for all possible failure modes in order to be able to accelerate the reliability testing. Acceleration of all failure modes would not be achieved equally by increasing certain loads. It is therefore possible that failure modes being dominant under actual service loading would not be dominant under increased loading conditions. The only way by which to address this problem would be to model all failure modes.

  Accelerated testing on component level would be considerably easier than full system testing since each component could be tested with different acceleration factors. It may not be possible to achieve uniform accelerated complete system testing. It may therefore be optimal to perform component level accelerated testing in conjunction with complete system testing (partially accelerated).

- Statistics
  Well established statistical methods exist to derive reliability data from test results. Classical statistics require a large number of specimens to be tested to enable practical confidence levels to be achieved. The next section deals with the viability of inferring practical reliability data from small sample testing. A more fundamental problem is however the fact that reliability data for the product must be inferred from testing only a sample of the total population, be it a large or a small sample, whilst it is, due to the complexity of the system, difficult to prove that all influences on the system have been taken into account in the reliability formulation.

- Statistics of limited sample testing
  It is possible to infer reliability data from limited sample testing using Bayesian Inference. The principle behind this method is that if prior knowledge of the expected distribution is obtained, fewer specimens are required to achieve practical confidence levels. It is therefore again necessary to establish failure models for all failure modes.

- Interaction
  When component testing is performed it will be necessary to determine loading conditions for each component. Therefore it is required to analyse the interaction between the different components of the system.

Comments from the literature concerning the above aspects are discussed in detail in the following sections.

3.4.6.1.2 Process

The purpose of durability testing is to determine the life to failure of the structure in terms of some measure of customer usage. According to Leese and Mullin (1991), many companies have spent decades relating (correlating) their proving grounds with typical customer service usage. This process is one of the main themes of the present study. If it is assumed that this work has already been done, the purpose of correlation is to ensure that any test method used, represents the same severity of testing than would the defined proving ground test sequence. This is mostly done in terms of fatigue damage. Leese and Mullin (1991) describe the process of performing fatigue calculations to correlate proving ground to proving ground, proving ground to laboratory test and test to test.

3.4.6.1.3 Acceleration factor

Two important concepts need further discussion. The obvious intention of laboratory testing is to accelerate the test in comparison with the proving ground test. This is already achieved through the fact the test rig could run for 24 hours per day. Additionally, however, the non-damaging sections of the proving ground test sequence may be edited out of the laboratory test sequence. These will obviously include sections which are unavoidable on a physical track such as turn-around spaces.

Proving grounds are usually already accelerated in relation to average customer usage (typically by a severity ratio of 5 – 10). It is normally possible to achieve a further compounding severity ratio in the laboratory of 2 – 5. Mathematically it is possible to accelerate testing almost by an unlimited factor by increasing the amplitudes of the stresses. This is sometimes done by multiplying the measured signals with a factor larger than one and then to apply drive signals to achieve this on the rig. This practice is

however not desirable, since it may imply a different failure mechanism to come into play, such as low cycle fatigue. Barton (1991) describes a method to minimize the maximum test stress whilst achieving the desired acceleration factor.

3.4.6.1.4 Equalised acceleration

Secondly, the requirement to achieve equal acceleration of all reference channels, may be commented on. If unequal acceleration is applied, it would mean that some parts of the structure would be tested faster than others. An example of this may be when a channel on a suspension component sensitive to braking wheel forces is less accelerated to a channel sensitive to vertical wheel forces on a four poster test rig, due to the fact that braking forces are not simulated on the rig. It is then obvious that such a test would not prove the integrity of the former component.

A further example may be a channel on a chassis crossmember sensitive to twisting of the chassis, compared to a bending gauge on the chassis beam, sensitive to vertical bending. In such a case, it will be possible, for instance, to include a correct mix of out-of-phase and in-phase sections in the final sequence. An algorithm to derive the optimal sequence in terms of equal and maximized acceleration was developed during a post-graduate study, supervised by the present author and is reported on by Niemand (1996). This process is also followed when designing a sequence on the proving ground to simulate customer usage.

The process of establishing an optimal test sequence with equalized acceleration for all channels, presents a very non-linear problem, as recognized by Moon (1997), where the application of neural networks in the development of testing sequences, is described.

3.4.6.1.5 Choice of fatigue exponent

It is important to note that, when using the stress-life approach, only the fatigue exponent (b) would influence relative fatigue calculations, since the fatigue coefficient, as well as other factors, such as stress concentration factors, would divide out. The calculation of a durability test severity ratio (or acceleration factor) would give different results with different b-values. This would be true for any accelerated test (levels 3 or 4), be it using simulated loading, block loading, or single amplitude loading.

It follows that it is of importance to choose the correct value for b when such relative damage calculations are performed (Niemand (1996)). b may typically vary between –0.05 for some parent metals, to –0.333 for welds in steel or aluminium (Olofsson et al. (1995)). A value between –0.25 and –0.3 is typical for failure of non-welded metal with significant stress concentrations. A value of –0.333 is normally chosen when weld failures are expected, otherwise a value of –0.25 or –0.27 is often used.

For a component test, the problem may not be relevant, since the component could have a single fatigue exponent (i.e. be of an homogeneous material, without welding). For component or assembly testing, where different fatigue exponents are relevant, it has to be accepted that different severity ratios will be achieved during a test for different details of the assembly or component.

The same considerations with regard to the choice of fatigue exponent also exist for all the analysis (as opposed to testing) methods employed during the present study.

Equivalent to testing methods, analysis methods also require input loading (in the case of analysis methods, being input loading for e.g. finite element analysis rather than for a physical test on a component or assembly), that is representative of in-service loading conditions by some fatigue damage ratio (e.g. five minutes of dynamic finite element analysis stress results represents the damage of one hour of real life). Again this ratio will be mathematically dependent on the fatigue exponent used for the damage calculations.

3.4.6.1.6 Synthetic test signals

The above paragraphs have concentrated on laboratory tests where the measured response on the proving ground is simulated in the laboratory. In terms of fatigue damage, the same calculation principles will also apply when using synthetic test signals, such as constant amplitude or block loading signals. A method is described by Lin and Fei (1991) to use a progressive stress (stress increasing over time) approach for accelerated testing.

3.4.6.1.7 Testing for modes of failure other than fatigue

Testing for wear, corrosion, lubrication failure, electronic component failure, rattle-and-squeak and many others, also require methods to accelerate the testing, whilst quantifying the relation between the laboratory test and real life.

Energy content is used for calculating acceleration for rattle-and squeak tests (Hurd (1992)). Moura (1992) describes temperature accelerated testing on electronic components, using the Arrhenius equation, which is similar to the stress-life equation, with temperature instead of stress.

Accelerated corrosion testing presents large difficulties and is not dealt with in the present study.

3.4.6.2 Laboratory load reconstruction

A laboratory test method, employed for both the minibus and the pick-up truck case studies, involves the accurate simulation in the laboratory of loads measured on a test track or road. The testing was performed under the supervision of the present author, by the Laboratory for Advanced Engineering (Pty) Ltd. The specialized mathematical technique required for this load reconstruction is described by Raath (1997).

Specialised software (Qantim^{TM}) was used for the calculation of the drive signals for the test rig, such that the remotely measured responses are accurately simulated. The basic steps utilised in this technique are briefly outlined below:

- The test rig is excited with a pseudo random white noise, while simultaneously recording all relevant responses (accelerations or strains). As many responses as there are drive actuators, are required. They are normally carefully chosen so as to be each sensitive to only one drive force, thereby limiting the cross influence.
- A time-domain based dynamic model is found from the input-output data using dynamic system identification techniques. This model is identified in the reverse sense, i.e. output response multiplied by dynamic transfer function yield random input.
- The transfer function is then used to calculate the actuator input signals from the desired measured response signals.

- The actuator input signals are then applied to the test rig, while recording the achieved response signals.
- By comparing the desired and the achieved responses, response errors are found, which are again simulated using the transfer function, to give the error in the actuator input signals. The input signals are then updated to give the new input signals.
- The above procedure is repeated until the achieved response signals match the desired response signals.

An equivalent method in the frequency domain, called Remote Parameter Control (RPC) is described by Dodds (1973). Dong (1995) describes a method using time domain series models, without the need for sophisticated software systems.

3.4.6.3 Synthetic signal laboratory testing

The testing of bus structures using synthetic laboratory signals, such as block loading and constant amplitude loads, is described by Kepka and Rehor (1993).

3.4.7 Statistical Analysis

3.4.7.1 Cause and effect of variations in fatigue testing results

Cutler (1998) discusses the cause and effects of variations in fatigue testing results. It is argued that the cause of variations in fatigue results should be investigated and where appropriate be linked to particular aspects, such as measurements, methods, machines, environment, people or materials. Plots of residuals against fits need to be checked for structure, trends or serial correlation.

3.4.7.2 Bayesian Inference

A method is described by Giuntini (1991) that enables true failure data to be combined with prior predictions to yield a posterior estimate of a failure distribution. This method is of importance, since with structural durability testing, it is often not possible to perform a sufficient number of tests to obtain a statistically significant sample, whereas years of experience with similar components do provide significant prior knowledge.

The method requires a choice of distribution, as well as an estimate of the parameters defining the prior distribution. The real failure data is then used to fit a failure distribution. Random samples are generated from these two distributions using the Monte Carlo method. The samples are combined according to a chosen proportion (indicating the user's relative confidence in the two prior distributions), which are then used to fit a posterior distribution. The method was employed during the pick-up truck case study presented later and also discussed by Slavik and Wannenburg (1998).

3.4.7.3 Statistical correlation between usage profile and durability test

A statistical methodology to establish the correlation between the usage profile and the durability test, is described by Beamgard et al. (1979). The methodology consists of a user survey, where information pertaining to cargo transported, annual vehicle mileage, as well as percentages of mileage driven on various categories of public roads are gathered, a measurement phase, where fatigue damage induced by the various categories of roads are quantified, as well as a statistical analysis using the Monte Carlo method, where the statistical correlation is derived.

The result is shown in the form of a graph of customer distance vs durability distance (severity ratio) for various percentile customers. It is argued that verification of the method against field failure data is imperative. It is also argued that, for such verification to be accurate, it is important to determine the mortality of vehicles for reasons other than structural failures. Such data is given by Libertiny (1993). A methodology similar to the above was employed for the minibus, as well as the pick-up truck case studies.

3.5 DETERMINATION OF INPUT LOADING

3.5.1 General

According to Grubisic (1994), the service life of a vehicle component depends decisively on the loading conditions in service. It is necessary that a representative loading spectrum is defined for both design and testing purposes. If not, the most sophisticated analysis or testing techniques will yield no useful results. In this section, some important current practices in this regard are described.

3.5.2 Sources and Classification of Loading

The contents of this and the following two sub-sections, are mainly taken from the paper by Grubisic, with some additions by the present author.

It is argued that the main influencing parameters on the loading spectrum may be defined as *usage* (vehicle utilization and driver), *structural behaviour* (vehicle dynamic properties and the design) and *operational conditions* (quality and type of road). This definition is similar to that used by Slavik and Wannenburg, where the terms *usage*, subdivided into *magnitude* (driver influence and vehicle utilization, e.g. distance per month) and *severity* (operational conditions), were used, together with the term *durability* (vehicle properties from design and manufacture).

It is also argued that the importance of the component under consideration needs to be taken into account. Primary components, subdivided into safety critical component and functional components, as well as secondary components are defined.

Loads originate from road roughness (strongly influenced by speed), manoeuvres (braking, accelerating, steering), power generation (engine), transmission, cargo/passenger interaction with structure, wind, accidental impact loads, as well as events such as driving over a curb.

Loads may be classified as (quasi-)static versus dynamic, random versus deterministic, transient (as in the case of events) versus stationary, fatigue versus overload, etc.

Consideration of both the sources and the classifications is important, as it facilitates better understanding, comprehensiveness and correct treatment.

As all structures represent more or less complicated elastic systems, time varying operational loads could excite natural modes. Stress response at a certain location on the structure will therefore show the effect of both the input loads, as well as the dynamic characteristics of the structure.

3.5.3 Design Load Spectrum

Most load histories are random in nature, implying the use of statistical functions which allow the derivation for the occurrence of certain values. Most methods to derive these statistical functions (generically called cycle counting methods, which included rainflow counting, PSDs etc.) are one-dimensional, i.e. only magnitude and number of occurrences are counted. Any such result may therefore be defined as a load spectrum (magnitude versus cumulative frequency).

The main parameters of the arguments of Grubisic are depicted in Figure 3-13, which is somewhat adapted from the reference by the present author. The characteristics of both the loading, as well as the material fatigue properties could be represented on a log-log plot of stress amplitude versus number of cycles. The loading, thus represented is the load spectrum, where-as the material properties are presented as SN-curves.

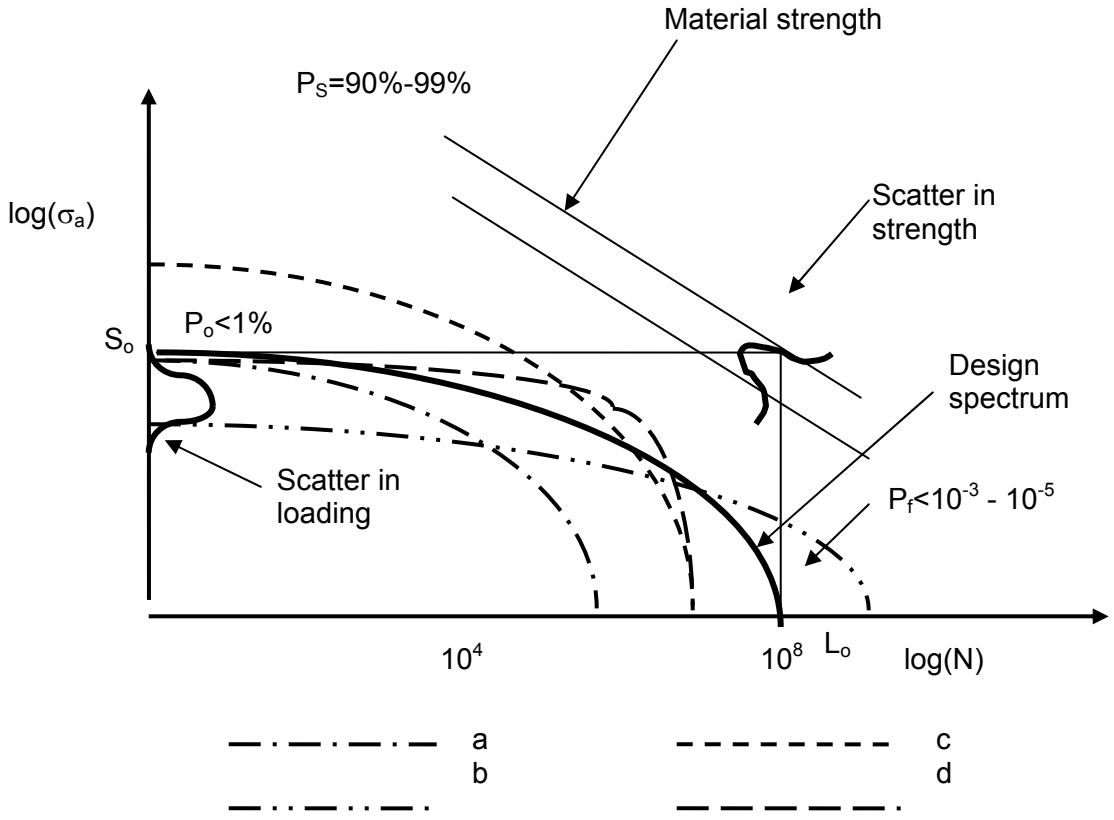

Figure 3-13 Load spectrum diagram (Grubisic)

Load spectrum curve [a] may for argument sake represent the loading on an automotive component in off-road conditions (high amplitudes, low number of cycles), where-as curve [b] may represent the same component loading under highway loading conditions (low amplitudes, high number of cycles). The two together and others in between represent the scatter in loading on a component.

From these, a design spectrum with a probability of occurrence of typically less than 1 %, must be defined, resulting in a probability of failure (which needs to be calculated taking into account the scatter in material strength and taking a 90 % survival probability for initiation and 99 % for fracture) of typically 10^{-3} to 10^{-5}.

Additional to the design spectrum, for some components it is necessary to take into account individual unexpected overloads coming from special events such as accidents. These loadings are predominantly impact loads and do not influence the fatigue behaviour.

The loading design spectra must be determined from measurements, taking into account different operational loading conditions (cornering, bad surface, straight driving, braking & acceleration, etc.), as well as customer usage. Strategies to quantify the latter may involve measurements with vehicles driven by several different test drivers over different road segments, measurements on a test vehicle following customer vehicles, or simple measurement devices installed on customer vehicles. In the present study, several detailed procedures for quantifying customer usage, are presented.

3.5.4 Test Load Spectrum

Methods for the derivation of test spectra are also presented by Grubisic. A test program should assure a reliable approval of the expected service life and have the highest possible acceleration to minimise test time and cost. The following possibilities to achieve this are listed:

- Increase the test load frequency. This may be used in uni-axial tests, where the testing frequency is not exciting any natural frequencies of the component.
- Increase the maximum load amplitudes (see curve [c] in Figure 3-13). This method has the danger of causing other failure mechanisms, such as plastic deformation, to come into play and is therefore normally avoided.
- Omit low non-damaging loads. Typically the level of omission would be at between 0.2 and 0.4 of the maximum loads.
- Do not exceed maximum load amplitudes, but increase other load amplitudes and omit non-damaging loads (see curve [d] in Figure 3-13). Typically, for a vehicle suspension component, achieving more than 100 million cycles in its life, a durability test would have between 2 million and 7 million cycles at similar frequencies, implying an acceleration factor of around 30.

3.5.5 Road Roughness as a Source of Vehicle Input Loading

It is recognized that road roughness plays a significant role as a source of vehicle input loading. From a pavement engineering point of view, substantial research has been conducted to establish measurable parameters to quantify road roughness (as quality and maintenance criteria). A method to predict vertical acceleration in vehicles through road roughness is described by Marcondes and Singh (1992). The method uses the International Roughness Index (IRI), together with dynamic characteristics of the vehicle, to predict the PSD of vertical acceleration of the vehicle.

The present author initiated a study, with the purpose to use the IRI to classify road types for durability requirement establishment. It was argued that the existing classifications, e.g. highway, secondary tar, gravel, etc., leave room for misinterpretation between questionnaire participants during user surveys and measurement engineers. The results of the study are presented by Blom and Wannenburg (2000).

The IRI statistic of a specific profile section is determined by accumulating the measured suspension motion linearly and dividing the result by the length (L) of the profile section.

$$IRI = \frac{1}{L}\int_0^{L/v} |\dot{x}_s - \dot{x}_u| dt$$

with

v = speed over section

$\dot{x}_s$ = vertical velocity of sprung mass

$\dot{x}_u$ = vertical velocity of unsprung mass

Eq. 3-24

The IRI value ranges from 0 (for totally smooth surface), through to 30 (for unpaved section traversable only at slow speeds. The strength of the method is that descriptive road classifications may be coupled to an IRI value (see Table 3-3). The correspondence between subjective classifications (by a range of typical vehicle users) and measured IRI values is depicted in Figure 3-14. A bias towards overestimating the IRI value for higher value roads, was observed. This would indicate that the descriptive classifications may need to be adjusted somewhat.

The correspondence between the measured IRI and the calculated relative fatigue damage is depicted in Figure 3-15. On a log-log plot, there is a linear relationship with a gradient approximately equal to the fatigue exponent used for the fatigue calculation. This result is interesting from the following perspectives:

- It indicates the viability of deriving fatigue loading from IRI data (since it is possible to derive PSD data from IRI values - Marcondes and Singh (1992) - and fatigue loading from PSDs - Sherratt (1996)), this result is to be expected.
- It shows the importance of correct estimation of usage of higher IRI valued roads, since there is a highly non-linear (power law) relationship between the IRI value and the fatigue damage.

The principle of using a roughness index to categorize roads for usage profiles is also discussed by Blom and Wannenburg.

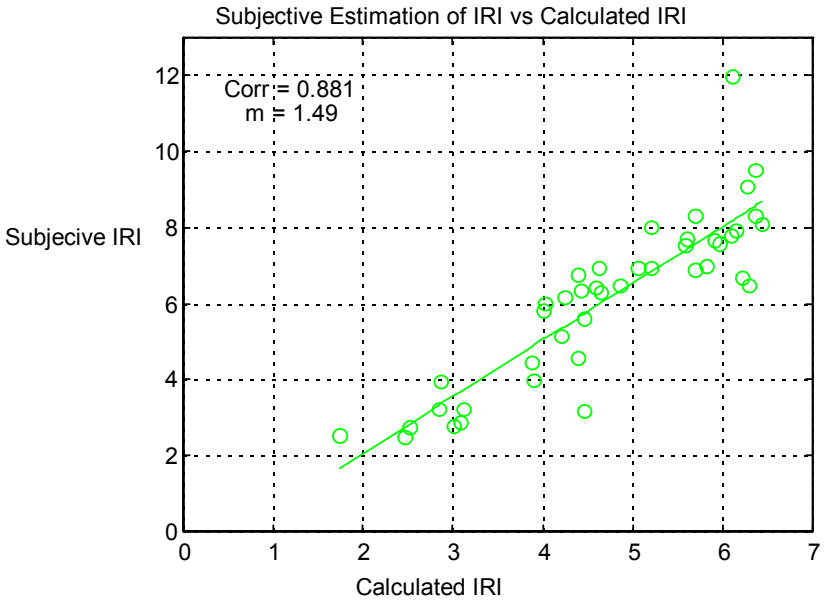

Figure 3-14 Subjective IRI vs calculated IRI (from Blom and Wannenburg)

Table 3-3 (from Blom and Wannenburg) Road classifications for subjective IRI

Description	IRI
Paved Roads	
A comfortable ride perception is obtained at speeds equal to or greater than 120km/h. No depressions, potholes or corrugations are noticeable. Surfaces with undulations are barely perceptible at a speed of 80 km/h with the roughness ranging from 1.3 to 1.4. High quality highway surface 1.4 to 2.3 and high quality surface treatment sections 2.0 to 3.0.	0 - 2
A comfortable ride perception is obtained at speeds up to 100-120km/h. Moderate perceptible movements or large undulations may be experienced at 80km/h on surfaces displaying no defects. Occasional depressions, patches or many shallow potholes are descriptive of a defective surface.	2 - 5
A comfortable ride perception is obtained at speeds up to 70-90km/h. Profound movements and swaying are perceived on surfaces with strong undulations or corrugations. Frequent moderate and uneven depressions or patches, or occasional potholes.	5 - 8
A comfortable ride perception is obtained at speeds up to 50-60 km/h. Frequent sharp movements and/or swaying associated with severe surface defects. Frequent deep and uneven depressions and patches, or frequent potholes.	8 - 10
It is inevitable to reduce speed to below 50 km/h. Surfaces display many deep depressions, potholes and severe disintegration.	10 - 12
Unpaved Roads	
Recently bladed surface of fine gravel, or soil surface with excellent longitudinal and transverse profile (usually found only in short lengths). A comfortable ride perception is obtained at speeds up to 80-100km/h. The awareness of gentle undulations or swaying.	0 - 6
A comfortable ride perception is obtained at speeds up to 70-80 km/h. An awareness of sharp movements and some wheel bounce. Frequent shallow-moderate depressions or shallow potholes. Moderate corrugations.	6 - 12
A comfortable ride perception is obtained at a speed of 50 km/h. Frequent moderate transverse depressions or occasional deep depressions or potholes. Strong corrugations.	12 - 16
A comfortable ride perception is obtained at 30-40 km/h. Frequent deep transverse depressions and/or potholes or occasional very deep depressions with other shallow depressions. Not possible to avoid all the depressions except the worst.	16 - 20
A comfortable ride perception is obtained at 20-30 km/h. Speeds higher that 40-50 km/h would cause extreme discomfort, and possible damage to the vehicle. On a good general profile: frequent deep depressions and/or potholes and occasional very deep depressions. On a poor general profile: frequent moderate defects and depressions.	20 - 24

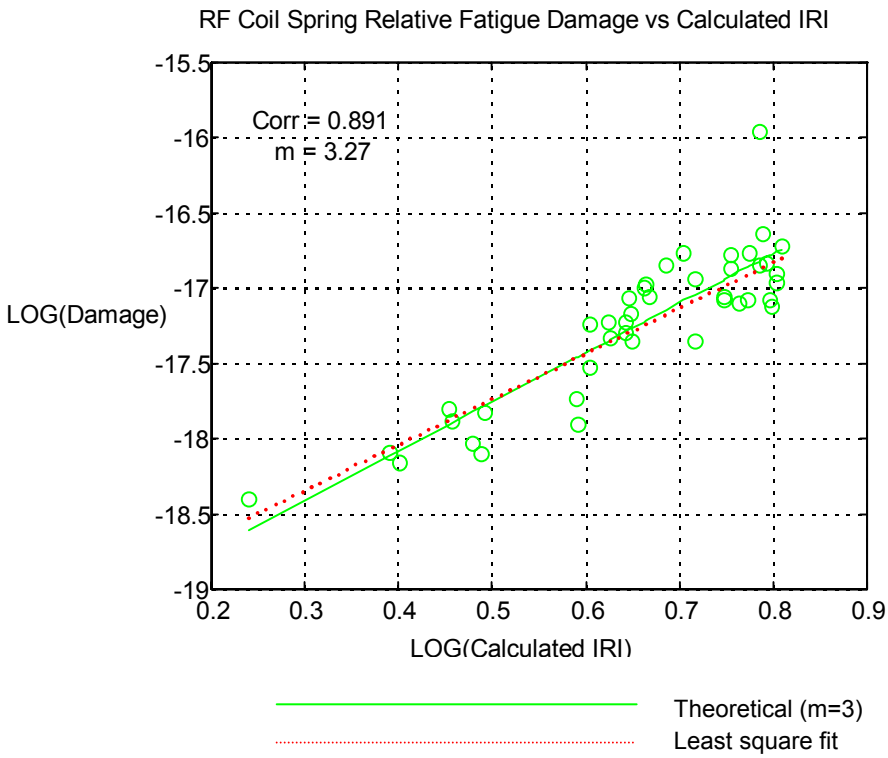

Figure 3-15 (from Blom and Wannenburg) Fatigue damage vs IRI

The results of this study were unfortunately not available at the time when the two relevant case studies (minibus and pick-up truck) were performed (the study was initiated by the author as a result of the work performed during the case studies). The more scientific road classification approach was therefore not incorporated at the time, but the developed method is proposed as part of the generalized methodology presented in Chapter 1.

3.5.6 Vibration

Richards (1990) presents a review of analysis and assessment methodologies for vibration and shock data to derive test severities, mainly for the transport industry. The following general observations are of importance:

- A significant proportion of the dynamic environment experienced by cargo on vehicles originates from the interaction between road wheels and road surface. This is fundamental to much of the work presented in the present study.
- Vehicle speed is one of the major influencing factors on the severity of vibrations.
- The vibration dynamics contain both continuous and transient responses, which are often difficult to separate, due to the irregularity of the transient occurrence intervals and amplitudes. Continuous response is traditionally termed vibration and the transient response is considered as shocks. These factors played a major role in the tank container case study presented later.

Four methods to determine vibration test severity are reviewed by Richards:

- PSD approach: The test severity is derived from the Power Spectral Density of measurements. The limitation of this method is that, due to the averaging, transient events and time varying data (non-stationary) cannot be described.
- Sandia approach: Based on comprehensive measurements, the most severe values of root-mean-square acceleration for each of several frequency bandwidths, are derived.
- Aberdeen Proving Ground approach: The method uses the mean acceleration PSD values using a 1 Hz bandwidth, along with the standard deviation in each band. One standard deviation is added to the mean to provide a testing envelope. The method can be distorted when non-stationary data is used. Measurements on a test track should therefore happen at constant vehicle speed over each section.
- Cranfield approach: The method included both the acceleration PSD and the Amplitude Probability Density Function (APD). The PSD gives the spectral shape, but the overall amplitude is modified using the APD. Transient events are thus included as short duration, high amplitude, random vibration.

To some extent the method used for the tank container case study, is similar to the latter approach. The tank container case study is interesting in the sense that it could be regarded as cargo being transported on vehicle (falling into the regime described in this section, namely so-called vibration testing), or can be seen as a vehicle structure in itself, where fatigue based methods are more commonly employed. The statement is made by Devlukia (1985) that PSDs and APDs are not sufficient to establish fatigue loading characteristics, advocating the use of rainflow counting.

A European research project, to establish an integrated system for the design of vibration testing, is described by Grzeskowiak et al. (1992). This process is called ‘tailoring’, a term used by vibration testing engineers. It would seem that fatigue domain analysis is recognized in this project. The present study, to a large extent, is aimed at the same objective.

3.5.7 Limit State and Operational State

In principle the process for static design is simple. Structural response (stresses, displacements, etc.) to some defined input loading is determined, either through analytical calculations, or finite element methods. These results are then evaluated against a set criterion for allowable quantities. The allowable quantities would be material property related (e.g. yield stress) or functional (e.g. maximum allowable displacements).

Traditionally, a strength design criterion is set in the following format;

Calculated maximum stress (function of defined loading & geometry)
<
Allowable stress,

where the allowable stress would be a material strength (e.g. yield stress) divided by a safety factor. The safety factor may then typically take the following into account:

- Uncertainty with regards to the material strength.
- Uncertainty with regards to the loading.
- Dynamic loading effects.

- Fatigue loading effects.
- Stress concentrations, welding etc.

In some cases, design criteria are set which incorporates an obvious safety factor on the prescribed loading, as well as an additional safety factor applied to the material strength. Such safety factors should rather be called factors of ignorance, since they attempt to take account of aspects not quantified scientifically.

A more logical approach, called the limit state design method MacGinley and Ang (1992), requires the designer to define limit states and operational states. Much smaller safety factors are then prescribed to allow mainly for statistical uncertainty of material properties. As an example, a designer of a tanker truck would then have to define the following limit states:

- Maximum vertical, lateral, longitudinal (separate and/or combined) loading for no damage to vehicle. Here travelling over a hump in the road at a high speed with a full load, may define the maximum vertical load. The maximum longitudinal load may be during maximum braking effort under full load and the lateral load could be during a high speed double lane-change manoeuvre, or during a scuffing event on a concrete tarmac.
- Maximum longitudinal load for no leaking of tank. This may be some accident situation, where the truck collides with another vehicle.
- Fatigue limit state loads, where vertical, longitudinal and lateral load amplitudes, as well as repetitions during the design life of the vehicle, need to be defined.
- Other limit states, such as energy to be absorbed during a roll-over without the tank leaking, penetration damage to the tank vessel, energy to be absorbed by bumpers and underrun bars during accidents.

With the responsibility of defining these design limit states being put on the designer, there is then no need for applying safety factors on the loads to be used in the design, but it does put an added responsibility on the design engineers.

In many industries, however, the more traditional approach is still adhered to in design codes. In the road tanker industry, a South African design code, SABS 1398 (1994), defines the following design criteria:

Maximum principal stresses calculated for the following separate loading conditions shall be less than 20% of the ultimate tensile strength of the material:

- Vertical load = 2 g
- Longitudinal load = 2 g
- Lateral load = 1 g

Since a 2 g longitudinal acceleration cannot even be approximated during hard braking and a 1 g lateral acceleration would overturn most road tankers, it is obvious that safety factors are applied to the loading side of the static design equation. Also, an additional safety factor of 5 is enforced on the material strength.

An equivalent American design code, Code of Federal Regulations, Title 49, requires that the maximum principal stresses calculated for the following combined loading condition shall be less than 25% of the ultimate tensile strength of the material:

- Vertical load = 1.7 g

- Longitudinal load = 0.75 g
- Lateral load = 0.4 g

In this case, the loads seem much closer to realistic limit state loads, but the safety factor of 4 on the material strength must involve more than just allowance for scatter in material properties. Both these codes do not prescribe any fatigue loading and it is therefore apparent that the safety factors incorporate allowance for fatigue.

A further factor contributing to the high safety factors in these codes is the fact that they assume very simple hand calculations to be performed, resulting in only global bending, tensile and shear stresses caused by the prescribed loads and not peak stresses at stress concentrations, such as will result from detailed finite element analysis. It would therefore be erroneous to evaluate localized high finite element peak stress results using such codes without further interpretation.

In the USA Federal Regulations code for the design of ISO tank containers, a criterion is prescribed for stresses resulting from a combined;
- Vertical load = 3 g,
- Longitudinal load = 2 g,
- Lateral load = 1 g,

to be lower than 80% of the yield stress of the material. When applying these loads to a detailed finite element model, it is doubtful whether any design in the world strictly complies.

Sophisticated design codes, such as the ASME code for pressure vessels, allow for the interpretation of detailed finite element stress results, where allowable local stresses can be more than twice the yield strength of the material, based on the fact that local yielding would occur with the resultant redistribution of stresses. Such peak stresses would therefore not be detrimental to the static integrity of the structure, but under repetitive or variable loading (to which vehicle structures are subjected), such areas would be of high concern for fatigue problems.

3.5.8 Design and Testing Criteria

3.5.8.1 Maximum load criteria

3.5.8.1.1 Automotive vehicles

A design criterion in terms of static inertial loads is described by Skattum et al. (1975).
- Vertical load = 3 g
- Longitudinal load = 2 g
- Lateral load = 1 g

The vertical load is substantiated from measurements, where it was found that a 3 g vertical load would be exceeded with a 3% probability.

Riedl (1998) describes an exercise to substantiate the design of aluminium components of the BMW 5-series rear axle, with particular consideration of extreme loads. Testing was performed using pendulum induced impact loads.

3.5.8.2 Fatigue loading

3.5.8.2.1 Inertial Loading

As discussed in paragraphs 3.5.7 and 3.5.8.1.1 above, it is typical to find loading criteria for automotive structures in design codes expressed in terms of inertial loading (also called g-loading). As argued in paragraph 3.5.7, it would seem that such criteria would often also make allowance for fatigue loading.

The obvious reason for using inertial loading in design criteria, is that inertial loading may be generic (independent of specific design, or more specifically, the specific design mass). Since it is a principal objective of the present study to establish fatigue loading design criteria for automotive and transport structures, a methodology was developed based on fatigue equivalent static g-loading.

Xu (1998) argues that g-loads are sufficient to capture the structural response to the three principal global loading modes experienced by vehicles, namely, bouncing (vertical g-load), pitching (longitudinal g-load) and rolling (lateral g-load). Xu introduces the concept of modal scaling to supplement the quasi-static g-loads, which would be able to address response modes beyond these three. The method is in principle equivalent to the modal superposition method discussed in paragraph 0. For the LTV case study, it was required to employ a hybrid g-loading / modal superposition method similar to that described by Xu.

3.5.8.2.2 Remote Parameter Analysis

A concept termed Remote Parameter Analysis (RPA), developed at Ford Motor Co. to integrate finite element analysis and simulation or road test data for durability life prediction, is described by Pountney and Dakin (1992). The method is of importance since it allows component optimisation earlier in the design process, due to the ability to derive free-body component forces from measurements on customer correlated routes. Since a finite element simulation process is some 30 times faster than laboratory simulation and some 90 times faster than proving ground simulation, the period of time spent in the design and development phases can be significantly reduced.

The method involves the following steps:

- Develop a free body diagram of the component under consideration.
- Construct a finite element model of the component.
- Select a constraint set and apply unit loads to the finite element model.
- Derive from the results, a load-to-gauge transfer matrix, taking care to choose the positions of the strain gauges such that effective decomposition is achieved. The inverse of this matrix is used to determine the loads acting on the component from the time data measured at the strain gauges.
- Derive also a load-to-response transfer matrix. This matrix enables very fast solution of the stresses on the component for each time step load set solved during the previous step, without having to perform the finite element analysis again.
- Fatigue analysis on the stress-time result at any position on the component can then be performed.

The method is based on static linear models, therefore disregarding the effect of dynamics (i.e. it is a quasi-static method). Poutney and Dakin state that most

engineering problems can however be solved using the static linear models. The majority of the methods employed in the present study are also based on this important simplifying assumption.

The RPA methodology is essentially an extension of the quasi-static method depicted in Figure 3-2. The RPA method is depicted on the summary diagram in Figure 3-16.

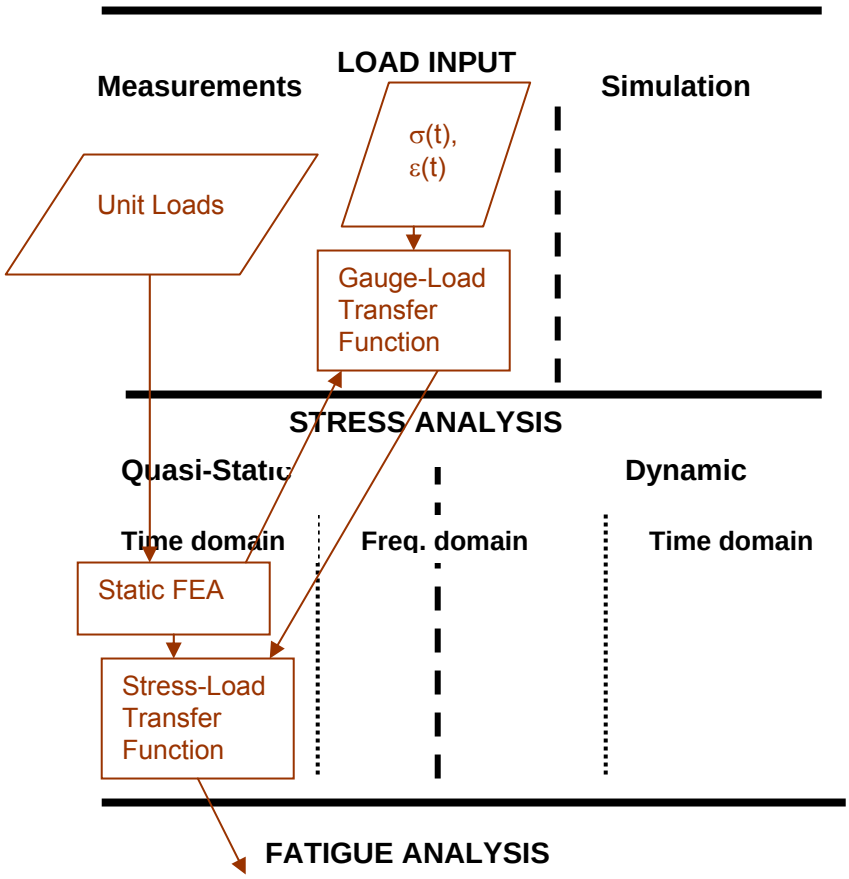

Figure 3-16 Remote Parameter Analysis

A fully dynamic method with similar steps may be derived from the mathematical process used to reconstruct real road input loading in the laboratory from remotely measured parameters such as strains, according to Raath (1997). Here the laboratory rig would be substituted by a dynamic finite element model, where time-domain or frequency domain transfer functions between dynamic identification input loads and dynamic responses at measuring positions are fitted on the finite element results, to be able to derive dynamic input loads (simulating the real loads) for dynamic finite element analysis.

3.5.8.2.3 Standardised load-time histories

Heuler et al. (2005) reviews a large number of Standardised Load Time Histories (SLH) developed over 30 years in the aircraft (e.g. FALSTAFF, Gerharz (1987)) and automotive industries. Such systems are the result of collaborative efforts by industry working groups and typically involve comprehensive measurement exercises, the results of which are statistically processed to obtain standardised load spectra. One such

system, named CARLOS (Schutz et al. (1990)), produced vertical, longitudinal and lateral random load sequences, being a mixture of 5 road types, which are used for front suspension durability testing.

3.5.8.2.4 Statistical domain

A statistical model of random vehicle loading histories is described by Leser et al. (1994). The load history is considered to have stationary random and non-stationary mean contents. The stationary variations are modelled using the Autoregressive Moving Average Model (ARMA), while a Fourier series is used to model the variation of the mean. The method enables the construction of time domain data for analysis or testing purposes.

3.5.8.2.5 Frequency domain

A novel approach to establish fatigue loading for road tankers is presented by Olofsson et al. (1995). A survey of more than 1000 gasoline road tankers in Sweden found that more than 40 % of the vehicles were impaired by cracks caused by fatigue, indicating that the existing design criteria are insufficient to guard against fatigue failure. The method is based on an extension of the Shock Response Spectrum (SRS) approach, commonly used to described shock loading (e.g. for earthquake analysis). The approach is called the Fatigue Damage Response Spectrum (FDRS) and is used in France to create fatigue test sequences for structures. The process to establish a FDRS can be summarized as follows:

- From measured acceleration data the response of a single degree of freedom dynamic system with varying dynamic properties (natural frequency and damping) is determined using FFT analysis.
- For each response, the fatigue damage is calculated using the stress-life approach, together with the Miner damage accumulation principle.
- The FDRS is then a plot of fatigue damage as a function of natural frequency (at various damping factors).

Assuming that stress levels ($\Delta\sigma$) will be proportional to the response acceleration (a) of the fundamental mass (m) ($\Delta\sigma = m \times a$) and combining this with the stress-life equation (Eq. 3-14) and the Miner equation (Eq. 3-22) yields the following expression for damage:

$$D = \left(\frac{m}{S_f}\right)^{-1/b} \sum n_i a_i^{-1/b} \qquad \textbf{Eq. 3-25}$$

The constants before the summation will cancel in a relative damage calculation and therefore again only the fatigue exponent (b) is unknown. As discussed in paragraph 3.4.2.4.3, a reasonable estimate can be made.

Olofsson describes an alternative cycle counting method to the rainflow method, called the HdM model, claimed to provide better results when stress histories are irregular and is easier to use. Counting of up crossings at levels of a ($n_+(a)$) is performed. The summation is then changed to an integral:

$$D = \int_{a_{\min}}^{a_{\max}} n_+(a) a^{-1/b} da \qquad \textbf{Eq. 3-26}$$

It is proposed that this formulation be used in design codes to specify fatigue loading. Enveloped curves, based on extensive measurements, will have to be used. Accelerations would typically be measured on bogeys and kingpins (rigid areas) and would thus be somewhat vehicle dependent. The curves would be normalised to exclude the S_f and b constants required to determine absolute fatigue damage. The practical use of such curves would therefore require the calculation of the first natural frequency of the tank structure under consideration, an estimation of the damping factor, as well as the determination of S_f and b for all critical points on the structure. Fatigue damage estimates, taking into account the simplified dynamic response of the structure, would then result. The method is depicted on the summary framework in Figure 3-17.

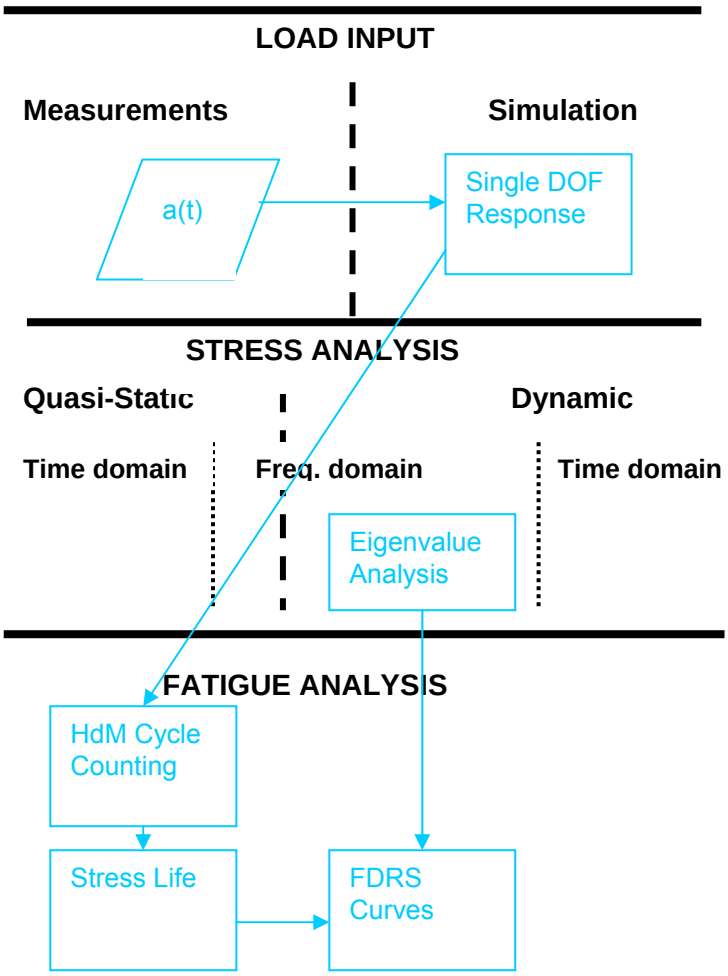

Figure 3-17: Fatigue Damage Response Spectrum (FDRS) Method

The methodology was not implemented as presented above by the present author for any of the case studies. For the light commercial vehicles, the dynamic response of the vehicles was inherently taken into account due to the fact that dynamic testing was performed. For the road tankers and the LHDs, it was demonstrated that the first natural frequency response would cause stress patterns proportional to those caused by static vertical inertial loading and that no other modes significantly contributed.

For the LTV industrial vehicle, higher order mode shapes were taken into account using the modal superposition method. In the latter case, there was no need to establish generic design criteria, which meant that the higher order mode excitation could be taken into account directly. In the case of the tank container, generic design criteria (valid for other designs), were required, a quasi-static methodology was followed, resulting in fatigue equivalent static g-loads. The above technique, however, may suitably address higher order dynamics in a way that would be generic for all designs and was therefore included into the generalised methodology formalised during this study.

3.6 CLOSURE

In this chapter, the fundamental theory underpinning the techniques applied for the case studies presented in the following chapters, was presented. Also dealt with were current practices with regard to the determination of input loading for vehicular structures.

Figure 3-18 depicts the summary framework, populated with all the durability analysis (as opposed to testing) methods described in this chapter. The diagram offers an holistic view of the different choices of methods and their relationships with each other. The advantages and disadvantages of the various methods are listed in Table 3-4. The colours used for each method in the diagram are listed in the legend column of the table. Black is used in the diagram for objects that are part of more than one method. The diagram and table are later employed to compare the newly developed methods employed during the present study, with the existing methods.

Table 3-4: Comparison of Durability Analysis Methods

	Type	Load Input	Stress Analysis	Fatigue Analysis	Legend	Advantages	Disadvantages
Multi-body Dynamic Simulation	Time domain	Road profile or measured accelerations	NA	NA	Dark green	May be used to obtain force inputs for FEA from measured accelerations or road profiles	Complex tyre models
Remote Parameter Analysis	Quasi-static, time domain	Straingauge measurements	Static FEA	Rainflow counting + various fatigue life analysis methods	Brown	Can use remote measured straingauge data, economic FEA	Not suitable for complex dynamic response, rainflow on each stress point, loading results not suitable for code = not design independent
Co-variance method	Quasi-static, frequency domain	Measured /simulated input forces	Static FEA	Dirlik formula + various fatigue life analysis methods	Light green	Takes account of complex dynamic response, economic FEA	Requires stationary random input data, Dirlik formula approximations, loading not design independent
Random Vibration	Dynamic, frequency domain	Measured /simulated input forces	Eigen value FEA	Dirlik formula + various fatigue life analysis methods	Pink	Takes account of complex dynamic response, economic FEA	Requires stationary random input data, forces must be measured, Dirlik formula approximations, loading not design independent
Fatigue Domain Reponse Spectrum	Dynamic, fatigue/ frequency domain	Measured accelerations	Eigen value FEA	HdM cycle counting + Stress Life	Light blue	Takes account of complex dynamic response, economic FEA, loading is design independent	Requires stationary random input data
Modal Superpositon	Dynamic, time or frequency domain	Measured /simulated input forces	Eigen value FEA	Dirlik formula + various fatigue life analysis methods	Violet	Takes account of complex dynamic response, economic FEA	Forces must be measured, Dirlik formula approximations, loading not design independent
Direct Integration with Large Mass, Relative Inertial, La Grange Multiplier	Dynamic, time domain	Measured accelerations	Dynamic FEA	Rainflow counting + various fatigue life analysis methods	Orange and Red	Takes account of complex and transient dynamic response, accelerations may be measured, can be design independent	Expensive FEA

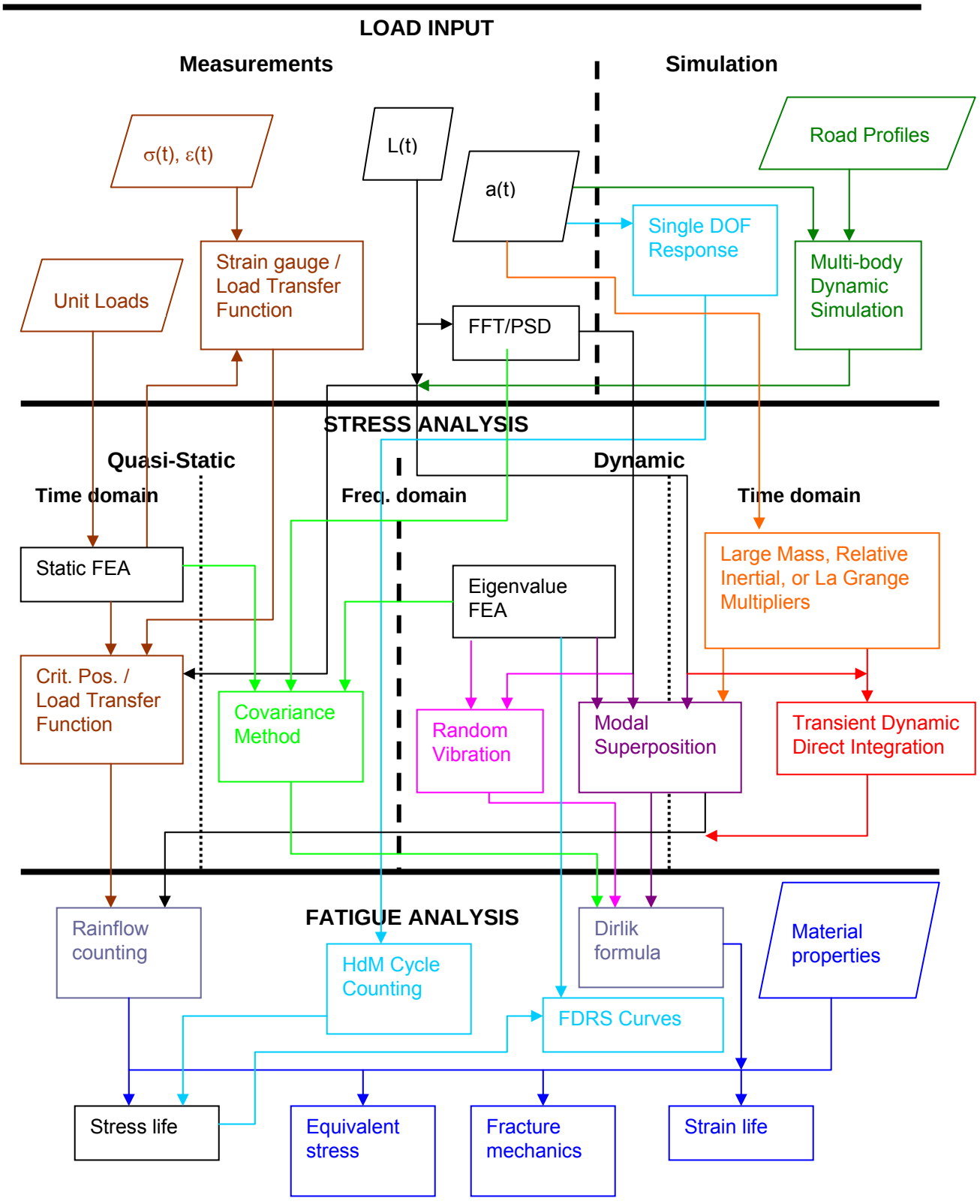

Figure 3-18: Summary diagram

4. MEASUREMENTS, SURVEYS AND SIMULATION

4.1 SCOPE

Input loading may typically only be derived from one or a combination of the following sources:

- Measurements
- Surveys
- Simulation
- Field failures

The first three of these sources are dealt with in this chapter in terms of the case studies, the last one being a derivative of verification of failure predictions with field failures and therefore dealt with in Chapter 6.

4.2 MEASUREMENTS

4.2.1 General

The most important source for deriving input loading must be measurements. Measurements can only be performed if vehicles are available, albeit prototypes or similar models. This would mostly be the case. Measurements were performed for all the case studies and are presented in the context of each case study.

4.2.2 Methodology

It is important to note that measurements, especially using strain gauges, are commonly and mostly mistakenly, regarded as exercises to quantify stresses. Strain gauge measurements are not very effective for such a purpose, due to two reasons:

- Strain gauges are placed at specific positions and can only measure where they were placed. To know where to measure is often not possible without finite element analysis.
- In terms of fatigue, the critical stress areas mostly exhibit high stress gradients. Placing strain gauges to accurately measure these gradients is mostly not practical.

It is therefore argued in the present study, that strain gauge measurements are purposed to quantify input loading and not stresses. Such loading is then used as inputs to finite element analyses (then only quantifying the stresses) or testing.

With the above in mind, the general measurements methodology involves the following basic steps:

- Planning: Measurements are a means to an end and careful consideration must be given to the end usage of the results. All possible input loads to the structure must be identified and decisions to leave some out must be well founded. Additional strain gauges, sensitive to such loads, would typically be placed to verify such assumptions.
- Configuration: Transducers must be placed at positions that will be sensitive to the inputs to be quantified. Preferably, each transducer should be sensitive to only one input, but normally cross coupling will be unavoidable. There will be a minimum of as many transducers as inputs to be measured, but it is good practice to have a few

redundant channels. Strain gauges should be positioned in areas of nominal (preferably uni-axial) stresses.

- Instrumentation: Details of the instrumentation must be well documented, including accurate positions, signs, gauge factors, calibrations, etc. Where possible, known loads must be used to record the calibration values with the same settings as used during the measurements. This must be done before and after the measurements, since adjustment of gains to avoid overloading, is often required during the measurements. Zero readings should be taken before and after the measurements and the zero conditions should be documented. A trial run, with inspection of the data, is good practice, to ensure optimum gain settings.
- Measurements: Measurements must be performed during representative operational conditions. Sampling rates must be chosen to ensure capturing of significant data. Typical fatigue causing frequencies from road inputs are between 0 Hz and 20 Hz. Sampling rates of 200 Hz would mostly ensure reliable data in the frequency band of interest. Possible resonant effects may require higher sampling rates.

4.2.3 Minibus

4.2.3.1 Instrumentation

A minibus vehicle was instrumented (refer to paragraph 2.2.1). The vehicle was of a model that has been on the market for several years and it was its replacement that prompted the project. During the life of the existing model, fatigue failures have occurred on chassis crossmembers. It was intended to use these failures to calibrate the mission profile results. Strain gauges measuring shear strains were applied to each torsion bar forming part of the front suspension. These measured signals are directly proportional to the relative displacement between the front wheels and the chassis, as well as therefore to the vertical spring loads induced by the front wheels on the suspension and through the suspension to the chassis. It was argued that these measurements would then be directly related to the major portion of the damage induced on the chassis and suspension components. For the failed crossmember this certainly would be the case, since only the torsion bar loads are reacted there. The shock absorber forces, which would be proportional to the derivative of the relative displacement (velocity), are reacted on a bracket to the front of the chassis.

It was subsequently demonstrated that relative damages calculated using the relative velocities were similar to those calculated using relative displacements. This may be explained by the fact that the damage calculated from the displacements underestimates the higher frequency content, but overestimates the lower frequency content, compared to the damage calculated from the velocity. Possibly more important is the fact that the damages were used in a relative sense (damage of one type of road divided by the damage of another), negating to some extent absolute errors.

A transducer was installed on one front wheel to measure the revolutions of the wheel. This signal was used to measure the distance travelled during the measurements.

The signals were amplified with a carrier wave amplifier and then stored on a magnetic tape recorder. After the measurements, the data was read into a computer at a sampling rate of 128 Hz. At the time, the capacity of the equipment available forced a compromise on the sampling frequency used.

The measurements were performed on different category roads typically used by taxis, as well as on the manufacturers vehicle test track.

4.2.4 Pick-up Truck

4.2.4.1 Instrumentation

The placement of the measuring positions on the vehicle was planned so as to include all major suspension, chassis and body structure elements. The aim was to have the transducers so placed as to collect the vehicle's measured response to the following fundamental types of input loading:

- Vertical wheel inputs
- Lateral wheel inputs
- Longitudinal wheel inputs
- Global twisting inputs
- Body vibrations

The following reasoning was applied. From experience it is known that the damaging inputs into the suspension and chassis of the vehicle can be characterised by measuring positions on the suspension components which are respectively sensitive to the vertical, longitudinal and lateral wheel forces. The twisting inputs induced into the vehicle have been collected by placement of a transducer on one of the chassis cross members. In order to characterise the relative independent body vibrations, transducers were placed at the left top door corner and the left rear panel of the load box. Table 4-1 lists the positions of the various measuring points.

Table 4-1 Pick-up truck measurement configuration

Channel number	Position	Transducer type
1	Left front wheel acceleration – vertical	Accelerometer – 30g
2	Right front wheel acceleration – vertical	Accelerometer – 30g
3	Right rear wheel acceleration – vertical	Accelerometer – 15g
4	Left rear wheel acceleration – vertical	Accelerometer – 15g
5	Left front coil spring	Strain gauge
6	Right front coil spring	Strain gauge
7	Right rear differential	Strain gauge
8	Left rear differential	Strain gauge
9	Left front strut	Strain gauge
10	Right front beam outside	Strain gauge
11	Left beam centre between wheels	Strain gauge
12	Round cross member	Strain gauge
13	Left top door corner	Strain gauge
14	Loadbox left rear panel	Strain gauge

The signals were amplified with a carrier wave amplifier and then stored on a magnetic tape recorder. After the measurements, the data was read into a computer at a sampling rate of 200 Hz.

4.2.4.2 Measurements

The measurements were performed on a wide range of typical road types across the country. Recordings were done for the laden and unladen conditions.

During the measurements, each section of road selected to be sampled was subjectively assigned to one of the same categories used for the questionnaires. Customer road (usage profile) measurements were performed throughout South Africa to ensure the inclusion of a wide range of roads that might be used by pick-up truck owners. The roads were divided according to their characteristics into the following categories:

- Rural good tar roads
- Rural bad tar roads
- Urban tar roads
- Mountainous and winding tar roads
- Rural good gravel roads
- Rural bad gravel roads

The suspension track at the Gerotek vehicle test facility near Pretoria was also measured with the purpose of obtaining sequences that might be used for the accelerated road simulator test.

4.2.5 Fuel Tanker

4.2.5.1 Instrumentation

After completion of the first prototype vehicle of the new design, comprehensive measurements were performed. Strain gauges and accelerometers were used.

The placement of transducers was divided into three categories:

- Transducers were placed to obtain fundamental kinematics and load inputs into the structure to be used as inputs to a dynamic finite element analysis. The finite element analysis will yield dynamic stress results to be processed to obtain fatigue life estimates for all critical areas of the structural design.
- Transducers were placed in known critical areas to measure stresses, which could be used as reference and verification for the finite element analysis. For this purpose, strain gauges were placed to measure nominal stresses in as many areas required to reasonably characterise the stress response of the structure. Fatigue life estimates are also obtained directly from these transducers for all the areas identified as critical after the static finite element analysis
- Gauges were placed in critical areas where the design for future vehicles has been changed, or manufacturability problems have been experienced during the construction of the prototype unit. The data from this third category was used directly, or indirectly, together with finite element analysis, to obtain fatigue life estimates.

4.2.5.2 Measurements

The measurements included a typical 300 kilometre trip with a liquid load, as well as a return empty trip.

4.2.6 ISO Tank Container

4.2.6.1 General

During this case study, a much more involved measurement exercise was performed compared to the other case studies. As introduced in Chapter 2, the objective was to establish the operational loading conditions for ISO tank containers. These containers are employed on road, rail and sea and travel (without drivers) all over the world. Special equipment, trade named 'XLG 2000 Data Logger', was developed for this purpose. A South African electronic firm, Datawave, was commissioned for this development.

4.2.6.2 Transducers

Transducers were specially chosen such that container design independent loads could be quantified, as well as verification of the processing algorithms could be achieved.

4.2.6.2.1 Accelerometers

For the former purpose, eight accelerometers were placed on the structure (seven at corner castings, implying reasonable independence of the specific tank container design) and one on the vessel itself. The positions and directions of measurements of the accelerometers are depicted in Figure 4-1.

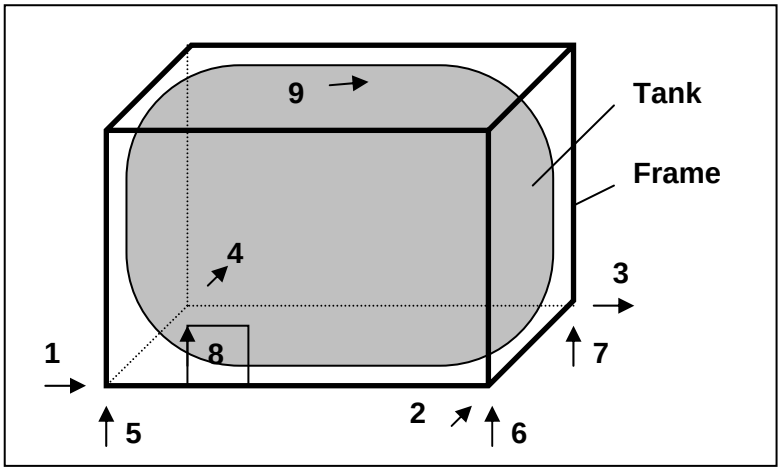

Figure 4-1 ISO tank container measurement configuration

- Channels 1 and 3 : Longitudinal accelerations at the corner castings.
- Channels 2 and 4 : Lateral accelerations at the corner castings.
- Channels 5 to 8 : Vertical accelerations at the corner castings.
- Channel 9 : Longitudinal accelerations recorded on the tank.

From this configuration of the accelerometers it is possible to determine the 6 rigid body modes of the frame, as well as the twisting movement:

- Vertical translation : (ch5 + ch6 + ch7 + ch8)/4
- Longitudinal translation : (ch1 + ch3)/2
- Lateral translation : (ch2 + ch4)/2
- Pitch : (ch5 + ch8 – ch6 – ch7)/2/length of tank

- Roll : (ch5 + ch6 – ch7 – ch8)/2/width of tank
- Yaw : (ch2 – ch4)/length of tank
- Twist : (ch5 – ch8) – (ch6 – ch7)

It is evident that there was one redundant accelerometer on the frame. This was a safety precaution in case of malfunctions. The accelerometer on the tank itself (channel 9) was used as a reference.

4.2.6.2.2 Strain gauges

The strain gauges were placed at the areas sensitive to vertical, longitudinal and lateral loading independently (not peak stress areas). From this data fatigue life predictions could be made for the specific tank design, which could then be compared to the calculated predictions of a finite element model, using the loads derived from the accelerometer data, for verification purposes.

4.2.6.3 Data recording domains

The datalogger records measured data in three different domains. The reason for this was that it would be impractical to store unprocessed data. The special data reduction algorithms that were part of the datalogger intelligence made it possible to store what would have been 460 GByte of data during a typical 6 week trip using only 3 MByte.

The datalogger stores one hour of continuously sampled data, which it then swaps into a buffer space for processing, whilst sampling the next hour. The data is then processed and stored in three domains (refer to Figure 4-2).

A: The overloads are short time events (approximately 2 seconds long) which incorporate high peaks (e.g. railway shunting or handling at the depots). The data logger is able to identify these overloads and stores it in memory with a capacity for 256 events. Each time a smaller event in the memory is overwritten with a larger one. The data is sampled with a sampling frequency of 602 Hz.

B: Data containing an hour's acceleration information is transformed to the frequency domain. The transformed data represents the statistics for the recorded hour. The memory is able to collect 1016 of these data files, with a sampling frequency of 301 Hz. From this data time domain data could be recreated, losing only the transient events.

C: Cycle and strain range counted information from the data measured by the strain gauges, is saved in the form of rainflow matrices. As mentioned before, this data is used to verify the fatigue calculations from the frequency domain data.

4.2.6.4 Data assembly and storage

Data was extracted by computer at certain depots after completion of typically 6 week trips. The data was sent via e-mail to the University of Pretoria, where the data was stored. After extraction, the dataloggers were reset, to commence a new set of measurements. Problems were encountered where the loggers were not reset, so that the data sent from the next depot, under a new name, was the same as the previous set. The files were named so as to link them to a specific tank, as well as the route followed.

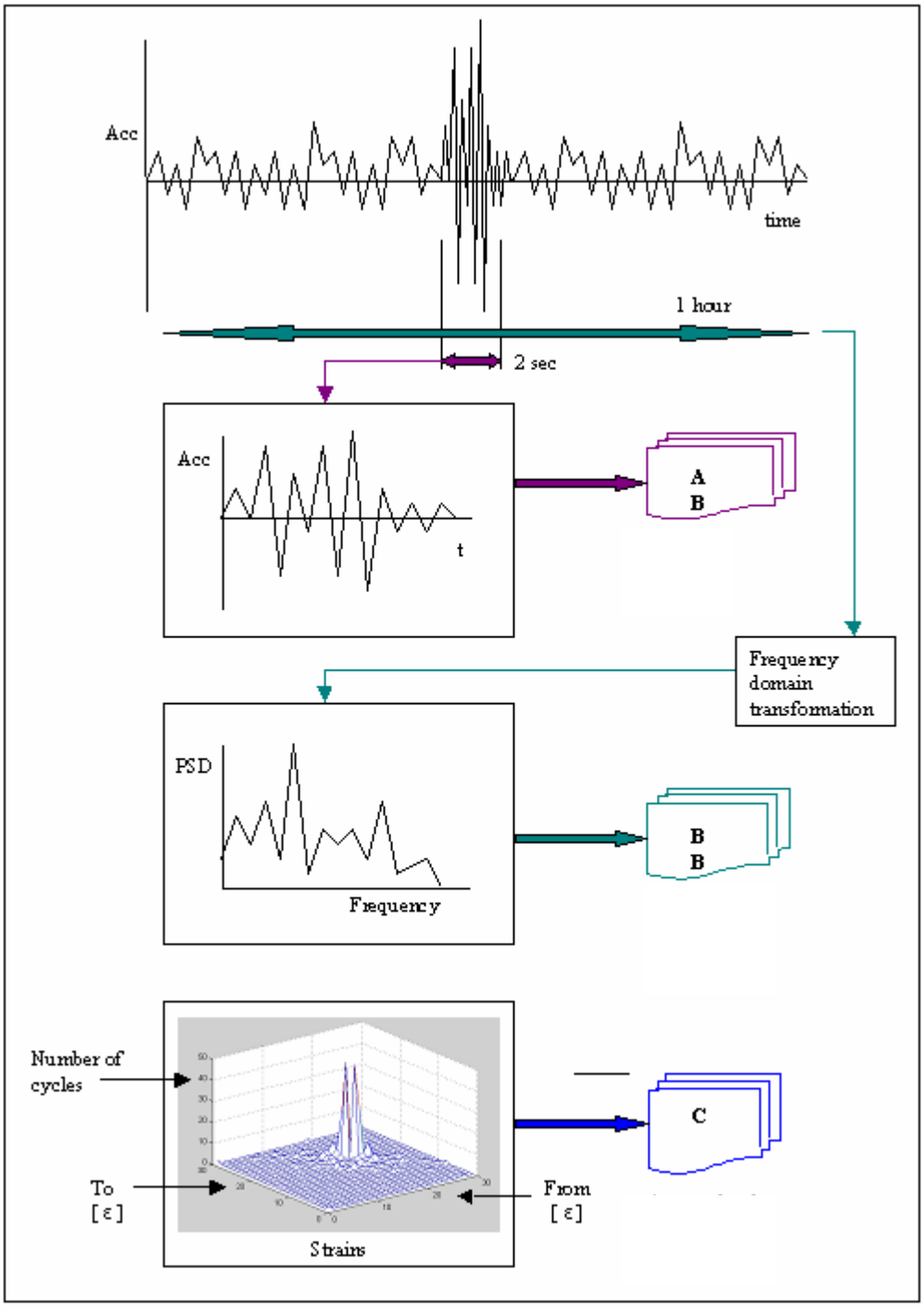

Figure 4-2 Data recording domains of datalogger

4.2.6.5 Datalogger

The components of the specially developed datalogger are diagrammatically depicted in Figure 4-3.

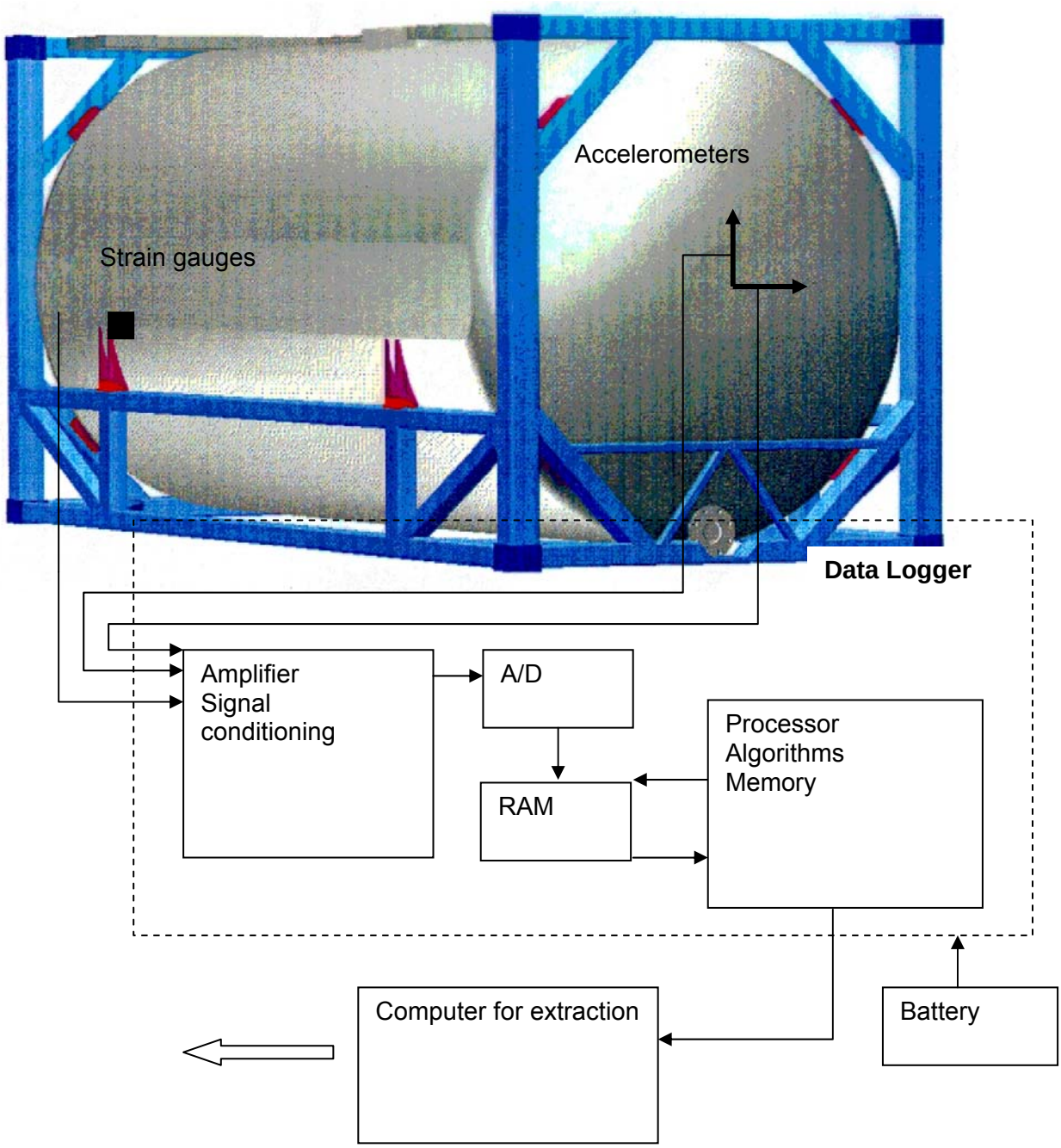

Figure 4-3 Components of datalogger

4.2.6.6 Routes and cargo

The establishment of the routes of the tank containers during measurement periods was of importance to be able to link events to certain conditions. Route logging data from the

operators was available for this purpose, being coupled to the dates stored with the data on the datalogger. Problems were experienced with the dates from both the datalogger and the operator information, which made some sets of data unusable. The operator data also did not include sufficient detail (only the point and time of departure and the point and time of arrival were available) to be able to know for certain which modes of transport were involved during the trip. Some intended linking was therefore not achievable.

Also of importance was to know whether the tank was full or empty for each hour of data sampled in the frequency and time domains (an acceleration multiplied with the gross mass gives a much higher load than when multiplied with the tare mass). The uncertainty concerning the events during a trip, made it impossible to determine this from the operator data. Special techniques had to be developed to determine from the frequency contents of the data (when full the frequencies tend to shift lower on the accelerometer placed on the tank), whether the tank was full or empty.

4.2.7 Load Haul Dumper

4.2.7.1 Instrumentation

The vehicle was instrumented with eleven strain gauges, two displacement transducers and two accelerometers. The two accelerometers were positioned on the axles of the vehicle and measured the vertical acceleration. The two displacement transducers were used to measure the displacement of the dumping and tilting hydraulic cylinders, but were damaged during the measurement by the low roof. The main purpose of the displacement transducers was to give an indication whether the bucket is up or down, and tilted or not. Fortunately a real-time camera was mounted on the vehicle, which took a photo every three seconds for the full duration of the measurement. The position and orientation of the bucket can be determined from these photographs.

The strain gauge positions are depicted in Figure 4-4 to Figure 4-7. Channels 7 and 8 were located on the widest section of the boom, about 25 mm from the bottom edge of the plate. These two channels measured stresses parallel to the bottom edge of the plate.

Channel 6 was located on the front chassis 100 mm below the top edge of the side plate, coincident with the front axle centre line. The gauge measured stresses in the horizontal direction. Channels 4 and 5 were located 105 mm below the bottom edge of the top plate on the rear chassis, also coincident with the axle centre line.

Channels 1, 2 and 3 were located on the articulation joint. Channels 2 and 3 were located on the bottom hinge plate on the front chassis, coincident with the centre line of the joint. Channel 2 was on the top side and channel 3 on the bottom side of the plate. Channel 1 was located on the bottom side of the lower plate of the top hinge of the articulation joint on the rear chassis, also coincident with the centre line of the joint.

Channels 9 and 10 were mounted on the canopy roof, with channel 10 measuring plate bending stresses in the centre of the roof, and channel 9 measuring stresses on the edge of the roof plate.

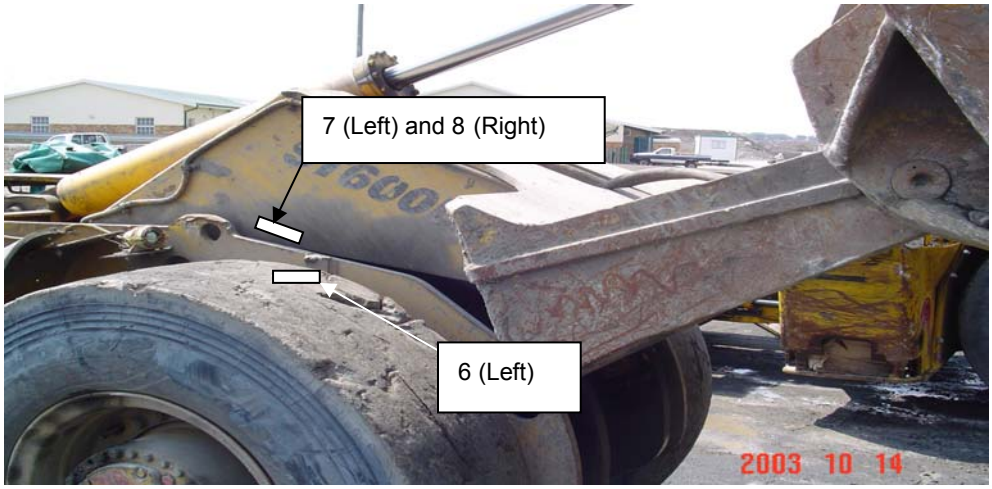

Figure 4-4 Channels 6, 7 and 8

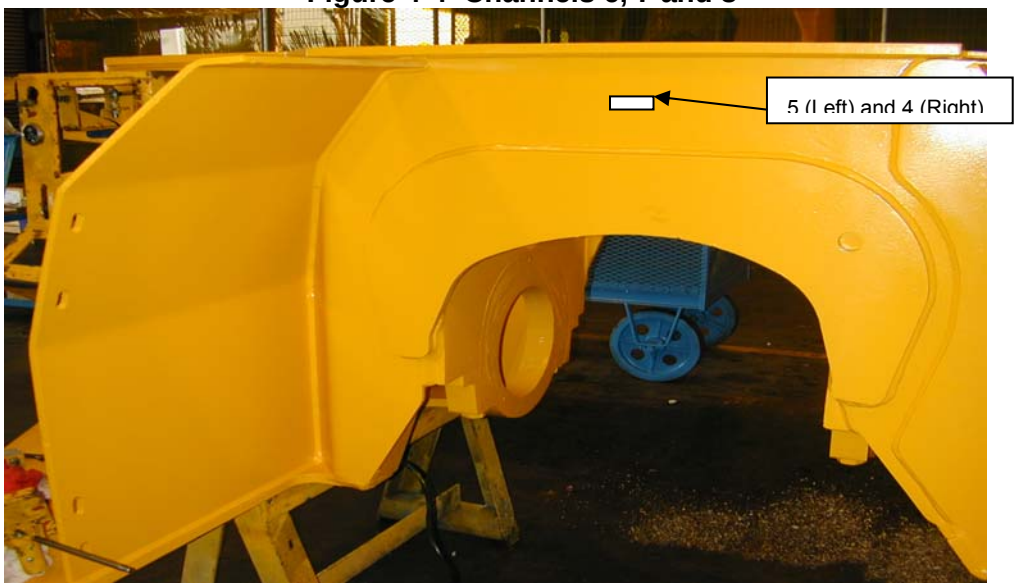

Figure 4-5 Channels 4 and 5

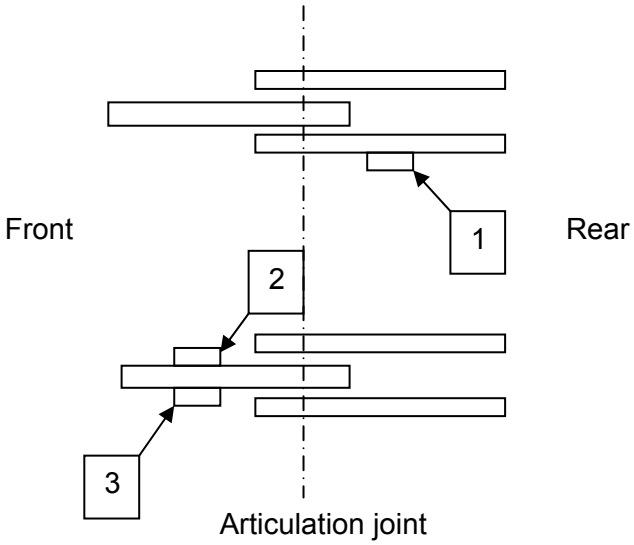

Figure 4-6 Channels 1, 2 and 3

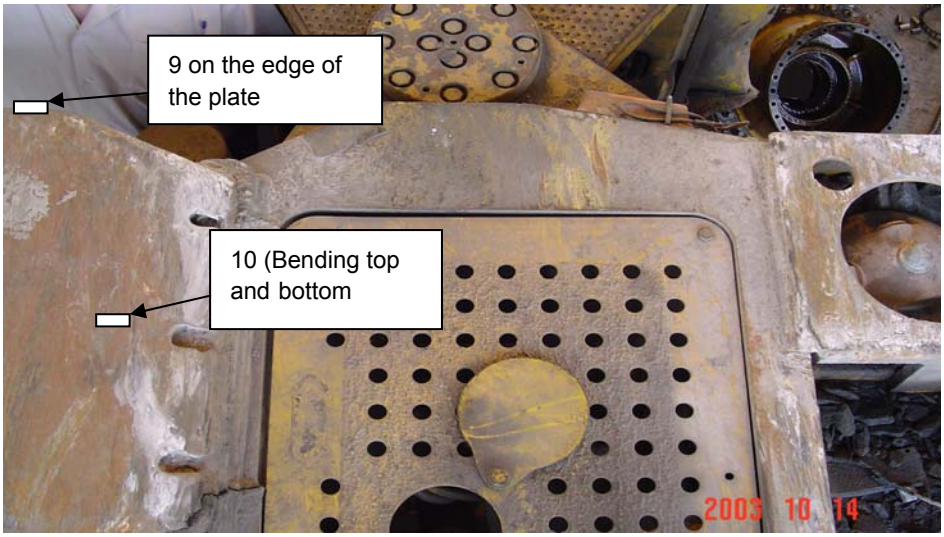

Figure 4-7 Channels 9 and 10

4.2.7.2 Measurements

The measurements were performed at the Waterval platinum mine near Rustenburg. The vehicle was underground for an hour and a half, and data was recorded for the full duration. The vehicle was operated by a regular LHD operator, performing typical tasks. The data was recorded with a SOMAT field computer at a sample rate of 200 Hz.

4.2.8 Ladle Transport Vehicle

4.2.8.1 Instrumentation

The configuration for the LTV measurements is detailed in Table 4-2.

Table 4-2 LTV measurement configuration

Channel No.	Position
1	Lid arm, above tower pivot, left side.
2	Lid arm, above tower pivot, right side.
3	Chassis, above bogie, left side.
4	Chassis, above bogie, right side.
5	Crank, above the main shaft, left side.
6	Crank, above the main shaft, right side.
7	Tower cross member quarter point, left side.
8	Tower cross member quarter point, right side.
9	90° element of critical gauge.
10	45° element of critical gauge.
11	0° element of critical gauge.

The data was recorded on an HBM Spider sampling at 200 Hz, and then downloaded onto a laptop computer.

4.2.8.2 Measurements

Measurements were performed with the vehicle operating typically in the Aluminium Smelter Plant. The events that occurred during the measurement exercise are described below.

Two trips were recorded for the LTV on two routes and stored separately. The events which occurred are shown in the tables below.

Table 4-3 Route 1 events

Event #	Description
1	Start vehicle.
2	Force cranks down to ensure that the bed is properly lowered.
3	Travel empty to fetch full ladle test weight.
4	Pick up full ladle test weight.
5	Travel forward and backwards.
6	Put down full ladle test weight.
7	Travel empty to weigh bridge to fetch empty ladle.
8	Pick up empty ladle #20.
9	Travel along route C2.
10	Put down empty ladle
11	Waiting for full ladle.
12	Picked up full ladle #25.
13	Travel to weigh bridge.
14	Put down full ladle
15	Travel empty approximately 40m forward to park and download data.

Table 4-4 Route 2 events

Event #	Description
1	Start vehicle.
2	Travel empty to weigh bridge to fetch empty ladle.
3	Pick up empty ladle #45.
4	Travel along route C1.
5	Put down empty ladle
6	Used the LTV to nudge the ladle and stand into the correct position and waited for full ladle.
7	Picked up full ladle #7.
8	Travel to weigh bridge.
9	Put down full ladle.
10	Travel empty to the mobile workshop.

4.3 SURVEYS

4.3.1 General

As discussed in paragraph 3.5.2, the influence of driver behaviour, driving patterns and road profile usage on the structural input loading of a vehicle is of importance. Often the only way to quantify these parameters is through user surveys. In this section, two user surveys, performed for the light commercial vehicles, are discussed.

4.3.2 Methodology

Thorough planning of user surveys is of utmost importance. The type of technical information required, makes it difficult to formulate the questions such that non-technical persons would be able to provide reliable answers. As an example, a question concerning the percentage distance of usage travelled on bad gravel roads, which has a significant influence on fatigue calculations, may attract biased answers for two reasons. Firstly, non-technical, or even technical persons will often over estimate this percentage, firstly due to the fact that such travelling makes a much larger impression on them than their every day travelling to work and back (being uncomfortable and typically during a special outing), and secondly, answering the question accurately in terms of distance instead of duration (travelling on bad gravel roads would typically be at very slow speed), is difficult. Care should therefore be taken to add redundant questions, so as to verify possible inaccurate answering.

A questionnaire exercise is best performed by professional companies which have access to manufacturer's sales databases. The optimal method is person-to-person surveys, which, for practical reasons, are normally conducted by phone. According to the market research company employed during the minibus case study, the return rate is typically less than 10 % for questionnaires sent out by post.

4.3.3 Minibus

4.3.3.1 Questionnaire exercise

A questionnaire was compiled, in collaboration with the Centre For Proactive Marketing Research, which was filled in by a number of taxi operators. The following information contained in the questionnaire was used for statistical processing:

- Percentage of total distance travelled on the following roads:
  - Highway
  - Central town
  - Suburban
  - Country
  - Smooth gravel
  - Rough gravel
  - Very rough gravel
- Average distance travelled per day

The questionnaire was filled in by 122 minibus taxi operators of all different makes and models operating in different regions in the country.

4.3.4 Pick-up Truck

4.3.4.1 Questionnaire exercise

A questionnaire was compiled, in collaboration with the Centre For Proactive Marketing Research, which was completed by 170 pick-up truck owners. The following information contained in the questionnaire was used for the statistical processing (differing somewhat from the definitions used during the minibus project due to lessons learned):

- Percentage of distance travelled on the following roads:
  - Rural good tar roads
  - Rural bad tar roads
  - Urban tar roads
  - Mountainous and winding tar roads
  - Rural good gravel roads
  - Rural bad gravel roads

- Average distance travelled per month

Data concerning different cargo loads and travelling speeds was also obtained and utilised in the fatigue processing of the measured data.

4.4 SIMULATION

4.4.1 General

In instances where a prototype vehicle, or a similar model do not exist, inputs can be derived through computer simulation. A multi-body dynamic model of the vehicle, including the suspended inertia, the springs and dampers and unsprung masses of the suspension systems and wheels, as well as sometimes, global stiffness characteristics of the vehicle structure, is excited by known terrain profiles, to produce time domain solutions of suspension forces that may then be used as inputs for finite element analyses.

Dynamic simulation also may be used as part of the establishment of maximum loads and static equivalent fatigue loads to avoid the demands of dynamic finite element analyses.

4.4.2 ISO Tank Container

Accelerations were measured on the corner castings of a tank container during normal operation. These inputs were transformed to six rigid base degrees of freedom. A finite element analysis of the container structure was used to derive the three translational and three rotational stiffnesses affecting the motion of the centre of gravity of the container relative to the input base motion. A dynamic simulation, described in paragraph 5.2.2.1.2 was performed, to solve for the six fundamental input loads on the tank.

4.5 CLOSURE

In this chapter, the methods to determine input loading were described for the various case studies. These inputs can then be used to derive design and testing requirements, which is the subject of the next chapter.

5. DESIGN AND TESTING REQUIREMENTS

5.1 SCOPE

This chapter deals with the derivation of design and testing requirements from the measurement, survey and simulation data discussed in the previous chapter. The extraction of fundamental input loading for the definition of the maximum loading limit state, as well as for dynamic finite element analysis, is firstly described.

An approach to establish fatigue equivalent static loading requirements (requiring only static stress analyses but taking fatigue loading into account in a scientific manner), is next presented.

A novel approach, developed by the author, to establish a statistical usage profile (defining both the severity, as well as the magnitude of usage in a fatigue sense, as a probability density function), is described.

The establishment of testing requirements, using both the fatigue equivalent static loading results, as well as the statistical usage profiles, is lastly presented.

As before, the methods are presented as applied to the appropriate case studies.

5.2 FUNDAMENTAL INPUT LOADING

5.2.1 General

In this section, the derivation of fundamental input loading from measured data (for category 1 transducers as defined in paragraph 4.2.5.1) is demonstrated as applied during the bulk tanker case study. Such input loading could be used as input for dynamic finite element analysis, as well as to obtain overload limit state loads.

5.2.2 Maximum Loading Limit State

5.2.2.1 ISO tank container

5.2.2.1.1 Scope

The datalogger recorded accelerations at carefully selected positions on the tank container. From these accelerations maximum loading events were identified. The logger is able to save 256 files that are approximately 1.7 seconds long with a sampling frequency of 602 Hz. The least severe event already recorded is continuously overwritten by more severe events, such that the data recorded at the end of a trip contains the most severe events that the container was subjected to during the measurement period.

The measured acceleration time events were then used as input signals to a mathematical tank container model. From this model the limit state loads (in terms of inertial acceleration [g]) that the tank containers had been subjected to, were determined.

5.2.2.1.2 Dynamic simulation

The measured accelerations at the corner castings serve as input signals for a mathematical model of the tank container. The purpose of the model is to determine the dynamic loads that are transferred between the frame and the tank (vessel) of the container. These loads are expressed in terms of g.

The assumption of an uncoupled six-degree of freedom model (three translational and three rotational degrees of freedom) is made. The model consisted of a mass element that is held into position by spring and damping elements. This is connected to a rigid frame. The measured accelerations are used to excite the frame (refer to Figure 5-1). Two models were used, one with the properties of a full tank container and one that simulated an empty container.

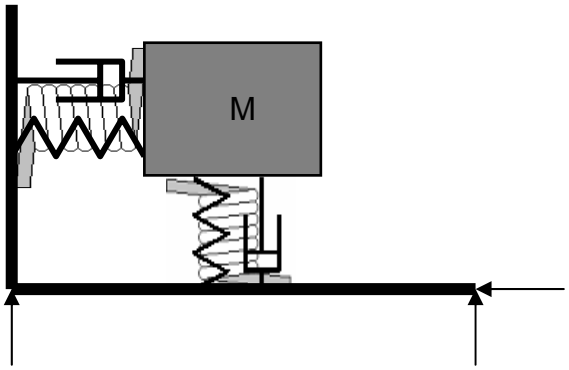

Figure 5-1 Dynamic model of tank container

The dynamic behaviour of the container is described by the equation of motion:

$$[m]\{\ddot{u}\} + [c]\{\dot{u}\} + [k]\{u\} = \{P\}$$

Eq. 5-1

The response was solved by means of the Runge-Kutta method for numerical integration.

From the response the transferred load between the tank and the frame can be calculated by adding the forces at the spring and damping elements. Figure 5-2 shows a typical calculated dynamic loading profile.

5.2.2.1.3 Results

Figure 5-3 shows the maximum amplitude loads, in terms of g, that were calculated for all the full tank container data (the vertical scale is blanks to protect propriety information).

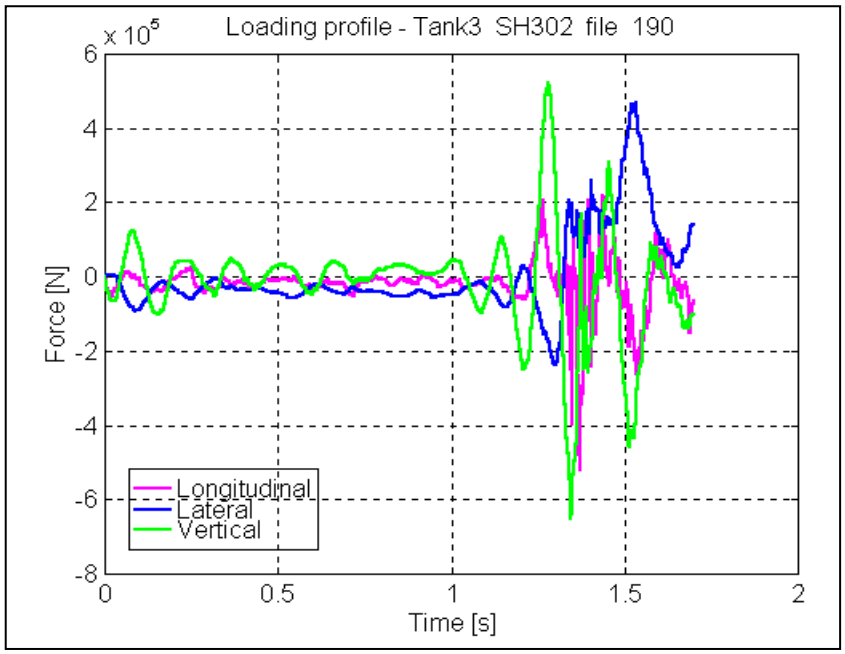

Figure 5-2 Dynamic translational loading profile

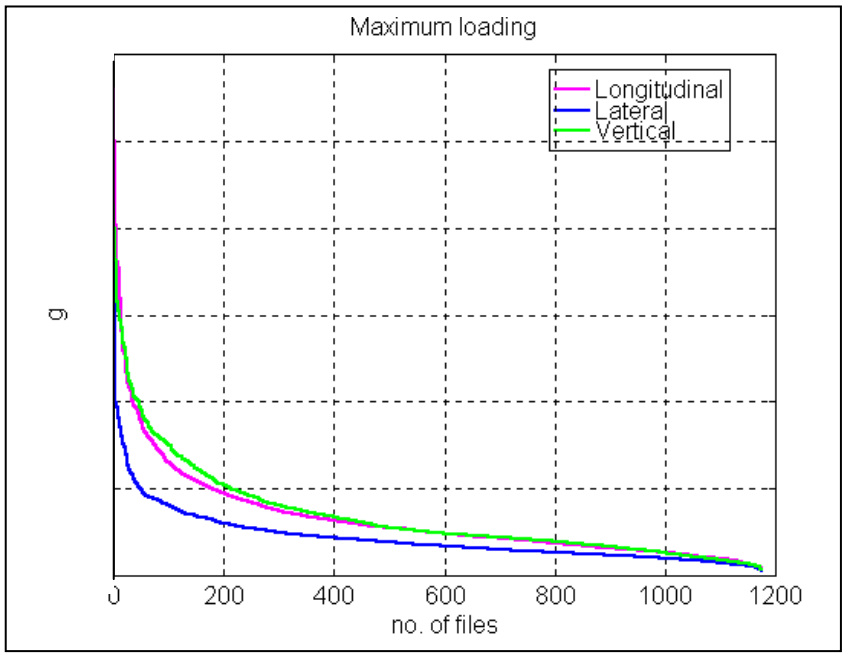

Figure 5-3 Maximum amplitude loads for tank containers

5.2.3 Dynamic Finite Element Analysis

5.2.3.1 General

Measured input loads may be used in a dynamic finite element analysis to calculate stress response.

5.2.3.2 ISO tank container

Figure 5-4 depicts the deformed shape of an ISO tank container at a time instant during a rail road shunting event, using the time domain measured data.

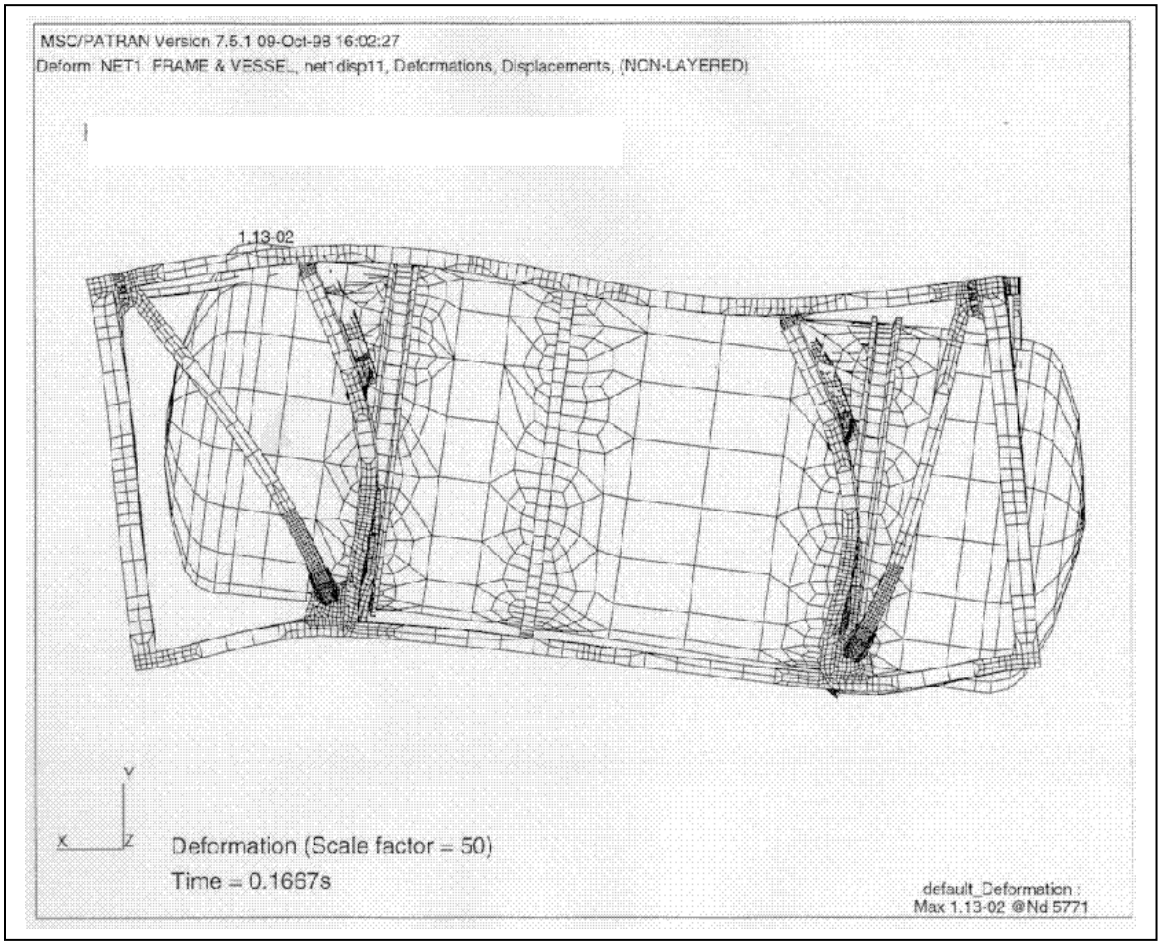

Figure 5-4 Deformed shape of tank container during shunt

The inputs for this dynamic finite element analysis were the measured accelerations on the corner mounts of the tank. Figure 5-5 depicts the correlation between the calculated stress response at a strain gauged position and the directly measured stress during the same event. The benefit of the dynamic finite element analysis method is that stress responses are obtained at all positions on the structure and not only at instrumented positions. The computational effort required is however restrictive. The 4 second event required hours of analysis time.

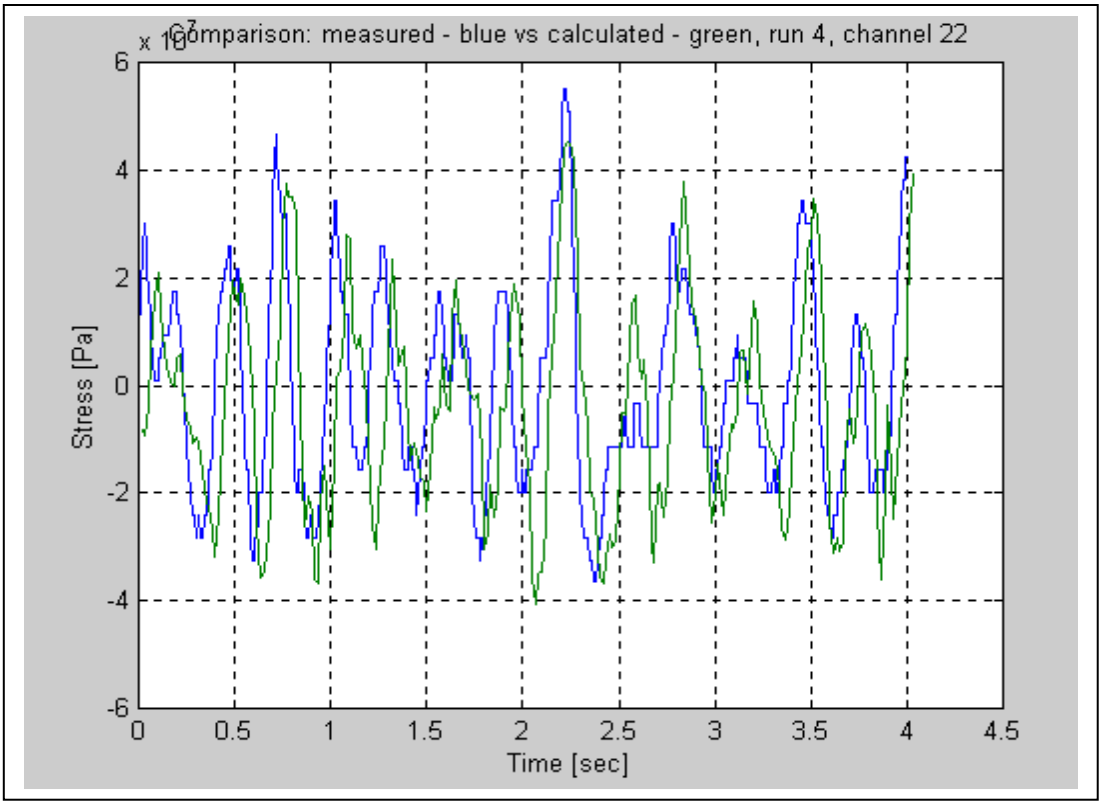

Figure 5-5 Comparison between measured and calculated stresses

5.3 HYBRID MODAL SUPERPOSITION / REMOTE PARAMETER METHOD

5.3.1 General

In paragraph 3.5.8.2.2, the Remote Parameter Analysis (RPA) method, was discussed. The method solves for input loads in the time domain by multiplying measured stresses (remote or indirectly measured parameters) with a transfer matrix between input loads and stresses at the strain gauge positions, which is established through linear-static finite element analysis using unit loads. In the paper by Pountney and Dakin (1992), the method is used to calculate suspension forces, but it could easily be adapted to solve for g-loads, as suggested in paragraph 3.5.8.2.1.

As also suggested in the same paragraph, higher mode response (which could not be described by g-loads), could be taken into account by supplementing the g-load approach with the modal superposition method. The mode-acceleration method discussed in paragraph 3.2.3.4.2 in fact inherently superimposes the quasi-static response with response of excited modes (truncated from the full set of modes).

For the Ladle Transport Vehicle case study, it was required to develop a hybrid methodology, using the RPA method to solve for the quasi-static g-loads, as well as for the modal scaling (participation) factors.

5.3.2 Ladle Transport Vehicle

5.3.2.1 Determination of loading

The measured data (discussed in paragraph 4.2.8) for all the channels were transformed to stresses. For channels 7 and 8, shear stresses were calculated. For the rosette gauge (channels 9,10 & 11), maximum and minimum principal stresses were calculated.

Dynamic loading that could be used together with the finite element model to calculate the dynamic stresses that would cause fatigue, were next derived from the measurement results. For this, the trip 2 data was mainly used, since this trip excluded the test weight event.

Data from channel 3 and 4 (bending gauges on the left and right of the chassis beams) were purposed to derive vertical and lateral loading. The vertical and lateral effects on these 2 channels were decoupled by adding them for vertical and subtracting them for lateral. This is depicted in Figure 5-6. The success of the decoupling can be observed by noticing that the lateral data excludes the effect of the ladle being lifted and put down, whereas the vertical data excludes the effect of turning.

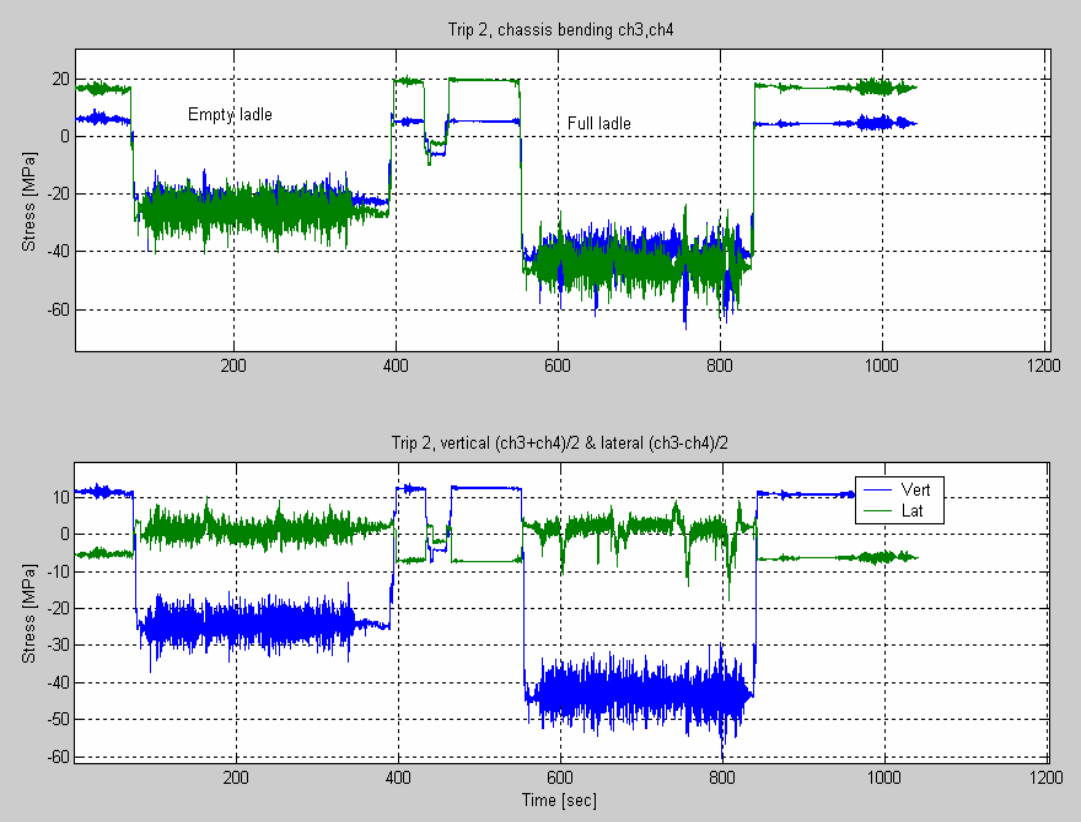

Figure 5-6 Coupled and de-coupled vertical and lateral channels

The frequency content of the channel 3 & 4 data is depicted in Figure 5-7 using a Power Spectral Density plot. Energies at 2.5 Hz, 3.5 Hz and 4.7 Hz were observed. From the decoupled data, it can be seen that the 3.5 Hz frequency belongs to the vertical motion (found to the second natural frequency - vertical bending - of the trailer on its wheels) and the 2.5 Hz frequency belongs to the lateral motion (found to be the first natural frequency – rolling – of the trailer on its wheels).

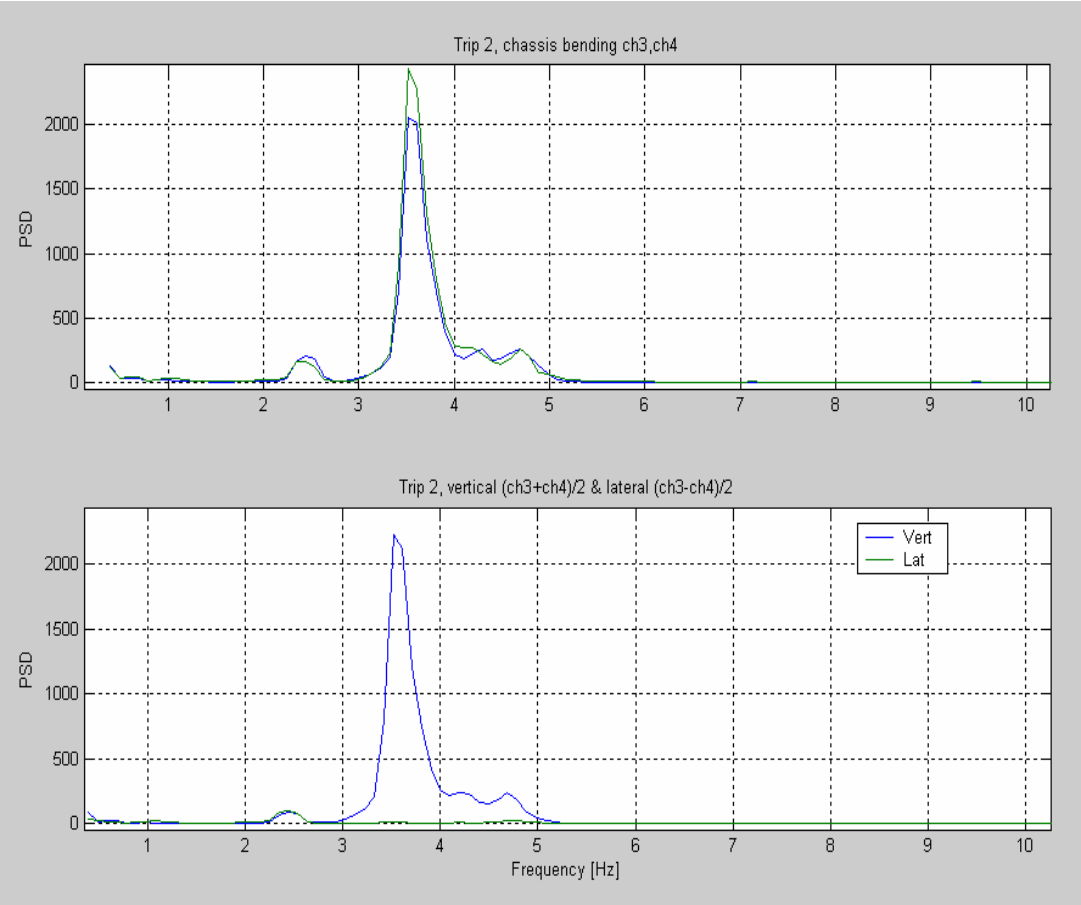

Figure 5-7 Frequency contents of coupled and de-coupled vertical and lateral channels

By also decoupling the data from channels 5 and 6 (crank left and right) and then comparing the vertical data to the vertical data obtained from channels 3 and 4, it was found that it was mostly proportional to each other by a constant factor, which is the same factor determined from the finite element model for pure vertical loading, implying that very little longitudinal loading was present.

The shear gauges (channels 7 & 8) and the rosette gauges (channels 9, 10 & 11), exhibited significant energy at a frequency of 4.7 Hz. This corresponds to the third natural mode, which is a twisting mode of the pillars, with the lid swinging laterally, as depicted in Figure 5-8.

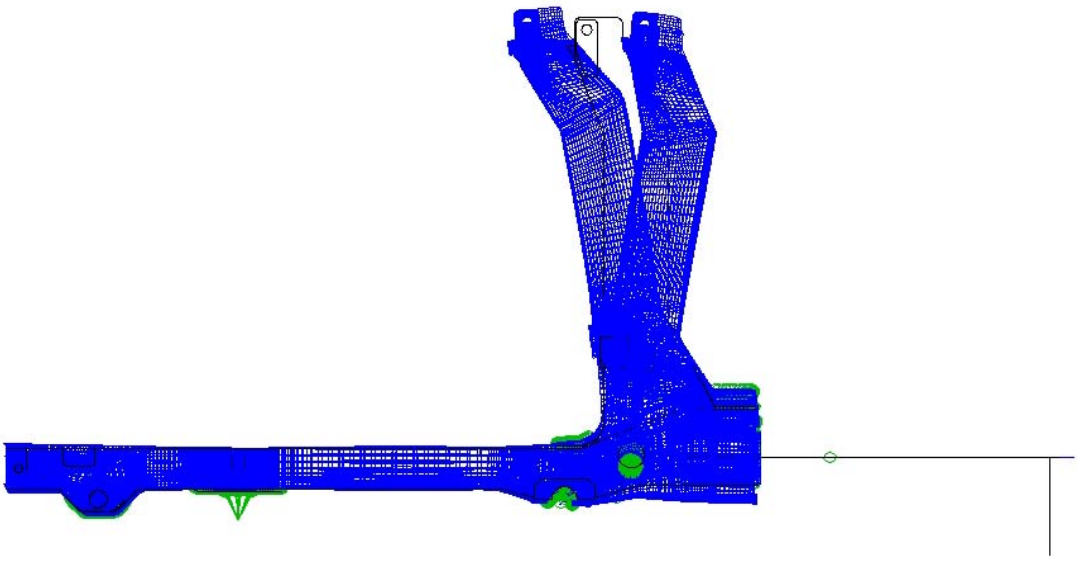

Figure 5-8 Pillar twisting modeshape

This mode cannot be excited if the lid is resting on the ladle, as was the design intent. From the measurements, it was observed that the lid sometimes was resting on the ladle (during trip 1 with a full ladle) and other times not (both trips with the empty ladles and trip 2 with the full ladle). The effect that this had on the strain gauges on the pillars (channels 7 – 11) is depicted in Figure 5-9, showing the significantly lower strains measured on channel 9 during trip 1 with a full ladle, compared to trip 2. The energy at 4.7 Hz during trip 2 and the corresponding reduction of this energy when the lid settles on the ladle during trip 1, can be observed from the frequency plots in Figure 5-10.

Three 'load cases' were therefore identified as having an influence on the dynamic stress/strain response of the structure, namely, vertical loading, lateral loading, as well as the excitation of the third mode shape, if the lid is not resting on the ladle.

The finite element results for these three load cases (unit g loads for the vertical and lateral and modal stresses for the third mode shape) were determined at the various strain gauge positions. The FEA results, as well as the measured results for channels 7 and 8 were identical and therefore only channel 7 was used. The three rosette gauge results were not converted to stress.

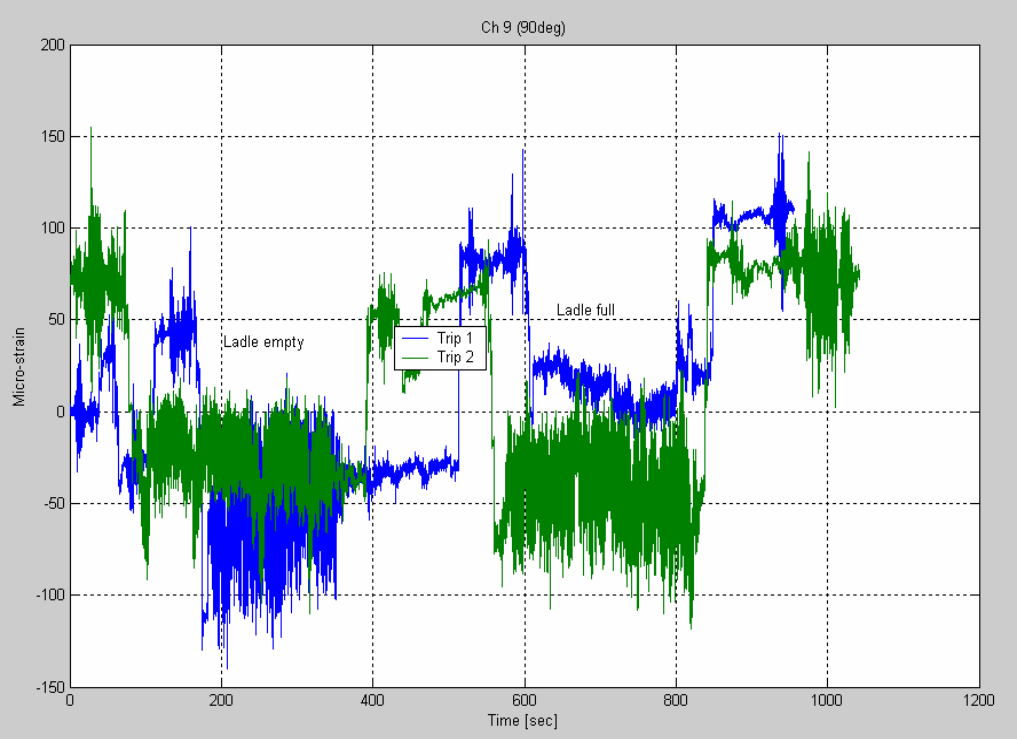

Figure 5-9 Pillar strain gauge for 2 trips

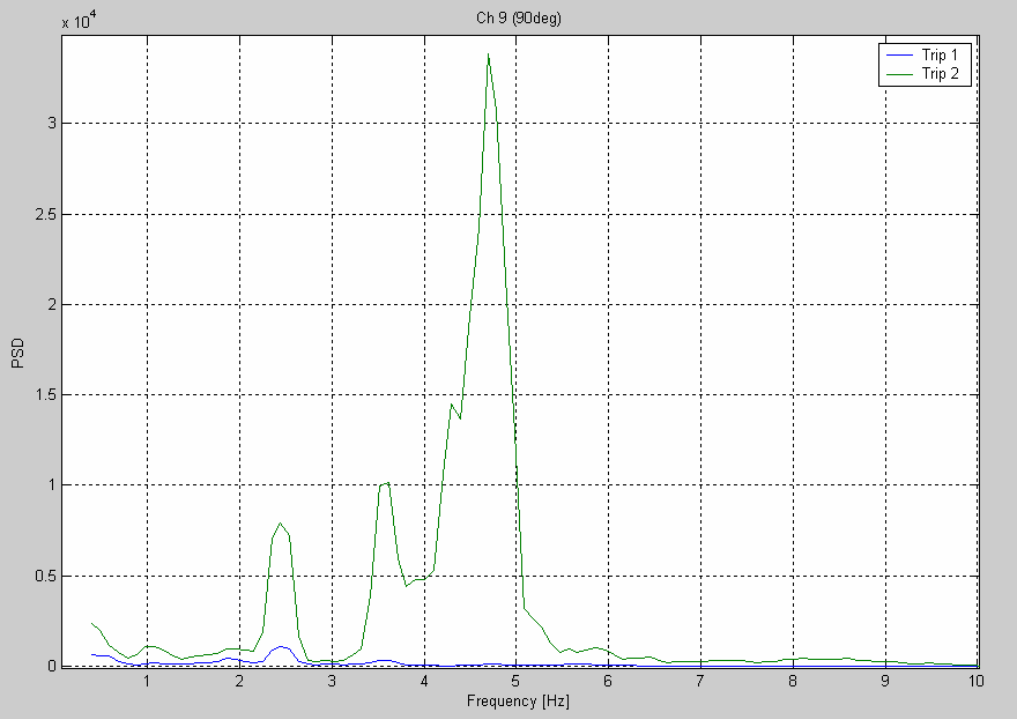

Figure 5-10 Pillar strain gauge frequency content for lid resting and lid not resting

The unit load results were written into the following matrix:

$$[K_{unit\_load\_\sigma\varepsilon}] = \begin{bmatrix} \sigma_{ch3,1gvert} & \sigma_{ch3,1glat} & \sigma_{ch3,modal} \\ \sigma_{ch4,1gvert} & \sigma_{ch4,1glat} & \sigma_{ch4,modal} \\ \sigma_{ch5,1gvert} & \sigma_{ch5,1glat} & \sigma_{ch5,modal} \\ \sigma_{ch6,1gvert} & \sigma_{ch6,1glat} & \sigma_{ch6,modal} \\ \sigma_{ch7,1gvert} & \sigma_{ch7,1glat} & \sigma_{ch7,modal} \\ \varepsilon_{ch9,1gvert} & \varepsilon_{ch9,1glat} & \varepsilon_{ch9,modal} \\ \varepsilon_{ch10,1gvert} & \varepsilon_{ch10,1glat} & \varepsilon_{ch10,modal} \\ \varepsilon_{ch11,1gvert} & \varepsilon_{ch11,1glat} & \varepsilon_{ch11,modal} \end{bmatrix} = \begin{bmatrix} 52.5 & -98 & 0.22 \\ 52.5 & 98 & -0.22 \\ 32 & -36 & -0.2 \\ 32 & 36 & 0.2 \\ 0 & 6 & 0.262 \\ 11.5 & 109 & 10.6 \\ -37.6 & 191 & 9.04 \\ -15.2 & 207 & 5.06 \end{bmatrix} \begin{matrix} MPa \\ MPa \\ MPa \\ MPa \\ MPa \\ \mu\varepsilon \\ \mu\varepsilon \\ \mu\varepsilon \end{matrix}$$

Eq. 5-2

In order to derive the vertical and lateral loads, decoupled channel 3 and 4 results were used, together with the channel 7 results, to solve for the modal contribution. The transfer matrix was therefore calculated as follows:

$$[K_{decoupled}] = \begin{bmatrix} \frac{(\sigma_{ch3,1gvert} + \sigma_{ch4,1gvert})}{2} & \frac{(\sigma_{ch3,1glat} + \sigma_{ch4,1glat})}{2} & \frac{(\sigma_{ch3,modal} + \sigma_{ch4,modal})}{2} \\ \frac{(\sigma_{ch3,1gvert} - \sigma_{ch4,1gvert})}{2} & \frac{(\sigma_{ch3,1glat} - \sigma_{ch4,1glat})}{2} & \frac{(\sigma_{ch3,modal} - \sigma_{ch4,modal})}{2} \\ \sigma_{ch7,1gvert} & \sigma_{ch7,1glat} & \sigma_{ch7,modal} \end{bmatrix}$$

$$[K_{decoupled}] = \begin{bmatrix} 52.5 & 0 & 0 \\ 0 & -98 & -0.22 \\ 0 & 6 & 0.262 \end{bmatrix}$$

Eq. 5-3

The vertical and lateral g-loads, as well as the modal participation factor (all three as time histories), could therefore be solved as follows:

$$[K]\begin{Bmatrix} Vert\_g \\ Lat\_g \\ Modal\_part\_fact \end{Bmatrix} = \{\sigma\}$$

$$[K_{decoupled}]\begin{Bmatrix} Vert\_g(t) \\ Lat\_g(t) \\ Modal\_part\_fact(t) \end{Bmatrix} = \begin{Bmatrix} \frac{(\sigma_{ch3,meas}(t) + \sigma_{ch4,meas}(t))}{2} \\ \frac{(\sigma_{ch3,meas}(t) - \sigma_{ch4,meas}(t))}{2} \\ \sigma_{ch7,meas}(t) \end{Bmatrix}$$

$$\begin{Bmatrix} Vert\_g(t) \\ Lat\_g(t) \\ Modal\_part\_fact(t) \end{Bmatrix} = [K_{decoupled}]^{-1}\begin{Bmatrix} \frac{(\sigma_{ch3,meas}(t) + \sigma_{ch4,meas}(t))}{2} \\ \frac{(\sigma_{ch3,meas}(t) - \sigma_{ch4,meas}(t))}{2} \\ \sigma_{ch7,meas}(t) \end{Bmatrix}$$

Eq. 5-4

This was done for trip 2, which included excitation of the third mode for both the empty and full ladle sections. The results are depicted in Figure 5-11 and Figure 5-12.

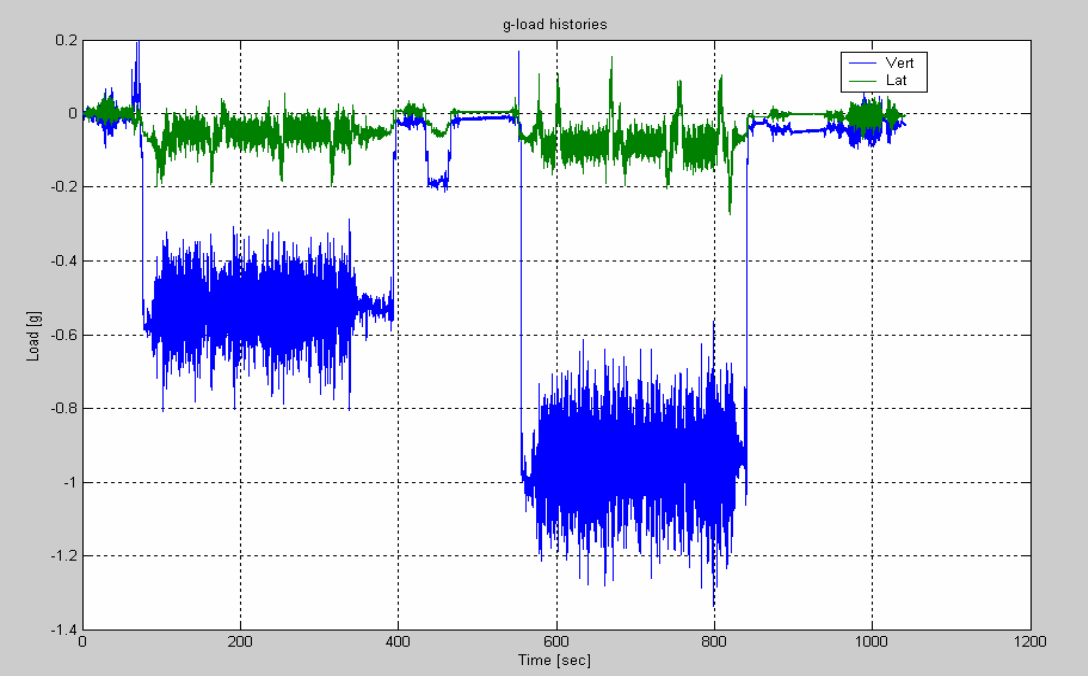

Figure 5-11 Vertical and lateral g-loads

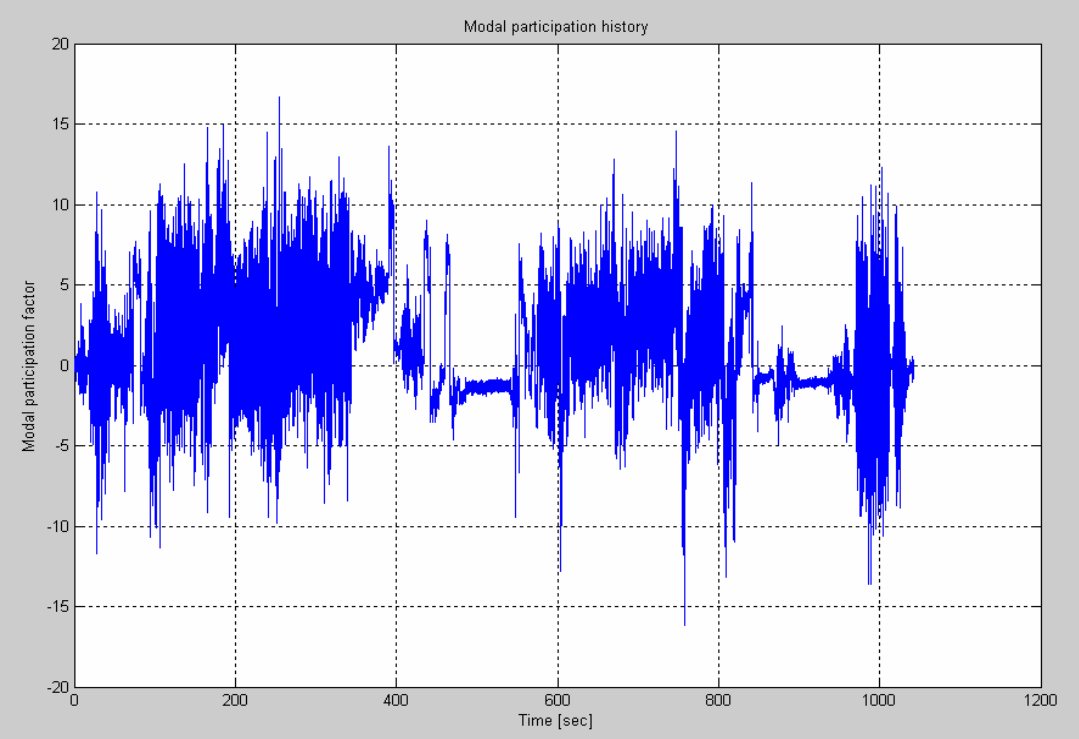

Figure 5-12 Modal participation factor

The loads thus derived could then be used to calculate time histories for all the measured channels, as follows:

$$\begin{Bmatrix} \sigma_3(t) \\ \sigma_4(t) \\ \sigma_5(t) \\ \sigma_6(t) \\ \sigma_7(t) \\ \varepsilon_9(t) \\ \varepsilon_{10}(t) \\ \varepsilon_{11}(t) \end{Bmatrix} = [K_{unit\_load\_\sigma\varepsilon}] \begin{Bmatrix} Vert\_g(t) \\ Lat\_g(t) \\ Modal\_part\_fact(t) \end{Bmatrix}$$

Eq. 5-5

These calculated results may then be compared to the measured time histories. For channels 3, 4 and 7 they are mathematically identical, whereas the success of comparison for the other (redundant) channels gives the confidence that the non-active loads were disregarded and that the results may be used to determine fatigue stresses on the total structure. The comparison is performed by comparing normalized fatigue damages, calculated using the Stress Life method from the measured, as well as the derived time histories. The results are listed in Table 5-1.

Table 5-1 Comparison between measured and calculated normalised damages

	Ch3	Ch4	Ch5	Ch6	Ch7	Ch9	Ch10	Ch11
Measured	97	107	68	77	18	354	483	342
Calculated	97	107	60	60	18	533	471	282

5.4 FATIGUE EQUIVALENT STATIC LOADING

5.4.1 General

Due to the cost of dynamic finite element analyses, as well as the restrictive number of critical positions that can be instrumented for direct fatigue analysis, there is an incentive to simplify the fatigue design process. Such a simplified procedure is also required for design codes, since codes could not stipulate the use of dynamic finite element analysis methods, or measurements, since this would restrict their usage to only sophisticated users, as well as requiring the availability of an existing structure for measurements.

In many industries, design codes or less formal design criteria are used where allowance for fatigue is simply made by prescribing higher than limit state design loads and/or incorporating safety factors on the allowable stresses. The origin and applicability of such criteria are often uncertain.

In the following paragraph, a methodology for deriving fatigue equivalent static criteria for fatigue design, is proposed.

5.4.2 Methodology

5.4.2.1 Uni-axial axis method

Using measured data, a fatigue design criterion can be developed that requires only static finite element analysis. In the case of heavy vehicles, the vertical bending stress (measured for example on the vehicle chassis) can be used, due to the fact that it is assumed that the vertical induced loads would represent most of the fatigue damage experienced on a vehicle structure.

5.4.2.1.1 Measurements

In the derivation below, a transport vehicle (considered to be typical in terms of weight, suspension etc. of all vehicles in its class) is assumed to have been instrumented with strain gauges on its main chassis beams, measuring vertical bending stresses. The vehicle is assumed to have been driven on roads representative of normal usage for a distance of 200 km whilst measurements were taken.

5.4.2.1.2 Measured damage calculation

The measured stress-time histories are cycle-counted, to yield a spectrum of stress ranges ($\Delta\sigma_i$) and number of counted cycles (n_i). A relative fatigue damage (relative because generic material properties, b and S_f are used) can be calculated using the stress-life approach. The exponent (b) of the stress-life equation is chosen as –0.33, being the gradient of almost all of the SN-curves in fatigue design codes (ECCS (1985), BS 8118 (1991)), whilst the coefficient S_f is arbitrary, since it will cancel out in the calculation.

Firstly, the number of cycles to failure at each stress range can be calculated with the reverse of Eq. 3-14:

$$N_i = \left(\frac{\Delta\sigma_i}{S_f} \right)^{1/b} \qquad \textbf{Eq. 5-6}$$

Then the total damage is calculated using Miner's damage accumulation theory (Eq. 3-21):

$$\text{Damage} = \sum \frac{n_i}{N_i} = \sum \frac{n_i}{\left(\frac{\Delta\sigma_i}{S_f}\right)^{1/b}} \qquad \textbf{Eq. 5-7}$$

5.4.2.1.3 Equivalent stress range calculation

The purpose then would be to obtain an equivalent bending stress range which would, when repeated an arbitrary (n_e) times, cause the same damage to the beam to what would be caused during the total life (e.g. 1 million km) of the vehicle, made out of repetitions of the measured trip.

This damage could be calculated as follows:

$$N_e = \left(\frac{\Delta\sigma_e}{S_f}\right)^{1/b}$$

$$\text{Damage}_e = \frac{n_e}{N_e} = \frac{n_e}{\left(\frac{\Delta\sigma_e}{S_f}\right)^{1/b}} \qquad \textbf{Eq. 5-8}$$

$\Delta\sigma_e$ can be solved by equating:

$$\text{Damage}_e = \text{Damage} \times 1 \text{ million km} / 200 \text{ km} \qquad \textbf{Eq. 5-9}$$

Therefore, combining Eq. 5-7, Eq. 5-8 and Eq. 5-9:

$$\sum \frac{n_i}{\left(\frac{\Delta\sigma_i}{S_f}\right)^{1/b}} = \frac{n_e}{\left(\frac{\Delta\sigma_e}{S_f}\right)^{1/b}}$$

$$\Delta\sigma_e = \left(\sum \frac{\Delta\sigma_i{}^m n_i}{n_e}\right)^{1/m} \qquad \textbf{Eq. 5-10}$$

With n_e=2 million

m= −1/b=3

n_i=cycles counted for each stress range from the total measured trip, multiplied by 1million/200

The arbitrary choice of n_e = 2 million was done because the fatigue classifications in the ECCS code are denoted by the stress range values in MPa at 2 million cycles, for each SN-curve.

5.4.2.1.4 Fatigue equivalent static loading calculation

The bending stress (σ_{1g}), caused by 1 g (unit) vertical inertial loading at the strain gauge position, is then calculated using finite element analysis.

The fatigue equivalent static loading (FESL), is then calculated as follows:

$$FESL = \frac{\Delta\sigma_e}{\sigma_{1g}}$$

Eq. 5-11

This load is a single axis (vertical), inertial load range (i.e. peak-to-peak), measured in [g], which, when applied 2 million times, would represent the fatigue loading of 1 million kilometres.

5.4.2.1.5 Life assessment

The FESL is then applied on the finite element model in a static analysis. The stresses thus calculated are interpreted as stress ranges, which would be repeated 2 million times during the life of 1 million kilometres. The fatigue life at each critical position may then be calculated, using the appropriate SN-curve relevant to the detail at each position.

The fatigue damage calculated at the strain gauge position (using the same SN-curve as for the measured damage calculation) would be equal to the measured damage, due to Eq. 5-9. It is then assumed that the operational dynamic stress responses at any other position on the structure, are proportional to the dynamic stress at the strain gauge position by the same constant factor as the ratio between the vertical-static-inertial-load stress responses at the other positions and the strain gauge position. If this is the case, the fatigue damages calculated at the other positions would be the same as what would have been calculated from measured dynamic stresses at those positions.

In the application of the FESL method, it would therefore be good practice to place redundant (not used for FESL calculation) strain gauges on the structure. The measurements from the redundant gauges may then be used to calculate fatigue damages that may be compared to those calculated using the FESL. Close correlation would imply a high confidence level in the validity of the assumptions made. The placement and number of redundant gauges are important and are demonstrated in paragraph 5.2.2.1.3.

5.4.2.2 Multi-axial loading method

In certain cases, the assumption that the contribution of loads other than vertical to fatigue damage may be neglected, cannot be made. Sedan vehicles are mostly used on well surfaced roads, but are cornering and braking more frequently and more severely than heavier vehicles, implying that longitudinal and lateral loads should be considered. Tank containers are subjected to severe longitudinal loading during rail shunting operations. Heavy vehicles with high centres-of-gravity may exhibit relatively high frequency and magnitude rocking response, implying lateral loading.

The single axis method described in the previous paragraphs may easily be adapted to take into account multi-axial loading. The vehicle chassis, used as an example in the single axis method derivation, will again be employed, but the assumption is now made that vertical, longitudinal, as well as lateral inertial loading, are to be considered.

5.4.2.2.1 Measurements

To be able to solve three FESLs, three non-redundant strain gauge channels are required. The correct placement of these gauges is non-trivial. Three bending gauges

next to each other on one of the chassis beams would obviously measure the same for any of the three loads and could therefore not be used to solve three unknown loads.

In this idealised example, three bending gauges are placed as depicted in Figure 5-13, representing a chassis frame, the four wheel positions, as well as two cross beams. The chassis would be loaded by inertial loads on some mass connected to the chassis beams at various places and is supported at the wheel positions. Channels 1 and 3 would respond the same for vertical and longitudinal loads, but differently for a lateral load, whereas channel 2 would respond differently to all three loads to the other two channels. Measurements are recorded on a typical route as before.

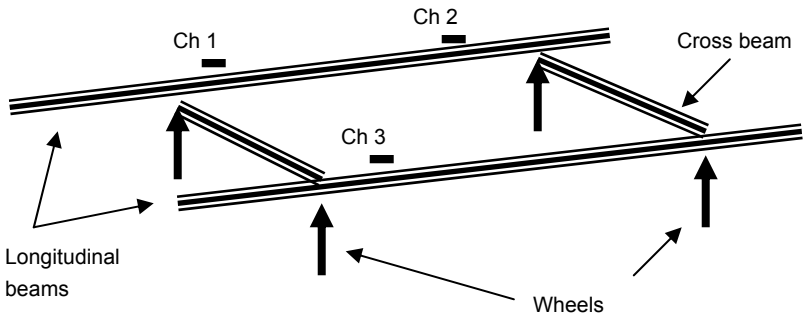

Figure 5-13 Idealised chassis with strain gauges

5.4.2.2.2 Measured damage calculation

As described in paragraph 5.4.2.1.2 above, rainflow cycle counting is performed on the data of all three channels, yielding σ_i and n_i results for all three.

5.4.2.2.3 Equivalent stress range calculation

Employing again Eq. 5-10, the equivalent stress range ($\Delta\sigma_{e,chj}$) for each channel (j) is calculated:

$$\Delta\sigma_{e,chj} = \left(\sum \frac{\Delta\sigma_i{}^m n_i}{n_e} \right)^{1/m}$$

5.4.2.2.4 Fatigue equivalent static loading calculation

The finite element model is loaded with separate unit inertial loads in the three directions and the stress responses ($\sigma_{load,chj}$) at each of the strain gauge positions and for each load, are determined. The stress response (σ_{chj}) at the three gauge positions due to a combined inertial load case would then be:

$$\begin{bmatrix} \sigma_{vert,ch1} & \sigma_{long,ch1} & \sigma_{lat,ch1} \\ \sigma_{vert,ch2} & \sigma_{long,ch2} & \sigma_{lat,ch2} \\ \sigma_{vert,ch3} & \sigma_{long,ch3} & \sigma_{lat,ch3} \end{bmatrix} \begin{Bmatrix} g_{vert} \\ g_{long} \\ g_{lat} \end{Bmatrix} = \begin{Bmatrix} \sigma_{ch1} \\ \sigma_{ch2} \\ \sigma_{ch3} \end{Bmatrix}$$

Eq. 5-12

Rearranging Eq. 5-12 and substituting the equivalent stress range results, enable the calculation of the FESL in three directions:

$$FESL = \begin{Bmatrix} \Delta g_{vert} \\ \Delta g_{long} \\ \Delta g_{lat} \end{Bmatrix} = \begin{bmatrix} \sigma_{vert,ch1} & \sigma_{long,ch1} & \sigma_{lat,ch1} \\ \sigma_{vert,ch2} & \sigma_{long,ch2} & \sigma_{lat,ch2} \\ \sigma_{vert,ch3} & \sigma_{long,ch3} & \sigma_{lat,ch3} \end{bmatrix}^{-1} \begin{Bmatrix} \Delta\sigma_{e,ch1} \\ \Delta\sigma_{e,ch2} \\ \Delta\sigma_{e,ch3} \end{Bmatrix}$$

Eq. 5-13

The above equation may be generalised for any number of inertial or non-inertial loads $\{L_{i=1\ to\ a}\}$, requiring (a) measurement channels to solve (a) fatigue factors $\{FF_{i=1\ to\ a}\}$, for every load:

$$FESL = \begin{Bmatrix} FF_1 \\ : \\ FF_a \end{Bmatrix} = \begin{bmatrix} \sigma_{1,ch1} & .. & \sigma_{a,ch1} \\ : & :: & : \\ \sigma_{1,cha} & .. & \sigma_{a,cha} \end{bmatrix}^{-1} \begin{Bmatrix} \Delta\sigma_{e,ch1} \\ : \\ \Delta\sigma_{e,cha} \end{Bmatrix}$$

Eq. 5-14

5.4.2.2.5 Life assessment

The calculated loads are applied simultaneously to the finite element model. The stresses thus calculated again may be interpreted as stress ranges to be applied 2 million times during a 1 million kilometre life. Using the appropriate SN-curves for each critical position, the fatigue life of the total structure may be calculated.

5.4.3 Comparison with Remote Parameter Analysis Method

The uni-axial FESL method would yield exactly the same results as the uni-axial RPA method, with the only difference being that the cycle counting is performed directly on the single measurement signal, thereafter using Fatigue Equivalent Static loads and stresses, instead of calculating load and stress, time histories first and then performing cycle counting on all critical stress histories. The FESL method therefore improves on the RPA method by being less computationally intensive.

A further important improvement is achieved due to the fact that the FESL method results in a single, design independent load requirement, which could be used in design codes.

The multi-axial FESL method achieves the same advantages over the multi-axial RPA method, but does not yield the same life prediction results on the total structure. This discrepancy is due to the fact that phase information is lost after the conversion of the multi-axial time histories to Fatigue Equivalent Static Loads.

If the idealised chassis example depicted in Figure 5-13 was subjected to exactly in-phase (or 180° out-of-phase) sine wave inertial loading in the vertical and lateral directions (with no longitudinal load), each load causing the same amplitude of stresses at channels 1 and 3, the measured result would be double the amplitude on one of the channels and zero amplitude on the other, resulting in the latter channel having a zero $\Delta\sigma_e$. The σ_{1g} results would be the same in absolute magnitude for both channels and both loads, but would be of the same sign for the vertical loading and of opposite signs for the lateral loading. The FESL result would then be correctly calculated, resulting in $\Delta g_{vert} = \Delta g_{lat}$.

If, however, the vertical and lateral loads are randomly out-of-phase, as would normally be the case, the FESL calculation may often result in $\Delta\sigma_{e,ch1}$ being approximately equal to $\Delta\sigma_{e,ch3}$, since the combined vertical and lateral loading would statistically cause similar stress responses on both chassis rails. In this case, the solution of Δg_{vert} and Δg_{lat} would be ill-conditioned. If the vertical and lateral loading were decoupled before cycle counting, by adding the two channels for vertical loading and subtracting them for lateral loading, 'more correct' results for Δg_{vert} and Δg_{lat} would be achieved, but application of these loads in a static finite element analysis would yield an overestimated damage on the one rail (where the two loads, now implicitly in-phase, are superimposed) and an underestimated damage on the other (where the loads would out-of-phase).

5.4.4 Fuel Tanker

5.4.4.1 Finite element analysis

Detailed finite element half models were constructed of the front and rear trailers, employing mainly shell elements. 1 g vertical inertial loading was applied. The liquid load was simulated using pressure loading. The front trailer model and results are depicted in Figure 5-14 and Figure 5-15.

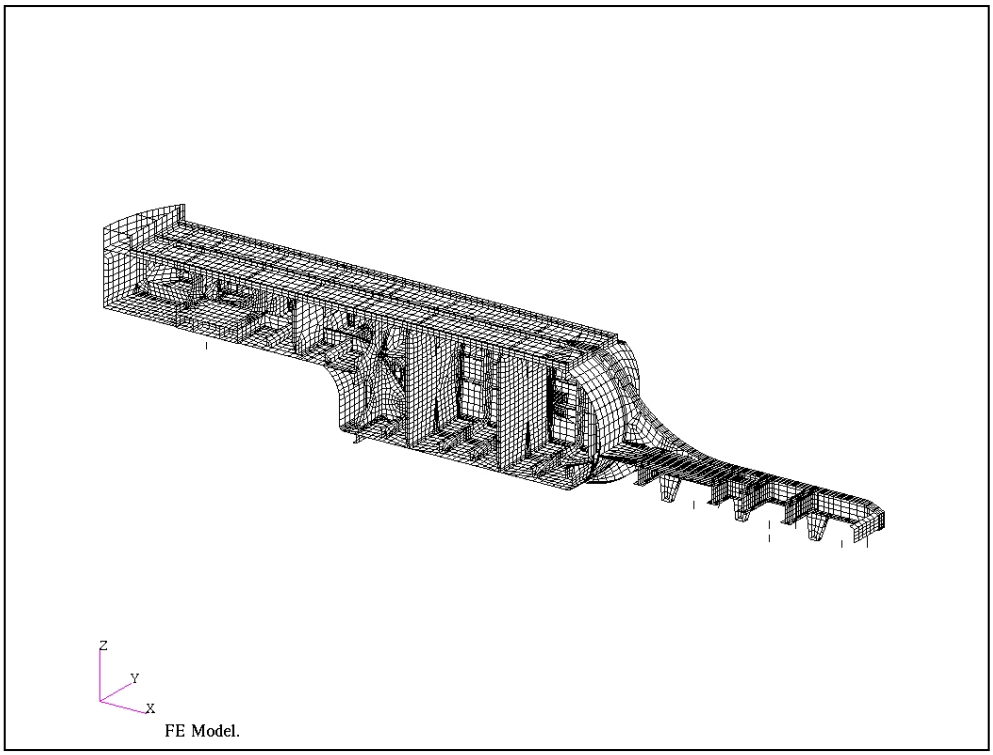

Figure 5-14 Finite element model of fuel tanker front trailer

5.4.4.2 Measured damage calculation

Fatigue damage calculations were performed on the measured data, using the process depicted in Figure 3-11. A fatigue exponent of b=-0.333 was used.

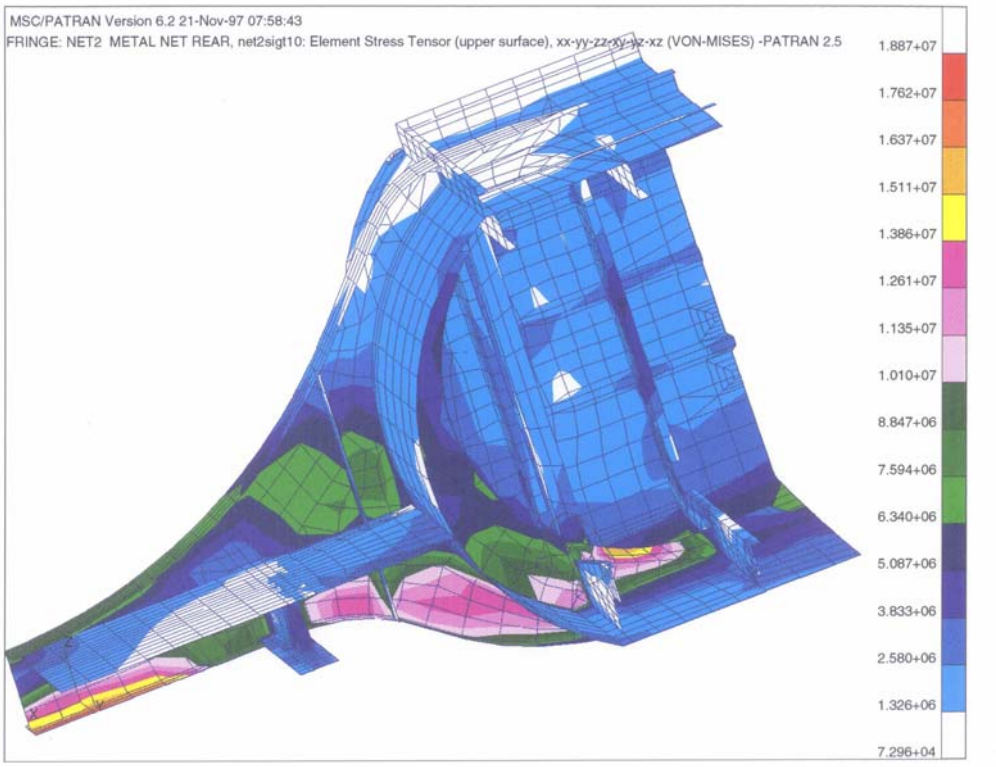

Figure 5-15 Finite element results on fuel tanker front trailer

5.4.4.3 Fatigue equivalent static load calculation

The bending stress measured by channel 34 on the front trailer chassis was used for the FESL calculation, due to the fact that it is again assumed that the vertically induced loads would represent most of the fatigue damage experienced on the vehicle structure. An equivalent stress range corresponding to 2 million cycles (arbitrarily chosen to correspond to the number of cycles at which the weld class is specified), was calculated which would cause the same damage to what was caused at that channel during the total measured trip extrapolated to a life distance of 2 million kilometres (the fact that the life distance is equal to the chosen cycles is coincidental). Eq. 5-10 was again used for this purpose with: N=2 million, m=3 and n_i=cycles counted for each stress range full the total trip, multiplied by 2 million/distance travelled during measurements.

This was done on the assumption that a life of 2 million kilometres would be expected of these vehicles.

The resultant equivalent stress range was found to be 15.5 MPa. The stress calculated by FEA for a 2 g load was 50 MPa. The equivalent vertical load therefore corresponds to a vertical acceleration of 15.5/50 x 2 g = 0.62 g. It is then implied that any stress calculated in the vehicle structure at 0.62 g vertical loading would be repeated 2 million times during a life of 2 million kilometres. All welds should then be of a class higher than the nominal stress at the weld calculated for 0.62 g loading. According to BS 8118 (1991), the class for a fillet weld would be 20 and for a butt weld 24.

5.4.5 ISO Tank Container

5.4.5.1 Scope

In this section, the processing of the fatigue domain data is described. The purpose of the processing is to determine fatigue loading criteria for the analysis or testing of tank containers. The multi-axial method derived in paragraph 5.4.2.2, was used.

5.4.5.2 Measured data and fatigue processing

A total of approximately 1100 days of data was processed. This included data received from 4 tank containers. The rainflow counting process was performed onboard of the datalogger in real time.

Due to a constraint in the datalogger design, the resolution of the stress ranges counted, together with the corresponding number of cycles, had to be fixed for all channels and all files. All stress ranges between 0 and 24 MPa (first bin) were counted as the same, and so were ranges between 24 and 48 MPa (second bin) and so forth up to 31 bins. For the less sensitive channels and files where the stresses were low, this implied that, if the maximum stress range was less than e.g. 48 MPa, only two bins of counting resulted. A method to improve the resolution after the fact, had to be devised, since it would be inaccurate to assume all counted cycles in e.g. the first bin were 24 MPa large (many smaller cycles would then be overestimated)

5.4.5.3 Improvement of cycle counting resolution

When a log-log plot is made of originally counted cycles vs ranges for well populated channels and files, it was found that the relationship is always linear (which is to be expected from a statistical point of view). This may be observed in Figure 5-16.

A mathematical process was therefore implemented, which repopulated all counting results, by enforcing a linear relationship between cycles and stress ranges on a log-log scale, with the maximum stress range being upper value of the highest bin for which cycles were counted and assumed then to be one cycle and the lowest range being the filter cut-off range of 3.7 MPa and at the same time enforcing the total number of cycles to be the same as the original count.

The results of such an exercise are depicted in Figure 5-17 (original count only in 2 bins) and Figure 5-18 (improved resolution result).

5.4.5.4 Equivalent stress range

The counting results (table of stress range-$\Delta\sigma_i$ and cycles-n_i) for each channel and file are used to calculate a fatigue damage, using Eq. 3-14 and Eq. 3-21:

$$\Delta\sigma = S_f N^b$$

$$S_f = \text{fatigue coefficient}$$

$$b = \text{fatigue exponent}$$

$$D_{ch} = \sum \frac{n_i}{N_i}$$

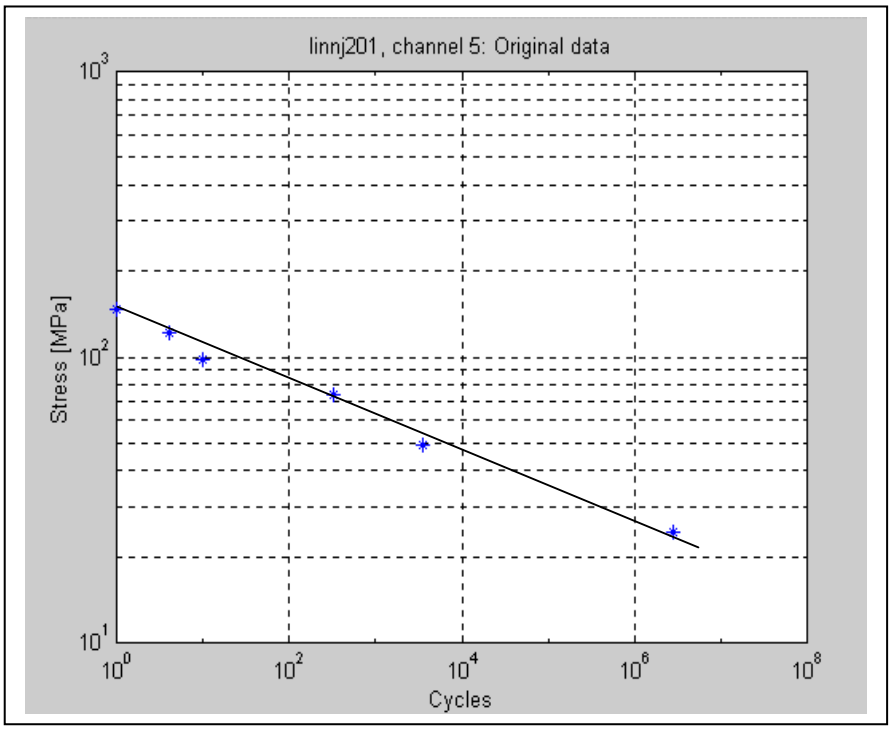

Figure 5-16 Log-log linearity between cycles and stress ranges

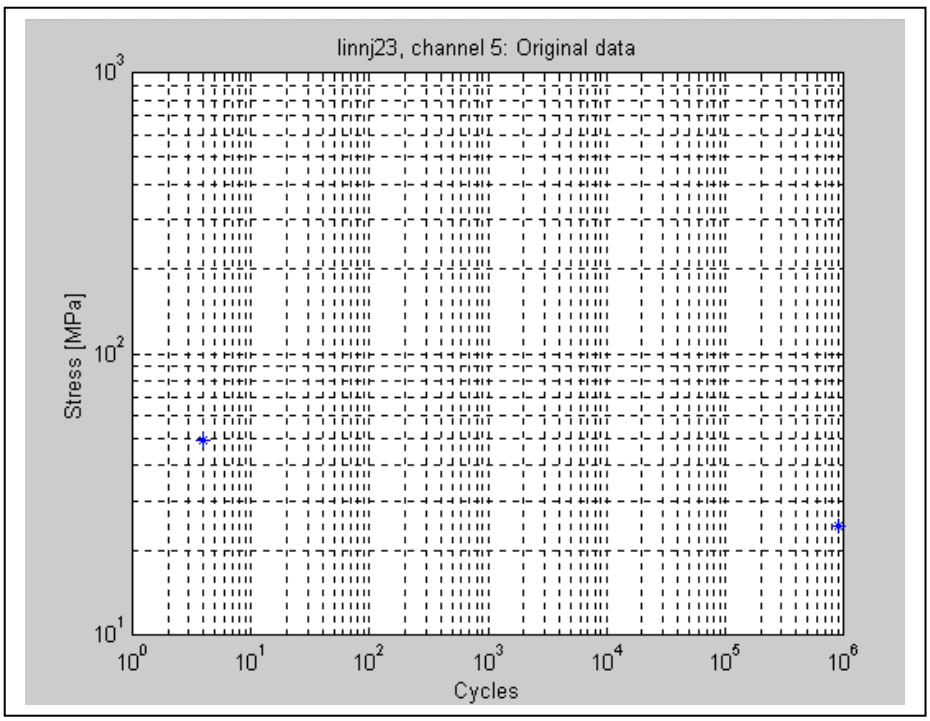

Figure 5-17 Data before improvement of resolution

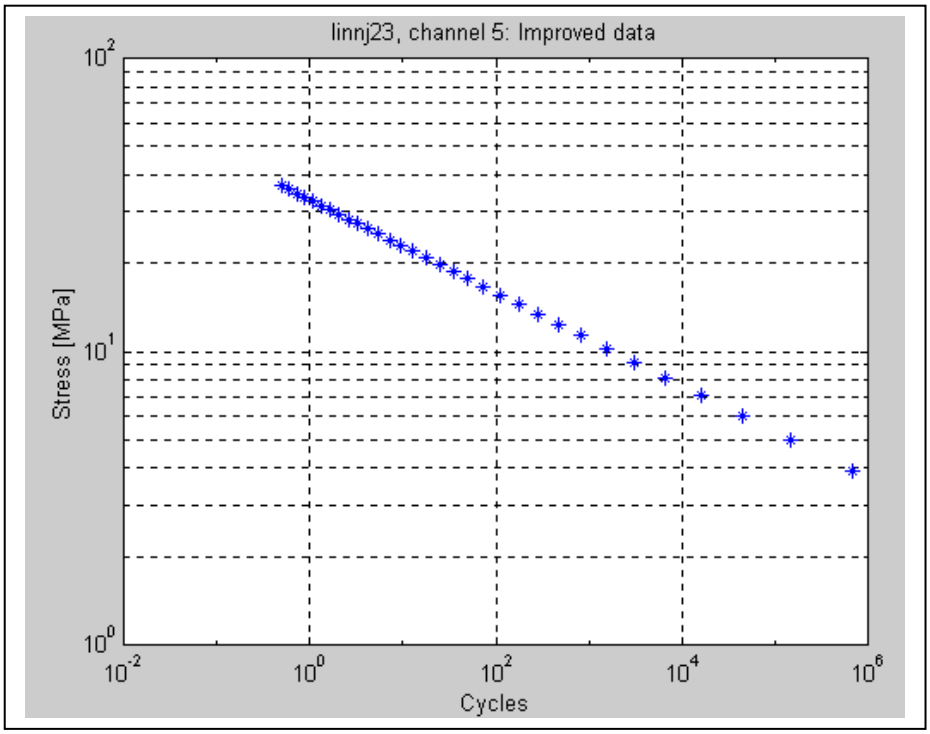

Figure 5-18 Data after improvement of resolution

The material property S_f is arbitrarily chosen (it cancels out later) and b is chosen as –0.33 (for welds). The damages are accumulated per channel for each file (a file typically representing 6 weeks of measurements). The damages per channel are then normalised ($D_{n,ch}$) to a damage per ten years of operation, by dividing it by the total accumulated measurement duration and multiplying it with the number of days in 10 years.

An equivalent constant amplitude stress range is calculated for each channel, which would cause the same damage as the normalised damage, if the range is applied an arbitrary 2 million times. This is achieved through the inverse of the above equations:

$$\Delta\sigma_{e,ch} = S_f \left(\frac{2 \times 10^6}{D_{n,ch}} \right)^b$$

Eq. 5-15

Each channel would then have an equivalent stress range, which would, if applied 2 million times, give the same damage as what was measured (extrapolated to 10 years).

5.4.5.5 Finite element analysis

Originally, pitching loading was not included as a load case. The result was that a longitudinal load was calculated that was higher than the vertical load. The high longitudinal result was explained by the fact that pitching of the tank when loaded with out of phase vertical loading back and front, would have a longitudinal influence. The high centre of gravity of the tank on a vehicle would imply that out of phase vertical loading would result in significant longitudinal effect, even though this would not translate in heavy loading onto the longitudinal bearing structures. It was decided to add a

pitching load (a positive inertial load on one end and an equal but negative load on the other), which would therefore be applied in combination with a lower longitudinal load that would then be calculated if the pitching effect was subtracted.

It is then required to determine the combination of g-loading (vertical, longitudinal, lateral and pitching) that would give this stress at the different strain gauge positions. For this, a finite element analysis was performed (model depicted in Figure 5-19). 1 g loading was applied on a full tank in each direction (L_i) separately and the stress results [$\sigma_{Li,ch}$] at the different strain gauge positions noted for each load case. For the pitching load the analysis was performed where the one end of the container was fixed and the other accelerated by 1 g.

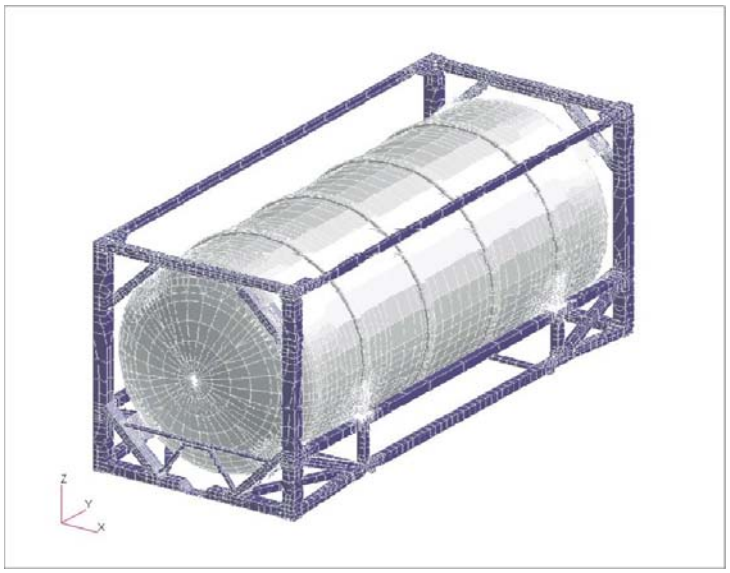

Figure 5-19 Finite element model of tank container

5.4.5.6 Fatigue equivalent static load calculation

The unit load FEA results are used as the elements in the transfer matrix of Eq. 5-14. The equivalent g-loading ranges are then determined by solving Eq. 5-14, with (a=4):

$$FESL = \begin{Bmatrix} FF_1 \\ : \\ FF_a \end{Bmatrix} = \begin{bmatrix} \sigma_{1,ch1} & .. & \sigma_{a,ch1} \\ : & :: & : \\ \sigma_{1,cha} & .. & \sigma_{a,cha} \end{bmatrix}^{-1} \begin{Bmatrix} \Delta\sigma_{e,ch1} \\ : \\ \Delta\sigma_{e,cha} \end{Bmatrix}$$

$$FESL = \begin{Bmatrix} \Delta g_{e,vert} \\ \Delta g_{e,long} \\ \Delta g_{e,lat} \\ \Delta g_{e,pitch} \end{Bmatrix} = \begin{bmatrix} \sigma_{vert,ch1} & \sigma_{long,ch1} & \sigma_{lat,ch1} & \sigma_{pitch,ch1} \\ \sigma_{vert,ch2} & \sigma_{long,ch2} & \sigma_{lat,ch2} & \sigma_{pitch,ch2} \\ \sigma_{vert,ch3} & \sigma_{long,ch3} & \sigma_{lat,ch3} & \sigma_{pitch,ch3} \\ \sigma_{vert,ch4} & \sigma_{long,ch4} & \sigma_{lat,ch4} & \sigma_{pitch,ch4} \end{bmatrix}^{-1} \begin{Bmatrix} \Delta\sigma_{e,ch1} \\ \Delta\sigma_{e,ch2} \\ \Delta\sigma_{e,ch3} \\ \Delta\sigma_{e,ch4} \end{Bmatrix}$$

Eq. 5-16

The fatigue equivalent static g-loads thus determined may then be used as a fatigue loading criterion (apply the g-loads 2 million times to simulate a 10 year life).

Since seven channels were available and only four unknown loads required solving, it was possible to produce several answers, using any four of the seven channels to give a 4x4 transfer matrix. There are 35 different such combinations, as listed below:

Permutations of 4 channels chosen from 7 =

1	1	1	1	1	1	1	1	1	1	1	1	1	1	1	1
2	2	2	2	2	2	2	2	2	2	3	3	3	3	3	3
3	3	3	3	4	4	4	5	5	6	4	4	4	5	5	6
4	5	6	7	5	6	7	6	7	7	5	6	7	6	7	7

1	1	1	1	2	2	2	2	2	2	2	2	2	2	3	3
4	4	4	5	3	3	3	3	3	3	4	4	4	5	4	4
5	5	6	6	4	4	4	5	5	6	5	5	6	6	5	5
6	7	7	7	5	6	7	6	7	7	6	7	7	7	6	7

3	3	4
4	5	5
6	6	6
7	7	7

The solutions thus obtained are depicted in Figure 5-20 below. The coloured stars represent the results for each of the 35 combinations for each of the four loads. Each load should be interpreted separately, but they are plotted using the same vertical scale, with zero g being at the origin of the graph. The vertical scale is blanked out to protect propriety information. Normal distributions (depicted in blue), were fitted to the 35 results for each load, exhibiting relatively narrow spreads around the four mean values of each distribution ($\Delta g_e(ver)_{me}$, $\Delta g_e(lon)_{me}$, $\Delta g_e(lat)_{me}$, $\Delta g_e(pit)_{me}$). The green line depicted on the graph merely connects the mean values of each load, showing the relative magnitudes of the loads.

It was decided to use these mean values of each load in order to minimise the differences across the 35 solution sets. The stability of the results across the 35 sets implies that the mean solution, applied as loads to the finite element model, would cause stresses approximately equal to the measurements based fatigue equivalent stresses at all of the seven measurement positions.

This in turn implies that, given that the seven measurement positions are representative of the total structural response, the fatigue equivalent static loads obtained through the above process, may be employed to accurately determine the fatigue life of the total structure.

The importance of the concept of placing redundant strain gauges is hereby demonstrated. Since the results are defined in terms of inertial loads, it is possible to use the results for any design.

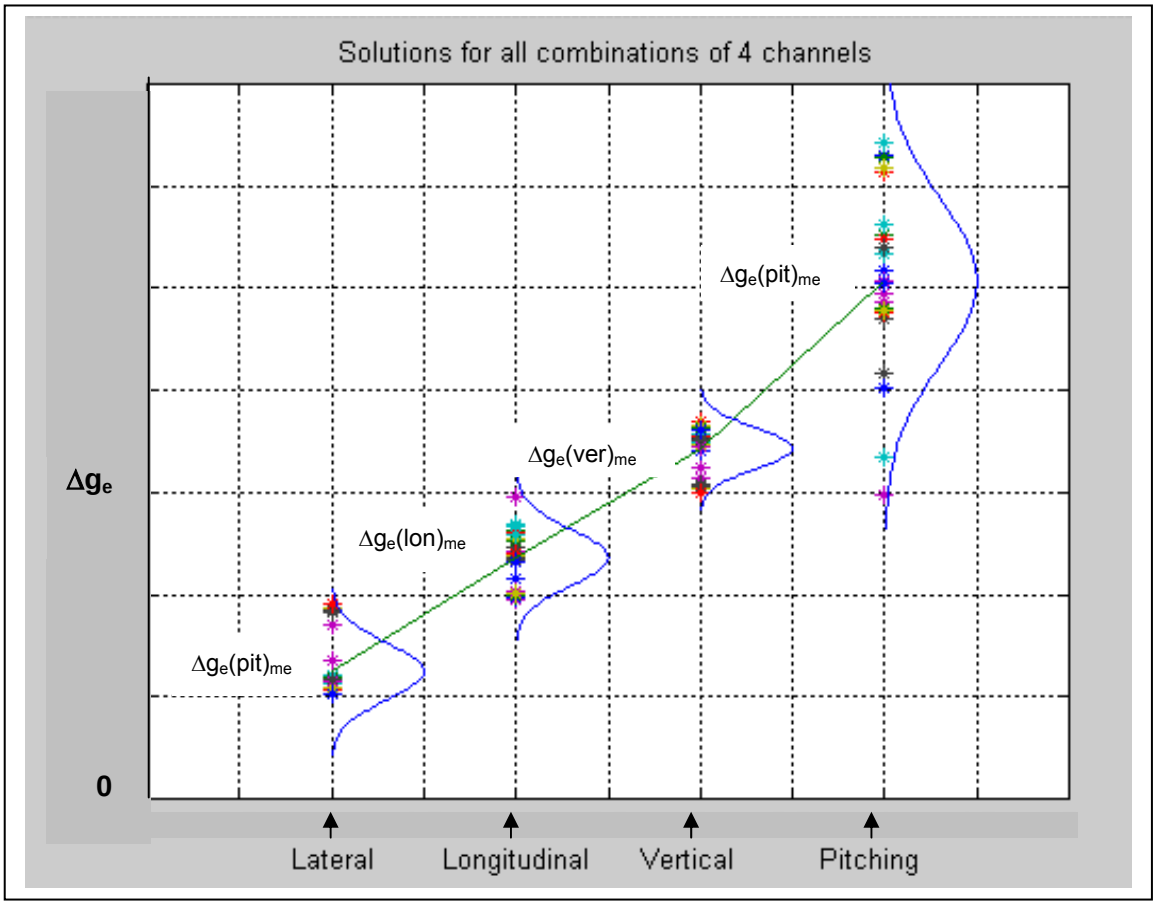

Figure 5-20 FESL solutions for different combinations of measurement chs

5.4.6 Load Haul Dumper

5.4.6.1 Finite element analysis

5.4.6.1.1 Model

The geometry and mesh of the vehicle structure were generated in MSC Patran. The model is depicted in Figure 5-21. The rear chassis and boom section of the vehicle was modelled. The front chassis was simulated in the model with rigid elements to ensure that the force transfer was correct.

5.4.6.1.2 Constraints and loads

The model was constrained at the rear wheel axle in the vertical (Y) and lateral (Z) directions to simulate the rear suspension. The model was constrained at the front axle in all three translations and rotation about the longitudinal axis.

The masses of the engine, bucket and front chassis were introduced to model as mass elements with the appropriate centre of gravity positions and masses. Three load cases, each implying a different model, were considered:

- Model A where the bucket is empty, the boom is resting on its stops and inertial loading is applied to simulate empty travelling.
- Model B where the bucket is full (6 000 kg), the boom is resting on its stops and inertial loading is applied to simulate full travelling.
- Model C where the boom is lifted and loading is applied on the boom to simulate the effect of forces on the bucket during loading or off-loading.

5.4.6.1.3 Quasi-static comparison with measurements

The finite element analysis was done for three conditions, with certain masses and loads, as described in paragraph 5.4.6.1.2. It is then possible to compare the static trends obtained from the stress results against the measured results.

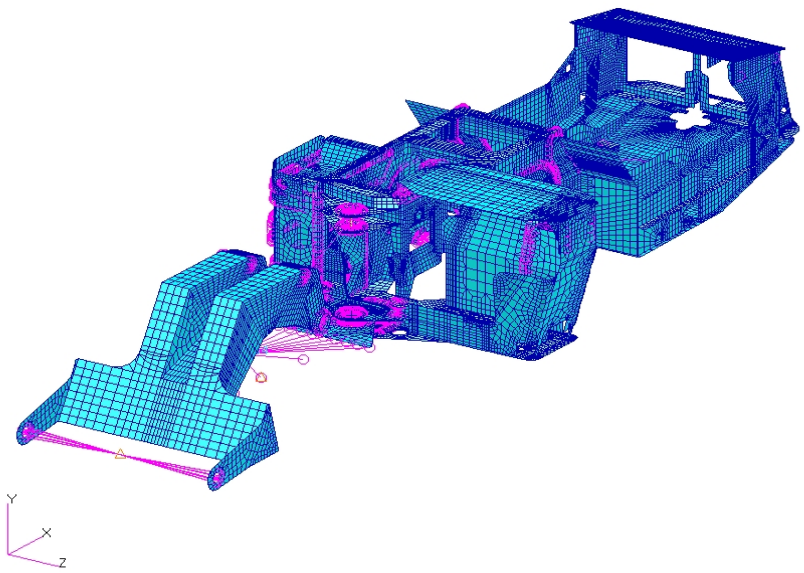

Figure 5-21 Finite element model

The first step in this comparison is to identify the periods in the measurement duration during which the vehicle was travelling empty or full, as well as when the bucket was lifted, to correspond with the three models. This was done by identifying the bucket position using pictures taken during the test by the real-time camera. These photos had a time stamp on and can be directly related to the measured signals. A channel that is

sensitive to bucket loads was selected and the finite element stresses at the location of that strain gauge for all three models were used to construct a quasi-static time history, corresponding to the measured events. This would not take the dynamic effects into account. The measured stress at channel 7 and the predicted stress according to FEA are depicted in Figure 5-22. The blue curve in Figure 5-22 corresponds to a bucket load of 5 tons. The trends of the stresses correlate well.

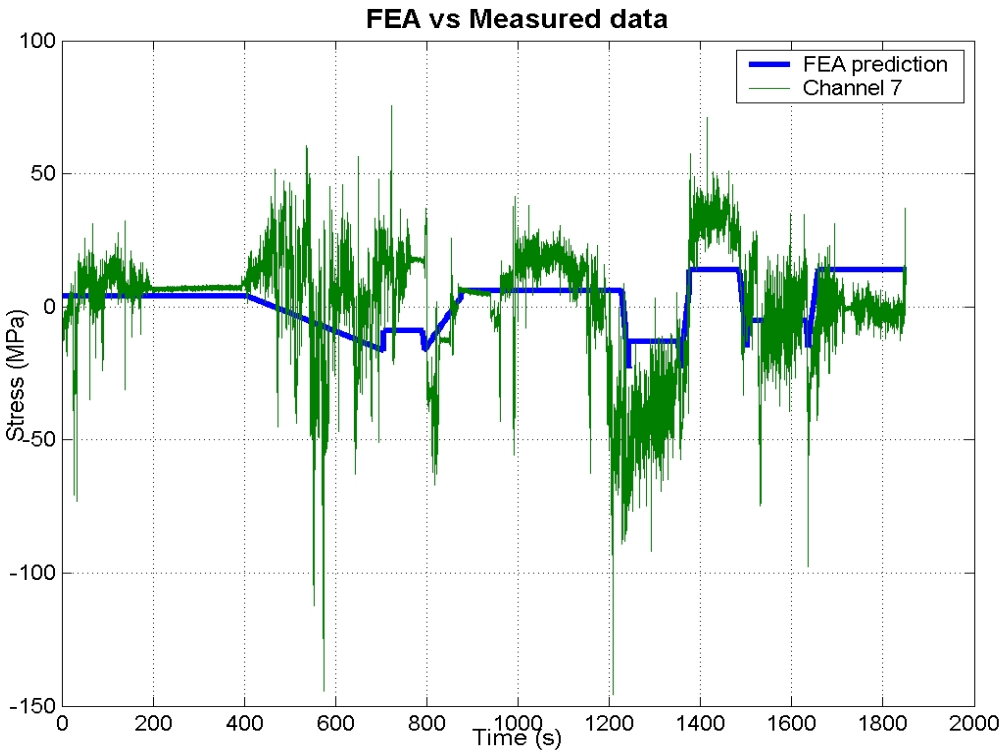

Figure 5-22 Quasi-static FEA vs measurements

5.4.6.1.4 Unit load analysis

It was decided to apply only vertical loading for all three models, since vertical loads would by far represent the largest proportion of fatigue damaging loads on the vehicle structure (horizontal loads due to hitting the side walls, ramming the bucket into a pile, braking, turning and accelerating, would occur far less frequently than vertical loads). Three strain gauges were therefore chosen in order to solve for the fatigue equivalent static loads (all vertical) for the three models, namely channel numbers 3, 4 and 7. The finite element stress results at each gauge position for 1 g load applied to each model were as follows:

$$\begin{bmatrix} \sigma_{1g,A3} & \sigma_{1g,B3} & \sigma_{1gC3} \\ \sigma_{1g,A4} & \sigma_{1g,B4} & \sigma_{1g,C4} \\ \sigma_{1g,A7} & \sigma_{1g,B7} & \sigma_{1g,C7} \end{bmatrix} = \begin{bmatrix} -3.5 & -12.5 & -12.5 \\ 12 & 12 & 4.34 \\ 5.8 & 25 & 35 \end{bmatrix} \text{MPa}$$

Eq. 5-17

5.4.6.2 Measured damage calculation

Relative fatigue damages for the measured runs for each of the three chosen channels were calculated. These damages (D_3, D_4, D_7) were calculated after performing Rainflow cycle counting (providing n_i and $\Delta\sigma_i$), using Eq. 5-7:

$$D_j = \sum \frac{n_i}{N_i} = \sum \frac{n_i}{\left(\frac{\Delta\sigma_i}{S_f}\right)^{1/b}}$$

$$\text{with } b = -0.33 \text{ as before}$$

$$S_f = \text{arbitrary}$$

Eq. 5-18

The calculated damages were extrapolated to total damages for a 10 000 hour life as follows:

$$TD_j = D_j \times 10\,000 \text{ hours / duration of measurement run (in hours)}$$

5.4.6.3 Fatigue equivalent static load calculation

The process that was followed in this case study to calculate fatigue equivalent static loads, differed from the single-axis (vertical loading only) methodology described in paragraph 5.4.2.1 in that three finite element models contributed to the total damage. The process was based on summation of damages, since the damages induced in the structure due to stresses on the three different models, are uncoupled (occur in separate durations).

For model (k) and strain gauge position (j), the damage (D_{kj}) induced by stresses (unit load stress (σ_{kj}) for model (k) at gauge (j) from Eq. 5-17, multiplied by the to-be-determined fatigue equivalent static load ($FESL_k$)), may be calculated using Eq. 5-8:

$$D_{kj} = \frac{n}{\left(\frac{\sigma_{kj} \times FESL_k}{S_f}\right)^{1/b}}$$

$$\text{with } b = -0.33 \text{ as before}$$

$$S_f = \text{same as in Eq. 5 - 27}$$

$$n = 2 \text{ million (chosen value)}$$

Eq. 5-19

The total damage at gauge position (j) must then be equal to the summation of the damages (D_{kj}) for k = A, B, C:

$$\frac{2\times10^6}{\left(\frac{FESL_A\sigma_{Aj}}{S_f}\right)^{-3}} + \frac{2\times10^6}{\left(\frac{FESL_B\sigma_{Bj}}{S_f}\right)^{-3}} + \frac{2\times10^6}{\left(\frac{FESL_C\sigma_{Cj}}{S_f}\right)^{-3}} = TD_j$$

Eq. 5-20

Three such equations exist, for each of the three channels (j = 3, 4, 7). From these three equations, the three unknown fatigue equivalent static loads could be solved as ($FESL_A$ = 4.2 g, $FESL_B$ = 1.1 g, $FESL_C$ = 1.85 g). When the above loads are applied to the three models, the stresses that are calculated are then used as stress ranges, applied 2 million times in a 10 000 hour life, and by using the appropriate SN-curves, damages at any critical position may be calculated by adding the damages for the three models, as depicted in Figure 5-23.

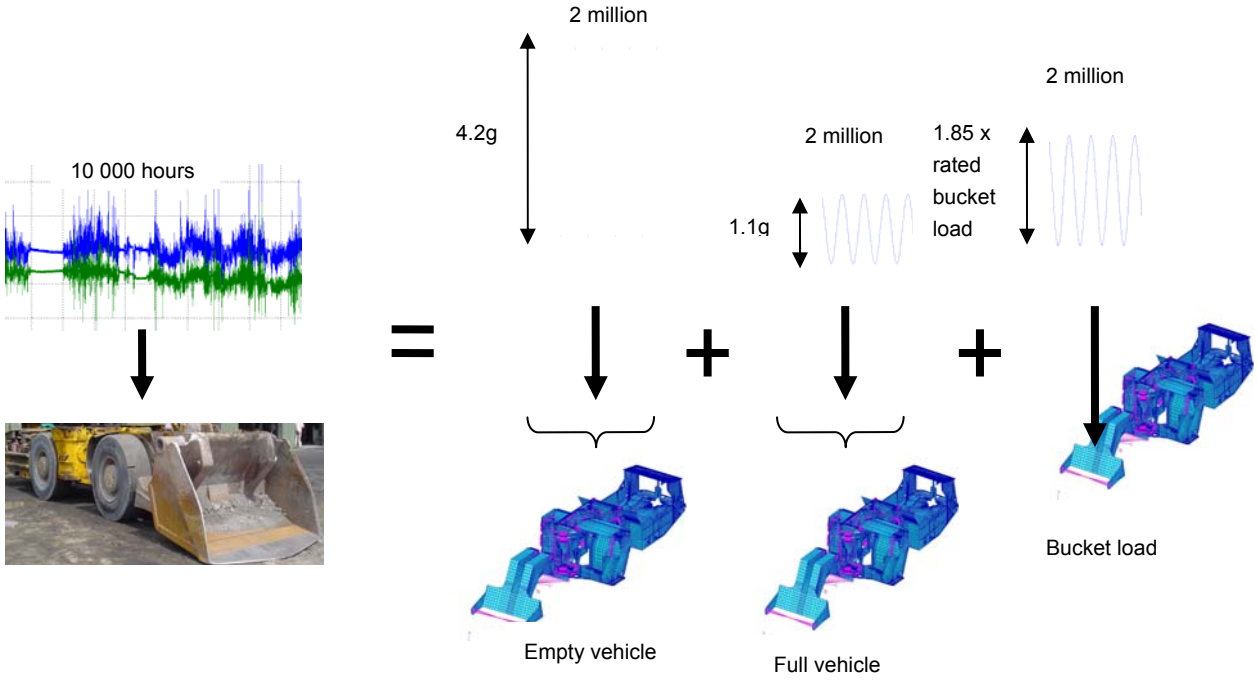

Figure 5-23 Equivalent fatigue loading

5.5 STATISTICAL MODEL

5.5.1 General

As was previously discussed, it is expected that several parameters defining the usage profile of a vehicle are not deterministic. Methods to establish a statistical model for usage profiles are dealt with in this section, using the light commercial vehicles as case studies.

5.5.2 Methodology

The methodology entails the following basic steps:

- Questionnaire exercise (dealt with in paragraph 4.2.7)
- Measurements (dealt with in paragraph 4.2)
- Fatigue processing of measurement data.
- Fitting probability density functions on parameters.

5.5.3 Minibus

5.5.3.1 Fatigue calculations

5.5.3.1.1 Method

The measured data obtained from the strain gauge bridge applied to the left torsion bar was employed to calculate relative damages induced on each route and road category. Sample calculations were performed on the other torsion bar data. It was observed that the damage ratios between different roads based on the left and right torsion bars were equivalent.

The measured data was organized in different files, each consisting of a certain category of road (categorized according to the questionnaire data), on the computer.

The measured strains were converted to stresses by assuming that the relationship between stress and strain was linear elastic. The range-pair-range algorithm was employed to count the fatigue cycles contained in the measured signals. The stress life criterion, together with the Miner damage accumulation law were employed to calculate the relative damage for each measurement file. An assumed SN curve with a gradient of b = -0.33 was employed.

The damage for each file was divided by the distance represented by the file, to obtain a damage/km for each terrain type.

5.5.3.1.2 Results

The damage/km results for files in each category were averaged to yield an average relative damage/km for each category. These results are listed in Table 5-2.

Table 5-2 Damage results per category

Category	Description	Average relative damage per kilometre
1	Highway	1.81×10^{-4}
2	Secondary tar	7.38×10^{-4}
3	Smooth gravel	2.53×10^{-3}
4	Rough gravel	3.16×10^{-3}
5	Very rough	3.78×10^{-3}

The relative damage per kilometre induced by the sequence measured on the durability track was calculated as 1.16×10^{-2}.

5.5.3.2 Statistical processing of questionnaire data

Based on the measurements that had been performed, it was attempted to calculate a relative damage per kilometre for every questionnaire participant. It was not possible to accurately distinguish between the damage caused by central town, suburban and country

roads and it was therefore decided to unite these three categories into one category, namely, secondary tar roads.

Table 5-2 lists the different categories that were used, together with the average relative damage per kilometre as obtained from the measurement results.

The average relative damage per kilometre for each participant was subsequently calculated as follows:

$$D_{average}/km = \sum_{category=1}^{5} \left(D_{average} / km_{category} \times \frac{percentage_{category}}{100} \right)$$

Eq. 5-21

A lognormal probability density function (PDF) was then fitted to these results:

$$f(x_1) = \frac{1}{x_1 \, \sigma_y \sqrt{2\pi}} e^{-\frac{1}{2}\left(\frac{\ln x_1 - \mu_y}{\sigma_y}\right)^2}$$

$$\text{with } x_1 = D/km$$

$$y = \ln x_1, \text{being normally distributed (mean} = \mu_y, \text{variance} = \sigma_y^2)$$

Eq. 5-22

The fitted curve together with the raw data histogram is shown in Figure 5-24. It may be observed that a good fit was achieved. A similar procedure was followed to obtain an expression for the statistical distribution of the km/day data:

$$f(x_2) = \frac{1}{x_2 \, \sigma_y \sqrt{2\pi}} e^{-\frac{1}{2}\left(\frac{\ln x_2 - \mu_y}{\sigma_y}\right)^2}$$

$$\text{with } x_2 = km/day$$

$$y = \ln x_2, \text{being normally distributed (mean} = \mu_y, \text{variance} = \sigma_y^2)$$

Eq. 5-23

The achieved fit is shown in Figure 5-25. Again a good fit was achieved.

It was however expected that the variables (D/km and km/day) would not be statistically independent. A participant logging high kilometres per day probably would primarily be using highways, implying low D/km. Statistical theory states that if two dependent variables can separately be fitted to lognormal distributions, then a bivariate lognormal PDF may be employed to obtain a two-dimensional distribution, defined by Eq. 5-24.

A 2-D plot of this function is shown in Figure 5-26.

$$f(x1,x2) = \frac{1}{x_1\, x_2\, \sigma_{y_1}\, \sigma_{y_2}\, 2\pi \sqrt{1-\rho^2}}\, e^{z}$$

$$\text{with } z = -\frac{1}{2(1-\rho^2)}\left[\left(\frac{\ln x_1 - \mu_{y_1}}{\sigma_{y_1}}\right)^2 - 2\rho\left(\frac{\ln x_1 - \mu_{y_1}}{\sigma_{y_1}}\right)\left(\frac{\ln x_2 - \mu_{y_2}}{\sigma_{y_2}}\right) + \left(\frac{\ln x_2 - \mu_{y_2}}{\sigma_{y_2}}\right)^2\right]$$

$$\rho = \frac{\sigma_{y_{12}}}{\sigma_{y_1}\sigma_{y_2}} \qquad \textbf{Eq. 5-24}$$

$$x_1 = \text{D/km}$$

$$x_2 = \text{km/day}$$

$$y_1 = \ln x_1, \text{being normally distributed (mean} = \mu_{y_1}, \text{variance} = \sigma^2_{y_1})$$

$$y_2 = \ln x_2, \text{being normally distributed (mean} = \mu_{y_2}, \text{variance} = \sigma^2_{y_2})$$

By definition:

$$\int_0^\infty \int_0^\infty f(x_1, x_2)\, dx_1\, dx_2 = 1$$

Eq. 5-25

Having thus achieved an excellent mathematical description of the D/km and km/day distributions pertaining to minibus taxi operators, it would be possible to extract durability requirements according to any company target (e.g. one year warranty for 90 % of the buyers, or 300 000 km for 90 % of the buyers). The process to extract durability requirements from these distributions is described later.

The results obtained thus far, however, have been based solely on theoretical exercises (fatigue calculations, questionnaires and statistical processing). In order to acquire sufficient confidence in these results, it was required to, in some way, verify the theoretical results. Such verification was subsequently attempted, based on the failure data that was available on a gearbox mounting crossmember of the vehicle. This verification firstly involved laboratory testing of the crossmembers, which is described in the next chapter.

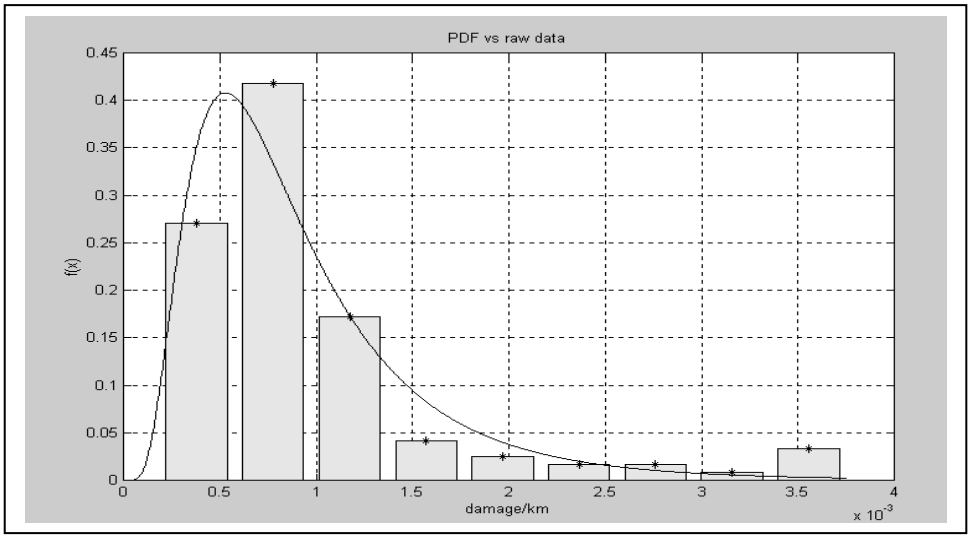

Figure 5-24 PDF of D/km versus raw data

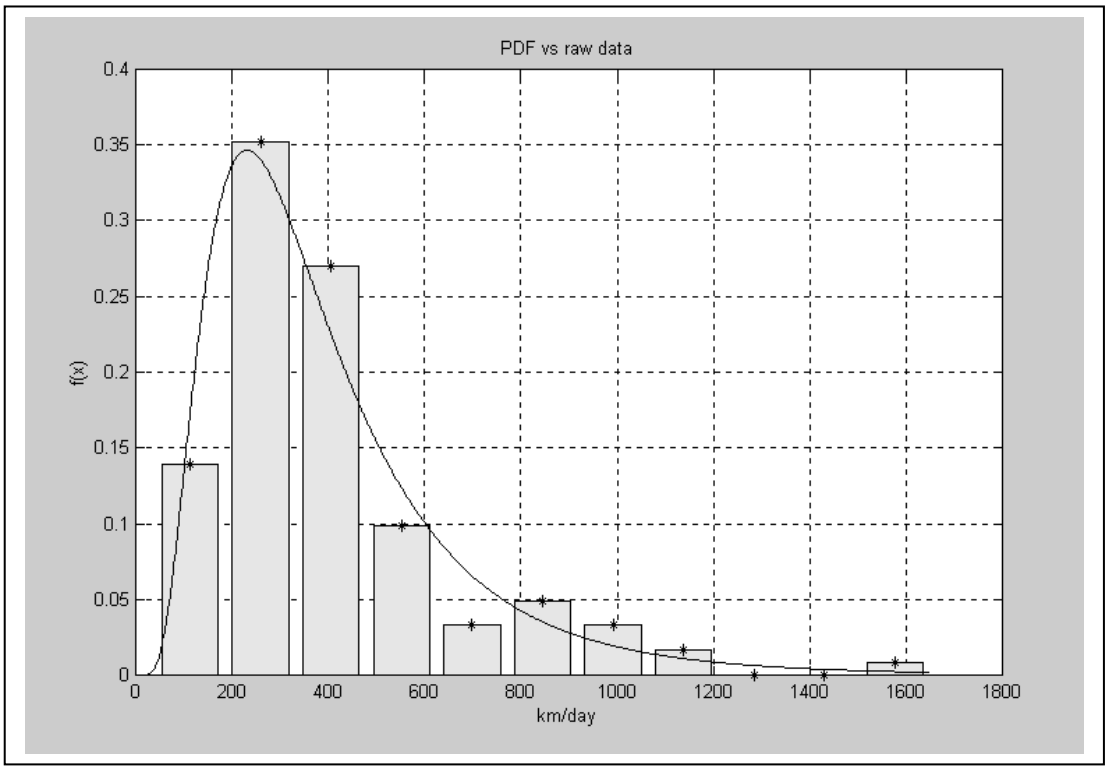

Figure 5-25 PDF of km/day versus raw data

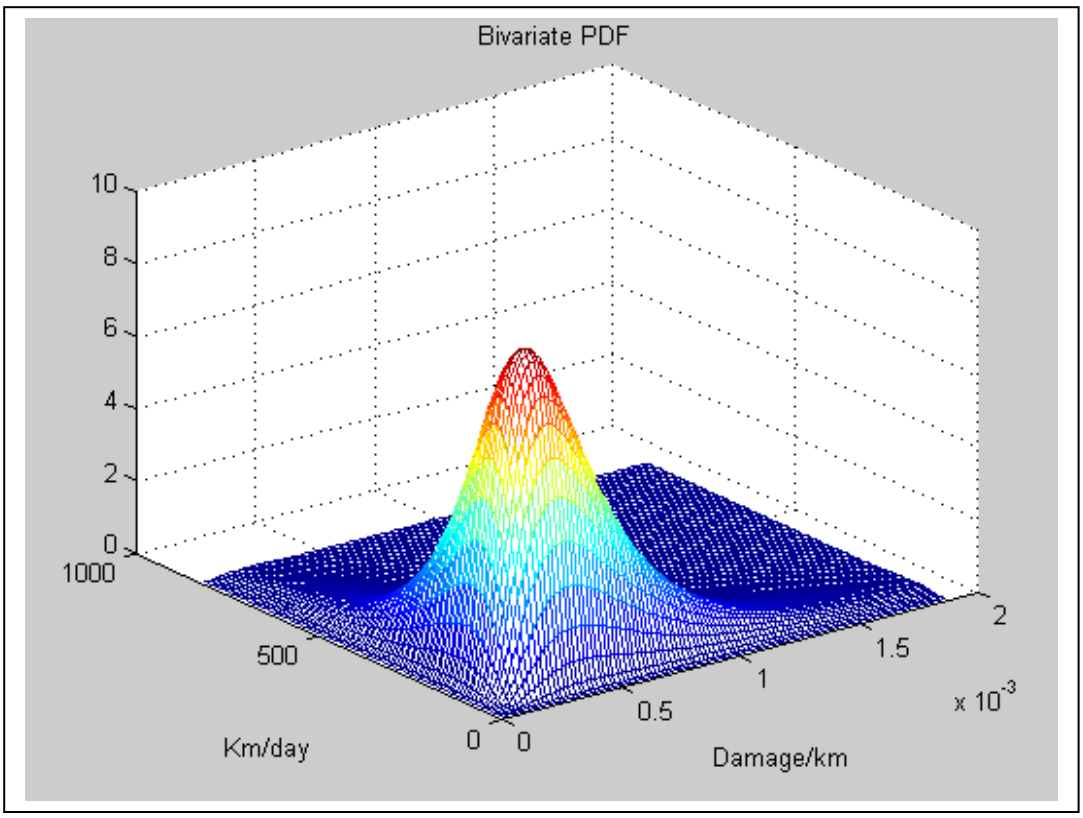

Figure 5-26 Bivariate distribution of km/day and D/km

5.5.4 Pick-up Truck

5.5.4.1 Fatigue processing

The measured data was downloaded onto computer and fatigue calculations were performed on each channel for each section of road. The damage was calculated using the same general material properties for all channels and road sections to obtain damage values that have no meaning in the absolute sense, but do give the relative severity between each road section for each channel. The damage for each road section was also divided by the distance to give a normalised damage per kilometre.

The damage per kilometre values for different road sections sampled for the usage profile and belonging to the same road category, were averaged to yield a single damage per kilometre value per channel per category. The results of these calculations are listed in Table 5-3.

Table 5-3: Damage/kilometre values for different road sections

Channel Description	Rural good Tar	Rural bad tar	Urban	Mountainous and winding	Good gravel	Bad gravel
Left front coil	2.73×10^{-8}	1.50×10^{-8}	1.60×10^{-7}	1.13×10^{-7}	2.70×10^{-7}	1.50×10^{-6}
Right front coil	3.75×10^{-8}	3.00×10^{-8}	2.20×10^{-7}	1.50×10^{-7}	4.40×10^{-7}	2.00×10^{-6}
Right rear diff	4.79×10^{-9}	2.30×10^{-9}	3.10×10^{-8}	1.10×10^{-8}	3.00×10^{-8}	1.50×10^{-7}
Left rear diff	5.30×10^{-9}	2.00×10^{-9}	2.10×10^{-8}	7.70×10^{-9}	3.40×10^{-8}	1.30×10^{-7}
Left front strut	2.50×10^{-10}	2.80×10^{-10}	1.30×10^{-9}	3.60×10^{-10}	2.00×10^{-9}	9.80×10^{-9}
Right front beam	5.90×10^{-9}	6.60×10^{-9}	3.00×10^{-8}	1.90×10^{-8}	3.10×10^{-7}	1.55×10^{-6}
Left beam centre	1.60×10^{-9}	2.80×10^{-9}	3.40×10^{-8}	1.00×10^{-8}	3.70×10^{-8}	2.20×10^{-7}
Round crossmem.	3.90×10^{-10}	8.20×10^{-11}	5.80×10^{-10}	5.50×10^{-10}	4.60×10^{-9}	2.60×10^{-8}
Left top door	3.50×10^{-10}	1.50×10^{-10}	6.10×10^{-10}	5.80×10^{-10}	6.60×10^{-9}	3.30×10^{-8}
Box left rear panel	3.40×10^{-10}	1.20×10^{-10}	1.80×10^{-10}	5.70×10^{-10}	1.33×10^{-10}	9.10×10^{-10}

The above results clearly show the relative severities of each category of road per channel. Comparisons of damage results between channels have no meaning (the damage on a coil spring and at a certain position on a differential are not comparable). A discrepancy concerning the relative damage calculated for the rural good surfaced category compared to the rural bad surfaced category can be observed. This may be ascribed to the subjective categorisation performed during the measurements.

5.5.4.2 Statistical processing of questionnaire data

A similar process to that described in paragraph 5.5.3.2 above for the minibus was followed for the pick-up truck. Eq. 5-21 was used to calculate the two parameters (km/month and damage/km). Lognormal probability density functions were fitted according to Eq. 5-22 and Eq. 5-23. The achieved fits are depicted in Figure 5-27 and Figure 5-28 below. These plots are for the average of channels 3 and 4, (left and right rear diff), which is indicative of the vertical loading on the rear axle. The same calculation can be done for any channel, but is shown here due to the fact that rear suspension leaf spring failures occurred on the vehicle during the durability testing. Again statistical dependence of the variables were assumed, implying the use of the bivariate distribution of Eq. 5-24.

From the questionnaire data it was found that the following distribution of cargo carrying could be assumed:
No load = 50%, Full load = 28%, Overload = 22%

The above results were used to compile test requirements and to perform failure prediction, as described in the next section.

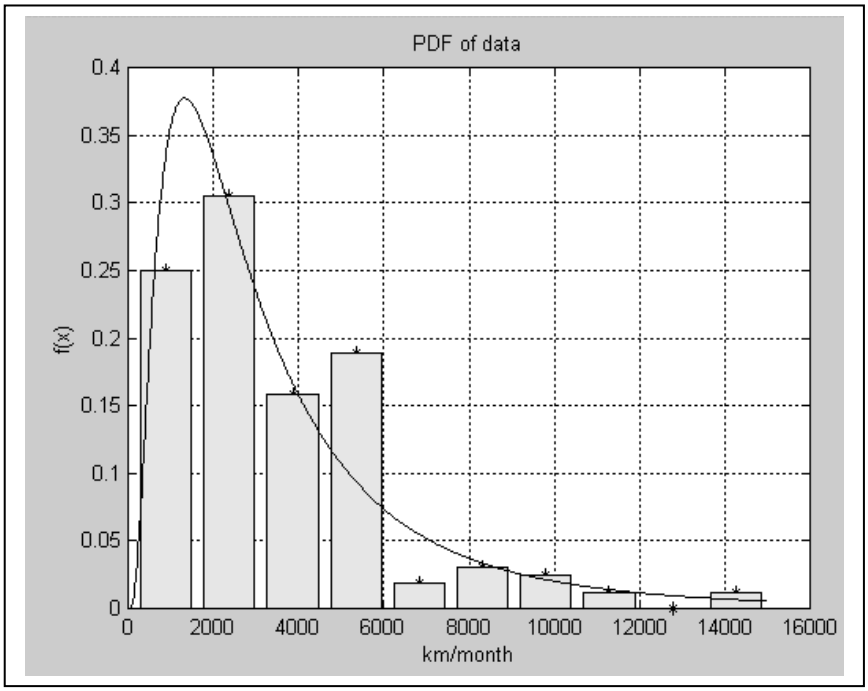

Figure 5-27 PDF of km/month vs raw data

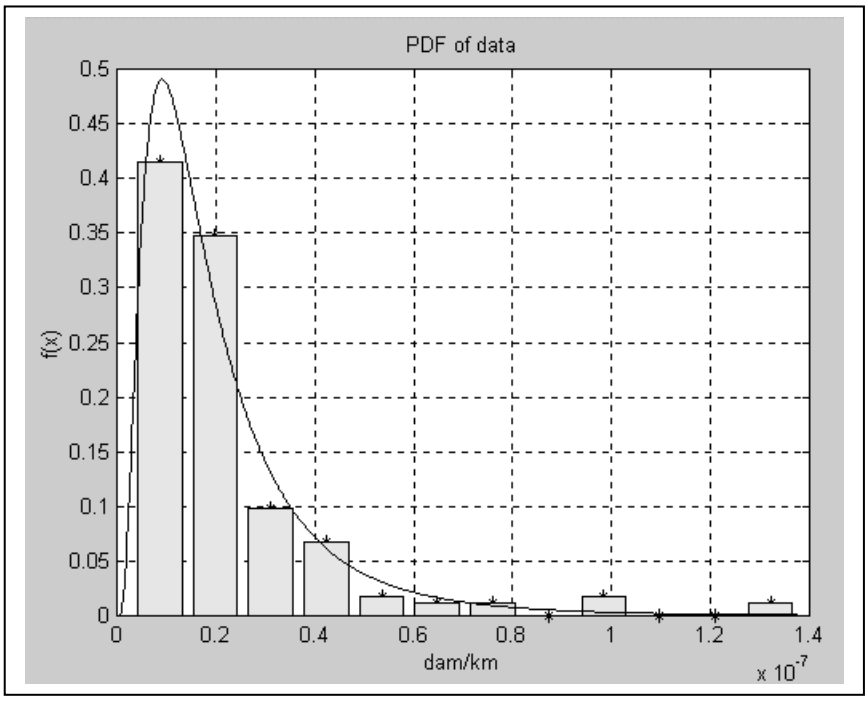

Figure 5-28 PDF of D/km versus raw data

5.6 TESTING REQUIREMENTS

5.6.1 General

In some instances, requirements, as derived from input loading determination, will be the same for design and testing. Representative dynamic loads could be used in dynamic finite element analysis, as well as for dynamic rig testing. Fatigue equivalent loads could be applied as sine wave, single amplitude loading in a test. Mostly, however, different requirements are set for testing, to what was used for the design. A physical test on a test track or a road simulator laboratory rig will apply load sequences that are of too long durations to be simulated by dynamic finite element analyses.

In this section, the derivation of testing requirements for the light commercial vehicles, as well as the ISO tank container, are dealt with.

5.6.2 Minibus

Although some aspects would require more detailed assessment, it was proposed that the statistical and fatigue presentation of the operational conditions which minibus taxi vehicles are subjected to, may be considered to be fairly accurate. Additionally, the methodology facilitates an extremely versatile means of deriving durability testing requirements.

Durability test requirements are established according to a target set by company policy. If this target is set in terms of distance without failure, the following method can be used to derive the appropriate durability requirement.

It is firstly necessary to also target a percentage users to be catered for, being defined as the percentage of vehicles which would reach the target distance without failure. The durability requirement will be set as a number of cycles to be completed on the test track without failure. The number of cycles implies a certain damage (D_{tt}). The required damage to be induced on the test track divided by the target distance without failure implies a vertical line on the D/km, km/day plane. D_{tt} should be chosen such that the percentage of the volume to the left of the straight line and underneath the surface defined by the 2-D PDF, would be larger than the target percentage users. Figure 5-29 depicts the results of such an analysis. Lines of different target distances are plotted on a plane of percentage users vs required cycles on the test track. As an example, if a target distance of 150 000 km without failure is set together with a percentage users of 96 %, the required number of cycles to be completed without failure on the test track may be read off as 10 000.

This result may also be presented in terms of a graph of percentage users vs required severity ratio (refer to Figure 5-30). This graph may be used to read off the required severity ratio for a certain percentage users (e.g. 7.6:1 at 95 %, implying that for every 1 kilometre on the test track, 7.6 kilometres of normal use, pertaining to 95 % of the users, will be simulated).

Similarly, if the company policy requires a target to be set in terms of years without failure (e.g. warranty period), the following procedure is followed:

Again a corresponding percentage users to be catered for must be set. The required damage to be induced by the test track (D_{tt}, which is related to the number of cycles on the test track) divided by the number of days without failure implies a hyperbola on the D/km,

km/day plane. D_{tt} must be chosen such that the percentage volume below this hyperbola and underneath the 2-D PDF, is more than the percentage users. Figure 5-31 depicts the results of such an analysis. Lines of different years without failure are plotted on a "cycles on test track" versus "percentage users" plane. As an example, a target of 10 years without failure for a percentage users of 95 % would require 30 000 cycles to be performed on the test track without failure.

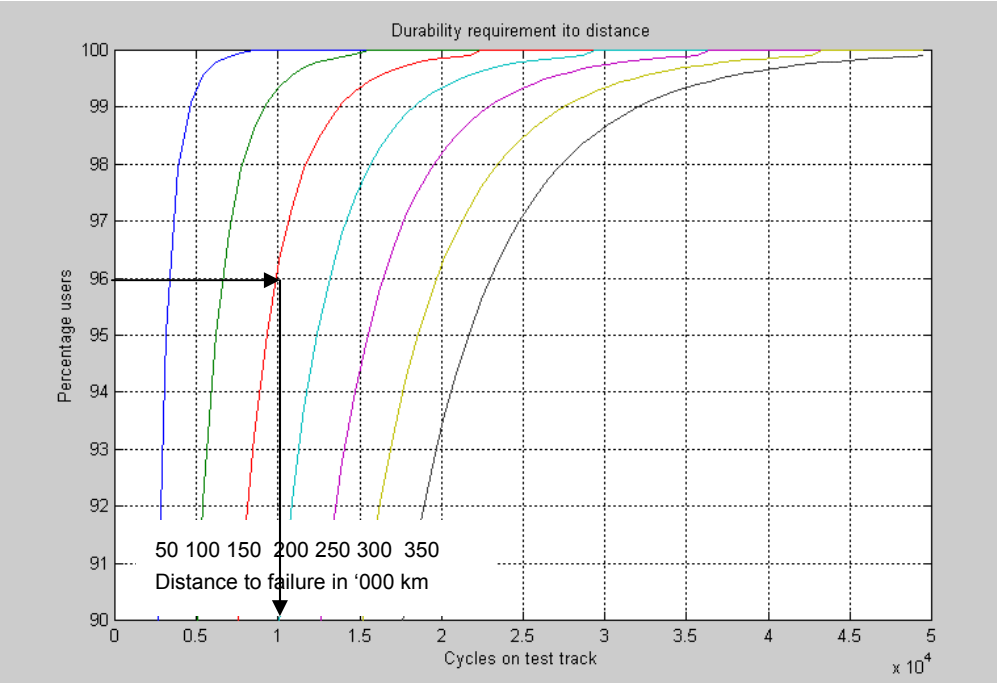

Figure 5-29 Durability requirements ito distance

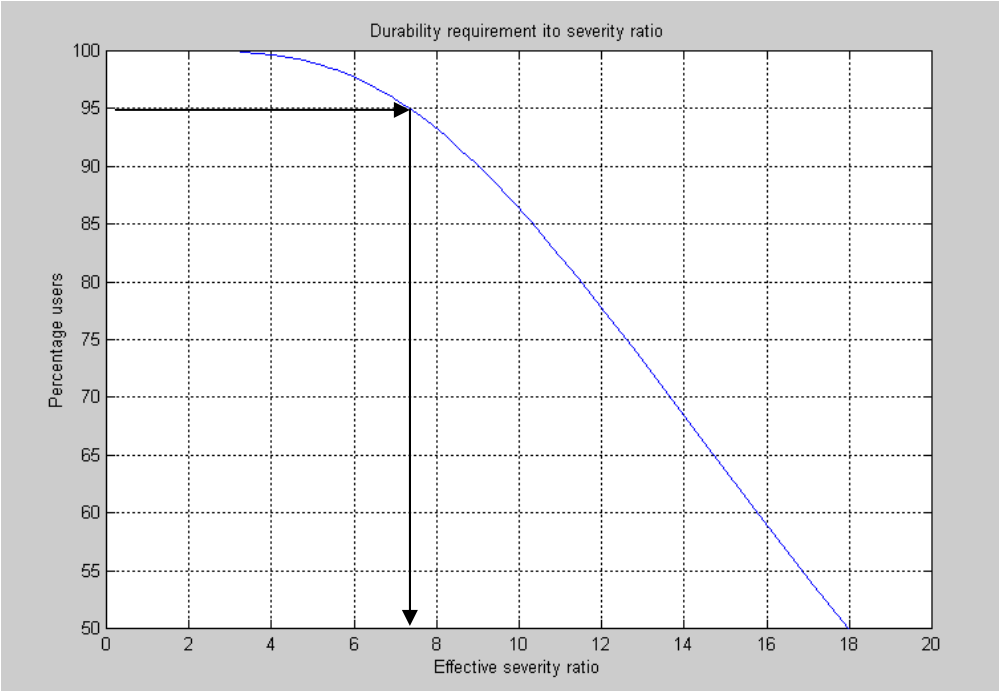

Figure 5-30 Durability requirements ito severity ratio

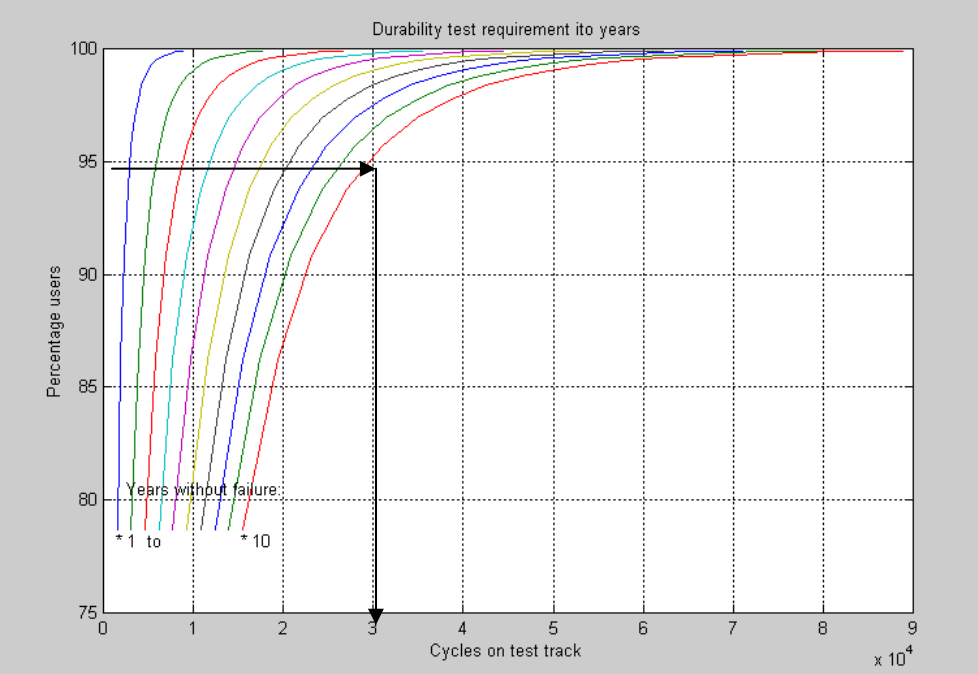

Figure 5-31 Durability requirement in terms of years

5.6.3 Pick-up Truck

5.6.3.1 Compilation of laboratory test sequence

From the fatigue damage calculations, only certain sections of the measured roads were selected to be simulated in the laboratory. This was necessary in order to equally accelerate the laboratory test for all channels by selectively replacing less severe road sections with more severe road sections. For this purpose the fatigue damages per unit time for each measured field file per channel were calculated

From this information, a laboratory durability sequence was compiled, utilising the measured field files with the highest damage per unit time. In order to achieve a similar test acceleration factor for all strain channels, it was necessary to find the right mix of field files and repetitions. This is achieved in a trial-and-error process. The solution would not be unique.

5.6.3.2 Monte Carlo establishment of durability test requirement

A process somewhat different to that followed for the minibus, but with the same aim, was used. It was decided to use the Monte Carlo approach, rather than an analytical approach, since it would then be possible to treat further parameters, such as the damage to failure, as well as the cargo loading, as statistical parameters. A flowchart of the process to establish 10 000 random samples of the parameters according to the distributions, is depicted in Figure 5-32.

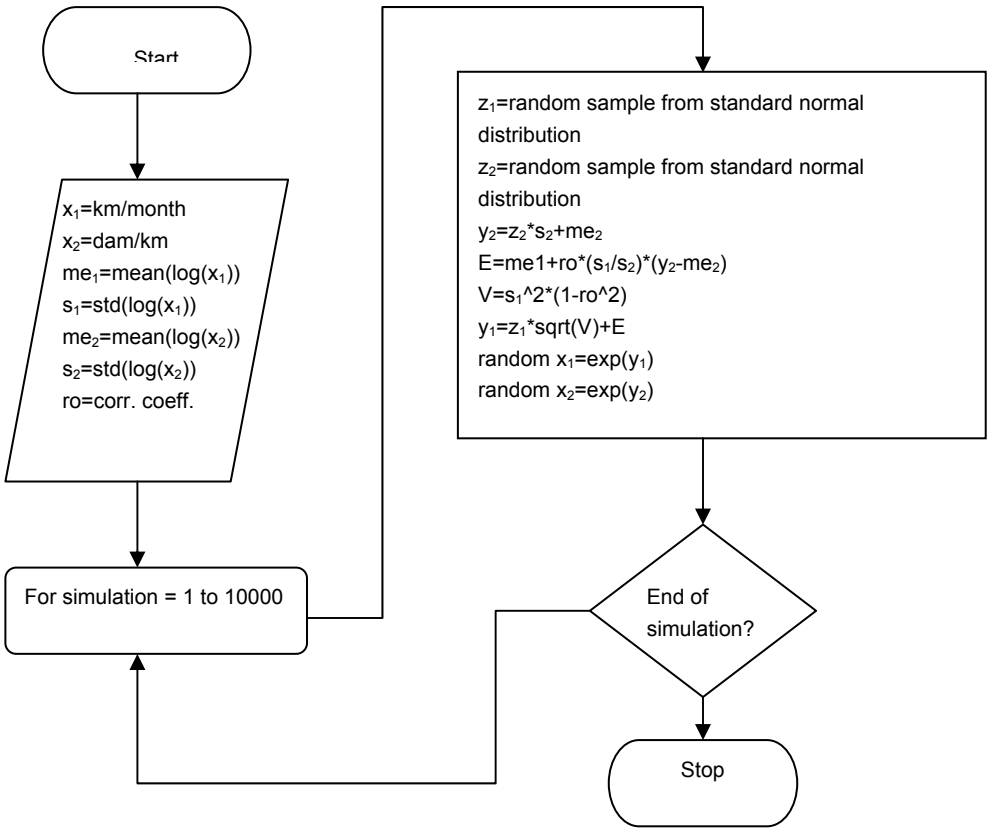

Figure 5-32 Monte Carlo process

Measurements with different cargo loads indicated that the damage reduces by a factor 0.4 for the no load case and increases with a factor 1.4 for the 20 % overload case. For each of the x_2 [D/km] samples these factors were applied, based on a uniformly distributed random number between 0 and 1 (if between 0 and 0.5 – multiply by 0.4, if between 0.78 and 1, multiply by 1.4). This shows the strength of the Monte Carlo method.

The 10 000 random samples of x_2 are then sorted from small to large and when plotted against it's index/10 000×100, yields a cumulative distribution function (refer to Figure 5-33).

The damage induced on the rear axle channels when applying the test sequence, was 7.9×10^{-6} per test cycle. If a target of 300 000 failure free kilometres are set for the vehicle, the number of cycles required from the testing can be calculated as 300 000 $\times$ x_2/damage per cycle. If the sorted 10 000 random samples of x_2 are used in this calculation and the result is plotted against the index/10 000×100, the required number of test cycles to achieve 300 000 km of usage is exhibited as a function of the percentage users (refer to Figure 5-34).

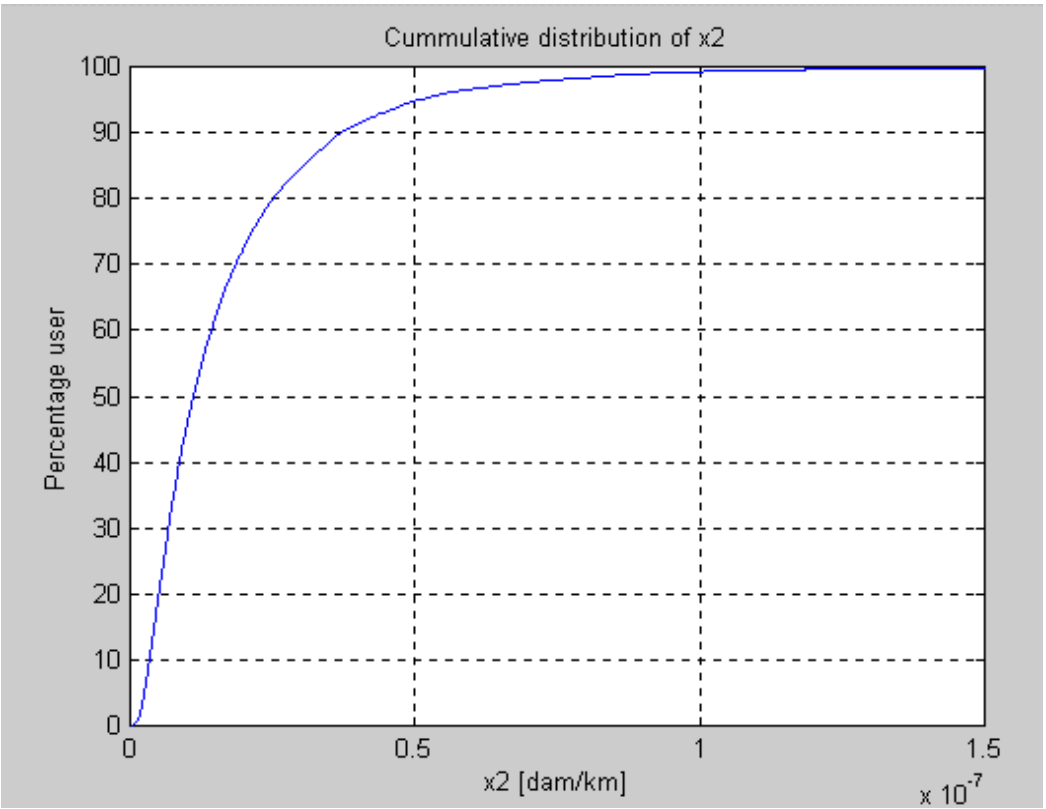

Figure 5-33 Cumulative distribution of x_2

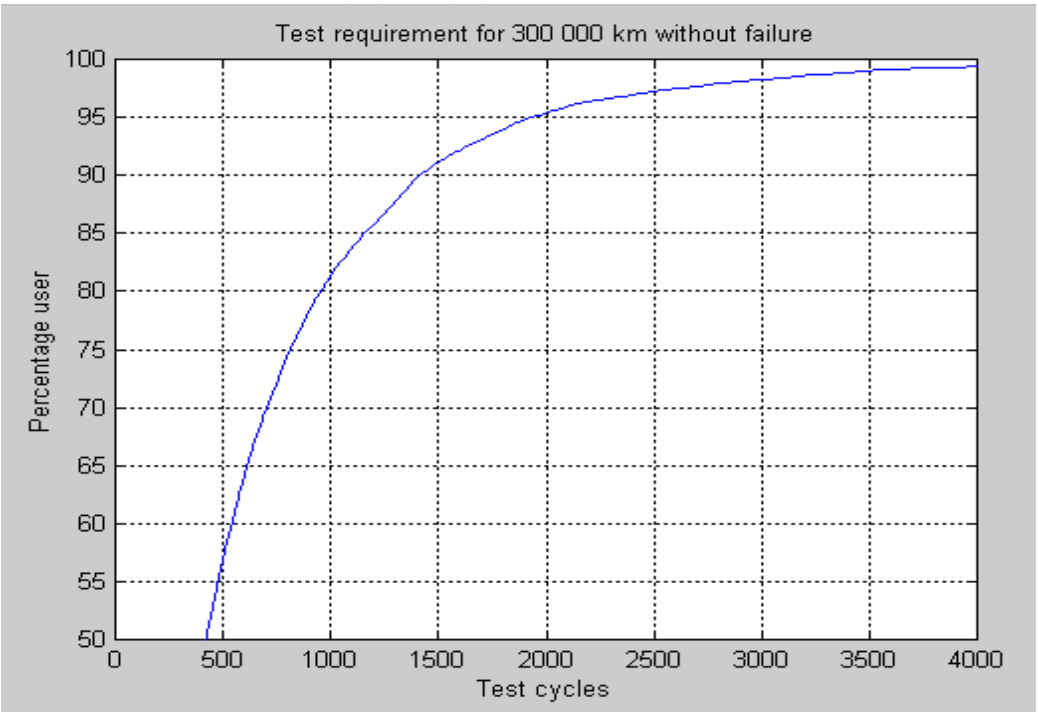

Figure 5-34 Test requirement for 300 00 km without failure

From Figure 5-34, the number of test cycles required to achieve 300 000 km of usage for any percentage of users can be determined. 2000 cycles are required if 300 000 km for 95 % of the users are to be achieved (only 5 % of users would induce more damage in 300 000 km). The duration of one test cycle was approximately one hour, which implied that at 24 hours per day and 7 days per week, the test would be completed in 3 months. At 300 000 km in 2000 hours, the effective simulation speed for the 95 % user would be 150 km/h. For the 50 % user, an additional acceleration of 2000/450 = 4.44 is achieved, implying an effective test speed of 666 km/h.

The testing performed according to the above criteria, as well as the failure predictions performed, based on the test results, are described in 6.2.3.

5.6.4 ISO Tank Container

Testing on the ISO tank container was performed on a servo-hydraulic test rig. In this instance, the requirements derived for fatigue design were also used for testing. The fatigue equivalent loads were used as inputs on the rig as sine waves. Care was taken to avoid frequencies at which resonant dynamics are excited.

A very important inadequacy of the testing method was that it was not practically possible to perform the testing whilst applying the vertical, longitudinal, lateral and pitching loads simultaneously, as is theoretically required to simulate the correct damage in all areas of the structure. The different loads were therefore applied in a series of tests. It was argued and substantiated through finite element analysis, that most of the critical areas were each only sensitive to one of the load directions. For those areas sensitive to more than one load affected the stresses, corrections were made to the results, taking into account the reduced stresses due to the loss of the combined effects and the increased number of cycles (2 million for each load).

5.7 CLOSURE

In this chapter, comprehensive techniques for deriving input loading requirements for design and testing, were demonstrated. As an alternative for performing dynamic finite element analyses, robust methods were presented to derive fatigue equivalent loads, applied in static finite element analyses, or single amplitude rig tests.

For test track or road simulator laboratory tests, powerful methods to establish testing requirements based on statistical targets, were developed.

In the next chapter, fatigue assessment and correlation of the results obtained in this chapter, are dealt with.

6. FATIGUE ASSESSMENT AND CORRELATION

6.1 SCOPE

There are in essence two methods which could be used to substantiate the results obtained in the previous chapter. Firstly, as the major aim of the design and testing requirements is to ensure that real operational loading conditions are accurately simulated, it is possible to verify such results by applying them to predict or reproduce failures that have been experienced in the field.

Secondly, the results can be compared to requirements set in design standards.

In this chapter, failure predictions and comparisons with actual failures experienced on the case study vehicles, or similar/older models, are dealt with. Comparison with design code loads are also described.

The chapter also contains a section dealing with a method to derive input loading from field failure data, without the need for measurements and surveys, that was developed during the minibus case study. This method is presented here since it is an inverse of the method to predict failures.

6.2 FATIGUE LIFE PREDICTION

6.2.1 General

Failure predictions and comparison with actual field failures are described for every case study.

6.2.2 Minibus

6.2.2.1 Method

To verify the theoretical distributions obtained from the measurements and questionnaires, it was attempted to use these distributions to obtain a theoretical prediction of the failures that had occurred in practice on the crossmembers. A methodology was subsequently developed to predict the failures that would have occurred before a certain reference date ($date_{ref}$), the result of which could then be compared to actual failure data on that date.

In paragraph 5.5.3 the average damage to failure (D_f) of the crossmember was based on the laboratory test results. A vehicle that was sold in a certain month would be on the road for a certain number of days (assumed 22 working days per month) up to $date_{ref}$. By dividing D_f by the number of days, a constant number for each month results:

$$constant_{month} = D_f \text{ / days on the road} \qquad \textbf{Eq. 6-1}$$

This constant then implies a hyperbola for each month on the D/km, km/day plane, since:

$$D/km \times km/day = D/day = constant_{month} \qquad \textbf{Eq. 6-2}$$

The probability that a vehicle that has been sold during a certain month preceding $date_{ref}$ would have failed before $date_{ref}$ can then be calculated by calculating the volume above

the hyperbola on the D/km, km/day plane and underneath the surface described by the fitted 2-D PDF. This volume can be calculated by double integration as follows:

$$P_{month} = \int_{x1=0}^{\infty} \int_{x2=\frac{constant_{month}}{x_1}}^{\infty} f(x_1, x_2)\, dx_2\, dx_1$$

$$\text{with } f(x_1, x_2) = \text{as defined by Eq. 5 - 33}$$

$$x_1 = \text{D/km}$$

$$x_2 = \text{km/day}$$

$$P_{month} = \text{probability that a vehicle sold in certain month will fail before data}_{ref}$$

$$constant_{month} = \text{as defined by Eq. } 6-2$$

Eq. 6-3

This process is graphically depicted in Figure 6-1, which depicts a contour plot of the 2-D PDF together with the hyperbolas for incremental age (only month=1 and month=2 are tagged, but the hyperbolas to the left are for one month increments up to month=9). The contour plot is essentially a top view of Figure 5-26. The contours represent constant values of probability density.

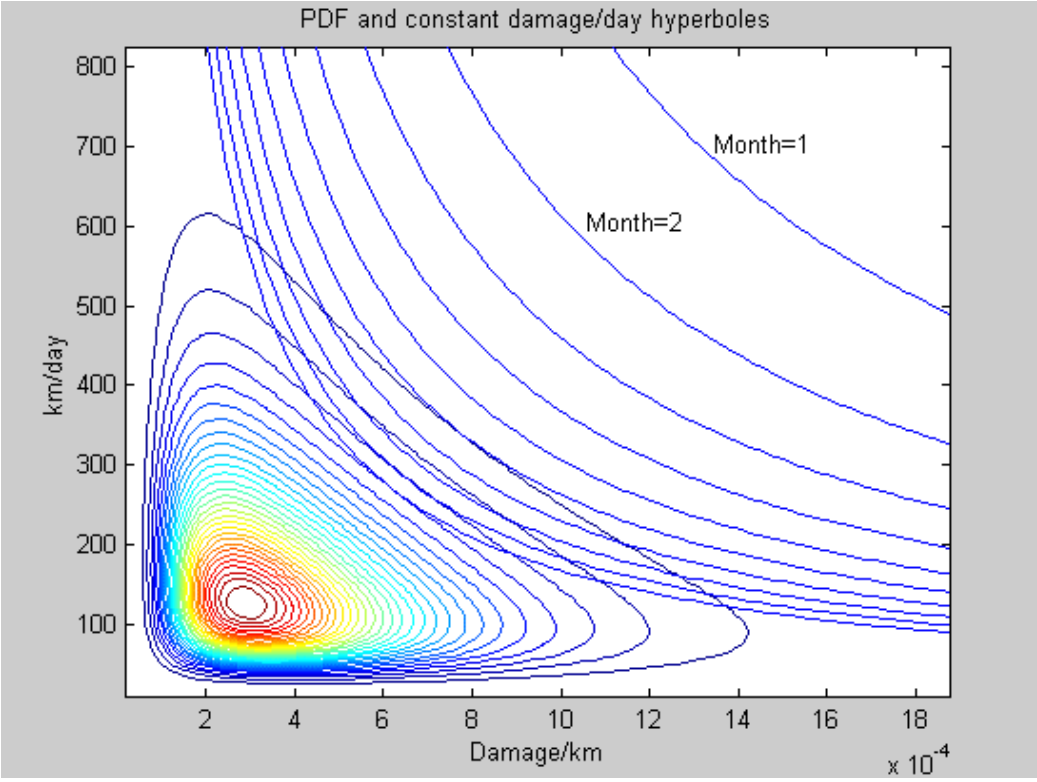

Figure 6-1 Integration of PDF

The total number of vehicles predicted to have failed by $date_{ref}$ may then be calculated as follows:

$$\text{Predicted number of failures} = \sum_{month=1}^{date_{ref}} \left(P_{month}\ sales_{month}\right)$$

Eq. 6-4

The distribution of distance to failure of the vehicles predicted to have failed can also be determined by calculating the number of vehicles for all months for each increment of x_1 (dam/km) which would have failed:

$$N(x_1) = \sum_{month=1}^{day_{ref}} \left[\left(\int_{x2=\frac{constant_{month}}{x_1}}^{\infty} f(x_1, x_2)\, dx_2 \right) \Delta x_1 \times sales_{month} \right]$$

$$\text{with } f(x_1, x_2) = \text{as defined by Eq. 5 - 33}$$

$$x_1 = \text{D/km, being incremented from } \Delta x_1 \text{ to } \infty \text{ in steps of } \Delta x_1$$

$$x_2 = \text{km/day}$$

$$N(x_1) = \text{number of vehicles predicted to have failed after } \frac{D_f}{x_1} \text{ kilometres}$$

$$constant_{month} = \text{as defined by Eq. } 6-3$$

Eq. 6-5

6.2.2.2 Testing

6.2.2.2.1 Test method

A test rig was erected which was able to simulate the relevant loads acting on the crossmember. The test rig consisted of three servo-hydraulic actuators. Two actuators were employed to simulate the vertical front wheel displacements and a third actuator was used to simulate the vertical inertial forces due to the gearbox acting on the crossmember. The test rig configuration is depicted in Figure 6-2.

Three signals measured on the test track were used as control signals, namely:

- Strain gauge on left torsion bar measuring torsional shear strains, used to control the left wheel actuator.
- Strain gauge on right torsion bar, measuring torsional shear strains, used to control the right wheel actuator.
- Strain gauge on gearbox mounting bracket, measuring strains caused by vertical inertial forces, used to control the gearbox actuator.

Drive signals for the three actuators were computed, using time domain based identification software, to accurately simulate the measured signals.

Three specimens were tested to failure. Failure was assumed to have occurred as soon as a crack developed in the crossmember.

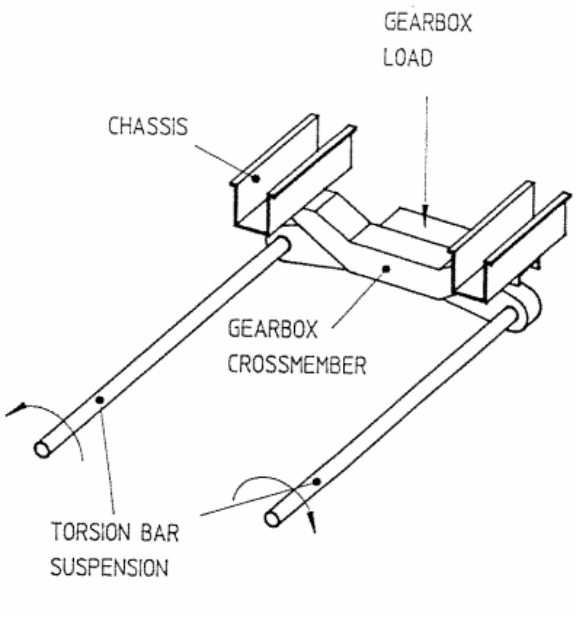

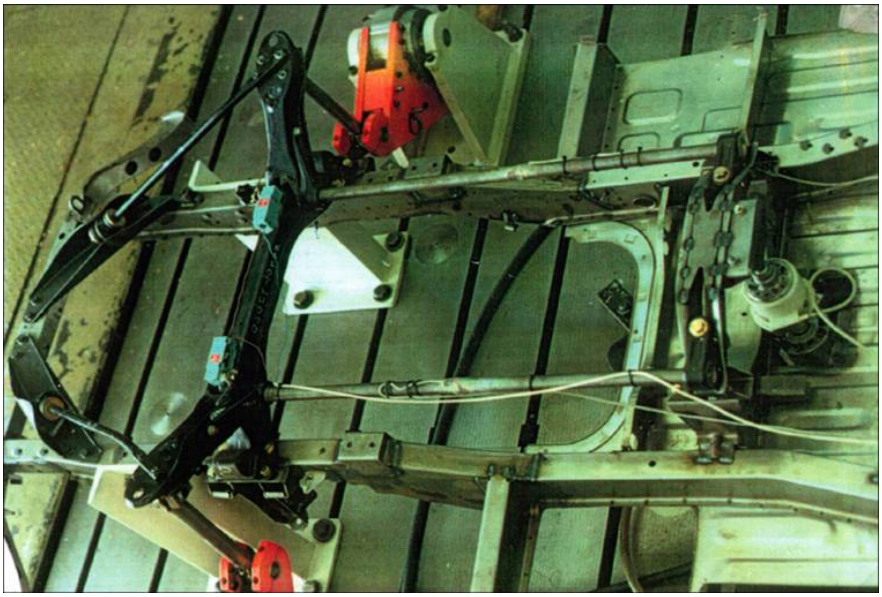

Figure 6-2: Test rig

6.2.2.2.2 Test results

The following number of test track cycles to failure was recorded for the three specimens that were tested:

Specimen no. 1:	1040 cycles	⇒ 26.87 relative damage
Specimen no. 2:	860 cycles	⇒ 22.22 relative damage
Specimen no. 3:	1240 cycles	⇒ 32.04 relative damage
Average :	1047 cycles	⇒ 27.06 relative damage

All cracks developed in the same position as had the field failures and there could be little doubt that the loading conditions had been the same. Some scatter was observed. It was

not possible to take account of this scatter in a statistical manner since too few specimens were tested. In subsequent analyses, the average damage to failure was therefore used.

6.2.2.3 Sales data

The specific minibus model was introduced to the market in December 1989. The sales for each month up to February 1991 (chosen as $date_{ref}$), are listed in Table 6-1.

Table 6-1 Sales figures for minibus

Month/Year	Sales	Month/Year	Sales
12/89	61	7/90	291
1/90	181	8/90	345
2/90	191	9/90	184
3/90	277	10/90	178
4/90	265	11/90	147
5/90	239	12/90	75
6/90	335	1/91	44

6.2.2.4 Results

The prediction calculations were subsequently performed using the theoretical distributions. The number of vehicles predicted to have failed was found to be more than the actual number of failures that had occurred up to February 1991 (308 vs 44).

Several reasons for this discrepancy could be put forward:

- The measurements were performed on a fully laden vehicle. Since it is probable that a certain portion of the distance reported by each participant would be travelled with an empty or half laden vehicle, the damage per kilometre would be overestimated.
- The questionnaire exercise may have been biased in relation to the total population of taxi operators. The number of participants may have been too small to obtain representative results. Also, the exercise involved only certain regions. Also it is not certain whether the percentages and distances per day quoted by the participants are applicable to 100 % of the distance covered by the vehicles and every day of the week. One participant quoted that he travels 1600 km/day, which seems unrealistic as an average distance per day. A better result would have been obtained if the average distance travelled per month had been asked.
- The damage to failure determined through laboratory testing was defined at the observance of a visible crack. Field failures may only have been reported after the crack had almost severed the crossmember. It was not possible to simulate this in the laboratory since the test had been performed in displacement control and not load control, implying that the induced force would diminish as the crossmember looses stiffness due to crack growth. The damage to failure may therefore have been underestimated by an unknown margin. This would cause an overestimation of the number of failures. A further test was subsequently performed on a cracked specimen to quantify this factor. The drive signals for the actuators were adjusted during the test to take account of the loss of stiffness of the specimen as the crack progressed, thus keeping the load inputs constant. The test was performed until final failure. A further 728 cycles resulted, implying that the damage to failure should be increased by a factor of 1.7.

- The number of sold vehicles utilized as taxis was unknown. It was assumed that 100% of the total sales had been utilized as taxis. An over estimation of the number of sales applicable to operational taxis (and therefore to the theoretical distributions) would cause an over estimation of the number of failures.
- Failures occurring in the field may not all have been reported.

It was not possible to quantify all of the above factors. A sensitivity study was however performed to study the influence of each factor on the prediction results. Adjustment factors were introduced within estimated reasonable ranges until a close correspondence between the actual failure results and the predicted results were obtained. The following factors were introduced:

- The damage per kilometre data was divided by a factor of 1.4.
- The kilometre per day data was divided by a factor of 1.8.
- The average number of operational days per month was taken as 20.
- The damage to failure was multiplied by a factor of 1.7, following the extended laboratory test.
- The number of vehicles utilized as taxis was taken as 0.6 times the total number sold.
- The number of failures reported was taken as 0.6 times the total number of failures.

The above set of adjustment factors does not represent a unique solution for obtaining a close correspondence between the prediction and the actual failure results, but was so chosen so as to result in a conservative estimation of the operational conditions pertaining to taxi vehicles.

The above process resulted in 45 vehicles being predicted to have failed in comparison to the actual 44. More importantly, however, is the good correspondence between the predicted and actual distributions of distance to failure. This comparison is shown in Figure 6-3. This result implied that the calibrated calculation process proved to be very successful.

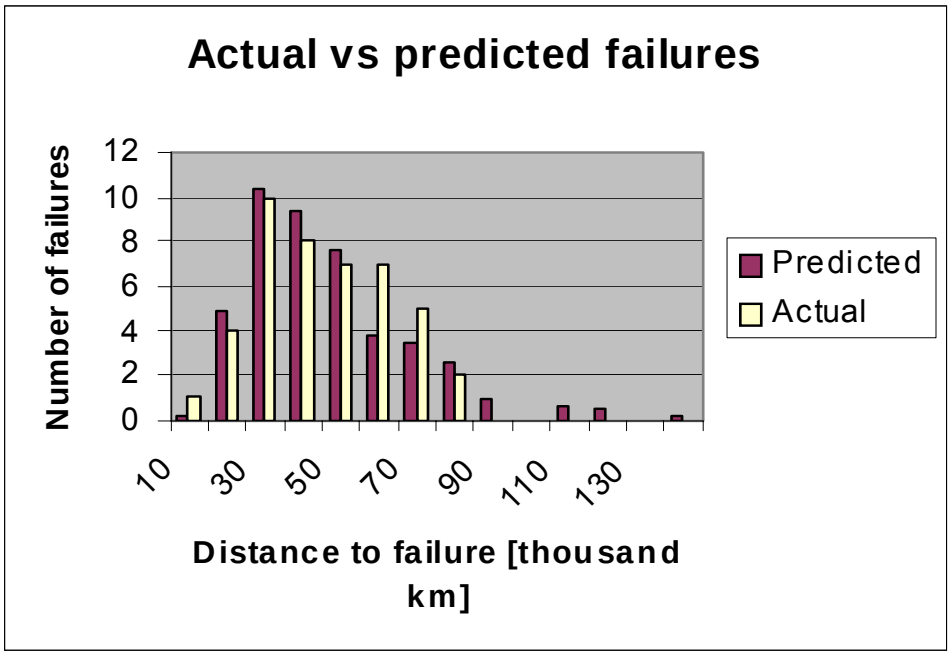

Figure 6-3 Actual vs predicted failures for minibus crossmember

6.2.2.5 *Monte Carlo simulation*

An alternative approach to the analytical approach used above for the prediction of failures, is the Monte Carlo simulation method discussed by Slavik and Wannenburg. The advantage of this approach is that it enables expansion of the number of variables treated as statistical variables. The Monte Carlo simulation method was applied to the pick-up truck case study, as described in paragraphs 5.5.4, 5.6.3 and 6.2.3. For the pick-up truck, no actual failure data was available and therefore the application of the method to the minibus case study, where correlation with actual failures can be demonstrated, serves as verification of the method.

As explained before and applied to the minibus, the method creates a large number of vehicles and randomly assigns to each one a D/km and a km/month parameter, such that the bivariate distribution of these two parameters for the created population, closely corresponds to the distribution derived above from the measurements and surveys. This is achieved through the process depicted in Figure 5-32.

It is then a simple matter to calculate the distance to failure (D_f / damage per km) and the months to failure (distance to failure / km per month) for each random vehicle. These results, together with the actual sales data, are used to predict the failure rates. The result of this analysis is depicted in Figure 6-4.

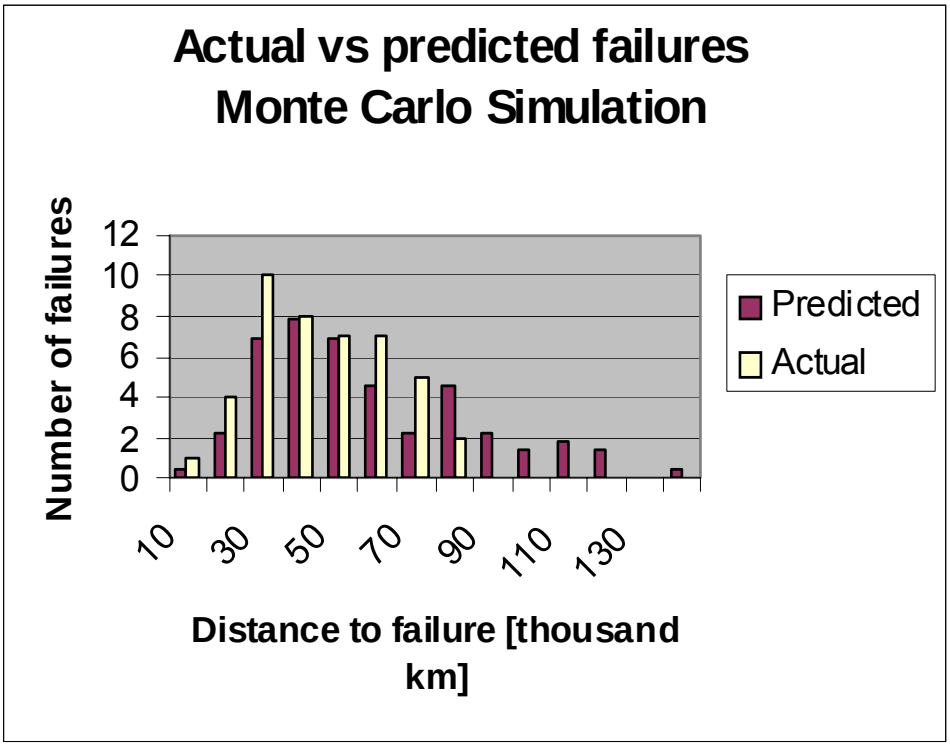

Figure 6-4 Actual vs Monte Carlo predicted failures for minibus crossmember

The results are similar to the results achieved with the analytical approach, as it should be, and therefore verifies the Monte Carlo approach.

6.2.2.6 *Summary*

A methodology has been developed to establish durability qualification test requirements for minibus vehicles based on South African conditions. The investigation involved a

statistical and fatigue representation of the operational conditions pertaining to taxi vehicles, based on the results of extensive measurements of road conditions, as well as data obtained from a questionnaire.

The theoretical results were used to predict the failures of gearbox mounting crossmembers that had failed in practice. The predicted results were compared to the actual failure results and with some adjustments, excellent correspondence was achieved. Durability requirements were subsequently derived.

The process thus established proved to be extremely successful. It is proposed that the methodology could be generalized to be applicable to any vehicle and could be used to address the establishment of durability test requirements in a powerful scientific manner.

A reverse method, based on the above is presented in paragraph 6.4 to derive a statistical representation of the usage profile of a vehicle in terms of fatigue damage, based only on failure data and sales data, without the use of questionnaires.

6.2.3 Pick-up Truck

6.2.3.1 Objectives

It was required to qualify the vehicle for South African conditions, which was to be defined by the usage profile exercise. It was aimed to perform the test for a sufficient duration such that all failures that may be expected to occur in the customer fleet within a reasonable life of the vehicle, would be reproduced on the test rig. The target was set as the equivalent of 300 000 km of 95 % of all users.

6.2.3.2 Laboratory test rig

The test rig consisted of four vertical servo-hydraulic actuators, with two 40kN actuators for the front wheels and two 100kN actuators for the rear wheels. (Dissimilar actuators were used simply due to equipment availability). Each actuator was equipped with a horizontal wheel platform that was provided with a mechanism preventing rotation of the actuator ram about the vertical axis. Restriction of fore-aft movement of the vehicle was provided by a small round bar at the front and rear of each of the front wheels, while lateral movement of the vehicle was prevented by side plates on the outsides of the four wheels on the wheel platforms. An axial fan with blow tubes was used as cooling aid for the vehicle's shock absorbers. The actuators were driven in displacement command mode and controlled via a digital to analogue interface system from a PC.

The test vehicle was placed on its wheels on the four poster road simulator. No side forces, braking or acceleration forces were therefore simulated. From previous experience, it is argued that a large portion of structural damage induced on pick-up truck vehicles would be caused by vertical inputs, since it is a vehicle intended to be used for carrying cargo on often rough road surfaces.

The test vehicle was fully laden since the field data sections used were all for the fully laden condition.

6.2.3.3 Calculation of actuator drive signals

It was necessary to perform two separate drive signal calculations. Low frequency drive signals were calculated from response data measured by the coil spring strain gauges and the differential strain gauges, filtered to contain frequencies between 0 and 5 Hz

only. High frequency drive signals were calculated from response data measured from the wheel accelerations, filtered to contain frequencies between 5 and 25 Hz (the accelerometers, although necessary to measure the high frequency inputs, do not respond at the low frequencies). The two drive signals were then superimposed to obtain the final drive signal.

The process to derive drive signals for the test rig is described in paragraph 3.4.6.2.

Due to hydraulic limitations, as well as safety considerations, it was not possible to achieve the same acceleration factors for the rear wheels to those achieved for the front wheels.

6.2.3.4 Relation between laboratory durability sequence and usage profile distance

The same fatigue damage calculation procedure was applied to the test rig measured responses for all the strain gauges. This resulted in the fatigue damage induced by the road simulator during one cycle of the laboratory test sequence.

The results are listed in Table 6-2. Again, comparison of the values for different channels has no meaning.

From this information, the required number of cycles to achieve the target test distance, pertaining to the 95 % user, could be determined, as described in paragraph 5.6.3.2.

Table 6-2 Test damage per cycle

Strain channel	Description	Test D/cycle $\times 10^{-6}$
1	Left front coil spring	179.3
2	Right front coil spring	261
3	Right rear differential	79
4	Left rear differential	6.5
5	Left front strut	1.1
6	Right front beam outside	111.4
7	Left beam centre between wheels	14.7
8	Round cross member	0.9
9	Left top door corner	1.6
10	Loadbox left rear panel	0

Although the intention was to achieve an equal acceleration for all channels, this was not achieved. The differences between the front wheel and rear wheel channels were ascribed to hydraulic limitations. The relatively low kilometre value of channel 10 could be attributed to the fact that a canopy that was fitted during the field measurements to protect the equipment, was not fixed onto the loadbox during the durability test. It is argued that a canopy changes the stiffness characteristics of the loadbox and hence affects the damage/kilometre results.

The test was terminated before achieving the target distance, due to failures.

6.2.3.5 Road simulator test failure results

When evaluating the test failure results, every failure can be related to one of the measurement channels by assessing which load input would primarily be causing the failure. All the failure events together with their corresponding cycles and damages to failure and assigned strain channel(s) are listed in Table 6-3.

Table 6-3 Road simulator test results

Damage	Cycles	Event	Corresponding Strain channel(s)
0.0024	302	Left rear leaf spring failure	3,4
0.0044	557	Right rear leaf spring failure	3,4
0.0033	416	Left rear leaf spring failure	3,4

The failures occurred well before the required 2000 cycles. The average cycles to failure was 425 and from Figure 5-34 it can be seen that this implies 300 000 km for the average (50 %) user.

6.2.3.6 Fatigue life prediction

Using the failure results, it was possible to perform a statistical failure prediction calculation. The first step was to use Bayesian inference to derive the statistical properties of the failure results. For this a prior mean and standard deviation had to be chosen, assuming a log-normal distribution. The posterior distribution was then derived from the combination of the prior distribution and the real failure results. The results of this calculation are depicted in Figure 6-5. A significantly smaller standard deviation was chosen for the prior distribution, but the relatively wide ranging failure results, implied a posterior distribution with a larger spread.

The Monte Carlo simulation method then requires a random failure damage (D_f) to be chosen according to the above distribution, for each of the 10 000 samples of x_1 (km/month) and x_2 (D/km) chosen using the process depicted in Figure 5-32.

The months to failure for each random sample (i) can then be calculated:

$$\text{months to failure}_i = D_{fi} / (x_{1i} \times x_{2i})$$

The results are then sorted from small to large and plotted against each sample's index (i) /1000 $\times$ 100, to yield a cumulative distribution of months to failure against cumulative percentage user, as depicted in Figure 6-6. The months to failure predicted for an improved design of the leaf springs which would survive the required 2000 test cycles can be calculated and similarly plotted:

$$\text{months to failure}_i = \text{D per cycle} \times 2000 / (x_{1i} \times x_{2i})$$

The distance to failure is calculated and plotted in Figure 6-7;

$$\text{distance to failure}_i = D_{fi} / x_{2i}$$

and for an improved design:

$$\text{distance to failure}_i = \text{D / cycle} / x_{2i}$$

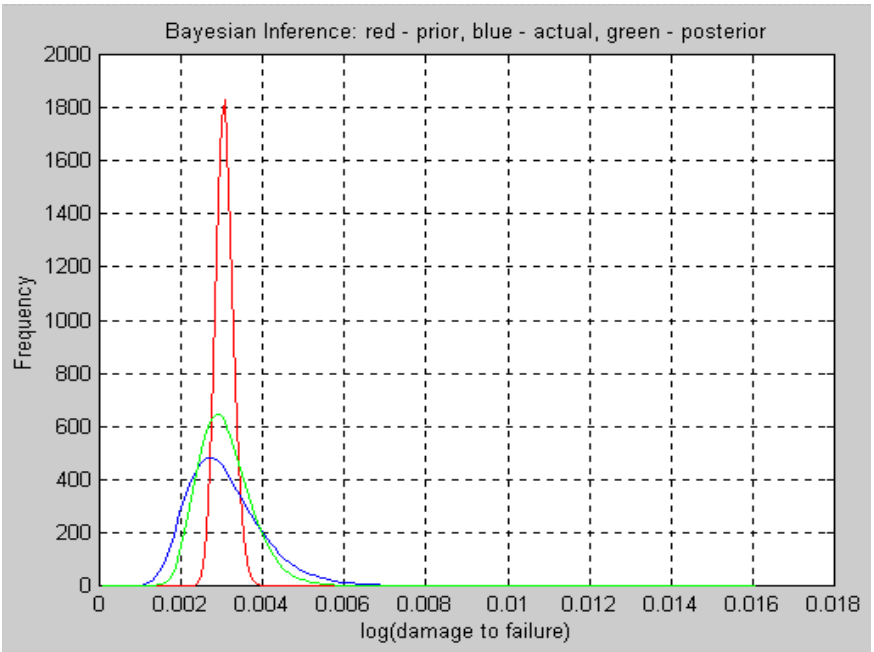

Figure 6-5 Bayesian inference of pickup truck damage to failure

From these graphs it can be seen that with the current design, 33 % of users will experience failures within 5 years (60 months) and 50 % will experience failure before 300 000 km. With the improved design, less than 3 % will experience failures within 5 years and less than 5 % before 300 000 km (as was intended).

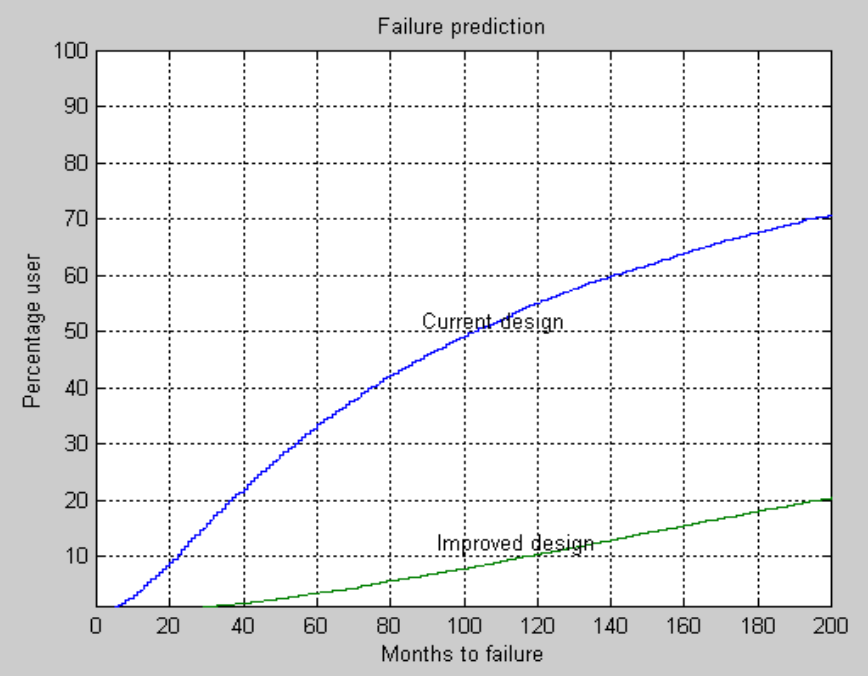

Figure 6-6 Time-to-failure prediction for pickup truck

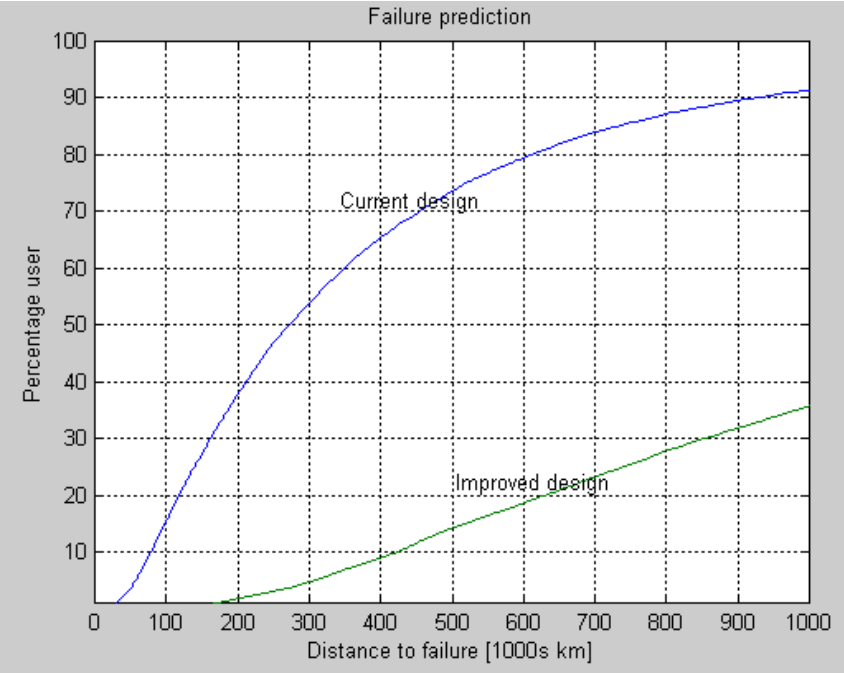

Figure 6-7 Distance-to-failure prediction for pickup truck

6.2.4 Fuel Tanker

6.2.4.1 Fatigue life prediction of prototype design

The fuel tanker design process described thus far, included comprehensive measurements on a prototype vehicle, based on which fatigue design criteria were derived (see paragraph 5.4.4). These criteria were subsequently used to estimate the fatigue life of the prototype design, according to the method described in paragraph 5.4.2.1.5. It was found that acceptable lives were estimated for all critical areas, except for a bulkhead support beam, the design of which therefore had to be modified. It was therefore expected to have no failures during the required life of the vehicles of 2 million kilometres. The majority of the fleet has to date exceeded the required life and in most cases no structural failures have been reported, thereby substantiating the FESL process. Premature field failures had been however reported on some vehicles, which were then investigated, as described in the following paragraphs.

6.2.4.2 Field failure description

The failures occurred on vehicles that were fitted with underslung axles, which were introduced due to availability problems with the overslung axles that were used in the original design. The engineering change procedure failed to highlight the fact that a large access hole (refer to Figure 6-8) for the airbag was to be introduced on the inside of the lower flange of the chassis beam in a critical stress area. The cracks experienced in the field all originated from this hole (after typically 800 000 km) and in some cases propagated into the web to almost sever the beam.

6.2.4.3 Prediction of field failures

6.2.4.3.1 Finite element analysis

The complete half model of the front trailer was used for the analysis (refer to paragraph 5.4.4.1). The access hole was modeled and the mesh was refined in the critical area. Vertical inertial loading was applied.

The stresses at the hole for a 1 g vertical loading are depicted in Figure 6-9. A maximum peak stress of 114 MPa is observed at the side of the hole.

6.2.4.3.2 Fatigue assessment

The fatigue design criterion established in paragraph 5.4.4.3 was that a fatigue life of 2 million kilometres on the vehicle is represented by 2 million cycles of a vertical loading range of 0.62 g. The fatigue equivalent peak stress range ($\Delta\sigma_e$) at the side of the access hole, to be experienced 2 million times during a 2 million kilometre life, would therefore be:

$$\Delta\sigma_e = 0.62 \times 114 = 71 \text{ MPa}$$

The material SN-curve for unwelded Aluminum in BS 8118 (1991) has a class of 60 (2.3% probability of failure), implying a fatigue strength (stress range) of 60 MPa at 2 million cycles.

The corresponding material fatigue properties as per Eq. 3-14 may be calculated as follows:

$$\Delta\sigma = S_f N^b$$
$$b = -0.333$$
$$\therefore 60 = S_f \left(2 \times 10^6\right)^{-0.333}$$
$$\therefore S_f = 7\,523 \text{ MPa}$$

The life to failure implied by the 71 MPa applied peak stress range can then be calculated:

$$\Delta\sigma = S_f N^b$$
$$\therefore N = \left(\frac{\Delta\sigma}{S_f}\right)^{1/b}$$
$$\therefore N = \left(\frac{71}{7523}\right)^{1/-0.333} = 1.2 \times 10^6 \text{ cycles}$$

Since 2 million cycles represents 2 million kilometres :

Predicted distance to failure $= 1.2 \times 10^6$ km

The predicted life correlates very well with the field failures, therefore again powerfully verifying the FESL method.

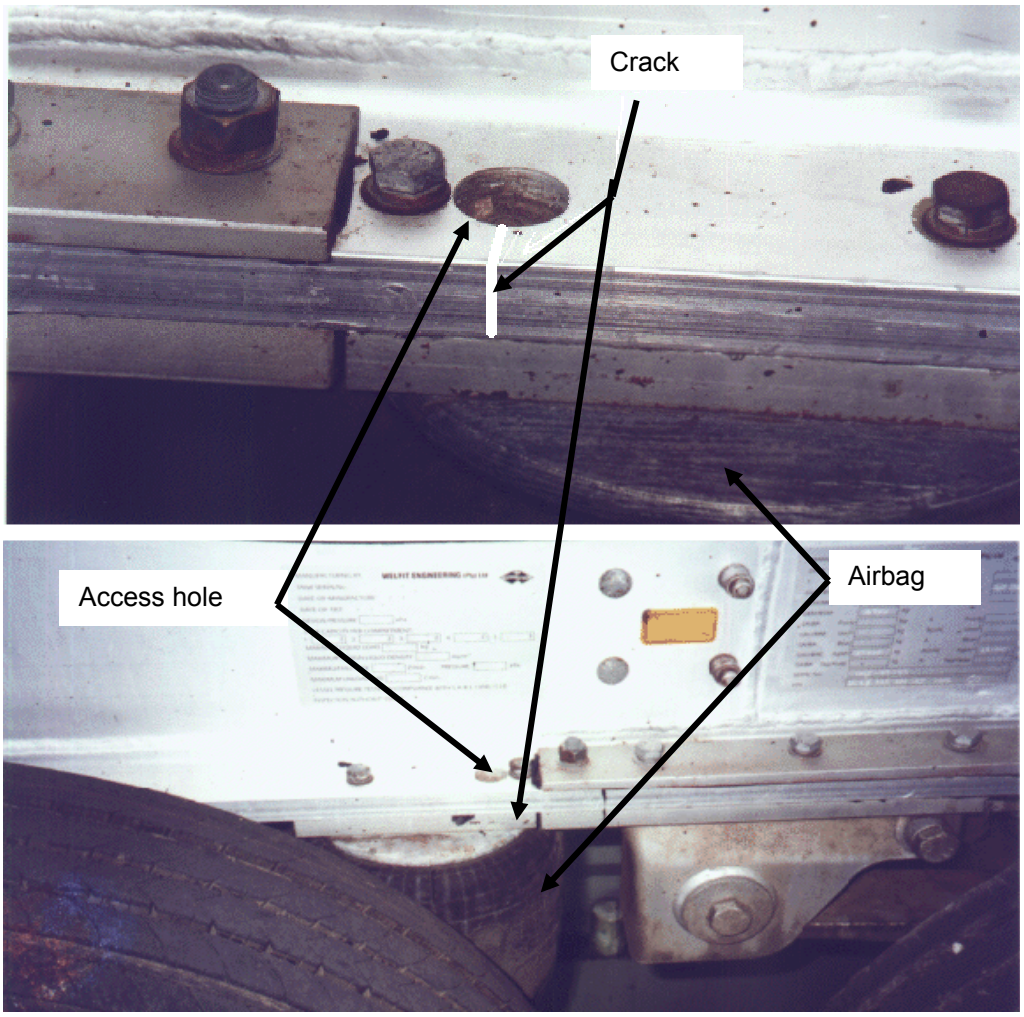

Figure 6-8 Field failure on fuel tanker

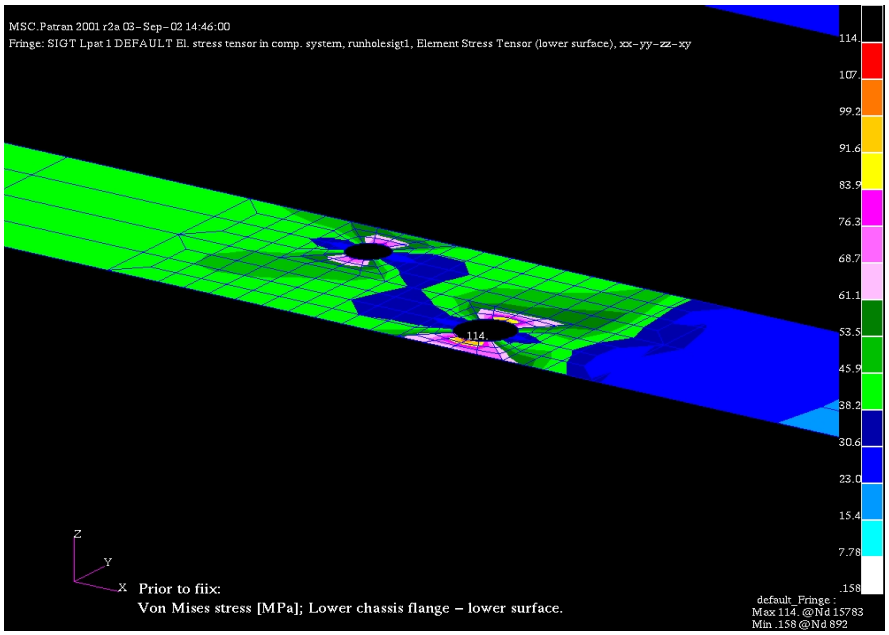

Figure 6-9 Fuel tanker chassis flange stresses

6.2.5 Ladle Transport Vehicle

6.2.5.1 Fatigue life prediction

The fatigue life estimation was performed using the Fatigue Module (based on nCode algorithms) of the MSC Patran software. The time histories of the vertical and lateral g-loads, as well as the modal participation factor (derived in paragraph 5.3.2.1), are multiplied separately with the unit load finite element stress results, obtaining stress histories for the total model. These stress histories are then superimposed to give total stress-time histories for the total model. Prescribing then the relevant SN material properties and understanding that the time histories would be repeated (80 000 hours / duration of histories in hours) times for a life, the hours to failure are calculated for the total model, based conservatively on the maximum absolute principal stresses. The software package performs the rainflow cycle counting and damage calculations internally and outputs contour plots of hours-to-failure.

6.2.5.2 Results

Some typical results are depicted in Figure 6-10 to Figure 6-13. Problem areas are pointed out with numbered arrows:

1) Web stresses perpendicular to cross member to web fillet weld.
2) Bottom flange stresses perpendicular to doubler plate fillet welds.
3) Top flange stresses perpendicular to doubler plate fillet wells.

Based on the above results, modifications were designed to achieve acceptable lives in the problem areas.

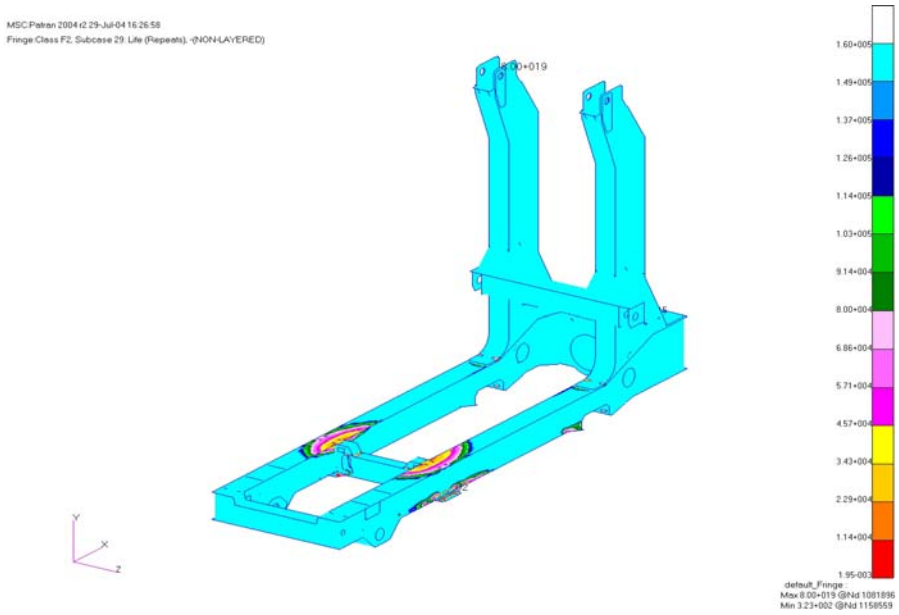

Figure 6-10 Estimated fatigue life for total model

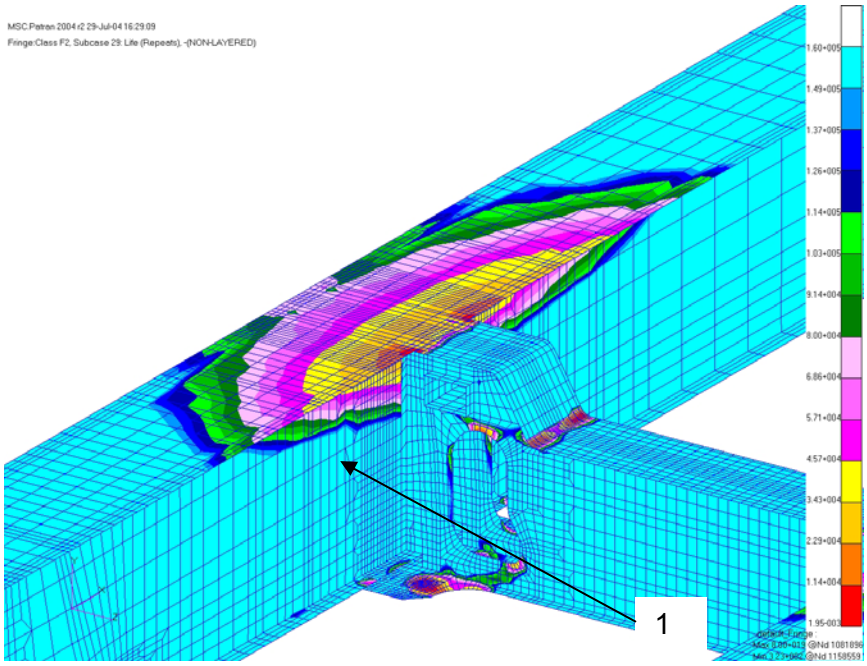

Figure 6-11 Fatigue life for crossmember to chassis welds

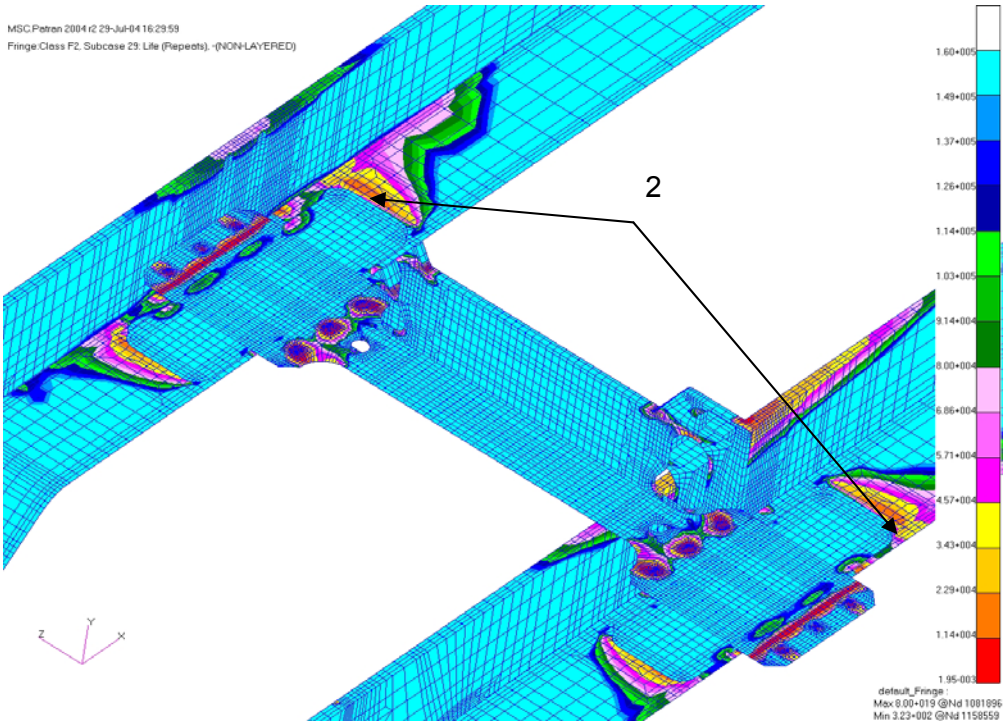

Figure 6-12 Fatigue life for doubler plate welds

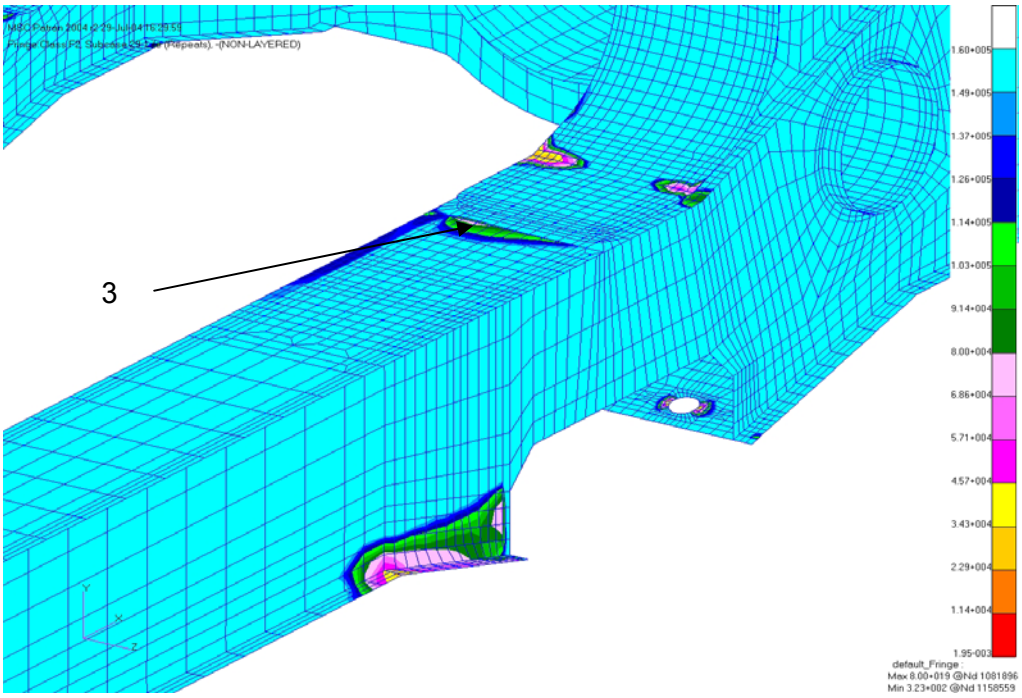

Figure 6-13. Fatigue life for chassis to pillar doubler plate welds

6.2.6 Load Haul Dumper

6.2.6.1 Fatigue life prediction

All the critical connections in the vehicle structure in the finite element model were divided into different groups, which correspond with the categories described in BS 7608 (1993). The parent metal, for example, was grouped as a category C, and a full penetration fillet weld as a category D, etc. The weld categories as chosen for the vehicle are depicted in Figure 6-14.

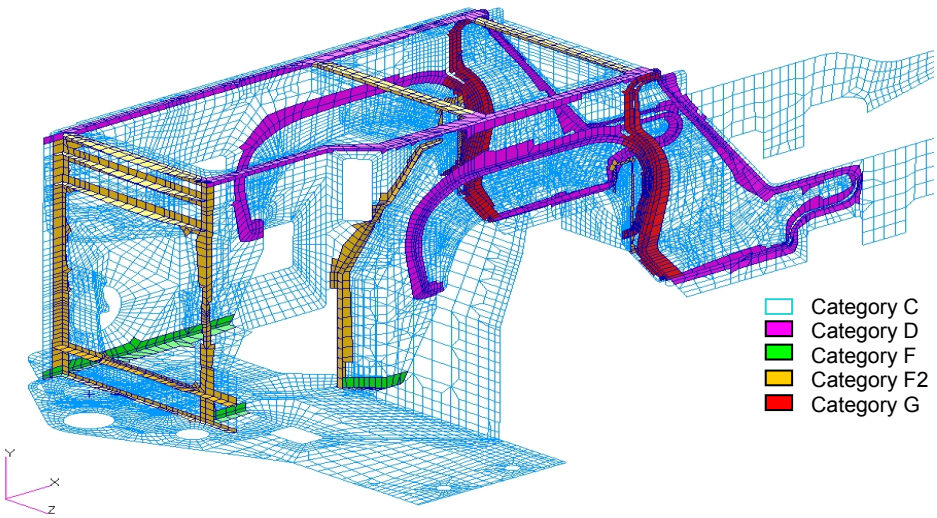

Figure 6-14 Weld categories according to BS7608

Using MSC FATIGUE solver, the stress results from the load factors as discussed in paragraph 5.4.6.3 were used to calculate the damage for the whole finite element model, using different S-N curves for each category. The result of this analysis would be the damage of one cycle for the whole model for each load case. The damages for the three load cases can then be summed, and then inversed again to give the number of cycles the structure will survive for the combined load case. As mentioned in paragraph 5.4.6.2, 2 million of these cycles corresponds to a life of 10000 hours. The result of this analysis is depicted in Figure 6-15.

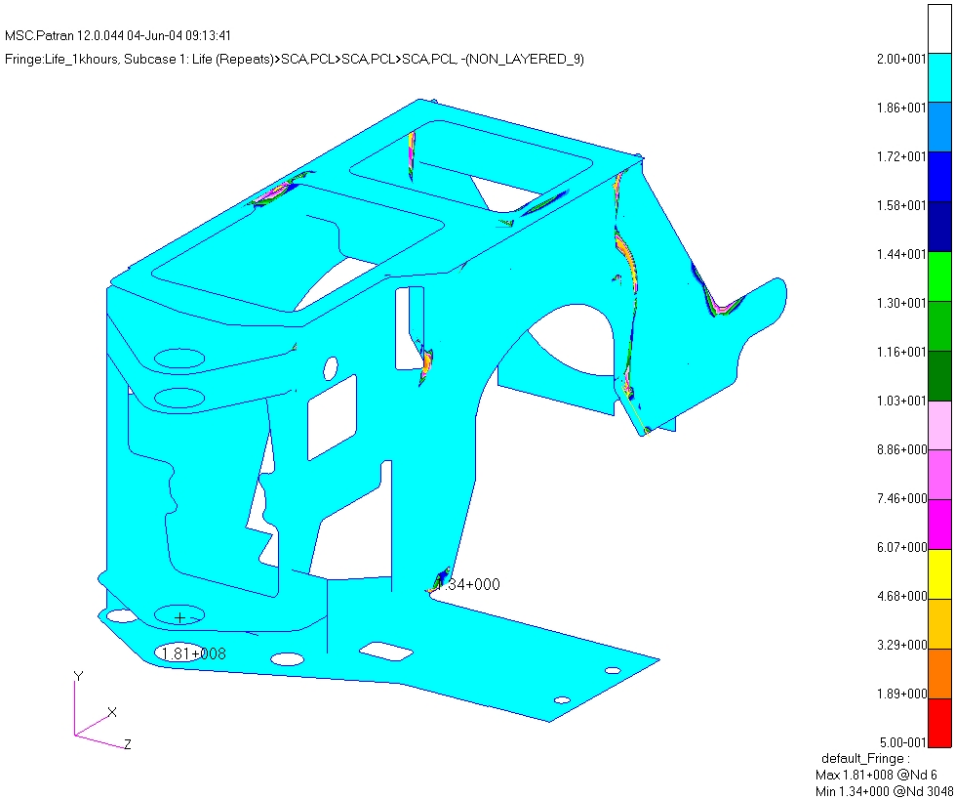

Figure 6-15 Fatigue life results for LHD

6.2.6.2 Correlation with field failures

Cracks were found on the chassis of a vehicle that was approximately 6 000 hours old. Photographs of these cracks, together with the corresponding fatigue life prediction contour plots, are depicted in Figure 6-16. Adequate correlation is achieved.

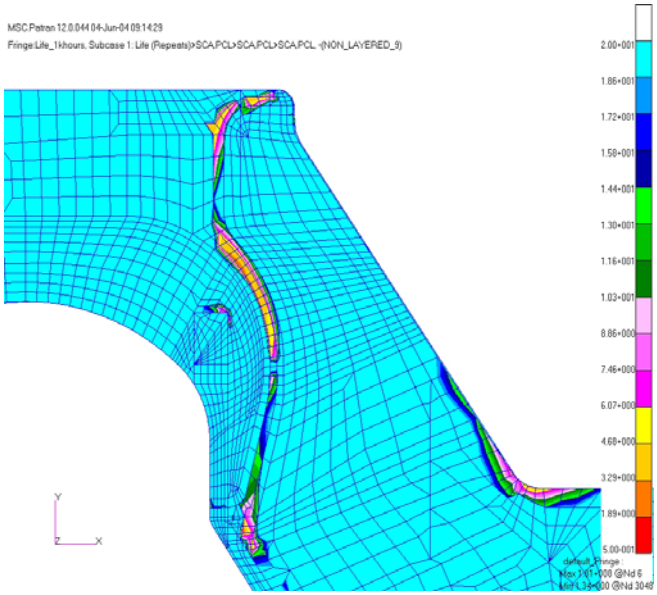

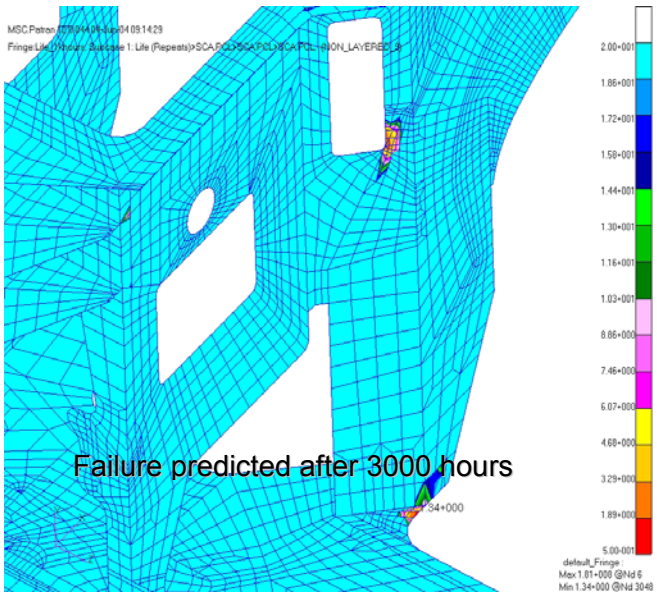

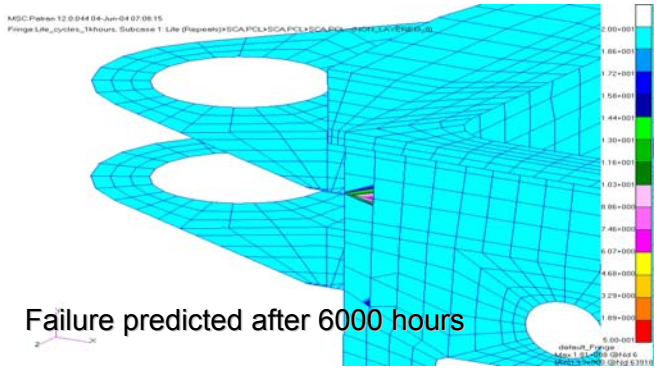

Figure 6-16 Correlation of predicted failures and field failures for LHD

6.3 DESIGN CODE CORRELATION

6.3.1 General

Comparisons of the input loads derived for the fuel tanker and the ISO tank container to relevant design codes, are performed in this section.

6.3.2 Fuel Tanker

6.3.2.1 Types of stresses calculated

South African fuel tankers are required by law to comply to two South African Bureau of Standards codes, namely:

- SABS (South African Bureau of Standards) 1398. (1994). *Road tank vehicles for petroleum based flammable liquids.*
- SABS (South African Bureau of Standards) 1518. (1996). *Transportation of dangerous goods – design requirements for road tankers.*

Both codes require the calculation of maximum principal stresses to be assessed against the allowable stresses. Any specific point at any position on the structure could be subjected to a combination of normal stresses (tensile or compressive in three possible directions) and shear stresses (also in three possible directions). At the surface (where maximum stresses always occur due to bending and torsion), the normal stress perpendicular to the surface, as well as the two shear stresses in the surface plane, must be zero, leaving two normal stresses and one shear stress to be determined. The maximum principal stress would be a normal stress caused by a combination of these three stresses in some principal direction in the plane of the surface.

During the finite element analysis, maximum principal stresses, TRESCA stresses, as well as sometimes Von Mises stresses, were calculated. The latter two types of stresses are basically equivalent. They differ from maximum principal stresses by virtue of the fact that they are equal to the difference between the maximum and the minimum principal stresses. They were calculated for the following reasons:

- The fatigue, as well as the yielding failure mechanism, are in fact driven by these stresses, rather than by maximum principal stresses.
- These stresses will always be equal or larger than the maximum principal stress on the surface, since one principal stress will always be zero and the maximum principal stress minus zero (if no negative principal stress exists) will be equal to the maximum principal stress. These stresses therefore yield more conservative (but necessarily so) results.

The calculated TRESCA or Von Mises stresses were therefore regarded as maximum principal stresses for the purpose of the codes.

A further interpretation required for assessing the calculated stresses in terms of the SABS codes, concerns the difference between local and global stresses. Both SABS codes are intended for simplified calculations of stresses on mostly cylindrical type tank vessels. Global bending, tensile and shear stresses are calculated by considering the vessel as a beam. When performing a detailed finite element analysis, especially on a complex geometry such as the fuel tanker structure, some very localised stresses are calculated at stress concentration positions. The allowable global stress criteria of the

codes are then inappropriate (sometimes being conservative or unconservative) and a more detailed assessment using BS 8118 (1991), is invoked.

6.3.2.2 SABS 1398

Acceleration forces are to be applied as separate load cases to the fully loaded vehicle. These are:

- 2 g longitudinal
- 2 g vertical
- 1 g lateral

For each of these load cases, the maximum allowable principal stresses in the tank wall are required to be lower than 20 % of the tensile strength of the material.

6.3.2.3 SABS 1518:1996

This code requires a combination of acceleration forces for load conditions expected during normal use. Additional to this, accident loads must be investigated according to other criteria. For normal use the design load requirements are:

- 0.75 g longitudinal + 1.7 g vertical + 0.4 g lateral

and the maximum allowable principal stresses must be less than 25% of the ultimate tensile strength of the material.

Design loads in the event of an accident are:

- 2 g longitudinal

and stress levels (maximum principal) must be less than 75% of the yield strength of the material.

6.3.2.4 BS 8118 (FESL)

BS 8118 does not specifically apply to tanker vehicles, but is a general structural design code for aluminium, which deals with static as well as dynamic loading conditions. For the limit state static design, the BS 8118 code requires the following loading.

Maximum expected loading factored by load factor (γ_f = 1.33):

- 0.75 g x 1.33 longitudinal + 1.7 g x 1.33 vertical + 0.4 g x 1.33 lateral

The resultant stresses should then be less than the factored resistance of the material (γ_m = 1.3), with material resistances given for the raw material, the heat affected raw material, the welding material, as well as the heat affected zone (HAZ) material. For dynamic loading, the BS code gives material properties for different details. The equivalent fatigue loading used is derived in paragraph 5.4.4.3.

6.3.2.5 Comparison of codes

Table 6-4 below gives a comparison of the different codes. If only regarding the vertical loading, the different codes compare as follows in terms of allowable stresses for the extrusions for 1 g vertical loading:

- SABS 1398: 28 MPa
- SABS 1518: 41 MPa
- BS 8118 static: 50 MPa (for HAZ)
- BS 8118 fatigue + FESL: 32 MPa (for weld class 20)

It is demonstrated that the FESL criterion derived for the fuel tanker, combined with BS 8118, is similar to the requirements of the SABS codes. The FESL method, however, has the benefit that it accounts explicitly for fatigue and differentiates between different fatigue strength categories in the design (for class 20 and higher categories, SABS 1398 would become progressively more conservative, but it would become unconservative for classes lower than 20.

Table 6-4 Comparison of different fuel tanker design code requirements

	SABS 1398	SABS 1518	BS 8118 Static	BS 8118 Fatigue
Longitudinal	2 g	0.75 g (2 g)	1 g	
Vertical	2 g	1.7 g	2.26 g	0.62 g
Lateral	1 g	0.4 g	0.53 g	
	Separate	Combined	Combined	
Allowable stress plates	62 MPa	77.5 MPa (232.5 MPa)	181 MPa for raw material 188 MPa for weld material 115 MPa for HAZ material	Typ. > 35 MPa for raw material Typ > 20 MPa for weld material (depending on classification)
Allowable stress extru.	56 MPa	70 MPa	185 MPa for raw material 146 MPa for weld material 112 MPa for HAZ material	

6.4 DERIVATION OF USAGE PROFILE FROM FIELD FAILURE DATA

6.4.1 General

Field failure data could be the most valuable source from which usage profiles may be derived. Goes (1995) argues that good or bad experiences of the ultimate tester, the customer, rarely find their way into the new product.

The successful mathematical model developed for failure prediction in paragraph 6.2.2 above prompted an attempt to develop a reverse method from which the two-parameter statistical usage profile could be derived by using only the available failure data, without the questionnaire and measurement data. This methodology is demonstrated based on the minibus case study.

6.4.2 Methodology

6.4.2.1 Probability density function

The bivariate lognormal PDF (Eq. 5.24), which defines the statistical usage profile, has five unknown constants:

- Mean of y_1 (μ_{y1})
- Mean of y_2 (μ_{y2})
- Standard deviation of y_1 (σ_{y1})
- Standard deviation of y_2 (σ_{y2})
- Correlation coefficient (ρ)

Ranges of interest for these parameters may be estimated. It is firstly assumed that the relative damage calculations are such scaled that the damage to failure for the structure/component for which failure statistics are known, is unity (i.e. $D_f = 1$).
Distances travelled before failure occurs could range from 10 000 km to 10 000 000 km, implying a total range for x_1 of D_f / distance = 1/10000 to 1/10000000 and for $y_1 = \ln(x_1)$ = -9.2 to –16.1. It is conceivable that one standard deviation in terms of distance to failure

may imply a maximum factor of 10 on the distance, or σ_{y1} = ln(10) = 2.3. Applying a standard deviation of 2.3 to the total range of y_1, it may then be argued that the range for the mean of y_1 could be estimated as μ_{y1} = -16.1 +2.3 = -13.8 to –9.2 –2.3 = -11.5.

Similarly, it may be estimated that x_2 for a population of vehicle owners may vary from 100 to 30 000 km/month (rather than km/day), implying y_2 = ln(x_2) = 4.6 to 10.3. Applying again a standard deviation of σ_{y2} = 2.3, the range for the mean of y_2 could be estimated as μ_{y2} = 4.6+2.3 = 6.9 to 10.3-2.3 = 8. These calculations are summarised in Table 6-5.

Table 6-5: Ranges of parameters

	Total min	-Max std dev	+Max std dev	Total max
Distance to failure	10000	100000	1000000	10000000
x1=1/Distance to failure	1.00E-04	1.00E-05	1.00E-06	1.00E-07
y1	-9.2	-11.5	-13.8	-16.1
x2=distance per month	100	1000	3000	30000
y2	4.6	6.9	8.0	10.3

The correlation coefficient (ρ) could vary between 0 (no correlation between two parameters y_1 and y_2) and –1 (full inverse proportionality). In practice, values between –0.1 and –0.5 would be expected, since some correlation would always exist (less distance on rough roads), but certainly not full proportionality. A typical set of values would therefore be:

μ_{y1} = -12.6 μ_{y2} = 7.5
σ_{y1} = 1 σ_{y2} = 1
ρ = -0.3

The bivariate Probability Density Function for these parameters is depicted in Figure 6-17. A contour plot of the PDF is depicted in Figure 6-18.

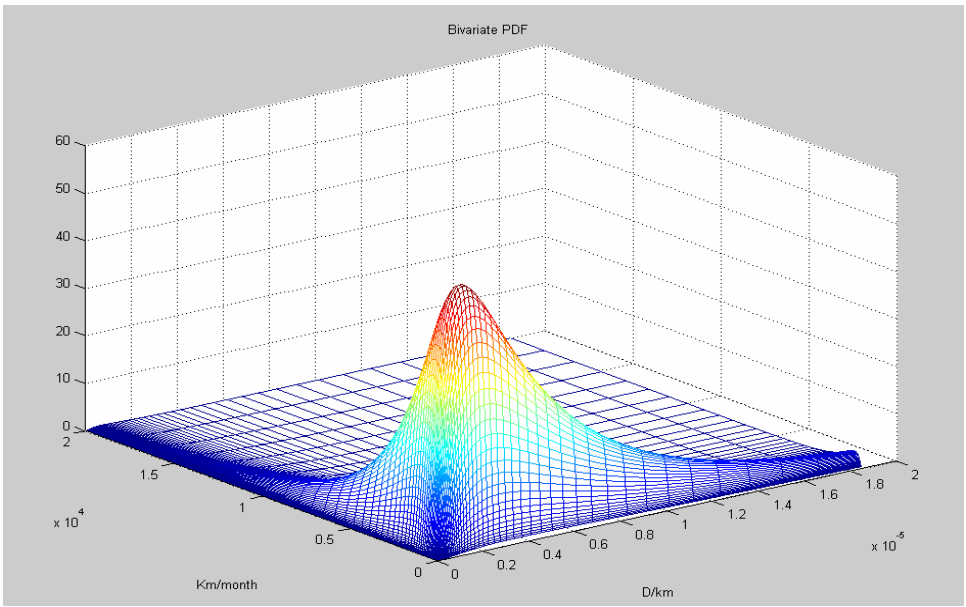

Figure 6-17: Probability Density Function for typical parameters

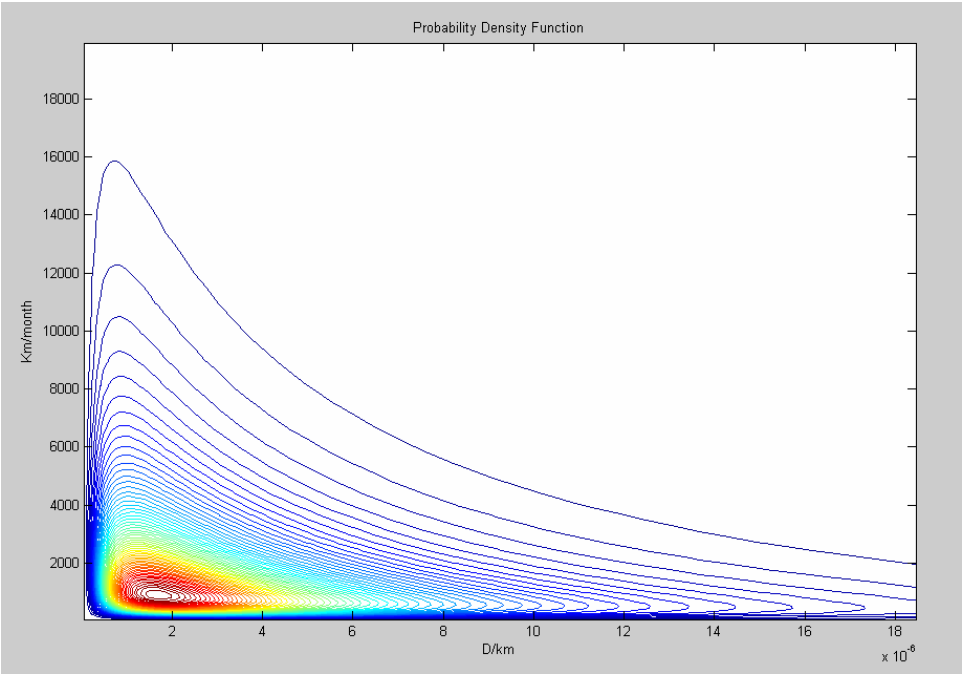

Figure 6-18: Contour plot of PDF for typical parameters

Plotting the PDF on a logarithmic scale for both axes (using the natural logarithm), yields a bivariate normal distribution, as depicted in Figure 6-19. On the same plot, the constant damage per time period (in this case, D = 1 and period = 12 months) lines, which are hyperbolas on a linear scale plot (see Figure 6-1), is depicted. The probability of a vehicle that is 12 months old, exceeding a damage of D = 1, can be calculated as the volume of the PDF to the right and above the 12 month line (the shaded area).

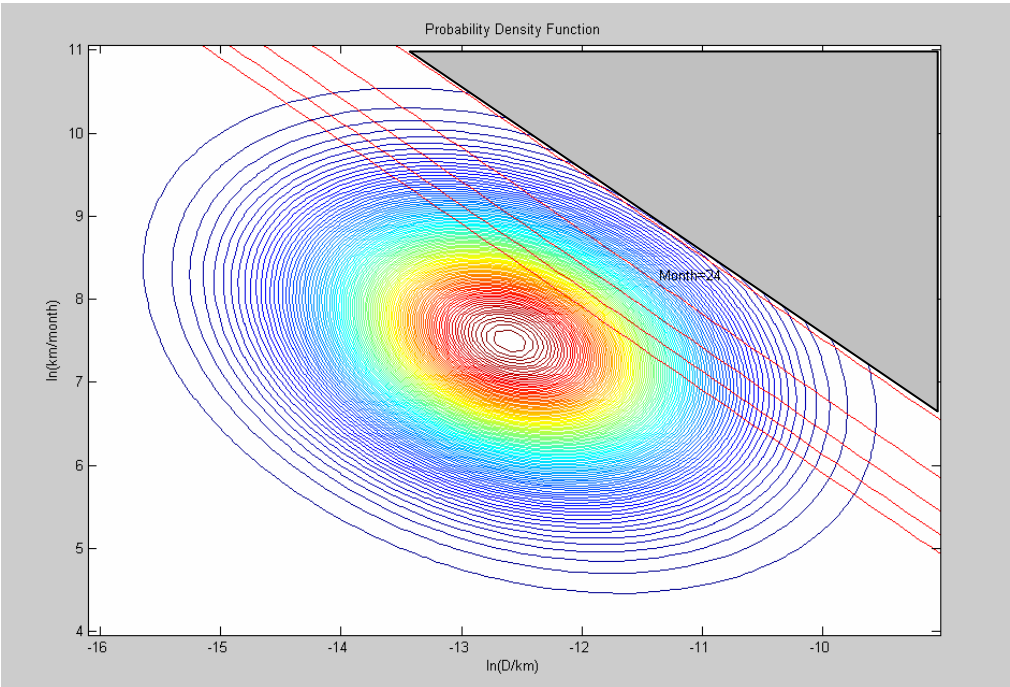

Figure 6-19: Contour plot of PDF for typical parameters on logarithmic scales

6.4.2.2 *Failure data*

Normally for any vehicle, available failure data would include the distance travelled by the failed vehicle, as well as its age. After performing a fatigue test to reproduce the experienced failure, the relative damage (D_f) to produce failure (with a known relation to cycles on the test track), would also be known. It is therefore possible to calculate the values of both parameters (dam/km and km/month) for each incidence of failure:

$$D/km = D_f / (\text{distance to failure})$$

$$km/month = (\text{distance to failure}) / (\text{age in months})$$

A Monte Carlo simulation method for predicting failures, depicted in Figure 6-20, was implemented as MATLAB code, in order to have a software tool to produce a simulated set of the above failure statistics for a given set of usage profile parameters.

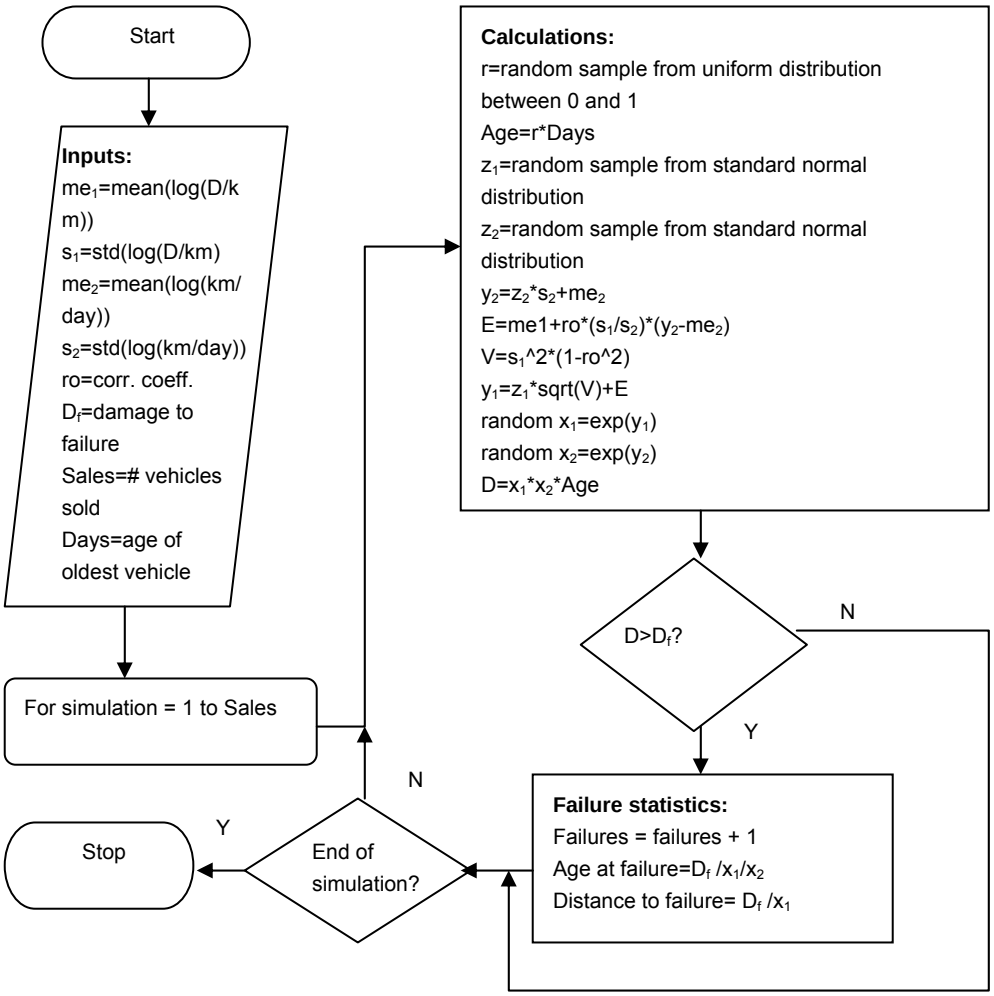

Figure 6-20: Monte Carlo simulation method

In all cases, it was assumed that the relative fatigue damages are scaled such that D_f = 1. The simulation was performed for a period of 5 years (60 months), with an assumed uniform sales distribution of 100 vehicles per month.

The first simulation was performed for the typical usage profile parameters listed above. 484 failures were simulated out of the total population of 6 000 vehicle (8 %). Figure 6-

21 depicts the contours of the PDF, the constant damage/month lines, as well as the failure parameters (D/km and km/month). Each failure incidence is represented by a star.

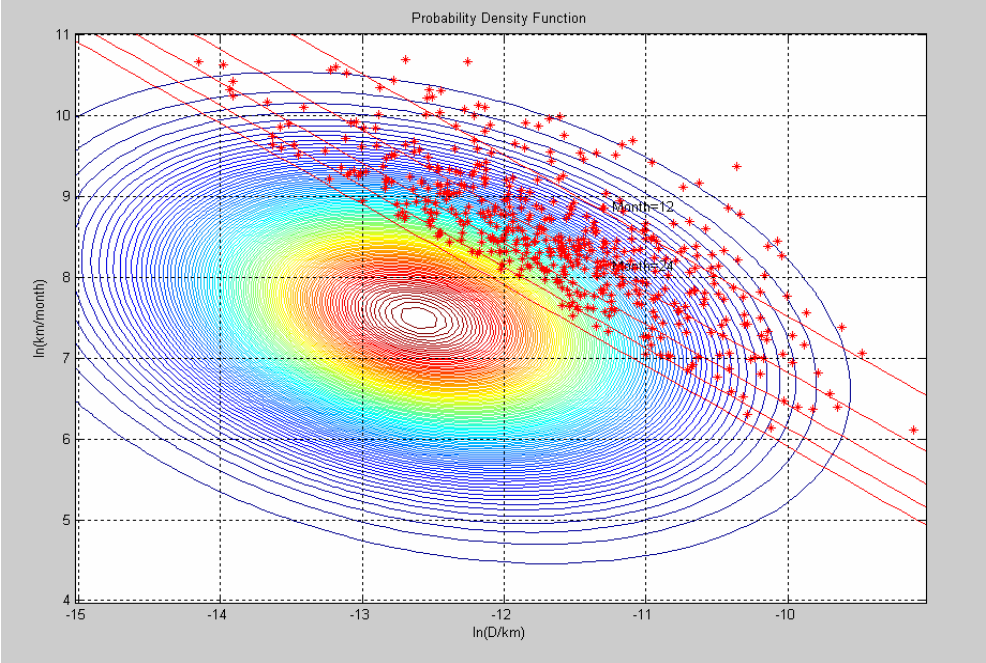

Figure 6-21: PDF contours and failure parameters

It is obvious that all failures would fall above the 60-month line (all vehicles are younger than 60 months), but it can be observed that the density of failures also exhibits some correlation with the contours of the PDF.

Although the failure parameters represent a sample of the total population, it is a particularly biased sample and can therefore not be used directly to estimate the means and standard deviations for the total population. The parameter values represent failed vehicles and should therefore be expected to be on the tails of the distributions.

The failure prediction method involves a complex process and a pure mathematical reversal cannot be achieved. However, based on the visible correlation between the density of the failures and the PDF contours, it was decided to develop a curve fitting technique to estimate usage profile parameters from failure statistics.

6.4.2.3 Curve fitting

The failure incidences are firstly binned into bins of constant ln(km/month) and ln(D/km) increments. The coarseness of these increments depends on the number of failures. These results are then normalised with respect to the exposure of each bin. Bins falling between two subsequent constant damage/month lines (e.g. between the lines of D/month = 1/50 and 1/51) could be populated with failed vehicles of any age older than 50 months, implying an exposure to a total number of 10 months (60 months – 50 months) multiplied by 100 vehicles sold per month = 1000 vehicles. The failure rate of each bin would therefore be proportional to the number of failures recorded in that bin, divided by 1000. Bins falling between the next set of lines (i.e. between the lines of D/month = 1/49 and 1/50) could be populated with failed vehicles of any age older than 49 months, implying an exposure to a total number of 11 months (60 months – 49 months) multiplied by 100 vehicles sold per month = 1100 vehicles.

The failures counted in each bin are therefore divided by the number of vehicles that could make up that count. The resultant value of each bin should then be proportional to the PDF value at the coordinates of the bin, since this PDF value is proportional to the number of vehicles out of a total population that would have the parameters of the bin.

The result of this exercise for the simulated failures is depicted in Figure 6-22.

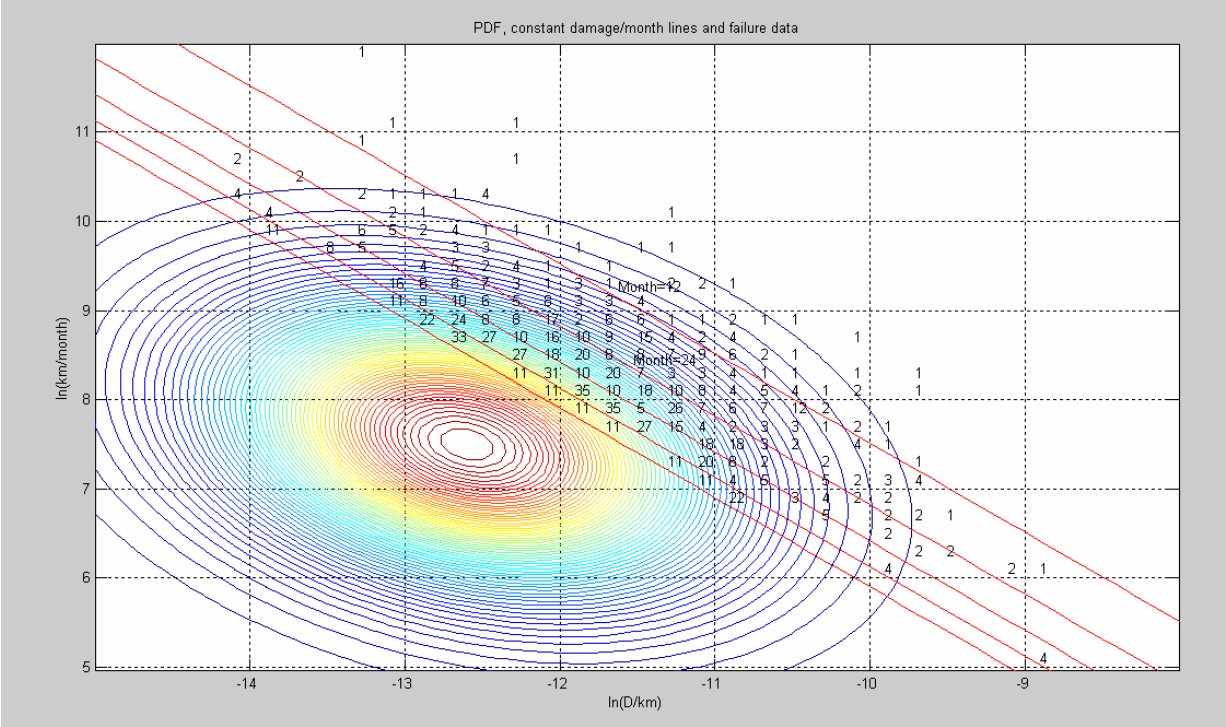

Figure 6-22 PDF contours with binned & normalised failure numbers

It is therefore argued that the binned and normalised failure values depicted in Figure 6-22, when multiplied by an unknown scale factor (K), would approximately fall on the PDF surface. The problem of estimating the usage profile parameters from failure data therefore reduces to curve fitting the PDF, divided by K, onto the set of binned and normalised failure values.

Mathematically, the problem is defined as follows:

> Solve the non-linear curve-fitting problem in the least-squares sense, that is, given input data xdata and output ydata, find coefficients P that "best-fit" the equation F(P, xdata), i.e.;
>
> $$\min_x \tfrac{1}{2}\left\|F(P,xdata)-ydata\right\|_2^2 = \tfrac{1}{2}\sum_i \left(F(P,xdata_i)-ydata_i\right)^2$$
>
> where,
>
> xdata = coordinates (ln(D/km),ln(km/month)) of the bins
> ydata = the normalised failure values of the bins
> F = PDF (defined by Eq. 4) / K
> P = unknown parameters (μ_{y1}, μ_{y2}, σ_{y1}, σ_{y2}, ρ, K)

Eq. 6-6

MATLAB provides a built-in function "lsqcurvefit", which uses the large-scale algorithm to solve the above problem. This algorithm is a subspace trust region method and is based on the interior-reflective Newton method described by Coleman and Li (1994), (1996). The values for (μ_{y1}, μ_{y2}, σ_{y1}, σ_{y2} and ρ), calculated from the failure data, together with an arbitrary K, are used as initial values of P, to commence the iterations. The values listed in Table 6-5 are used to bind the parameters.

Using this algorithm and the failure data depicted in Figure 6-22, the following result was obtained:

	μ_{y1}	μ_{y2}	σ_{y1}	σ_{y2}	ρ
True values	-12.6	7.5	1	1	-0.3
Curve fit results	-12.27	8	1.13	1.05	-0.5

These results are graphically represented in Figure 6-23. The accuracy of the curve fitted result is considered to be adequate. Using the estimated parameters to predict failures during the 5-year period, results in a failure percentage of 15 % instead of the 'true' 8 %, which would be an acceptable prediction, given the accuracy and cost of alternative prediction methods.

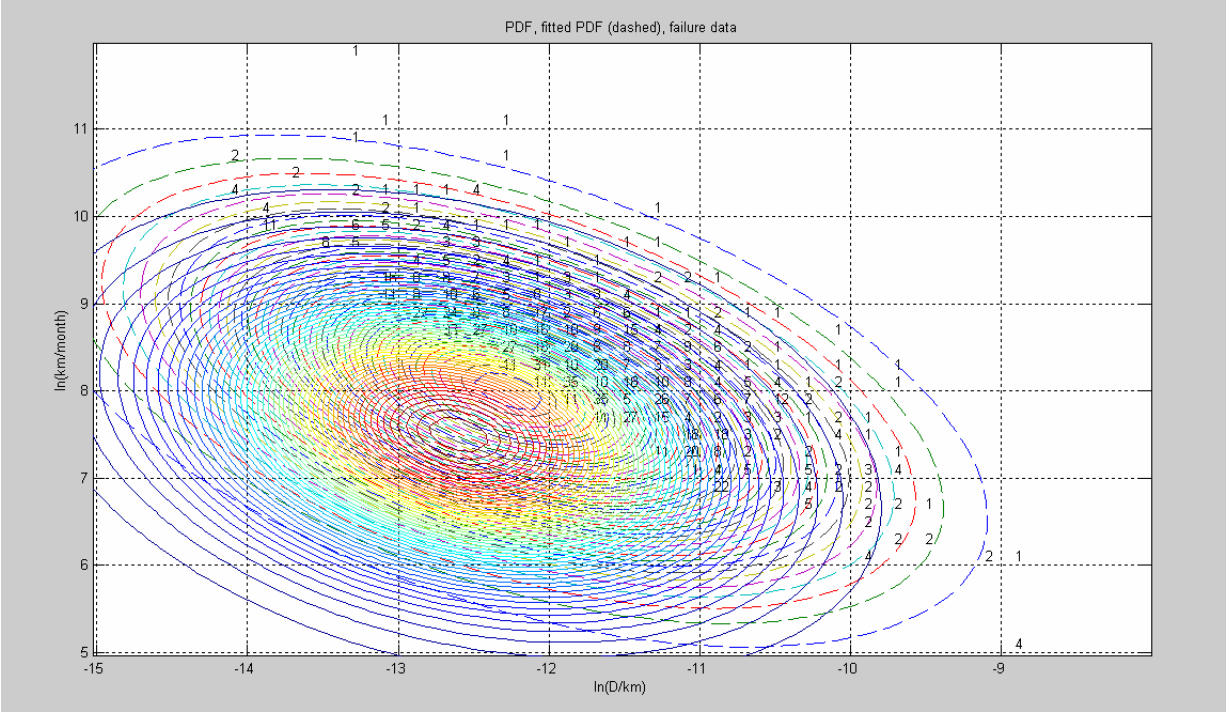

Figure 6-23 PDF of typical values, curve fitted PDF & failure data

Several more trials were performed to test the method. In each case a random set of usage profile parameters were generated (within the boundaries discussed before). These values were used to perform the Monte Carlo simulation to produce failure statistics. The curve-fitting algorithm was then applied to the normalised failure data. The results of these trials are presented in graphical and tabular form below.

	μ_{y1}	μ_{y2}	σ_{y1}	σ_{y2}	ρ
True values	-13.25	7.28	0.36	1.37	-0.26
Curve fit results	-13.07	7.76	0.46	1.41	-0.5

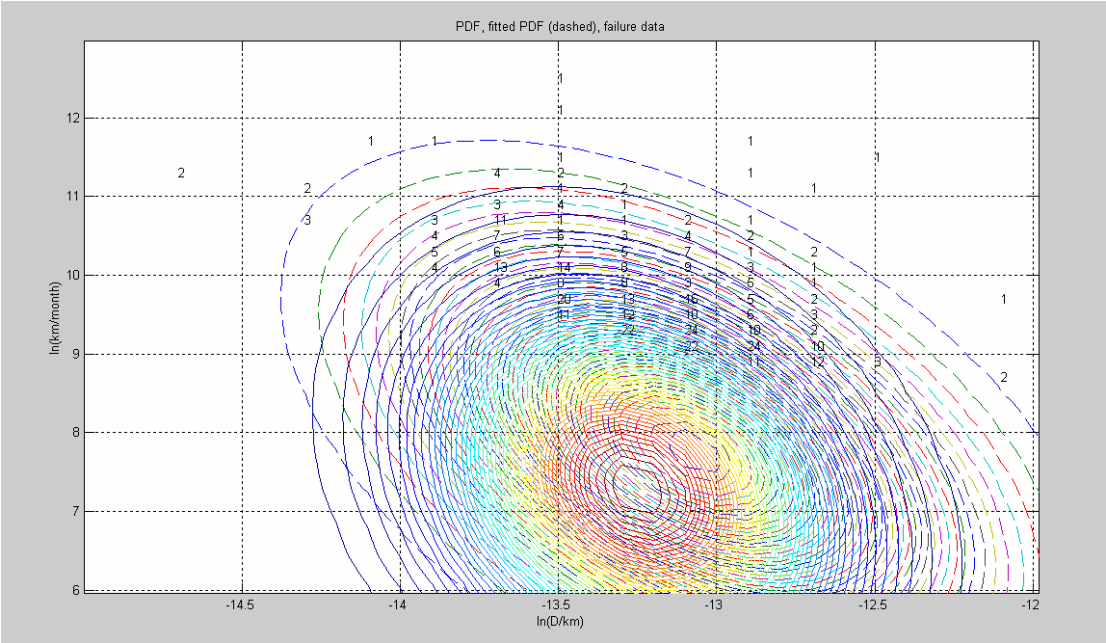

Figure 6-24 Case A – 3 % failures

	μ_{y1}	μ_{y2}	σ_{y1}	σ_{y2}	ρ
True values	-12.28	7.17	0.78	1.83	-0.11
Curve fit results	-12.43	6.9	0.89	1.89	-0.1

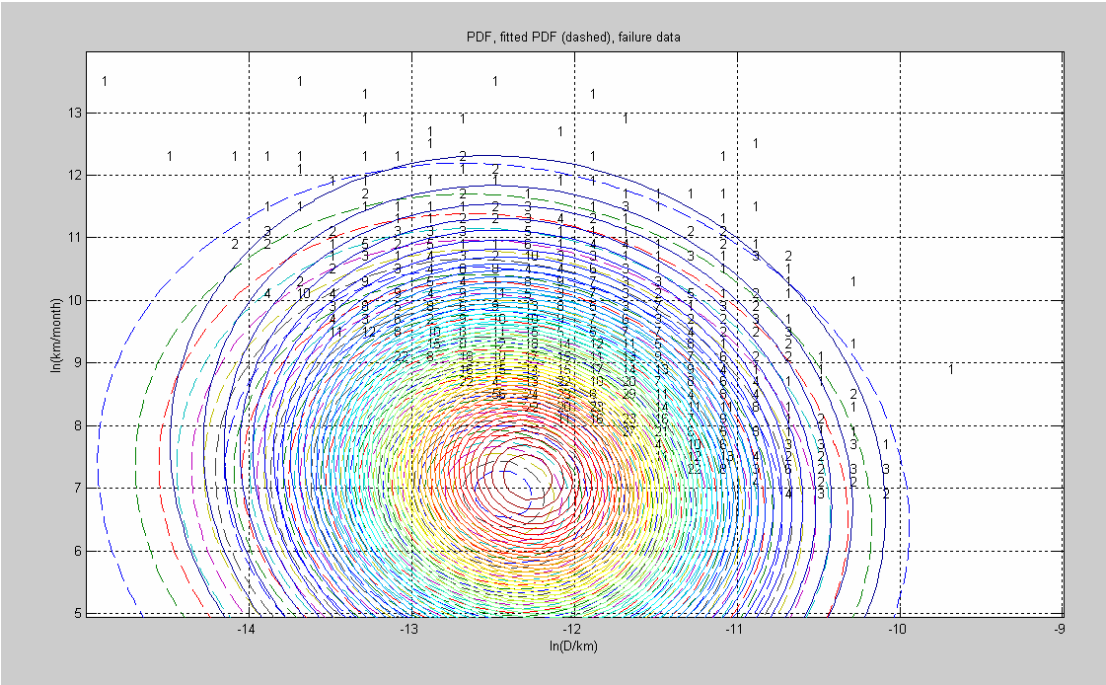

Figure 6-25 Case B – 16 % failures

	μ_{y1}	μ_{y2}	σ_{y1}	σ_{y2}	ρ
True values	-13.5	7.0	0.8	0.8	-0.2
Curve fit results	-13.8	6.9	1.16	1.18	-0.46

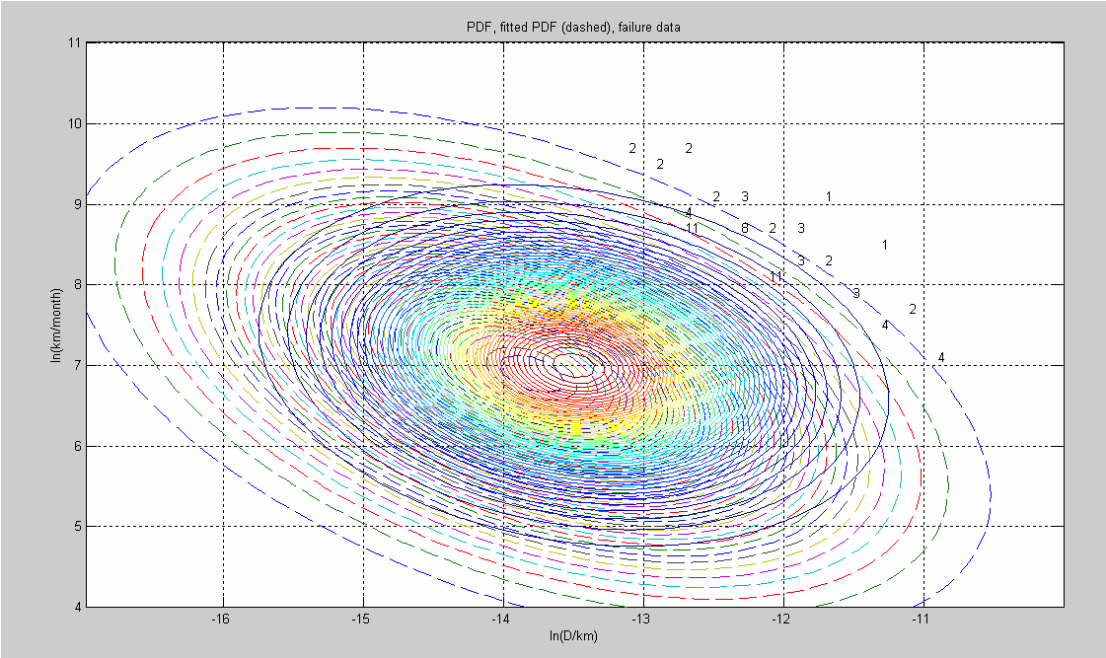

Figure 6-26 Case C – 0.4 % failures

It is clear from the above trials that the accuracy improves for higher failure percentages, which is to be expected. It is however argued that the method would still be useful for failure percentages as low as 0.5 %.

A methodology was presented that would enable vehicle designers to derive a statistical fatigue loading profile of the total population of users of a vehicle model from failure data recorded on the same or a previous model. The method is radically more economic than existing methods and entails a few hours of running a software program, together with performing a failure test on the component for which failure data is available to determine the damage to failure. It was demonstrated that reasonable accuracy could be achieved, even if the failures represent only a small fraction of the total population. The two-parameter usage profile thus determined can powerfully be used to predict failures or derive statistically based durability test or design requirements.

7. FORMALISATION

7.1 SCOPE

The methods dealt with in Chapters 4 to 6 have been presented (and developed) according to the specifics of the various case studies. In the present Chapter, these methods are generalised, as well as unified, into a cohesive methodology.

7.2 GENERALISED UNIFIED METHODOLOGY

7.2.1 General

Figure 7-1 depicts the components of a combined flow diagram for the establishment of input loading for vehicle and transport structures, incorporating all the techniques developed during this study.

The diagram is divided by the bold dashed lines into three regions, namely, the essential data sources (measurements, surveys, simulation, failure data, sales data), the analysis and testing exercises (fatigue processing, statistical calculations, Monte Carlo simulation, durability testing, finite element analysis), as well as the results (maximum loading, fatigue design requirements, durability testing requirements). The above logic is similar to the logic adopted for the structure of this thesis.

The flow of the diagram commences at the red decision block. The two additional decision blocks are yellow and green, the former representing the important decision of how to utilise measurement data and the latter representing the comparison between predicted failures and failure data.

In the following paragraphs, each component in the diagram, as well as the diagram logic, are described.

7.2.2 Commencement of Input Loading Establishment (Red Decision Block)

The availability of data sources drives the decisions made at the commencement of input loading establishment. If no prototype or similar vehicle (such as a previous model) exists, the only choice would be to perform a dynamic simulation. Such a case study has not been dealt with, but a typical example would be a new special purpose vehicle.

If a prototype or similar vehicle exists and no failure data exist for the structure or similar structures, measurements should be performed. Survey data is required if it is not possible to measure either a representative usage cycle, as was done for the road tankers and industrial vehicles, or to perform comprehensive measurements, as was done for the tank container.

7.2.3 Measurement Profile

The measurement profile relates to the transducer configuration, as well as the operational cycles, events, terrain categories, etc. to be measured.

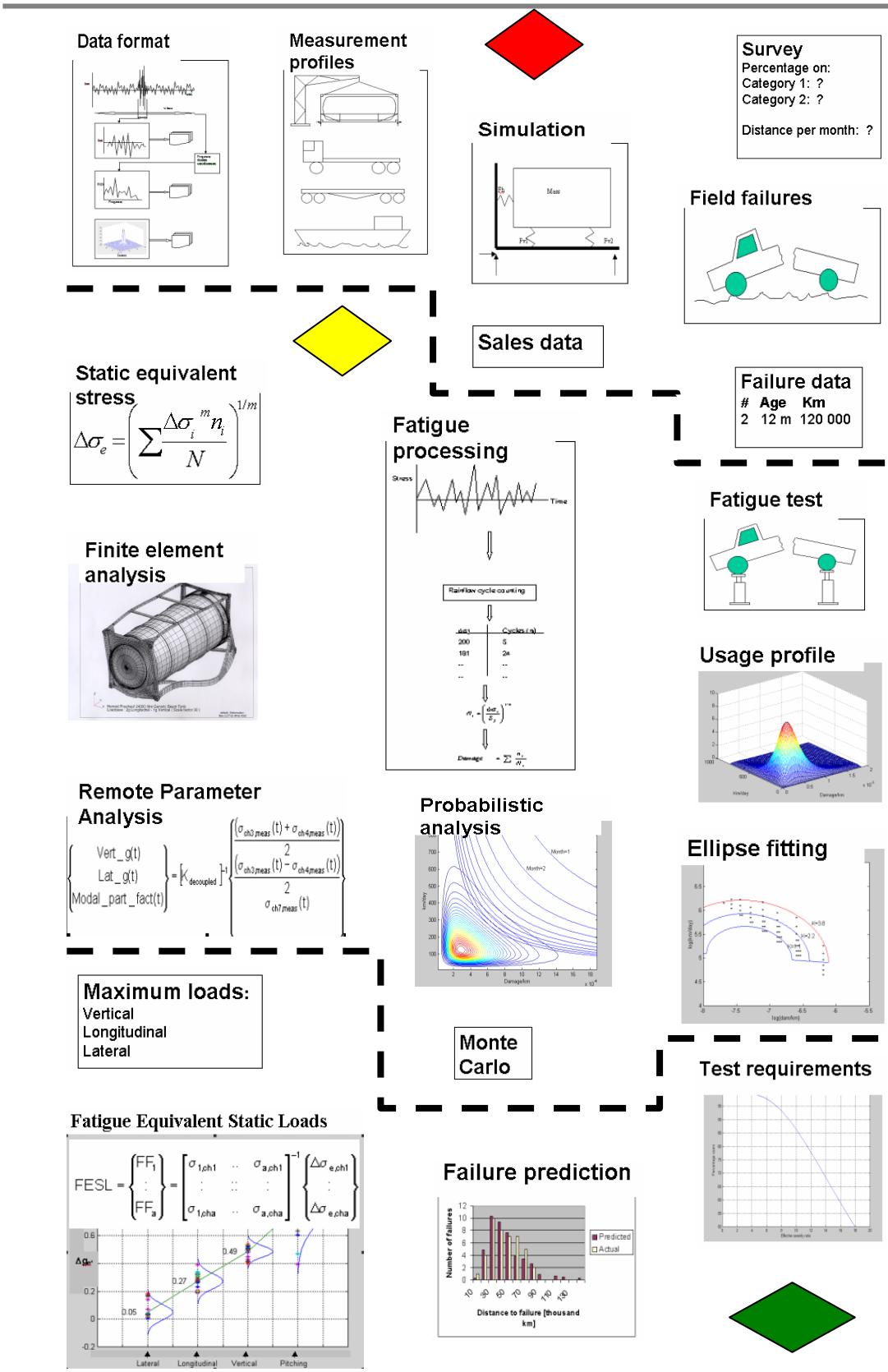

Figure 7-1 Components of generalised process

7.2.3.1 Transducer configuration

As discussed in paragraph 4.2.5.1, the transducers should be grouped into three categories, namely:

- Transducers (strain gauges and accelerometers) should be placed to be able to deduce the fundamental load inputs to the vehicle structure. This would typically entail instrumenting the suspension components (e.g. strain gauges on an axle could be used to measure vertical and longitudinal wheel loads), the kingpin area (in the case of road tankers, to measure the loads transferred through the hitch), as well as accelerometers to measure the six rigid body degrees of freedom accelerations of the total structure. Calibration of loads from the measured strains may involve isolated finite element models or laboratory calibration. The loads measured are used as direct inputs for static or dynamic finite element analyses, or as control channels for load reconstruction laboratory testing. When inputs are required for dynamic finite element analyses, the choice of analysis method would decide which transducers are required, as discussed in paragraph 3.2.3.7.
- Strain gauges should be placed in 'clean' stress areas to measure nominal stresses sensitive to global bending, tensile and shear stressing due to vertical, longitudinal and lateral, mainly inertial, loading. Accelerated test track, or road testing, is performed using these channels for severity ratio calculation. Such results are also very valuable in combination with finite element analyses, enabling the derivation of fatigue equivalent static loading. Strain gauges to measure nominal bending stresses on the chassis beams of a vehicle structure, is an example of this category. These gauges are placed away from stress concentration areas to ensure that slight misplacement of the gauge does not influence the results. Strategically placed gauges may be used in combination with finite element analysis, to obtain stress vs time histories at critical positions in the vicinity of the gauges, for fatigue life calculation.
- The third category involves placing strain gauges in known high stress areas, where the results can directly be used to calculate fatigue damage. Placement of such gauges and correct interpretation of the results are involved exercises. Fatigue design codes generally require nominal stress histories, where the stress concentration caused by the weld detail, hole, etc., are already taken into account by the SN – curve.

7.2.3.2 Operational cycle

An exercise based on a measured representative usage cycle, will only be valid in cases where the mission profile of the vehicle is well defined. In the case of the road tankers, it was argued that the measured trips would be representative of what the vehicles will be subjected to during their operational lifetimes. Formally, that assumption is rather unscientific, since it is based on a subjective choice of the measured trip. Such an assumption would be more valid in the cases of the industrial vehicles, where the only missions of the trucks are to carry loads on a reasonably static route.

In the case where comprehensive measurements are performed, as with the commercial vehicles case studies, the tacit assumption is made that all loading conditions are captured by the measurements. Again, fundamentally, such an assumption cannot be correct, since there will always remain a probability for more severe loading to occur. The uncertainty could be allowed for using an appropriate safety factor on the resulting loading requirements, but even then, the safety factor should be determined based on statistical processing of the measurement data.

7.2.3.3 Events

In some cases, specific events may contribute significantly to the usage profile in terms of fatigue damage. Examples of this may be shunting of tank containers, or driving over a curb for vehicles. Measurements of such events should be performed as separate exercises and the damage contributions added to the stochastic data on the basis of estimated occurrences during a lifetime.

7.2.3.4 Terrain categories

The IRI method, discussed in paragraph 3.5.5, provides the best scientific basis for defining terrain categories.

7.2.3.5 Driver influence

Driver influence may be taken into account by using a representative profile of drivers during measurements.

7.2.4 Data Format

7.2.4.1 Time domain

Data recorded in the time domain allows editing and therefore the best integrity, but, in the case of comprehensive measurements such as was performed on the tank containers, may not be possible due to storage space restrictions. A combination of short duration events stored in the time domain, together with frequency domain and/or fatigue domain storage, is then recommended.

7.2.4.2 Frequency domain

Storing data in the frequency domain allows reconstruction of time domain signals, but transient events would be lost.

7.2.4.3 Fatigue domain

Data processing from fatigue domain data is discussed in paragraph 5.4.5. Reconstruction to time domain data is possible to some extent, as discussed in paragraph 3.4.3.2.

7.2.5 Simulation

Multi-body dynamic simulation techniques to derive input data are discussed in paragraph 3.3. When measured data is not available, synthetic road profile data can be employed to derive dynamic loads for input into a fatigue assessment. Dynamic simulation may also be employed to derive dynamic loads when measured accelerations are available.

7.2.6 Survey

Survey methodologies are dealt with in paragraph 4.2.7. Care should be taken in the design of the questionnaire, such that redundant questions are built in to allow cross checking. Typically 1% of the total population may be sufficient to obtain representative data, but then care must be taken to obtain an unbiased sample. The terrain categories discussed in paragraph 3.5.5 should be used.

7.2.7 Field Failures

A powerful methodology to derive usage profiles from field failures is presented in paragraph 6.4. When field failure data is available, it should always be used to verify the testing or analysis results. Baseline tests, to reproduce field failures, should always be performed before qualification testing of a new or improved design. If this is done, the time-to-failure can very accurately be determined as the ratio between the times-to-failure of qualification test and the baseline test, multiplied by the time-to-field-failure. The complex, non-experimental processes used to arrive at fatigue life predictions can also be deterministically adjusted or calibrated using field failure information.

7.2.8 Ellipse Fitting

The proposed curve fitting procedure, forming part of the methodology to derive usage profiles from field failure data, is described in paragraph 6.4.

7.2.9 Sales Data

Sales data is required as input to failure rate predictions, as performed for the minibus.

7.2.10 Fatigue Processing

The stress life approach, detailed in paragraph 3.4.2.1, is in most cases adequate to perform fatigue processing of measured data. Calculations can mostly be performed in the relative sense, where only the gradient on the SN-curve would have an influence. A gradient of –0.25 (for parent metal failures) or –0.33 (for weld failures) would typically be used. When input loading has been established and fatigue life predictions are performed, appropriate SN-curves need to be used, available from design codes.

The statement concerning the use of stress-life specifically refers to fatigue processing as opposed to fatigue life prediction, which implies mostly calculations in the relative sense, which is then only dependent on the fatigue exponent. Such relative calculations are not practical to be performed using strain-life methods, since then all four material properties would have an influence on the results and therefore it is common practice to use stress-life methods for such calculations.

For predicting fatigue life, strain-life methods would most commonly be used in the automotive environment, except for spot welds. The substantial additional complexity is mostly hidden from the analyst, since computer programs are used. It is however not very certain whether a substantial benefit is derived from using the more complex method in cases of high cycle fatigue. Berger et al. (2002) discuss a comparative study on 6 different steels, for 144 different cases. It was found that the nominal-stress approach gives a slightly more accurate prediction of fatigue life than the local-strain method. It is proposed that the reason for this may be that the latter is more susceptible to erroneous estimations of input data.

For heavy vehicles, fatigue problems are mostly associated with welding, implying the use of the stress-life method for life prediction.

7.2.11 Hybrid Remote Parameter Analysis / Modal Superposition Method

Figure 3-18 was compiled in Chapter 3 to summarise the different existing fatigue assessment methods based on measurements and finite element analyses. During the ladle transport vehicle case study (paragraph 5.3) a hybrid method was developed, combining the remote parameter analysis and modal superposition methods. This

process is depicted by the thickened black arrows on Figure 7-2. *Unit loads* are used in a *static finite element analysis* to provide, together with the results of an *eigenvalue finite element analysis*, the elements for a *strain gauge / load transfer matrix*, as well as a *critical position / load transfer matrix*. The former is used to convert the *measured stresses, $\sigma(t)$*, to loads (including modal participation factors) in the time domain. The loads are inputs into the latter matrix, resulting in stresses in the time domain, which then are used for *fatigue analysis*.

The method allows for taking into account excited modes, requiring only dynamic finite element analysis to solve for the relevant mode shapes. The method, however, does not result in design independent design loads, which could be published in design codes. A method, incorporating the benefits of the hybrid remote parameter / modal superposition method, but resulting in design independent design loads, is proposed in the next paragraph.

7.2.12 Fatigue Equivalent Static Loading

The fatigue equivalent static loading method is described in paragraph 5.3. The method avoids the need for dynamic finite element analyses and results in design independent loads.

The process is depicted on the summary diagram in Figure 7-3, using thickened black arrows. *Measured stresses, $\sigma(t)$*, are cycle counted, using the *Rainflow counting* technique. The results are used to calculate *equivalent stress ranges* for each strain gauge position. *Unit loads* are used in a *static finite element analysis* to provide the elements for a *strain gauge / load transfer matrix*. This matrix is used to convert the equivalent stresses to equivalent load ranges. The loads are inputs into a *static finite element analysis*, resulting in equivalent stress ranges, which then are used for life prediction using the *stress-life* (or strain-life) method.

The method can be used for multi-axial loading (not to be confused with multi-axial fatigue), but may result in inaccuracies due to the loss of phase information. If care is taken concerning the direction of loads and the choice of measurement channels, conservative assessments can however be achieved.

The important assumption made for the FESL methodology to be valid, is that stresses due to dynamic vertical loading at all positions in the structure would have the same relative ratios to each other, as would be the case with a static finite element analysis with a simple vertical inertial loading. Under vertical dynamic loading, a vehicle structure would typically be excited in its first global bending mode of vibration, which would yield stress responses similar to a static inertial load response. Higher bending modes, twisting modes and local structural modes could however also be excited, which may cause high stresses in different areas. Resulting fatigue problems would then be due to resonance and would not necessarily be identified from a static analysis.

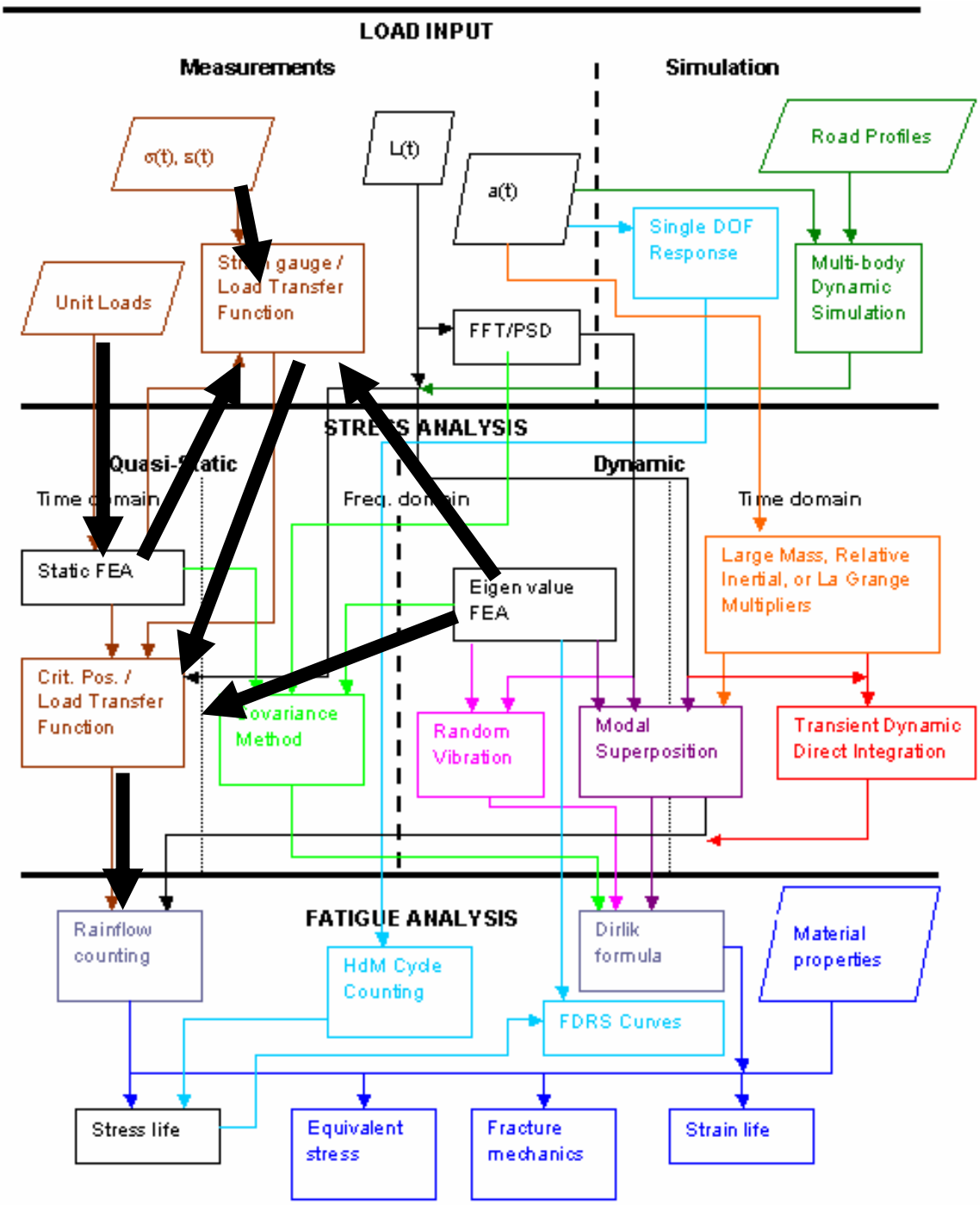

Figure 7-2 Hybrid remote parameter / modal superposition method

Although not pursued during the present study, it is proposed that, by combining aspects of the Fatigue Damage Response Spectra (FDRS) method, described in paragraph 3.5.8.2.5, with the modal superposition method, as well as the FESL method, this disadvantage could be overcome. The proposed concept would be that the FDRS are published, together with FESLs. The designer would obtain finite element eigenvalue solutions for the specific design and determine fatigue based, modal participation factors from the spectra, for modes found to be within the responding bandwidth. The analysis would then proceed as per the multi-axial FESL method, with the modal loads treated as additional 'static' loads. The additional aspects of the proposed process are depicted in Figure 7-3, using a thickened dashed arrow.

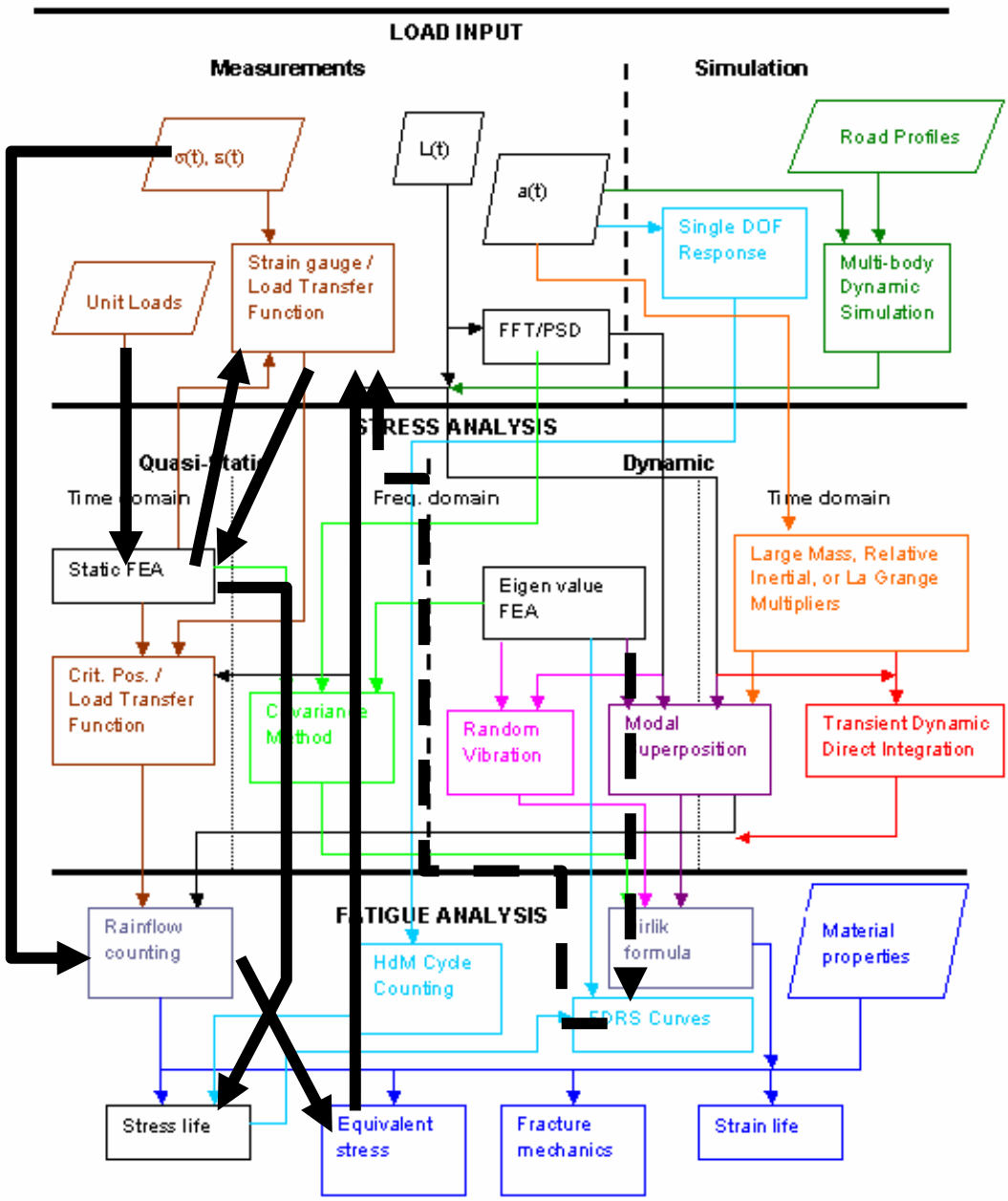

Figure 7-3 FESL process

7.2.13 Fatigue Test

The diagram depicted in Figure 7-4 captures the essence of the process of laboratory test development and correlation.

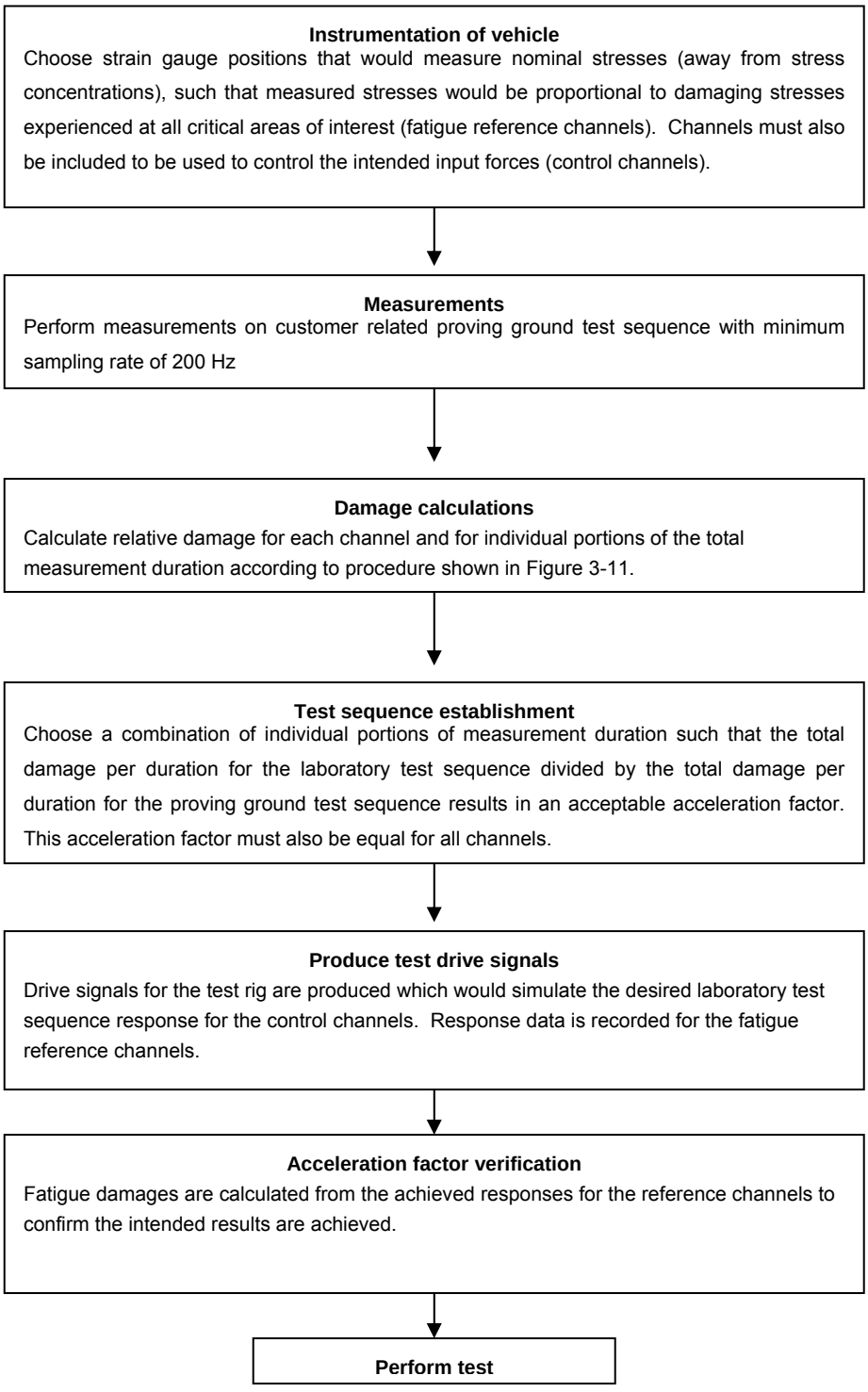

Figure 7-4 Durability testing procedure

7.2.14 Finite Element Analysis

7.2.14.1 Static analysis

Static analyses are used as part of the input loading establishment process as calibration. For maximum loads, or fatigue equivalent static loads, it may then also be used to calculate the resulting stresses.

7.2.14.2 Dynamic analysis

The use of dynamic analyses is restricted by computing power and is therefore avoided when possible. The choice of which dynamic analysis technique is used (refer paragraph 3.2.3), is highly dependent on the measurement configuration used, or vice versa. Methods to include dynamic effects without the need for complete model dynamic analyses, are discussed in paragraph 3.2.3.8.

7.2.15 Usage Profile

The statistical usage profile is an outcome of a process to establish input loads and is discussed in paragraph 5.4.6.

7.2.16 Monte Carlo

The Monte Carlo simulation technique may be used to predict failure rates from statistical usage profiles and is discussed in paragraph 6.2.2.5.

7.2.17 Probabilistic Analysis

The probabilistic analysis is used after the establishment of a statistical user profile to perform failure predictions or derive test requirements, as discussed in paragraph 5.6 and paragraph 6.2 respectively.

7.2.18 Failure Prediction

The failure prediction is the outcome of the probabilistic analysis, or a finite element analysis with static equivalent or maximum loads, or of a dynamic finite element analysis. Comparison of these results with existing field failure results happens in the green decision block and should be done when possible.

7.2.19 Test Requirements

Test requirements are the outcome of the probabilistic analysis (in terms of cycles to be completed on a test track or test rig), or of the FESL process, where these loads may be induced as sine waves on a test rig. In the latter case, if multi-axial loading is involved, the phase information will be lost, which may lead to inaccurate testing results, as discussed before.

Testing on a test rig may also be performed, directly using the measured results. The test severity would then be determined, based on fatigue processing of the measured results.

7.2.20 Fatigue Design Loads

Fatigue design loads are the outcome of the static equivalent calculations, without the transfer matrix for uni-axial loads, or through the transfer matrix for multi-axial loads.

7.2.21 Maximum Loads

Maximum loads are derived from measurements, through the dynamic simulation if fundamental loads are required from indirect measurements.

7.3 CASE STUDIES ACCORDING TO GENERALISED PROCESS

7.3.1 Minibus

The minibus case study logic is depicted on the process diagram in Figure 7-5.

- Commencement: The process commences at the red decision block by employing three of the four possible sources of input loading, namely, measurements, surveys and field failure data.
- Measurement profile and data format (paragraph 4.2.3): Extensive measurements are performed on routes typically used by taxis, organising the data into files on different road categories, to capture all profiles. It is proposed that the use of the International Roughness Index (described in paragraph 3.5.5) to characterise the road types, would improve the methodology. The data is stored in the time domain.
- Processing decision: This case study did not involve any finite element analyses, since fatigue life prediction is achieved through physical testing.
- Fatigue processing (paragraph 5.5.3): The data is therefore fatigue processed, yielding damage per distance values for each category of road.
- Customer survey results (paragraph 4.3.3)
- User profile (paragraph 5.5.3.2): Survey results are combined with the fatigue processed output of the measurements to define a probabilistic definition of the user profile, in terms of two parameters, namely damage per distance and distance per time.
- Probabilistic analysis (paragraph 5.6.2): This profile is then employed to derive durability testing requirements, using two different methods. The analytical method is depicted in red.
- Failure prediction (paragraph 6.2.2).
- Monte Carlo (paragraph 6.2.2.5): Depicted in blue.
- Fatigue testing: In both cases, the results from fatigue testing are required. The fatigue testing is performed on a test rig, using measured data to derive drive signals.
- Failure data and comparison: Failure prediction results are successfully compared to field failure data, verifying the techniques employed.
- Ellipse fitting (paragraph 6.4): An alternative method for determining a user profile, employing only field failure data and fatigue testing results, is developed. This process is depicted in green.

The methodology developed during this case study, is similar to that found in literature (as described in paragraph 3.5.8.2.3), but it was compellingly substantiated through accurate field failure prediction. Also, its unique analytical formulation made it possible to develop a potentially powerful technique for deriving a probabilistic user profile from field failures.

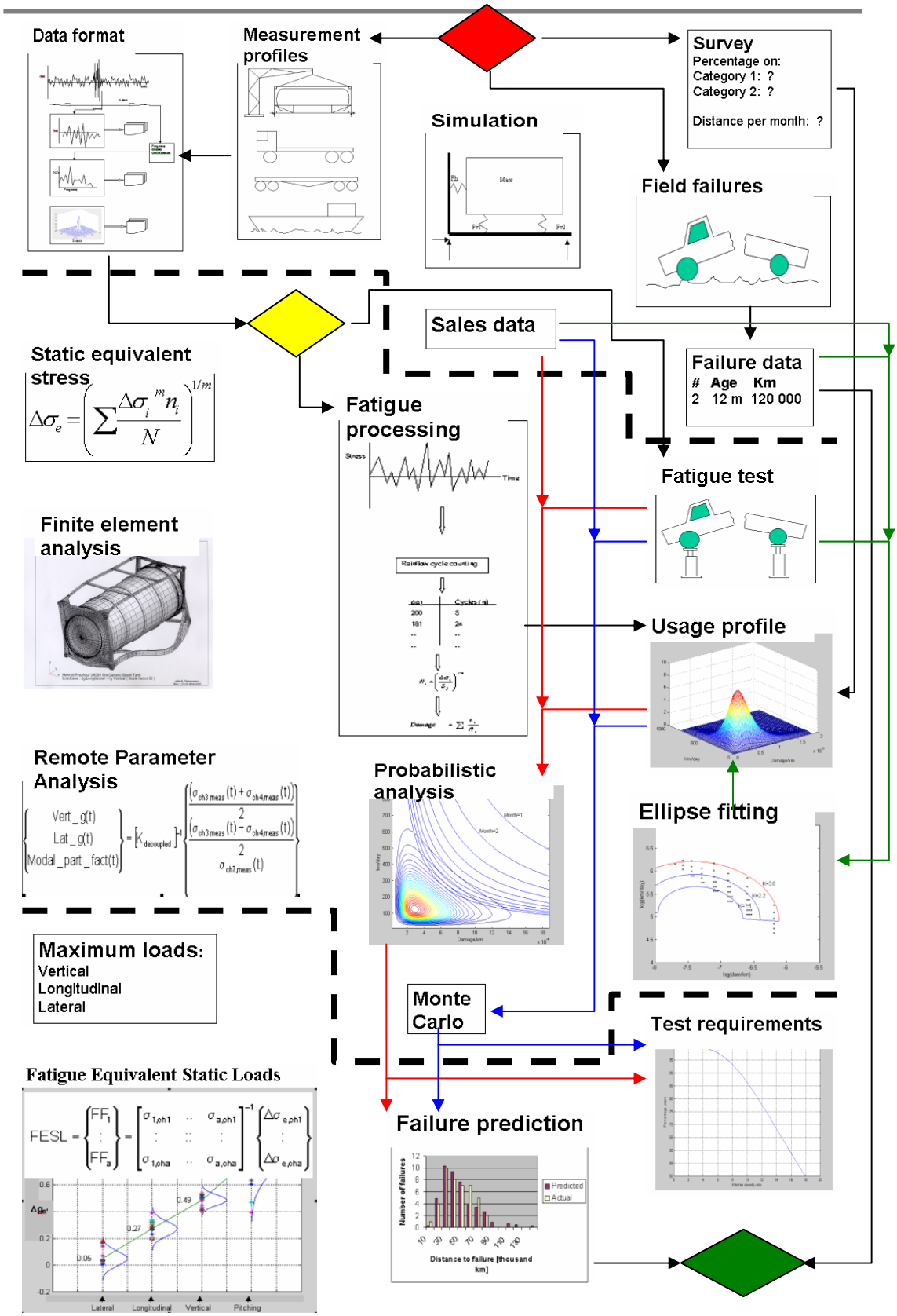

Figure 7-5 Minibus process

7.3.2 Pick-up Truck

The pick-up truck case study logic is depicted on the process diagram in Figure 7-6. This case-study was similar to the minibus case study, described above, differing only with respect to the fact that field failures were not available for verification purposes and that only the Monte Carlo method was used.

- Commencement: The process commences at the red decision block, employing measurements and surveys as sources for input data.
- Measurement profile and data format (paragraph 4.2.4): Extensive measurements are performed on routes typically used by pick-up trucks, organising the data into files on different road categories, to capture all profiles. The data is stored in the time domain.
- Processing decision: This case study did not involve any finite element analyses, since fatigue life prediction is achieved through physical testing.
- Fatigue processing (paragraph 5.5.4.1): The data is therefore fatigue processed, yielding damage per distance values for each category of road.
- Customer survey results (paragraph 4.3.4)
- User profile (paragraph 5.5.4.2): Survey results are combined with the fatigue processed output of the measurements to define a probabilistic definition of the user profile, in terms of two parameters, namely damage per distance and distance per time.
- Monte Carlo analysis (paragraph 5.6.3): This profile is then employed to derive durability testing requirements, using the Monte Carlo method.
- Fatigue testing (paragraph 6.2.3): The results from fatigue testing are required for failure prediction. The fatigue testing is performed on a test rig, using measured data to derive drive signals.
- Failure prediction (paragraph 6.2.3.6).

The case study demonstrated the Two Parameter Approach can be generically applied.

7.3.3 Fuel Tanker

The fuel tanker case study logic is depicted on the diagram in Figure 7-7.

- Commencement: The process commences at the red decision block, employing measurements and failure data as sources for input data.
- Measurement profile and data format (paragraph 4.2.5): Measurements are performed on a route typical of the mission of the vehicle. The data is stored in the time domain.
- Processing decision: The measured data is processed in terms of fatigue loading.
- Fatigue processing (paragraph 5.4.4.2): The data is fatigue processed, yielding stress ranges and number of cycles.
- Finite element analysis (paragraph 5.4.4.1): Firstly, the unit load stress at the measurement position is calculated to serve as input for the FESL calculation. After the FESL is calculated, it is induced as loading in a static finite element analysis to yield stresses, assumed to be ranges which are repeated 2 million times during the life.
- Equivalent stress calculation (paragraph 5.4.4.3): From the fatigue processed results, an equivalent stress range is calculated.
- FESL calculation (paragraph 5.4.4.3): The equivalent stress range is divided by the unit load stress to yield the FESL.

- Failure prediction (paragraph 6.2.4): The FESL finite element results are used to calculate fatigue lives at all critical positions.
- Comparison with field failures (paragraph 6.2.4): The predicted results are successfully compared to an actual field failure.

The case study also demonstrated and substantiated the uni-axial FESL method. The vehicles designed according to the process have achieved their design lives, except for failures caused by the unchecked design modification. A comparison between the FESL design criterion and design criteria for fuel tankers according to design codes, is presented in paragraph 6.3.2, demonstrating the improved sophistication achieved by the FESL method.

7.3.4 ISO Tank Container

The tank container case study logic is depicted on the diagram in Figure 7-8. The case study incorporated four parallel approaches, differentiated on the diagram using different coloured lines. Steps common to more than one approach are indicated using black lines.

7.3.4.1 Fatigue assessment through FESL finite element analysis

- Commencement: The process commences at the red decision block, employing measurements as the source for input data.
- Measurement profile and data format (paragraph 4.2.6): Measurements are performed on five tank containers, over long durations, using specially developed dataloggers, on typical land sea and rail routes. The data is stored in the time domain, frequency domain and fatigue domain.
- Processing decision: The data is processed in terms of fatigue loading.
- Fatigue processing (paragraph 5.4.5.2): The data is fatigue processed in real time on the datalogger, yielding stress ranges and number of cycles.
- Finite element analysis (paragraph 5.4.5.5): Firstly, the unit load stresses at the measurement positions are calculated to compile a unit load transfer matrix for the FESL calculation.
- Equivalent stress calculation (paragraph 5.4.5.4): From the fatigue processed results, equivalent stress ranges are calculated for the seven strain channels.
- FESL calculation (paragraph 5.4.5.6): The multi-axial FESLs are calculated from the equivalent stress ranges, using the unit load transfer matrix. 35 different unit load transfer matrices are used (from the 35 combinations of 4 channels chosen from the possible 7) to yield 35 sets of FESL solutions. The mean values are chosen as the final result.
- Finite element analysis (paragraph 5.4.5.5): After the FESLs are calculated, they are induced as loading in a static finite element analysis to yield stresses, assumed to be ranges which are repeated 2 million times during the life. This exercise is depicted with red lines on the diagram.
- Failure prediction: The FESL finite element results are used to calculate fatigue lives at all critical positions, as indicated by the red line.

7.3.4.2 Fatigue assessment through FESL testing

- Fatigue testing (paragraph 5.6.4): The same FESL results described in the previous exercise are used as input to fatigue testing in a laboratory, as indicated by the blue line.
- Failure prediction: The FESL fatigue testing results are used to calculate fatigue lives at all critical positions, as indicated by the blue line.

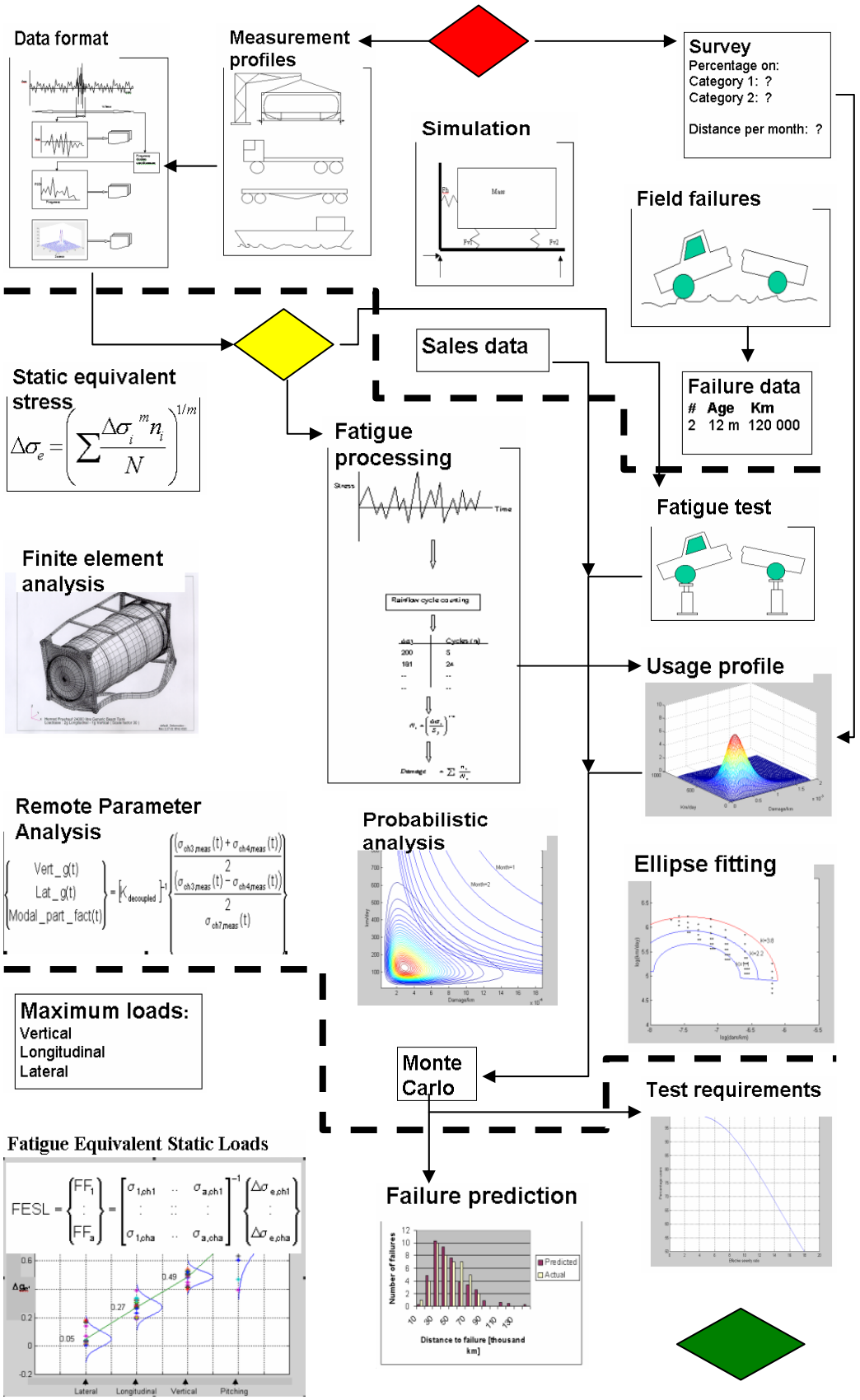

Figure 7-6 Pick-up truck process

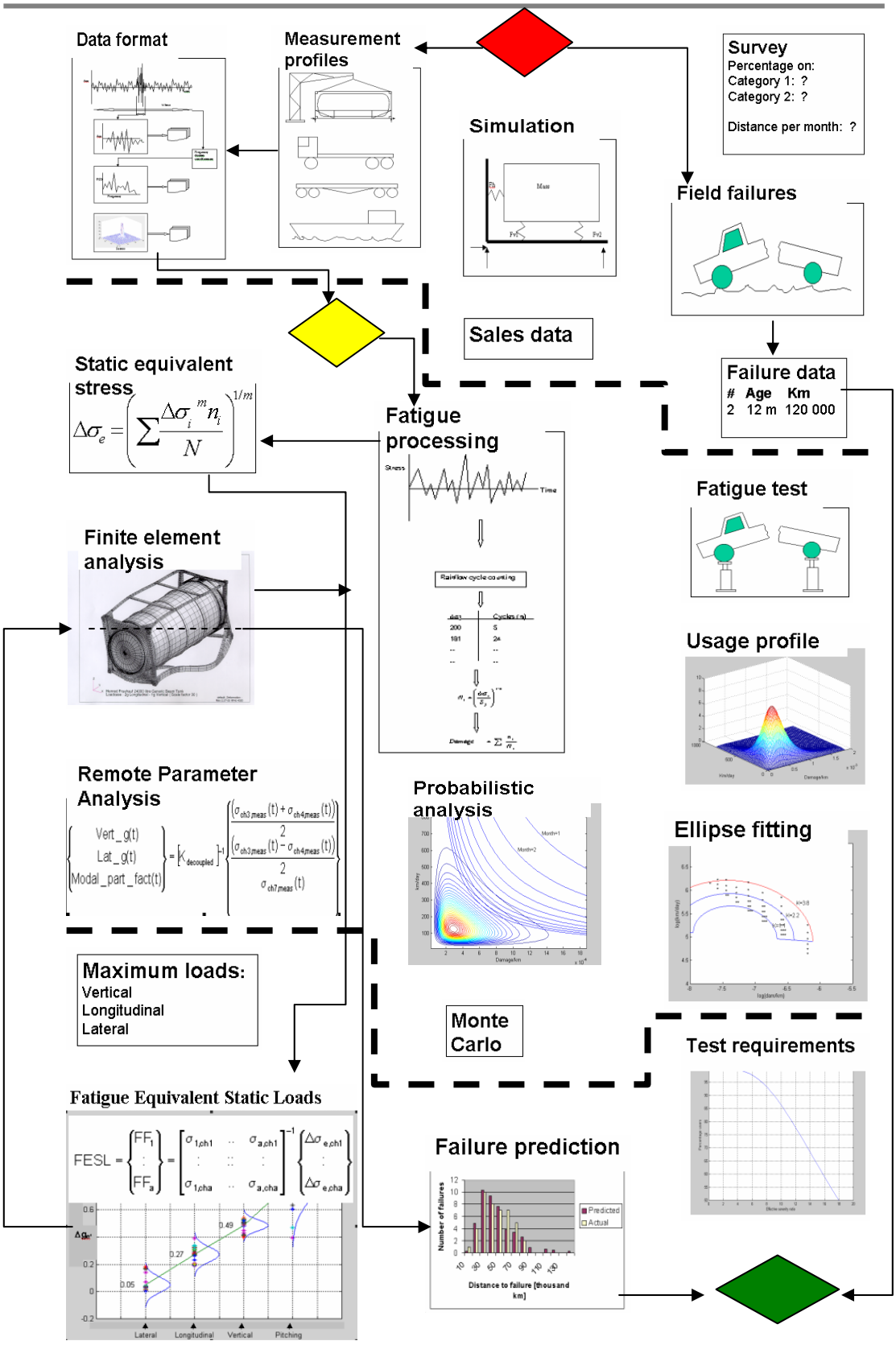

Figure 7-7 Fuel tanker process

7.3.4.3 Fatigue assessment through dynamic finite element analysis

- Processing decision: The accelerometer results, measured in the time domain, are used as inputs for the dynamic finite element analysis, as indicated by the green line.
- Dynamic finite element analysis (paragraph 5.2.3.2): A dynamic finite element analysis is performed.
- Fatigue processing: The stress results are fatigue processed, yielding stress ranges and number of cycles, as indicated by the green line.
- Failure prediction: The fatigue processed results are used to calculate fatigue lives at all critical positions, as indicated by the green line.

7.3.4.4 Maximum load determination through multi-body dynamic simulation

- Processing decision: The accelerometer results, measured in the time domain, are used as inputs for the multi-body dynamic simulation, as indicated by the pink line.
- Multi-body dynamic simulation (paragraph 5.2.2.1.2): A multi-body dynamic simulation is performed.
- Maximum loads: The simulation results are used to derive maximum g-loading.

The case study demonstrated the multi-axial FESL method. Several different tank container models have been successfully designed and tested using these results. The case study demonstrated the use of extensive measurements, with data recorded in different domains. The use of dynamic finite element analysis, as well as multi-body dynamic simulation, are also demonstrated.

7.3.5 Ladle Transport Vehicle

The ladle transport vehicle case study logic is depicted in Figure 7-9.

- Commencement: The process commences at the red decision block, employing measurements as the source for input data.
- Measurement profile and data format (paragraph 4.2.8): Measurements are performed on a prototype vehicle, on a typical operational route. The data is stored in the time domain.
- Processing decision: In this case study, the measured data is directly converted into load-time histories.
- Finite element analysis: Firstly, the unit load stresses (for vertical and lateral loads) at the measurement positions are calculated to compile a unit load transfer matrix for the load-time history calculation. Additionally, the modal stresses of a mode that was found to be excited during the measurements, are included in the transfer matrix. After the loads are calculated, they are induced as loading in a quasi-static finite element analysis to yield stress-time histories.
- Remote parameter analysis (paragraph 5.3.2.1): The measured results are multiplied with the transfer matrix to obtain load-time histories.
- Fatigue processing (paragraph 6.2.5): The stress-time histories are fatigue processed, yielding stress ranges and number of cycles.
- Failure prediction: The fatigue processed results are used to calculate fatigue lives at all critical positions.

This case study demonstrated the use of a combination of the remote parameter analysis method and the modal superposition method.

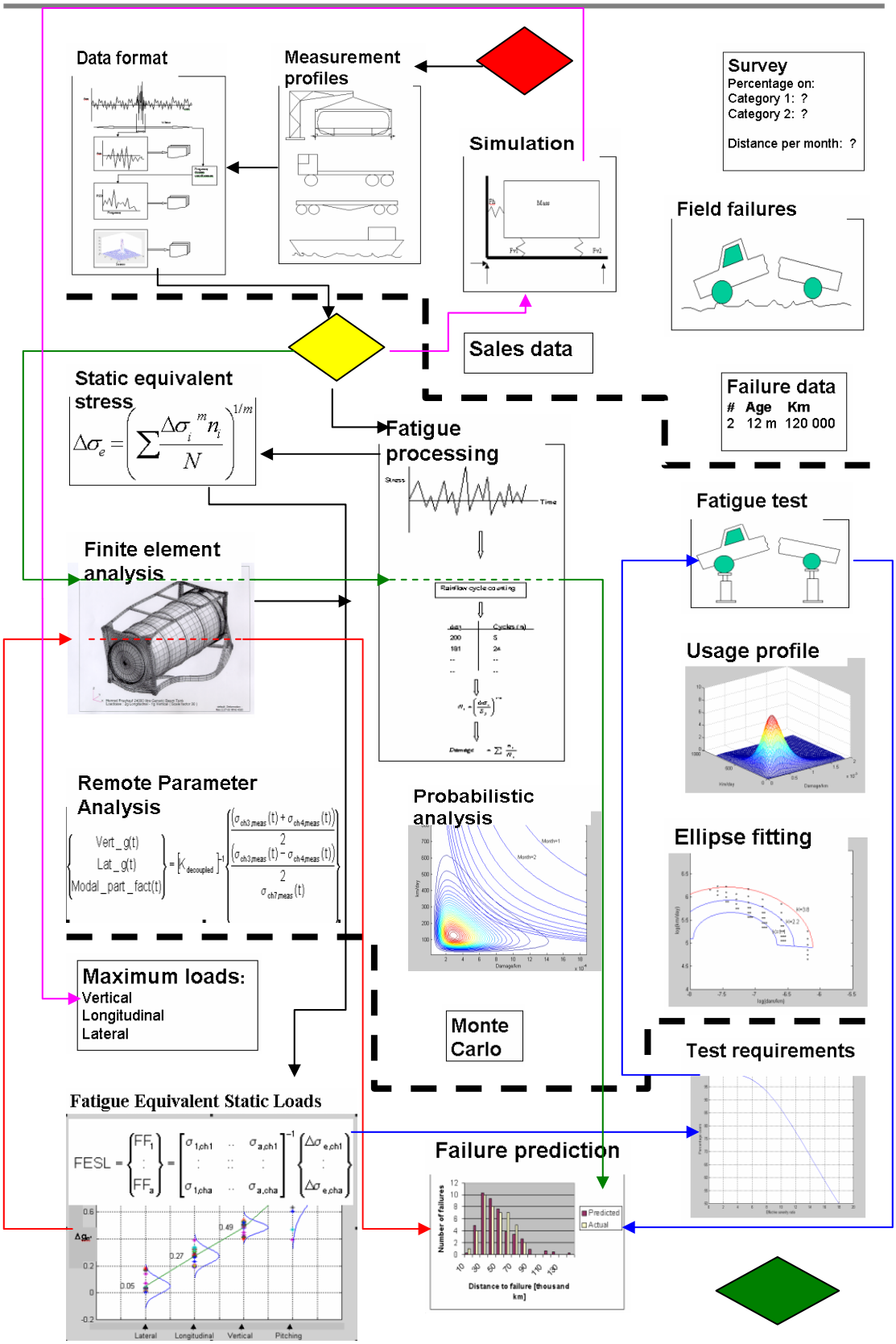

Figure 7-8 Tank container process

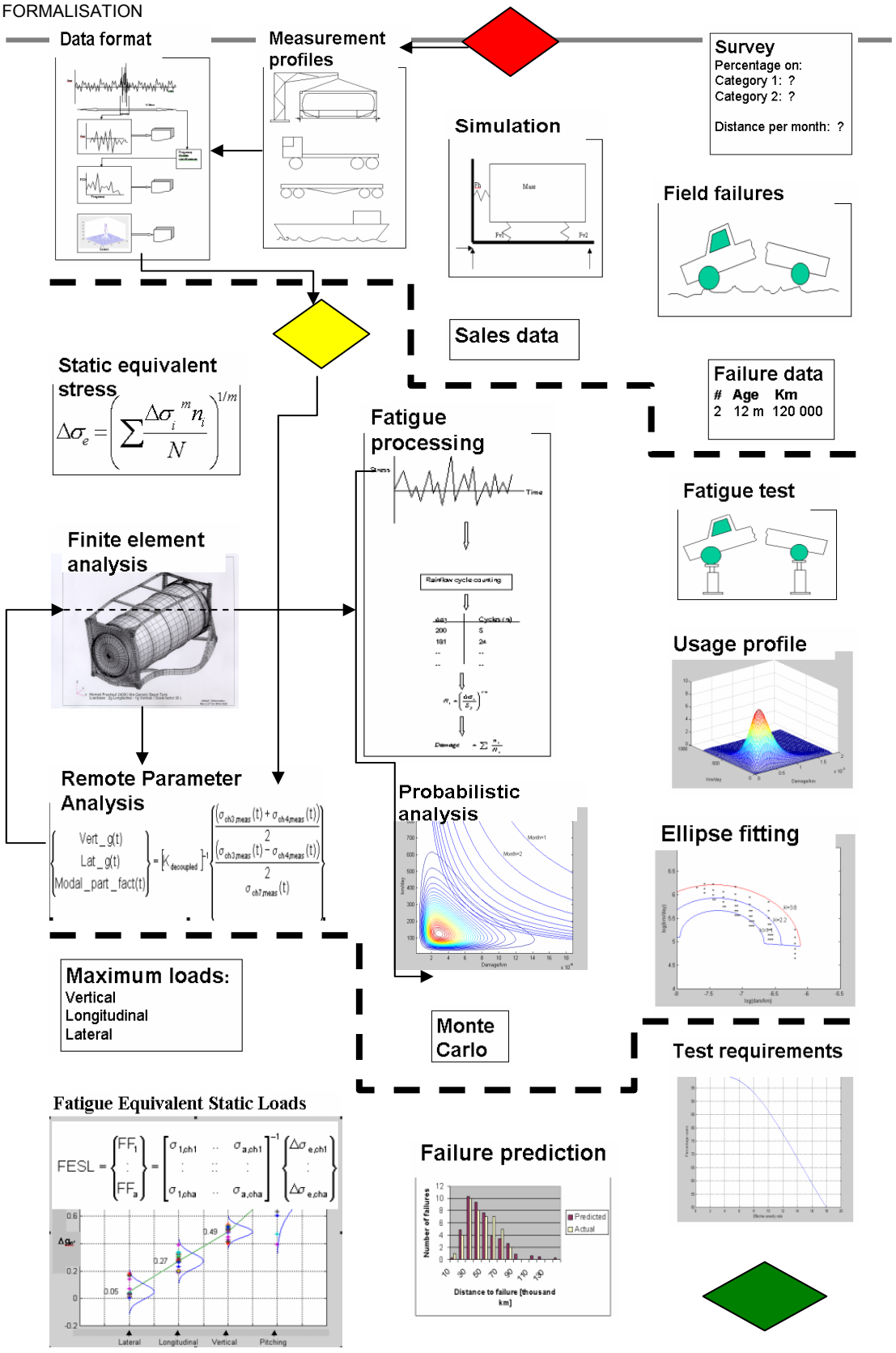

Figure 7-9 Ladle transport vehicle process

7.3.6 Load Haul Dumper

The load haul dumper case study logic is depicted on the diagram in Figure 7-10.

- Commencement: The process commences at the red decision block, employing measurements and failure data as sources for input data.
- Measurement profile and data format (paragraph 4.2.7): Measurements are performed on a route typical of the mission of the vehicle. The data is stored in the time domain.
- Processing decision: The measured data is processed in terms of fatigue loading.
- Fatigue processing (paragraph 5.4.6.2): The data is fatigue processed, yielding stress ranges and number of cycles.
- Finite element analysis (paragraph 5.4.6.1): Firstly, the unit load stress at the measurement position is calculated to serve as input for the FESL calculation. Two models are used to represent the travelling condition, as well as the condition while loading and tipping. After the FESL is calculated, it is induced as loading in a static finite element analysis to yield stresses, assumed to be ranges which are repeated 2 million times during the life.
- Equivalent stress calculation (paragraph 5.4.6.2): From the fatigue processed results, an equivalent stress range is calculated.
- FESL calculation (paragraph 5.4.6.3): The equivalent stress range is divided by the unit load stress to yield the FESL.
- Failure prediction (paragraph 6.2.6.1): The FESL finite element results are used to calculate fatigue lives at all critical positions.
- Comparison with field failures (paragraph 6.2.6.2): The predicted results are successfully compared to an actual field failure.

The case study also demonstrated and substantiated the uni-axial FESL method. Excellent correlation between predicted and actual failures is achieved. The expansion of the uni-axial FESL method to incorporate more than one constraint condition, is demonstrated.

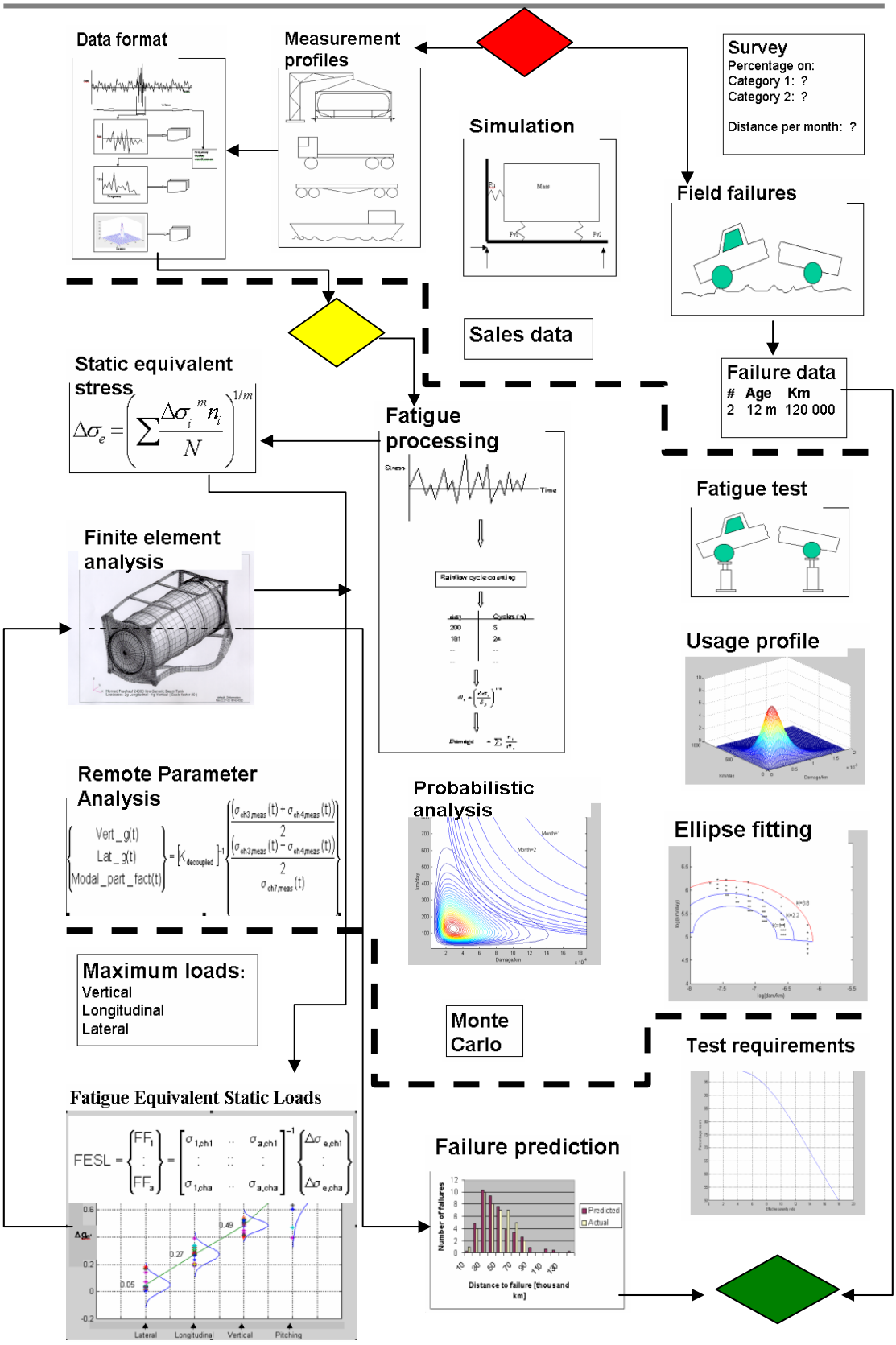

Figure 7-10 Load haul dumper process

8. CONCLUSION

The principal aim of the present study was the development of a generalised methodology for the determination of input loads for vehicle and transport equipment. This was achieved by combining researched current theory and best practices, with lessons learned during application on, as well as new techniques developed for, a number of complex case studies. The use of the generalised process diagram, depicted in Figure 7-1, to map the processes used during each case study, demonstrates the successful generalisation of the methodology. Apart from the above, the present study offers four individual, unique contributions.

Firstly, two methods, widely applied by industry, namely the Remote Parameter Analysis (RPA) method, which entails deriving time domain dynamic loads by multiplying measured signals from remotely placed transducers with a unit-load static finite element based transfer matrix, as well as the Modal Superposition method, are combined to establish a methodology which accounts for modal response without the need for expensive dynamic response analysis. This hybrid method, summarised in Table 8-1, may be compared to the existing alternatives, summarised in Table 3-4.

Secondly, a concept named *Fatigue Equivalent Static Load (FESL)* is developed, where fatigue load requirements are derived from measurements as quasi-static g-loads, the responses to which are considered as stress ranges applied a said number of times during the lifetime of the structure. In particular, it is demonstrated that the method may be employed for multi-axial g-loading, as well as for cases where constraint conditions change during the mission of the vehicle. The method provides some benefits compared to similar methods employed in the industry, such as the RPA method. The FESL method, summarised in Table 8-1, may be compared to the existing alternatives, summarised in Table 3-4.

Table 8-1: Summary of FESL and Hybrid methods

	Type	Load Input	Stress Analysis	Fatigue Analysis	Advantages	Disadvantages
FESL method	Quasi-static, time domain	Straingauge measurements	Static FEA	Rainflow counting + various fatigue life analysis methods	Can use remote measured straingauge data, economic FEA, loading results suitable for code = design independent, rainflow only for measured channels	Not suitable for complex dynamic response
Hybrid method	Dynamic, time or frequency domain	Straingauge measurements	Eigen value FEA	Dirlik formula or Rainflow + various fatigue life analysis methods	Takes account of complex dynamic response, economic FEA, can measure remotely	Loading not design independent

The concept of defining fatigue load requirements as quasi-static loads, the responses to which are considered as stress ranges applied 2 million times during the lifetime of the structure, provides the same fatigue prediction results as would the RPA method for uni-axial loading, but with some benefits. The need for a load-stress area transfer function, with cycle counting for each critical element, falls away due to the fact that cycle counting is performed directly on the measured results, requiring only one finite element analysis with unit loads there-after and direct fatigue interpretation of scaled results in terms of the classification of joints and other critical areas. The incorporation of such requirements into design codes, in the traditional format of prescribed static loads with allowable stresses, is also achieved, with the only complexity added, being the fact that the allowable stress would be dependent on the critical area fatigue classification.

Thirdly, a complex analytical model named *Two Parameter Approach (TPA*) is developed, defining the usage profile of a vehicle in terms of a bivariate probability density distribution of two parameters (distance/day, fatigue damage/distance), derived from measurements and surveys. The method provides the same results achieved with a Monte Carlo simulation, employed before. Based on an inversion of the TPA model (which would not be possible using the Monte Carlo approach), a robust technique is developed for the derivation of such statistical usage profiles from only field failure data.

Lastly, the applicability of the methods is demonstrated on a wide range of comprehensive case studies. Importantly, in most cases, substantiation of the methods is achieved by comparison of predicted failures with 'real-world' failures, in some cases made possible by the unusually long duration of the study.

Sensible future work may be concentrated around three main objectives. Firstly, the most promising technique with which to circumvent the principal weakness of all the methods based on static equivalent fatigue loads, without having to perform time consuming dynamic finite element response analysis, but still resulting in design independent results, seems to be the *(Fatigue Damage Response Spectrum – FDRS*) method. This method could be combined with the FESL method, resulting in additional FESLs as a function of the principal natural frequencies of the structure.

Secondly, the use of the proposed techniques to compile new design codes for various applications, would be of benefit. Such an exercise would identify impractical aspects and other weaknesses of the methodology, as well as allow comparison with existing design codes, with which experience have been built up over years.

Thirdly, since all the work presented in this study disregards the possible accuracy benefits inherent in using the Strain Life approach rather then the Stress Life approach and also disregards the effects of multi-axial fatigue, further work on incorporating these more advanced theories into the generalised process, would be of interest.

9. REFERENCES

Aja, A.M. (2000). Sub-modelling techniques for static analysis. *MSC Software first European Tecnology Conference*.

ASTM (American Society for Testing of Materials) E 1049-85. (1989). *Standard practices for cycle counting in fatigue analysis*.

ABAQUS Standard User's Manual, Vol. I, Version 5.6. (1996). Hibbitt, Karlsson & Sorensen Inc.

Bannantine, J.A., Comer, J.J. & Handrock, J.L. (1990). *Fundamentals of metal fatigue analysis*. Prentice-Hall.

Barton, R. (1991). Optimal accelerated life-time plans that minimize the maximum test-stress. *IEEE Transactions on reliability*. 40(2).

Bathe, K. (1996). *Finite element procedures*. Prentice Hall.

Bathe, K. and Wilson, E.L. (1976). *Numerical methods in finite element analysis.* Prentice Hall.

Beamgard, R.S., Snodgrass, K. P. & Stornant, R. F. (1979). A field performance technique for light truck structural components. *SAE 791034*.

Bekker, M.G. (1969). *Introduction to terrain-vehicle systems*. Ann Arbor: The University of Michigan Press, 1969.

Berger, C., Eulitz, K.-G., Heuler, P., Kotte, K.-L., Naundorf, H., Schuetz, W., Sonsino, C.M., Wimmer, A. and Zenner, H. (2002). Betriebsfestigkeit in Germany – an overview. *International Journal of Fatigue,* 24(6).

Bishop, N.W.M. and Sherratt, F. (2000). *Finite element based fatigue calculations*. Glasgow: NAFEMS Ltd.

Blom, T.F. and Wannenburg, J. (Sept. 2000). Rough with the smooth: Durability testing gets a boost from a new international roughness index. *Testing Technology International*.

British Standards Institution. (1993). Fatigue design and assessment of steel structures. *BS 7608*.

British Standards Institution. (1991). Structural use of aluminium. *BS 8118. Part 1*.

Broek, D. (1989). *The practical use of fracture mechanics*. Dordrecht: Kluwer Academic Publishers.

Bogsjo, K. and Forsen, A. (2004). Fatigue relevant road surface statistics. *Vehicle System Dynamics*, v 41.

Butkunas, A.A. and Bussa, S.L. (1975). Quantification of inputs for vehicle system analysis. *SAE 750133*.

Captain, K.M., Boghani, A.B. & Wormley, D.M. (1979). Analytical tyre models for dynamic vehicle simulations. *Vehicle system dynamics*, 3.

Chu, C.C. (1998). Multi-axial fatigue life prediction method in the ground vehicle industry. *International journal of fatigue*, 19(1).

Code of Federal Regulations. *Title 49 – Transportation*. US Goverment Printing Office, 178.

Coleman, T.F. and Li, Y. (1994). On the Convergence of Reflective Newton Methods for Large-Scale Nonlinear Minimization Subject to Bounds, *Mathematical Programming*, Vol. 67, Number 2, pp. 189-224.

Coleman, T.F. and Li, Y. (1996) An Interior, Trust Region Approach for Non-linear Minimization Subject to Bounds, *SIAM Journal on Optimization*, Vol. 6, pp. 418-445.

Conle, F.A. and Mousseau, C.W. (1991). Using vehicle dynamics simulations and finite element results to generate fatigue life contours for chassis components. *International journal of fatigue*, 13(3).

Conle, F.A., Chu, C.C. (1998). Fatigue analysis and the local stress-strain approach in complex vehicular structures, *International journal of fatigue*, 19(1).
Cutler, A.N. (Jan. 1998). Modern statistical ideas in fatigue testing. *Journal of the engineering integrity society*.
Devlukia, J. (1985). Correlating endurance performance on roads, proving grounds and rigs. *Colloquium on vehicle test data collection and analysis*. Institution of Electrical Engineers (Great Britain).
Dietz, S., Netter, H. & Sachau, D. (1998). Fatigue life prediction of a railway bogie under dynamic loads through simulation. *Vehicle system dynamics*, 29.
Dodds, C.J. and Robson, J.D. (1973). The description of road surface roughness. *Journal of sound and vibration*, 31.
Dodds, C.J. (1973). The laboratory simulation of vehicle service stress, *ASME Paper*, 73(24).
Dong, J. (1995). Time series models for vehicle random vibration simulation tests. *International journal of vehicle design*, 16(6).
Dressler, K. and Kottgen, V.B. (1999). Synthesis of realistic loading specifications, *European journal of mechanical engineering*, 41(3).
European Agreement on the Transport of Dangerous Goods (ADR), Her Majesty's Stationary Office, London.
European Convention for Constructional Steelwork (ECCS). (1985). *Recommendations for the fatigue design of steel structures*.
Faria, L.O., Oden, J.T., Yavari, B., Tworzydlo, W.W., Bass J.M. & Becker, E.B. (1992). Tyre modeling by finite elements. *Tyre science technology*, 20.
Gerharz, J.J. (1987). Standardised environmental fatigue sequence for the evaluation of composite components in combat aircraft (ENSTAFF = ENvironmental FalSTAFF).
Giuntini, M.E. and Giuntini, R.E. (1991). Development of a weibull posterior distribution by combining a weibull prior with a actual failure distribution using bayesian inference. *American institute of aeronautics and astronautics*, AIAA-91-4133.
Goes, F. (1995) Back to Basics: If cavemen could understand the principles of product testing, surely today's advanced man can? *Testing technology international*.
Gopalakrishnan, R. and Agrawal, H.N. (1993). Durability analysis of full automotive body structures. *Simulation and development in automotive simultaneous engineering*, SAE SP-973.
Grubisic, V. (1994). Determination of load spectra for design and testing, *International journal of vehicle design*, 15(1).
Grzeskowiak, H., Fortunet, N. & Leuridan, J. (1992). System for tailoring the mechanical vibration environment - progress and results of the EUREKA project 420, ENVIB. *Annual Technical Meeting - Institute of Environmental Sciences.*
Gurney, T.R. (1976). Fatigue design rules for welded steel joints. *The welding institute research bulletin*, 17.
Hawking, S. H. (1989). *A brief history of time*. Bantam Press.
Heuler, P., Bruder, T., Klaetschke, H. (2005). Standardised load-time histories – a contribution to durability issues under spectrum loading. *Mat.-wiss. u. Werkstofftech*, 36(11).
Hines, W. H. and Montgomery, C. D. (1980). *Probability and statistics in engineering and management science*. John Wiley & Sons.
Hurd, A. (March 1992). Using data energy content to accelerate road simulation tests. *Environmental engineering*.
Kepka, M. and Rehor, P. (1993). Methodology of experimental research into operating strength and fatigue life of bus and trolleybus bodywork, *International journal of vehicle design*, 13(3).

Kuo, Y. and Kelkar, S.G. (July 1995). Body-structure durability analysis. *Automotive engineering*.
Lee, Y.L. (1995). Durability design process of a vehicle suspension component. *Journal of testing and evaluation*, 23(5).
Leese, G.E. and Mullin, R.L. (1991). The role of fatigue analysis in the vehicle test simulation laboratory. *SAE technical paper series*, 910166.
Leever, R.C. (1983). *Application of life prediction methods to as-welded steel structures*. International conference on advances in life prediction methods. ASME, New York.
Leser, C., Thangjitham, S.; Dowling, N.E. (1994). Modelling of random vehicle loading histories for fatigue analysis. *International journal of vehicle design*, 15(3).
Libertiny, G.Z. (1993). A new look at the service life expectancy of passenger cars in the United States. *Simulation and development in automotive simultaneous engineering*, *SAE* SP-973.
Lin, Z. and Fei, H. (1991). A non-parametric approach to progressive stress accelerated life testing. *IEEE Transactions on reliability*, 40(2).
Lund, R.A. and Donaldson, K.H. (1992). Approaches to vehicle dynamics and durability testing. *SAE* 820092.
MacGinley,T.J. and Ang, T.C. (1992). *Structural steelwork – design to limit state theory*. Butterworth Heineman.
Mann, R.N. (1992). *Methods for statistical analysis of reliability and life data*. New York: John Wiley & Sons.
Marcondes, J. and Singh, S. P. (1992). Predicting vertical acceleration in vehicles through road roughness. *Journal of transportation engineering*, 118(1).
Miner, M.A. (1945). Cumulative damage in fatigue. *Journal of Applied Mechanics*, 12, Trans. ASME, 67.
Moon, S-K. (1997) *Application of neural networks in development of vehicle durability testing method*. 30th International symposium on automotive technology & automation, Italy.
Moura, C.M. (1992). A method to estimate the acceleration factor for sub-assemblies. *IEEE Transactions on reliability*, 41(3).
MSC Software Corporation. (2002). *MSC Fatigue 2003 User's Manual*.
MSC Software Corporation. (1997). *MSC/NASTRAN V70 Advanced Dynamics User's Guide*.
Neuber, H. (1969). Anisotropic non-linear stress-strain laws and yield conditions. *International Journal of Solids & Structures*, v 5, n 12.
Niemand, L.J. (1996). *Probabilistic establishment of vehicle fatigue test requirements*. Masters degree thesis. University of Pretoria.
Niemi, E.J. and Marquis, G.B. (2003). Structural hot spot stress method for fatigue analysis of welded components. In *Metal structures – design, fabrication, economy*. Edited by Jarmai & Farkas. Rotterdam: Millpress.
Olagnon, M. (July 1994) Practical computation of statistical properties of rainflow counts, *Fatigue*, 16.
Olofsson, U., Svensson, T. & Torstensson, H. (1995). Response spectrum methods in tank-vehicle design, *Experimental mechanics* , v 35, n 4.
Oyan, C. (1998). Dynamic simulation of Taipei EMU train. *Vehicle system dynamics*, 30.
Pountney, R.E. and Dakin, J.D. (1992). Integration of test and analysis for component durability. *Environmental engineering*, 5(2).
Raath, A.D. (1997). A new time domain parametric dynamic system identification approach to multiaxial service load simulation testing in components. *International journal of fatigue,* 19(5).

Rhaman, A. (Autumn 1997). Towards reliable finite element analysis. *Environmental engineering*.
Richards, D.P. (Dec. 1990). A review of analysis and assessment methodologies for road transportation vibration and shock data. *Environmental engineering*.
Riedl, H. (Jan. 1998). Test substantiation of aluminium chassis with particular consideration of extreme loads. *Journal of the engineering integrity society.*
Rixen, D.J. (2001). Generalized mode acceleration methods and modal truncation augmentation**.** *Collection of Technical Papers - AIAA/ASME/ASCE/AHS/ASC Structures, Structural Dynamics and Materials Conference*, v 2, p 884-894.
Rui, Y., Borsos, R.S., Gopalakrishnan, R., Agrawal, H.N. & Rivard, C. (1993). The fatigue life prediction method for multi-spot-welded structures. *Simulation and development in automotive simultaneous Engineering, SAE* SP-973.
Rupp, A. (1989). Ermittlung von ertragbaren Schnittkraften fur die betriebsfeste Bemessung von Punktschweissverbindungen im Automobilbau. *Forschungsvereinigung Automobiltechnik EV*, 78.
Ryu, J., Kim, H. & Wang, S. (1997). A method of improving dynamic stress computation for fatigue life prediction of vehicle structures. *SAE 971534*.
SABS (South African Bureau of Standards) 1518. (1996). *Transportation of dangerous goods – design requirements for road tankers*.
SABS (South African Bureau of Standards) 1398. (1994). *Road tank vehicles for petroleum based flammable liquids*.
Schutz, D. et al. (1990). *Standardized load sequences for car wheel suspension components (car loading standard)- CARLOS*. LBF – Bericht No. FB-191/IABG – Bericht No. TF-2695.
Sherratt, F. (1996). Current applications of frequency domain fatigue life estimation, *Environmental engineering*, 9(4).
Skattum, K.S., Harris, J.F. & Howell, L.J. (1975). Preliminary vehicle structural design for comparison with quantitative criteria. *SAE* 750136.
Slavik, M.M. and Wannenburg, J. (1998). *Prognosis of vehicle failures due to fatigue*. Conference proceedings of Risk, economy & safety failure minimisation and analysis: Failures '98. Rotterdam: AABalkema.
Socie, D.F. and Pompetzki, M.A. (2004). Modeling variability in service loading spectra. *Journal of ASTM International,* Vol. 1, No. 2.
Society of Automotive Engineers Inc. (1988). *SAE Fatigue design handbook*. 2nd Edition. Warrendale, PA: SAE.
Society of Automotive Engineers Inc. (1997). *SAE Fatigue design handbook* AE-22. 3rd Edition. Warrendale, PA: SAE.
Stephens, R.I., Dopker, B., Haug, E. J., Baek, W. K., Johnson, L. P. & Liu, T. S. (1987). Computational fatigue life prediction of welded and non-welded ground vehicle components. *SAE* 87967.
Svensson, T. (1997). Prediction uncertainties at variable amplitude fatigue. *International journal of fatigue*, 19(1).
Van Rensburg, W., and Wannenburg, J., (1996). *Validating design life-times using vibrational measurements*. Proceedings of international conference on noise & vibration engineering, ISMA21. Leuven.
Wannenburg, J. (1999). *The applicability of static equivalent design criteria for the fatigue design of dynamically loaded structures*. Proceedings of the fifth international colloquium on ageing of materials and methods for the assessment of lifetimes of engineering plant. Edited by Penny, R.,K. Chameleon Press Ltd.
Wannenburg, J. (1993). The probabilistic establishment of durability requirements based on field failure data. *Iron & Steelmaker (I&SM)*, v 20, n 9.

Wannenburg, J.J. (1966). *'n Studie van die vloei van lemroosters*. PhD proefskrif. Universiteit van Stellenbosch.
Xu, H. (1998). An introduction of a modal scaling technique: An alternative and supplement to quasi-static g loading technique with application in structural analysis. *SAE* 982810.

1. Broek (1985)
2. Svensson (1997)
3. Dressler and Kottgen (1999)
4. Rhaman (1997)
5. Hawking (1989)
6. Wannenburg (1993)
7. Van Rensburg and Wannenburg (1996)
8. ISO 1496-3:1991(E)
9. Kuo and Kelkar (1995)
10. Bathe (1996)
11. MSC/NASTRAN User's Guide
12. Dietz et al. (1998)
13. Oyan (1998)
14. Captain et al (1979)
15. Faria et al. (1992)
16. SAE Fatigue Design Handbook (1997)
17. Gopalakrishnan and Agrawal (1993)
18. Conle and Chu (1991)
19. Bannantine et al. (1990)
20. Gurney (1976)
21. Niemi and Marquis (2003)
22. ECCS (1985)
23. BS 8118 (1991)
24. Stephens et al. (1987)
25. Leever (1983)
26. Rupp (1989)
27. Rui et al. (1993)
28. Chu (1998)
29. ASTM E 1049-85 (1989)
30. Olagnon (1994)
31. Lund and Donaldson (1992)
32. Sherratt (1996)
33. Leese and Mullin (1991)
34. Barton (1991)
35. Niemand (1996)
36. Moon (1997)
37. Lin and Fei (1991)
38. Hurd (1992)
39. Moura (1992)
40. Raath (1997)
41. Dong (1995)
42. Kepka and Rehor (1993)
43. Pountney and Dakin (1992)
44. Cutler (1998)
45. Giuntini (1991)
46. Slavik and Wannenburg (1998)
47. Beamgard et al. (1979)
48. Libertiny (1993)
49. Grubisic (1994)
50. Marcondes and Singh (1992)

51. Blom and Wannenburg (2000)
52. Richards (1990)
53. Devlukia (1985)
54. Grzeskowiak et al. (1992)
55. MacGinley and Ang (1992)
56. SABS 1398 (1994)
57. SABS 1518 (1996)
58. Code of Federal Regulations, Title 49
59. Skattum et al. (1975)
60. Riedl (1998)
61. Leser et al. (1994)
62. Olofsson et al. (1995)
63. European Agreement on the Transport of Dangerous Goods (ADR)
64. Code of Federal Regulations, Title 49
65. Miner (1945)
66. Niemand (1996)
67. ISO 1496-3:1991(E)
68. Gurney (1976)
69. Miner (1945)
70. Wannenburg (1966)
71. MSC/NASTRAN V70 Advanced Dynamics User's Guide (1997)
72. Bathe (1996)
73. Craig (1981)
74. Dodds (1973)
75. Bishop and Sherratt (2000)
76. ABAQUS/Standard User's Manual (1996)
77. MSC.Fatigue 2003 User's Manual (2002)
78. Ryu et al. (1997)
79. Xu (1998)
80. BS 7608 (1993)
81. Goes (1995)
82. Hines and Montgomery (1980)
83. Niemi and Marquis (2003)
84. Bathe and Wilson (1976)
85. Rixen (2001)
86. Bogsjo et al. (2004)
87. Neuber (1969)
88. Socie and Pompetzki (2004)
89. Coleman and Li (1994)
90. Coleman and Li (1996)
91. Gerharz (1987)
92. Heuler et al. (2005)
93. Schutz et al. (1990)